Biomarkers of Donor Kidney Quality as Predictors of Transplantation Outcomes

Maria Kaisar

Nuffield Department of Surgical Sciences
&
The Queen's College

A thesis submitted for the degree of
Doctor of Philosophy in Transplantation Science
University of Oxford
Michaelmas Term 2016

Biomarkers of Donor Kidney Quality as Predictors of Transplantation Outcomes

SUPERVISORS

Rutger J Ploeg

Professor of Transplant Biology & Consultant Transplant Surgeon

Nuffield Department of Surgical Sciences

Benedikt M Kessler

Professor of Biochemistry & Mass Spectrometry

Nuffield Department of Medicine

Biomarkers of Donor Kidney Quality as Predictors of Transplantation Outcomes

Maria Kaisar
The Queen's College, University of Oxford

A thesis submitted for the degree of Doctor of Philosophy in Transplantation Science
Michaelmas Term 2016

ABSTRACT

Kidney transplantation is a lifesaving treatment for end stage kidney disease that offers considerable benefits to recipients in terms of survival and quality of life. The growing demand for transplants to treat conditions stemming from a rising prevalence of end stage renal disease, diabetes and cardiovascular diseases has to be met increasingly with donors who are older with a high incidence of comorbid conditions. Organs obtained from these higher risk donors are more likely to have either suboptimal short and long-term transplant outcomes or even fail to function altogether. Transplant clinicians, who have to balance the risk of patients dying while waiting for a transplant against the uncertainty of outcomes, often decline organs as transplants. These clinical challenges entail difficult decisions, and more refined tools to assess and quantify the risks of marginal donor organs are lacking. Diagnostic markers of donor kidney quality that can predict transplantation outcomes are highly desirable in order to discriminate the suboptimal from those allografts that will recover and have good long-term function.

My doctoral research using donor samples collected within the Quality of Organ Donation (QUOD) programme has shown for first time that it is possible, on the basis of a tissue proteomic profile, to discriminate donor kidneys at the time of retrieval that will have suboptimal allograft function from those kidneys that could recover and have good function at three and 12 months post transplantation. Despite AKIN classification and Remuzzi scoring showing no evidence of acute kidney injury or chronic kidney disease in the analysed biopsies, quantitative mass spectrometry and degredomics experiments with a subsequent validation analysis on an independent cohort of biopsy samples confirmed the increased levels of inflammation and pro-fibrotic proteins in the allografts with suboptimal function, while increased levels of cytoprotective proteins were detected in the kidneys that recovered with a good function one year after transplantation. Furthermore, the kidneys with suboptimal function demonstrated enhanced degradation of cytoskeletal proteins that are vital in sustaining the glomerular basement membrane cytoskeleton.

In addition, I conducted a pilot study using proteomic analysis of serum and urine of donors whose kidneys either developed delayed graft function or functioned immediately. This study confirmed that is feasible to identify alterations in the blood and urine proteome that are biologically meaningful.

In preparation of the discovery and development of diagnostic biomarkers of long-term outcome after kidney transplantation using QUOD plasma samples, I assessed the pre-analytical variability associated with the processing of whole blood during QUOD sample collection in order to identify a baseline proteomic and peptidomic profile against which candidate protein markers relevant for clinical correlates can be selected.

Based on the findings reported in this thesis, future work should aim to identify and develop better diagnostic tools that can more reliably predict donor organ quality. In addition, novel intervention strategies can be explored that either attenuate pro-fibrotic and proteolytic activities or enhance antioxidant and cytoprotective mechanisms in deceased donor kidneys prior to transplantation.

ACKNOWLEDGEMENTS

My DPhil journey has been a life changing experience professionally and personally and on this path my supervisors, colleagues, friends and family have been a constant source of inspiration and unreserved support.

My utmost gratitude goes to my supervisors Professor Rutger Ploeg and Professor Benedikt Kessler for inspiring, challenging and guiding me through my DPhil. It is their achievements in medicine and science that will inspire me for the rest of my academic career.

Professor Ploeg guided my learning through the clinical aspects of my research, with wisdom and enthusiasm, authority and empathy, focusing my scientific endeavour to the most important endpoint, the patient. His leadership in establishing landmark projects such as QUOD and COPE offered me training prospects for which I am indebted. His mentorship went beyond transplantation science. His optimistic view of life and his counsel "you will get there" will echo in my every uphill moment through life.

Professor Kessler offered me the space and the freedom to experiment and develop as a scientist in an environment of significant scientific accomplishments and high expectations. His support and the offer of so many incredible opportunities in his lab made me a better more rounded scientist and I am grateful for this.

I am deeply indebted to my employer NHS Blood and Transplant for offering me numerous opportunities through my career and support through my DPhil. I would particularly like to mention Professor Marion Scott who has supported and encouraged me and has played an instrumental role in establishing career development opportunities for clinicians and researchers within R&D NHSBT.

My deepest gratitude goes to the families of organ donors for their participation in the QUOD research program that has made this work possible.

My DPhil years were enriched by shared moments with colleagues and friends. My sincere thanks goes to Dr Zee Akhtar who has been a friend and colleague, Mr Leon van Dullemen, Dr Honglei Huang, Dr Sergei Maslau, Mrs Sandrine Rendell, Dr Roman Fischer, Ms Marie Laëtitia Thézénas who were always willing to impart knowledge and to help when required and, on occasions, offered me accommodation for the night to ensure an early start the next morning.

This incredible venture was shared with my family, my husband Gary and my son Alex. My DPhil would not have started without your encouragement and reassurances that "together, we can make it work". In challenging moments your unconditional love, patience and encouragement sustained me. Gary- this research has been enriched in so many ways by your scientific expertise and critical thinking and from our endless thought provoking and inspirational discussions and for this I thank you.

The completion of my DPhil can only be dedicated to you, to my family, to Alex and Gary.

DECLARATION

All the work presented in my DPhil thesis is my own research except were otherwise stated.
I have undertaken my research work with the support and guidance of my supervisors.
Mr Leon van Dullemen has provided support in performing a number of western blots described in my thesis. Dr Roman Fischer and Ms Marie Laëtitia Thézénas have run my samples in the mass spectrometer in the Kessler laboratory. Dr A Klooster performed the Remuzzi scoring in the University Medical Centre, Groningen, The Netherlands.

During my DPhil working within the QUOD National Management Team, I contributed in establishing the Quality in Organ Donation (QUOD) biobank coordinated by Professor Ploeg. My main contribution was developing the standard operating protocols of clinical sample collection, processing and storage aiming to minimise pre analytical variability to preserve the integrity of clinical samples for future research.

With shared responsibility with Dr Zeeshan Akhtar I worked to establish the Consortium for Organ Preservation in Europe (COPE) biobank that houses biological samples, clinical and demographic data collected from UK and Continental Transplant Centres of three clinical trials in kidney and liver preservation coordinated by Professor Ploeg.

I participated in establishing the Oxford Transplant Biobank. I have used the knowledge and expertise I developed in participating in the QUOD project to support the development of a local biobank that collects biological samples and clinical data from living donors and kidney recipients in Oxford Transplant Centre.

Table of Contents

Table of Figures

Table of Tables

List of Abbreviations

AKI	Acute kidney injury
ACN	Acetronitrile
ANOVA	Analysis of variance
ATP	Adenosine triphosphate
BCA	Bicinchoninic acid assay
BSG	Basigin
CAD	Chronic allogarft dysfunction
CAT	Catalase
CID	Collision induced dissociation
CIT	Cold ischaemic time
CKD	Chronic kidney disease
CLU	Clusterin
CPFP	Central proteomic facility pipeline
DBD	Heart beating donors
DC	Dendritic cells
DCD	Non heart beating donors
DGF	Delayed graft function
DOC	Sodium deoxycholate
DTT	Dithiothreitol
ECD	Extented criteria donor
eGFR	estimated Glomerular Filtration Rate
eGFR	estimated Glomerular Filtration Rate
ESI	Electron spray ionisation
ESRD	End stage renal disease
FA	Formic acid
FDR	False discovery rate
FTKAS	Fast track kidney allocation system
GBM	Glomerular basement membrane
GST	Glutathione s transferase
HCA	Hierarchical clustering analysis
H-FABP	Heart-fatty acid binding protein
HLA	Human leukocyte antigen
HPLC	High performance liquid chromatography
IAA	Iodoacetamide
ICAM-1	Intracellular adhesion molecule-1
IL-18	Interleukin 18
IL-6	Interleukin-6
IL-8	Interleukin 8
IPA	Ingenuity pathway analysis
IRI	Ischaemia reperfusion injury
JNK	c-Jun N-terminal kinases
KDPI	Kidney donor profile index

KEGG	Kyoto encyclopedia of genes and genomes
KIM-1	Kidney inflammation molecule -1
LAMB-2	Laminin beta chain 2
LC-MS/MS	Liquid chromatography tandem mass spectrometry
LD	Living donors
L-FABP	Liver fatty acid binding protein
LFQ-Ms/MS	Label free quantitaive mass spectrometer
m/z	mass /charge
MAPK1	Mitogen activated protein kinase 1
MDRD	Modification of diet in renal diseases
MRC	Medical research council
MS	Mass spectrometer
NAG	N-acetyl-β-glucosaminidase
ng	nanogram
NGAL	Neutrophil gelatinase associated lipocaline
NHSBT	NHS Blood and Transplant
NORS	National organ retrieval service
ODT	Organ Donationa and Transplantation
OPN	Osteopondin
PDGFRa	Platelet derived growth factor-β
PNF	Primary non-function
PROTOMAP	Protein topography and migration analysis platform
Prx3	Peroxiredoxin-3
QUOD	Quality in Organ Donation
ROS	Reactive oxygen species
SBP	Systolic blood pressure
SCD	Standard criteria donor
SCr	Serum creatinine
SDS-PAGE	sodium dodecyl sulfate polyacrylamide gel electrophoresis
SINQ	Spectra index normalised quantitation
SNOD	Specialist nurse of donation
STAT-1	Signal transducer and activator of transcription-1
TCA	Trichloroacetic acid
TNFa	Tumour necrosis factor a
Tris	Tris(hydroxymethyl)aminomethane
Trx-1	Thioredoxin-1
TRXR	Thioredoxin reductase
UNOS	United Network for Organ Sharing
VCAM-1	Vascular cell adhesion molecule-1
WI	Warm ischaemia
EDTA	Ethylenediaminetetraacetic acid
DSA	Donor specific antibodies
TSP-1	Thrombospondin-1
C1	Complement C1
C3	Complement C3
C4B	Complement C4B

CHAPTER 1

Introduction

1.1 Kidney transplantation

End stage renal disease (ESRD) concerns advanced loss of kidney function that, without intervention, will lead to the death of the patient. Renal replacement therapies such as haemodialysis and peritoneal dialysis are life-saving treatments but impact adversely on quality of life and are associated with high rates of mortality in the longer term[1]. Renal transplantation is both life-saving and life-enhancing and, as such, the preferred treatment for ESRD.

The first successful kidney transplantation was performed on December 23rd, 1954 at the Peter Bent Brigham Hospital in Boston by the team of John Merrill, Joseph Murray and Hartwell Harrison. A brother offered one of his kidneys to his identical twin sibling[2]. The transplanted kidney functioned immediately and the recipient survived for 9 years with a functioning graft that eventually succumbed to recurrent glomerulosclerosis, the original cause of his kidney disease[3].

To put this medical landmark into context, this first successful transplantation occurred before the introduction of adequate immunosuppressive therapies and prior to the option of histocompatibility cross matching between donor and recipient. The degree of histological compatibility and 'tolerance' between the siblings was assessed using a skin graft from the donor sibling engrafted in the recipient[2].

1.2 The clinical challenge in renal transplantation in the UK

The first successful kidney transplantation in the UK was performed in The Royal Infirmary of Edinburgh on 30th October 1960 by Sir Michael Woodruff. The renal transplant was among identical twin brothers. Sir Michael Woodruff

subsequently designed and, with the support of the Medical Research Council, established in Edinburgh the world's first purpose built transplant unit[4].

Since these early days, the success of kidney transplantation as a life-saving and life improving treatment for ESRD has led to a high demand for donor kidneys. As of March 2015, 5,686 patients were registered on the active transplant list for a kidney transplant in the UK (figure 1.1).

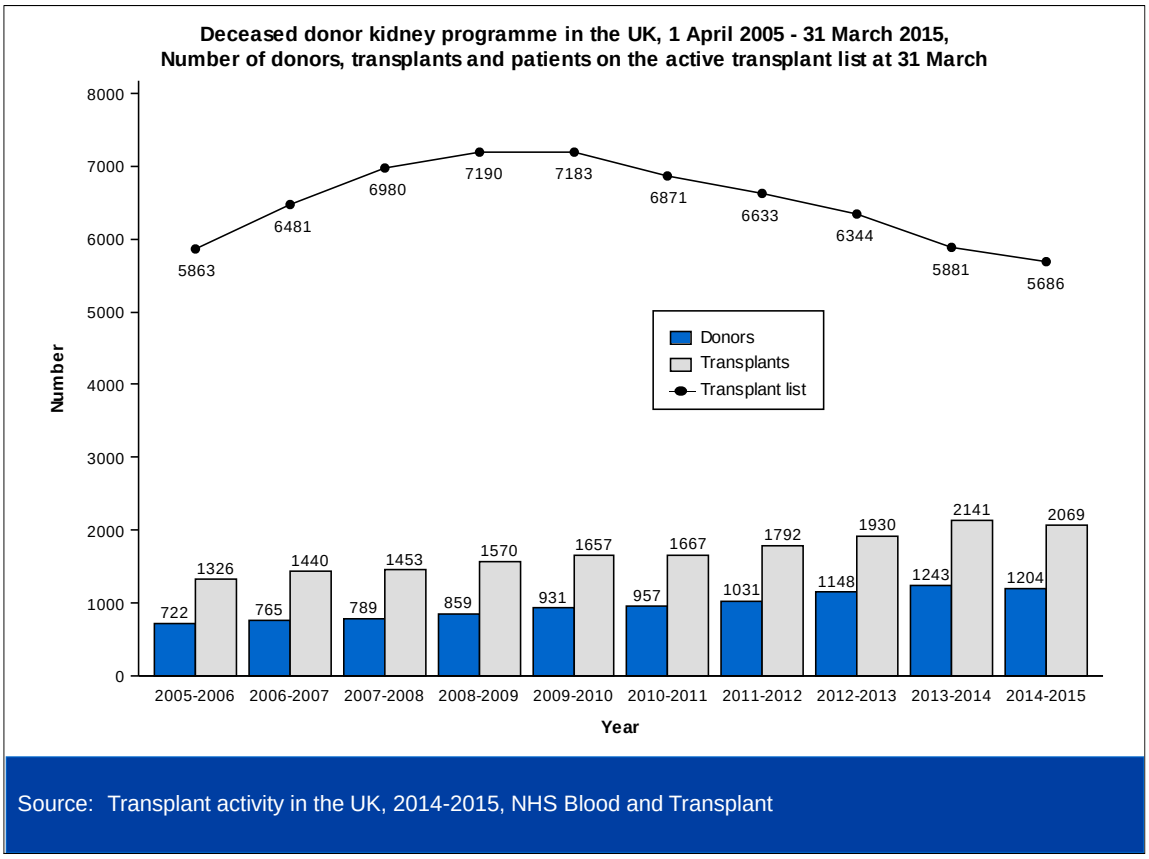

Figure 1.1 Number of patients with end stage renal disease waiting for a transplant compared to the number of deceased donors and transplants rmed in the UK in the period April 2005 to March 2015
The line represents the number of patients on the waiting list for a kidney transplant. The blue bars represent the donors and the grey bars the number of kidney transplants performed every year in the period March 2005-April 2015[5].

In the UK between April 2014 and March 2015 a total of 3,579 new patients joined the kidney waiting list representing an increase of 4% over the previous year[6]. This upward trend reflects a steadily aging population in addition to increased prevalence of kidney related diseases. Older patients joining the list tend to have an increased level of co-morbidities such as diabetes, cardiovascular diseases and obesity, which are conditions that, in themselves, have led to an increased demand for transplants.

A higher incidence of diabetic kidney disease has resulted in a gradual increase in the numbers of patients needing renal replacement therapy, from 12.3 patients per million (ppm) in 1995 to 27.6 ppm in 2009 in the UK[7].

Furthermore, the incidence of moderate to severe chronic kidney disease (CKD), defined by an estimated glomerular filtration rate (eGFR) < 60ml/min /1.73m^2 using the Modification of Diet in Renal Disease (MDRD) equation was estimated to 6.1% (95% CI 5.3%-7%) of the population aged 16 years in 2011[8]. Public Health England has predicted that in 2036, 8.3% of the population will have moderate to severe CKD[8]. Patients with CKD are at higher risk of progression to ESRD and an increased need for either dialysis or renal transplantation.

Unfortunately, the increased demand for donor kidneys for transplantation in the last decade has not been met by a similar increase in organ donation and, paradoxically, has even coincided with more deceased donor organs discarded than before. This clinical challenge associated with the shortage of donor organs and high discard rates is discussed below.

Shortage of donor organs

In the UK between April 2014 to March 2015 8,945 patients were listed with ESRD and from this cohort 5,686 adult patients were active on the waiting list for transplantation (figure 1.1). However, only 2,069 kidney transplant operations (obtained from 1,204 donors were performed due to a chronic shortage in supply). As a consequence, 243 patients died whilst waiting for a transplant[6]. Although the total number of patients in need of a kidney transplant increased from 7,437 to 8,945 in the period April 2014 to March 2015, the number of patients active on the waiting list did not reflect this increase with 5,881 patients in 2014 compared to 5,686 in 2015. In 2015 the number of patients with ESRD on the waiting list was similar to that in 2005 revealing that the number of suspended patients had more than doubled from 1,569 in 2005 to 3,529 in 2015[6]. The shortage of donor organs disproportionately affects patients of Asian and African-Caribbean descent who are 3 to 4 times more likely to develop ESRD compared to the white ethnic background population. Asian and African-Caribbean patients with ESRD currently represent 24% of the patients on the waiting list. However, only 3% of donor kidneys are obtained from these minority population cohorts[6].

Kidneys for transplantation can be obtained from either living or deceased donors, the latter including Donation after Brain Death (DBD) and Donation after Circulatory Death (DCD). The relative contribution of deceased and living donors to the donor pool has changed significantly over time with an almost doubling in the number of living donor (LD) kidneys transplanted in the period April 2005 to March 2015 (from 541 in 2005 to 961 in 2015)(figure 1.2). However, deceased donor kidneys are still the main source for transplantation. Due to the donor

shortage, in the last 10 years especially, a significant increase in the use of DCDs has occurred. NHS Blood and Transplant (NHSBT) recorded from April 2014 through March 2015, 961 living donations and 1,832 deceased donations. The number of donor kidneys obtained from DCDs has increased by three fold since 2005 (from 214 in 2005 to 711 in 2015)[5] (figure 1.2).

A key problem at time of offering is the perceived uncertainty by the clinician whether a particular donor kidney is suitable for the recipient. This is brought about by the lack of clinically relevant surrogate markers reflecting the quality of the graft-to-be and potential for subsequent allograft function. The multifactorial reasons for high kidney discard rates will be extensively discussed in this chapter. Failing to fully utilise all the available donor kidneys further contributes to the problem of organ shortage.

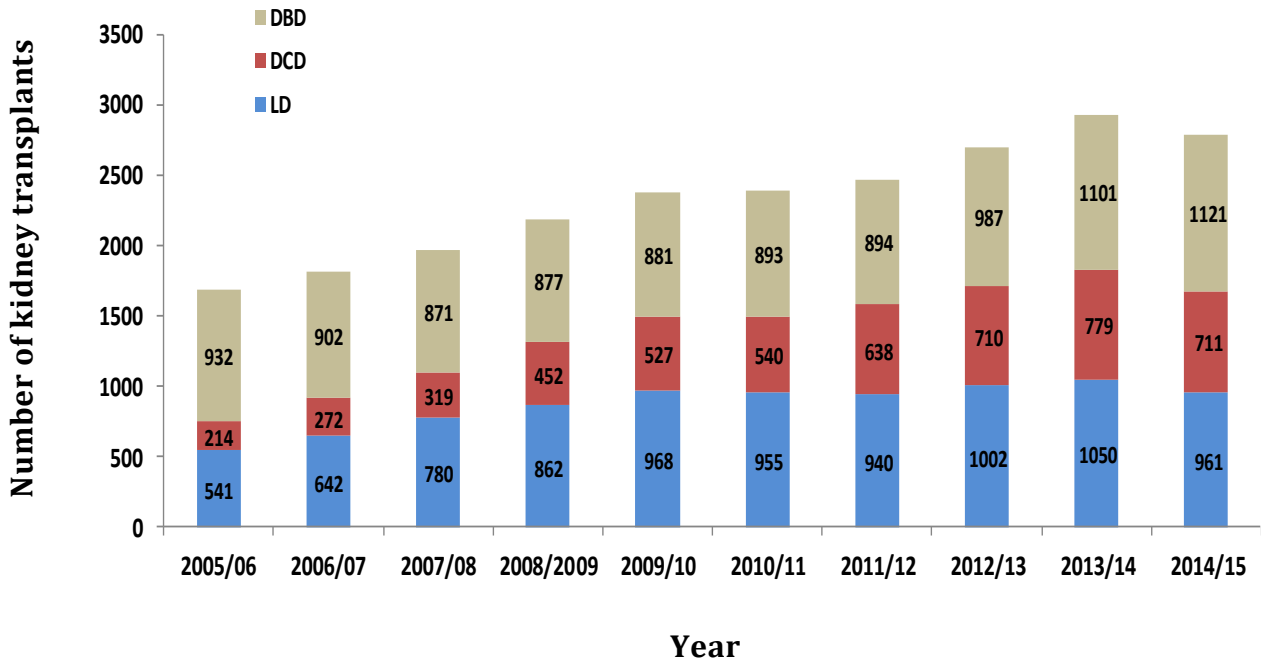

Figure 1.2 The number of kidney transplants performed and obtained from each donor type between April 2005 to March 2015[5]**.**
Adult kidney-only transplants and the contribution of DBDs, DCDs and LDs.

Discarded organs

In an effort to bridge the gap between the need for transplantation and the limited availability of deceased donor organs, clinicians have started to accept organs from older and higher risk donors including unstable DBDs, extended criteria donors and DCDs with more comorbidities.

Extended-criteria donors (ECDs) refer to kidney donors who are either 60 years and older or aged 50 to 59 years with at least two of the following three clinical presentations of hypertension, terminal serum creatinine >1.5 mg/dl, or death from cerebrovascular accident. The utilisation of ECD kidneys is hampered by the uncertainty of post transplantation outcomes and, as a result, a high percentage of these organs are not utilised. ECD kidneys are more likely to have suboptimal function or graft failure when compared to kidneys obtained from standard criteria donors (SCDs)[9] and as results a high percentage of ECD organs are either not retrieved or are discarded following retrieval.

In recent years, organ discard rates have followed the increased trends of donation rates from ECDs and DCDs. In the UK, 15% of retrieved kidneys from DCDs were discarded compared to 8% DBDs according to the NHSBT April 2014 to March 2015 kidney activity report[6] (figure 1.3). However, when we consider how many kidneys were declined from the overall number of donated kidneys it becomes apparent that 15% of DBD and 20% of DCD kidneys were not utilised.

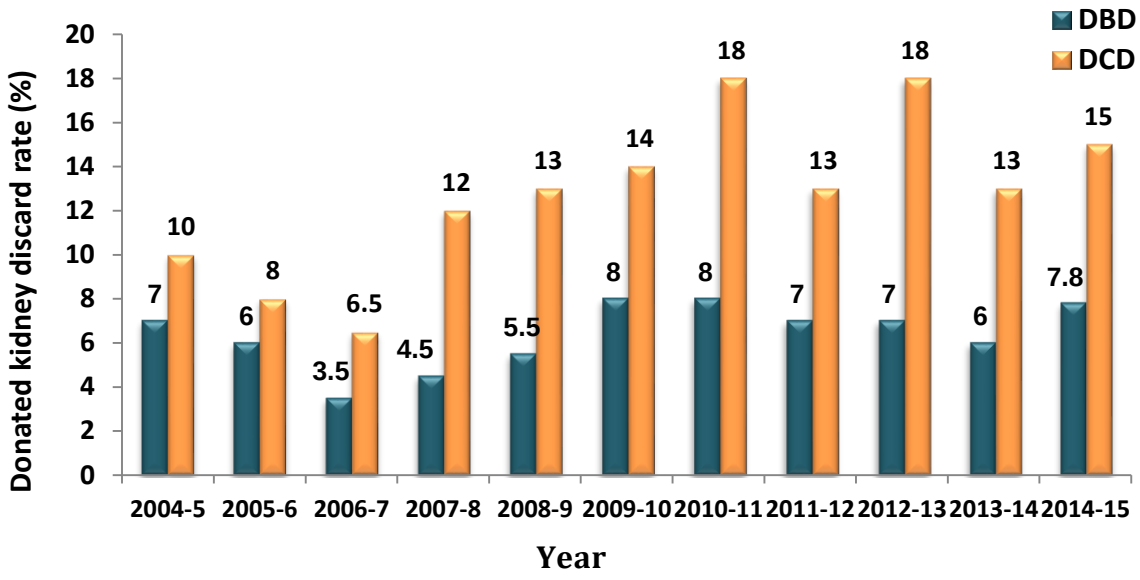

Figure 1.3 Rate of donor DBD and DCD kidneys discarded in UK in the period 2004-15[6].

The rate of discarded kidney is expressed as a percentage of the number of kidneys discarded / number of kidneys retrieved.

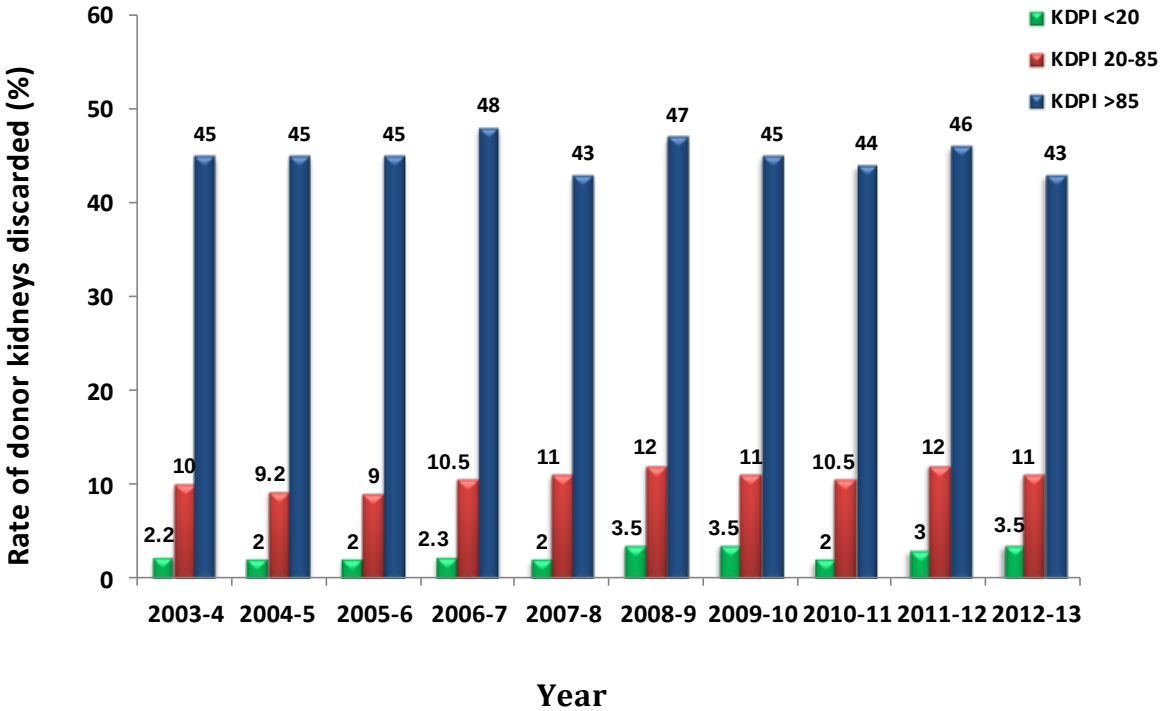

Figure 1.4 The rate of donor kidneys discarded according to KDPI score in USA[10].

The utilisation rate of donor organs varies greatly between countries and among different transplant centres within countries such as the USA or UK. Different allocation systems between countries and a more accommodating approach of some transplant centres to accept kidneys retrieved from ECDs account for some variability in discard rates. In the USA, the United Network for Organ Sharing (UNOS) data show that the discard rate of deceased donor kidneys increased almost 4-fold for donors with a kidney donor profile index (KDPI) > 85 when compared to a KPDI <85 (figure 1.4). The KDPI is an algorithm based assessment that produces a predictive score of the risk for allograft failure when ten donor clinical and demographic factors are considered (discussed in 1.6)[11]. The application of KDPI has been expanded to become an important assessment tool of donor kidney quality to decide whether kidneys should be discarded or transplanted. Its utility is discussed below. As Figure 1.4 shows, the discard rate increases as the KDPI increases with scores over 85 resulting in almost half of the donor kidneys discarded[10,12].

The decision to decline a donated kidney and provide a life-saving opportunity to a patient on the transplant list is not an easy decision for transplant surgeons. Callaghan *et al.,* looked into the potential utilisation of kidneys by assessing 20 discarded kidneys to determine if the decision to discard was medically justified or if some of the rejected kidneys were transplantable. The assessment method used was visual inspection by surgeons who had to re-evaluate the discarded kidneys in conjunction of donor demographic and clinical data. The study concluded that four of the twenty discarded kidneys were deemed 'usable' and nine were 'possibly useable' indicating that potentially 20% of the discarded kidneys could be transplanted with good outcomes[13]. A significant outcome of

this study was the implementation by NHSBT of the 'fast track kidney allocation system, (FTKAS)' to facilitate utilisation of discarded kidneys. The utility of the 'high risk' donor kidneys increases when the risk of dying on the waiting list is taken to account for certain cohorts of patients. Massey *et al.,* assessed the benefit of accepting a kidney with a given KDPI score compared to waiting for an offer of a lower KDPI (higher quality) kidney against the risk of dying on the waiting list. The study concluded that for older recipients or for patients who wait a long time for a transplant there is a benefit to long term survival in accepting a 'high risk' kidney[14].

The importance of increasing the utilisation of deceased donor kidneys is highlighted in the NHSBT strategy document 'Taking Organ Transplantation to 2020'[15]. The document highlights the need to develop new objective criteria for donor organ quality predicting transplantation outcomes. This will enable surgical teams to make better decisions on whether to transplant certain organs or decline them as unsuitable. The document concludes that the discovery of novel biomarkers to provide diagnostic tools predictive of long term organ function should be a priority research area[15].

1.3 Donor types

Donation after brain stem death

Donation after brain death (DBD) is the primary source of organs for transplantation and currently concerns 40% of all the donor pool[6] (, figure 1.2). Between April 2004 and March 2010 an initial decline in DBD donors (DBDs) was observed followed by a steady increase after 2010 to a level that exceeded all previous levels of donation following brain stem death. The initial reduction in

DBDs most probably was the result of a number of significant improvements in neurosurgical practise and intensive care that reduced deaths following brain trauma. However, the expansion of donor criteria and the acceptance of older donors then led to increased numbers of DBDs post 2010.

The pathophysiological causes of brain death in DBDs involve brain stem herniation caused by cerebral injury as a result of trauma or haemorrhage or an extended anoxic period due to cardiopulmonary arrest, leading to neuronal death with terminal brain stem dysfunction. Traumatic brain injury, with a progressive development of oedema and increase of intracranial pressure, can lead to brain stem herniation with the neurological characteristics of brain death. Onset of ischaemia and the reduced perfusion of the brain as a result of oedema and intracranial pressure lead to the 'Cushing reflex', which is characterised by hypertension and bradycardia and is a response that aims to re-establish brain perfusion. The progression of ischaemia across the medulla oblongata and hypothalamus leads to sympathetic nervous system activation and a parallel release of endogenous catecholamines in the circulation, which is known as the 'catecholamine storm' that promotes hypertension, tachycardia, and systemic vasoconstriction. A second phase emerges when, due to progression of ischaemia in the brain spinal cord axis, sympathetic deactivation leads to haemodynamic instability as a result of cardiac dysfunction and heart failure. Changes in systolic blood pressure cause hypoperfusion in the abdominal organs and can be detrimental to kidney function[16–18].

Apart from haemodynamic instability, several hormonal changes occur as the increased intracranial pressure affects the function of anterior and posterior pituitary glands in the brain. The onset of diabetes insipidus and hypothalamus

ischaemia following brain injury is characterised by endocrine dysregulation causing an imbalance between water and electrolytes. A decrease in antidiuretic hormone secretion such as vasopressin results in polyuria[17]. Hormonal resuscitation therapy such as insulin replacement can prevent hypovolemia, hypernatremia and haemodynamic collapse in the donor and this has been shown to lead to better functioning kidneys with lower levels of terminal serum creatinine (SCr) levels[19].

Brain injury induces a local and systemic state of inflammation that can damage donor kidneys. Increased levels of cytokines in circulation, following brain death and upregulation of pro-inflammatory genes, promote endothelial activation with adhesion molecules such VCAM-1, ICAM-1, P-selectin, E-selectin mediating a state of inflammation and migration of leucocytes to kidney compartments. The upregulation of adhesion molecules occurs as early as 30 minutes following brain death in animal models[20]. At the cellular level disruption of intracellular Ca^{+2}, ATP synthesis and energy production causes oxidative stress and dysregulation of reactive oxygen species (ROS) homeostasis that promotes further injury (figure 1.5).

A study by Nagareda *et al.,* described that the onset of diabetes insipidus following brain death increased urine output and histological examination of kidneys revealed injury related morphological changes that included necrosis of renal proximal and distal tubules with deposition of inflammatory cells[21]. Akhtar *et al.,* using a rodent model of haemorrhagic stroke and an unbiased –omics approach showed the dysregulation of metabolic pathways and morphological damage to the kidneys[22]

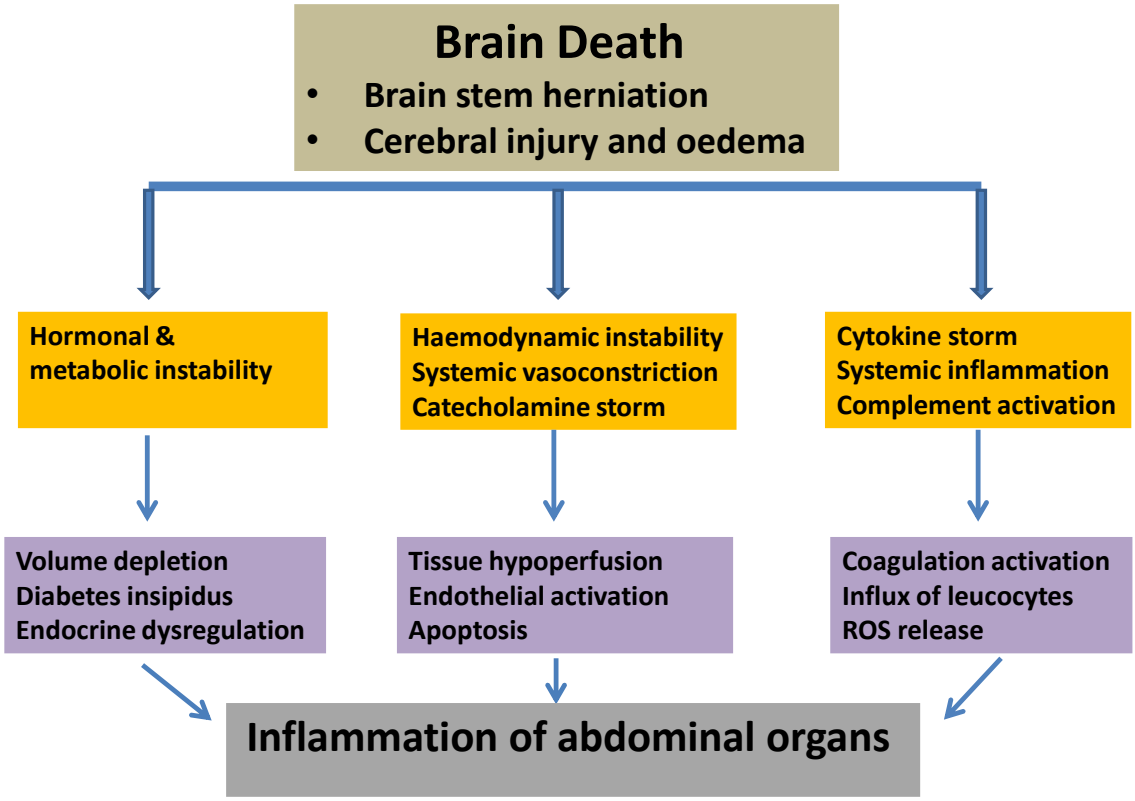

Figure 1.5 Summary of the pathophysiological canges in DBDs
A schematic summary of the main biological processes underlying the pathophysiological cascade that leads to injury of peripheral organs following brain stem death[16]*. Intracranial pressure and stem brain herniation activates the parasympathetic nervous system leading to a gradual decrease in blood pressure. During brain ischaemia the sympathetic system is activated generating the colloquially termed 'catecholamine storm' leading to vasoconstriction, elevation of blood pressure and tachycardia, an increase of vascular resistance, heart load and oxygen consumption. Catecholamines increase intracellular* Ca^{+2} *and disrupt the production of ATP synthesis causing ROS and oxygen free radical production. When catecholamine levels fall below baseline, vascular tension decreases leading to cardiac dysfunction and heart failure. This haemodynamic instability causes intense vasoconstriction in the abdominal organs resulting in hypoperfusion and the potential of onset of systemic ischaemia*[16,17,23]*.*

Donation after circulatory arrest

Contrary to donation following brain death, donation after circulatory arrest (DCD) is confirmed upon cessation of arterial circulation rather than neurological criteria. Depending on the circumstances that resulted in circulatory arrest, DCDs are grouped into four categories according to the Maastricht classification system (table1.1). Although in the UK 60% of the deceased donor organs are obtained from DBDs, retrieval of DCD organs has increased by more than 3-fold in the last decade[6] (figure 1.2).

In the UK, 90% of the DCD organs are obtained from Maastricht III donors. These donors have suffered an irreversible, catastrophic brain injury without brain stem herniation and the continuation of medical treatment is considered futile. Following consent for donation these patients undergo a controlled withdrawal of support. The period following withdrawal of life support, before circulatory arrest, determines whether donation is possible. The period from withdrawal of support to asystole may have a significant impact on the quality of the organs and subsequent transplantation outcomes. Withdrawal of life support starts with the disconnection of ventilator support and the donor enters the agonal phase characterised by haemodynamic instability and poor delivery of oxygen to the peripheral organs until asystole. The period of warm ischaemia (WI) starting from the withdrawal of life support extends until *in-situ* cold perfusion has started and has been subdivided into the agonal period, functional warm ischemic period (SBP<50mmHg) and asystolic warm ischemic period[24], as shown in figure 1.6.

Table 1.1 **Maastricht classification of DCDs**

Category	Description	Type of DCD
I	Dead on arrival	Uncontrolled
II	Unsuccessful resuscitation	Uncontrolled
III	Anticipated cardiac arrest, awaiting cardiac arrest following withdrawal of life support	Controlled
IV	Cardiac arrest in a brain-dead donor	Controlled
V	Unexpected arrest in ICU patient	Uncontrolled

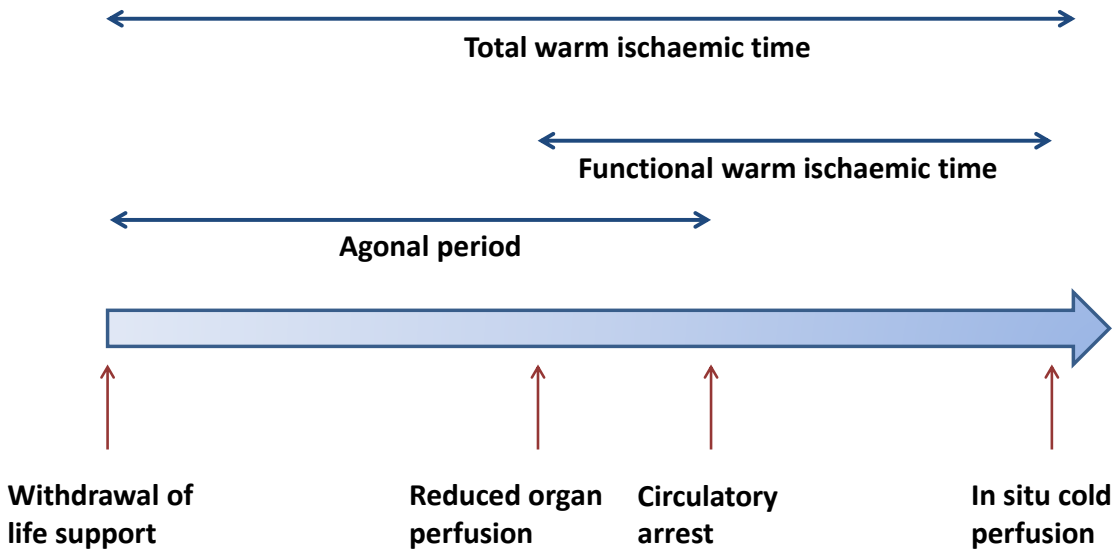

Figure 1.6 Sub-divisions of warm ischaemictime in DCDs[24]
The agonal period is defined as the time from withdrawal of support to asystole. Asystolic WI extends from the time of circulatory arrest following withdrawal of life support to in-situ perfusion. The functional warm ischaemic period starts from the moment that the systolic blood pressure falls below 50mmHg until in-situ perfusion of organs[24,25].

The longer the period of functional WI, the greater is the chance that the donor organs will not be utilised for transplantation due to the uncertainty of their quality and post-transplant function.

The extent of the biological impact of the duration of WI on the kidney is unclear and information is primarily derived from animal models. WI due to oxygen deprivation and nutrient depletion has an adverse impact on the cellular level and subsequent organ function[26]. Energy depletion dysregulates the cellular membrane permeability and causes cell swelling. Similarly, cellular oxygen depletion dysregulates the mitochondria respiratory chain and results in the generation of free radicals[27,28].

Following kidney procurement, after a period of WI a prolongation of anoxic conditions under static hypothermic preservation during transit for transplantation can have an irreversible impact on the allograft quality. Ceased circulation and the lack of O_2 delivery to the abdominal organs causes metabolic dysfunction, cytoskeletal dysregulation, endothelium activation, initiation of transcriptional activity that leads to autophagy, activation of apoptosis and necrosis regulated cell death mechanisms and activation of innate and adaptive immunity[29,30].

Restoration of the blood flow during reperfusion initiates a second insult to the already susceptible kidney and closes the cycle that is known as ischaemia reperfusion injury (IRI)[31]. IRI affects the kidneys that have been subjected to a period of hypoxia resulting from haemodynamic instability in DBDs or a warm ischemic period in DCDs. While in ischaemia the lack of O_2 becomes destructive for cellular function and tissue integrity, the restoration of O_2 during reperfusion

may become deleterious to the cell from involvement of ROS reacting with excess oxygen during reperfusion[31–36]. The clinical manifestation of IRI is delayed graft function (DGF) in DBDs and DCDs and has a significant impact on the onset of acute kidney injury (AKI) and long term kidney function in the kidney recipient. This will be discussed further in chapter 5.

Another period of WI rarely considered and not well studied is the period after the donor kidney is removed from cold storage to the commencement of reperfusion that includes the surgical anastomotic time. A recent study by Tennankore *et al.,* which included almost 138,000 kidney recipients from all donor cohorts, convincingly demonstrated that incremental 10 minute increases in WI from 20 minutes to 60 minutes was associated with an increased hazard ratio of graft loss. WI ≥60 minutes increased the relative hazard of graft loss by 23% even after adjustment for donor and recipient characteristics and cold ischaemic time[37] (CIT).

Extended criteria donors

The medical need for more transplants for life-saving treatments has forced transplant surgeons to utilise organs from donors who do not conform to the standard donor criteria.

ECDs are either older DBDs (age>60yrs) or aged 50-59 with comorbidities such as hypertension, terminal SCr >1.5mh/dl and death from cerebrovascular causes. ECDs are also known as marginal or high risk donors as the transplantation outcomes of kidneys obtained from these donors is expected to be less favourable in comparison with SCDs or associated with an increased possibility of graft failure.

Aging impacts on kidney function[38]. The normal ageing process is associated with morphological and structural changes in tissues and organs that will gradually result in functional decline. Aging kidneys undergo structural changes such as atherosclerosis, glomerulosclerosis and intestinal fibrosis. In combination with a gradual loss of glomeruli and renal mass this leads to a reduced capacity to filter urea and a decreased glomerular filtrate rate (GFR)[38,39]. With age, healthy kidneys without any underlined diseases undergo an average decline in GFR between 6-7 ml/min for each decade of life[40].

Utilisation of kidneys obtained from older deceased donors carries the inherent risk of not only already limited function related to donor age but also reduced regeneration capacity from ischemic injury from the donation and transplantation process.

The age of the deceased donor has been identified as an independent predictor of graft function and graft survival following transplantation. Summers *et al.,* have shown that first time recipients of older (>=60yr) DCD kidneys have increased risk of graft failure[41]. Similarly, Ojo *et al.,* identified donor age as an independent predictor of five-year recipient survival with recipient mortality increasing by 5% for each extra decade of donor age[42].

Although transplantation outcomes of older donor kidneys are less favourable than those of kidneys obtained from younger donors, utilisation of ECD kidneys offers the benefit of improving and prolonging the recipients survival when compared to the risk of remaining on dialysis[43,44]. The older the recipient is the more beneficial will be the receipt of an older kidney compared to dialysis.

In the UK, ECD kidneys are a significant source of allografts. In the period 2014-15, 58% of donors were older than 50 and 33% older than 60 years[5]. Considering the importance of this source of organs, studies have focused on improving the utilisation and outcomes from these donors.

Living donors

Living donors (LD) kidneys are obtained from healthy individuals and offered to either a genetically related family member (related) or to a spouse (unrelated) or offered as altruistic donations. LDs have not experienced the detrimental physiological trauma associated with brain or cardiovascular death and the offered kidneys have a shorter cold ischaemic time compared to kidneys obtained from deceased donors.

1.4 Outcomes in renal transplantation

Recipients of LD kidneys have superior graft and patient survival rates at one and five years post-transplantation compared to kidneys obtained from deceased donors. Terasaki *et al.,* in a seminal paper in 1995, were the first to show that donor kidneys obtained from LDs have higher survival rates than deceased donor kidneys even when there is higher degree of HLA mismatching between LDs and recipients[45].

In kidney transplantation after deceased donation, donor type, age and CIT are important factors and their impact is well established on short and long transplantation outcomes in the recipient[46–49]. Aubert *et al.,* in a prospective population study of 6,891 transplant recipients, compared the transplantation outcomes of kidneys offered by ECDs and SCDs. Univariate and multivariate analyses identified the donor, recipient and graft factors that were independent

predictors of graft loss. The study showed that allograft survival was lower for kidneys obtained from ECDs compared to SDCs (80% vs 88%, P<0.001) but there were additional factors that significantly and independently determined long term outcomes. These were donor-specific circulating antibodies, CIT (longer than 24hr) and the number of HLA mismatches. For recipients of ECD kidneys, the presence of donor-specific antibodies and extended CIT increased the risk of graft loss considerable in a seven year follow-up[50]. Similarly, Summers *et al.,* reported, in a similar size study using NHSBT data, that the risk of graft loss increased with donor age (for donors older than 60years) and extended CIT>24hr impacted adversely on grafts obtained from DCDs[51].

Primary non-function

Primary non-function (PNF) is defined as the absence of kidney function following transplantation. El-Zoghby *et al.,* in a single centre study of 1,317 kidney recipients, reported that 3% of transplants never functioned post-transplant for reasons which included venous or arterial thrombosis and factors related to donor kidney quality[52]. Donor kidney quality was highlighted as one of the main reasons that kidney allografts developed PNF based on the observation that both allografts from the same donor developed PNF[52]. Dahmane *et al.,*[53] reported the incidence of PNF as higher for kidneys obtained from ECDs, 7.7% compared to 1.8% in SCDs kidneys. The rate of PNF for kidneys obtained from DBDs in the UK is approximately 3% while for DCD kidneys it is between 3-5 %[48,51].

Delayed graft function

Delayed kidney function (DGF) is a common complication in kidney recipients with an incidence that ranges from 24-50% following transplantation of deceased

donor kidneys[54,55] but is a rare event following transplantation of LD kidneys with a frequency of 2-4%[56].

Although there are many definitions of DGF, the most common and widely reported as an endpoint in clinical studies is the need of dialysis in the first 7 days post transplantation once urinary tract obstruction or hyperkalemia have been excluded as the cause of kidney dysfunction. The onset of DGF is associated with extended hospitalisation and correlates in DBDs with reduced graft and recipient survival[57–59]. The association of DGF with long term allograft and recipient survival was not always obvious and has been debated in many studies [55,57,60,61]. Troppman *et al.,* showed that DGF and acute rejection increased the incidence of graft failure compared to DGF alone[62–64]. Other studies demonstrated a significant association with DGF to increased risk of acute rejection and graft loss in deceased kidney recipients[55,65]. The damaging impact of DGF on the long term function and survival of the kidney has been widely reported. A recent study by Wu *et al.,* demonstrated that recipients who had experienced DGF had a significant increased risk of biopsy proven acute rejection at one-, three- and five-years post-transplantation compared to an immediate function cohort[56,58].

The importance of donor factors on the development of DGF was recently confirmed by the study of Louvar *et al.,* who reported that, when kidney pairs from a common donor were transplanted, a recipient was at least twice as likely to develop DGF if the recipient of the contralateral kidney had developed DGF[59].

The donor type has been independently associated with the incidence of DGF[41,59]. With increased utilisation of DCD and ECD kidneys, the incidence of DGF has

increased. In 2010, a study of the transplant outcomes of 7,680 kidney transplants reported that the incidence of DGF was 49% for kidneys obtained from DCDs versus 24% for DBD kidneys[41]. However, the recipients who received DBD kidneys and developed DGF had significantly reduced kidney function a year after transplantation and reduced graft survival five years post-transplantation compared to recipients who did not develop DGF[66]. Conversely, recipients of DCD kidneys who developed DGF had no long term adverse outcomes. Nagaraja *et al.,* drew similar conclusions[67]. As discussed earlier in this chapter, brain stem death can lead to systemic abdominal organ inflammation in the donor that renders donor kidneys susceptible to IRI and subsequent onset of DGF. Following transplantation, the acute kidney dysfunction that underlies DGF can progress to long term suboptimal function in some recipients. The risk of onset of DGF increases with the age of kidney donor above 60 years of age[46,53]. Of note, the uncertainty about transplantation outcomes of older donor kidneys leads transplant surgeons to transplant older kidneys to older recipients. This could potentially introduce a bias in observations on the incidence of DGF and the associations of long term graft survival.

Chronic allograft dysfunction

Following transplantation of a deceased donor kidney, immunological factors may play a role in the immediate and longer term transplantation outcomes. The humoral or cell mediated immune response of the recipients to the allograft can lead to acute rejection of the graft. The extent of rejection spans from the rare, hyperacute allograft rejection with a total graft loss in less than 24 hours to chronic allograft rejection that manifests as a progressive microvascular and arterial injury leading to declined function and eventual graft loss[68]. Considerable advances in HLA cross matching in the last two decades has resulted in significant improvements in allograft and recipient survival. Despite the development of new immunosuppressant drugs to prevent acute rejection, many kidneys suffer a progressive decline of kidney function and the development of chronic kidney dysfunction leads to the loss of 50% of kidney transplants within 10 years, a clinical outcome that has been unchanged since 1989[69,70].

Following transplantation, acute and chronic rejection events, nephrotoxicity from immunosuppression medication, on-going co-morbidities such as diabetes and hypertension can lead to the recurrence of the original end stage kidney disease and graft loss. Reduced graft tolerance with associated chronic rejection and the development of chronic kidney dysfunction are associated with reduced graft survival in the long term post-transplantation[71–75].

Chronic allograft dysfunction may also result from non-compliance of allograft recipients with immunosuppression. Studies looking into non-compliance with medication in adults and younger recipients have concluded that the risk of graft

loss is 7-fold higher for the non-compliant recipients and affects almost 25% of all kidney recipients[76–78].

We have limited tools to monitor the development of chronic allograft dysfunction. Current assessment tools include post-transplantation kidney biopsy evaluation, glomerular filtration rate and serum creatinine (SCr) measurements. SCr is a surrogate marker of kidney function and is used as a clinical end point to predict long term graft survival and the development of chronic kidney disease. However, monitoring SCr levels can underestimate the early onset of allograft dysfunction[79].

Early identification of the allografts with declining function increases the options for medical interventions. Kidney function at 12 months post-transplantation is a strong indicator of long term outcome[80]. A large, retrospective cohort study following 13,670 kidney recipients for 10 years found a correlation between CKD stages at 12 months post transplantation and long term graft failure. Kidney recipients who had developed CKD stages 4 (defined as having an estimated GFR (eGFR) between 15-29ml/min/1.73m2) and CKD stage 5 (eGFR <15 ml/min/1.73m2) were more likely to suffer graft failure or death with or without an associated functioning kidney[81]. The same study identified associations in the rate of decline in eGFR levels between 3 and 12 month post transplantation and graft failure[81].

It is not yet clear if a decline in eGFR is an accurate predictor of the progression of kidney injury and a decline of allograft function and further studies are needed. The use of eGFR as a surrogate marker of allograft kidney function in recipients has some limitations. The equations for GFR calculation were

developed to predict kidney function decline in patients of renal disease rather transplant recipients. Transplanted patients on immunosuppression regimes face additional clinical challenges from nephrotoxicity related to medicines such as calceneurin inhibitors. In addition, eGFR has low sensitivity and specificity in predicting kidney dysfunction as changes to eGFR may not be observed until irreversible damage in kidney function has already occurred.

1.5 Current assessment tools of donor kidney quality

The quality of the donor kidney plays a major role in both the immediate function of the allograft and in the longer term outcome. The ability to accurately assess kidney quality and predict post-transplant function would be of considerable benefit to potential recipients.

Currently, transplant clinicians have limited tools to assess kidney quality. Macroscopic assessment of the donor kidneys is carried out by the retrieval team in association with donor demographic and clinical factors. This preliminary screen may rule out obviously unsuitable kidneys but is insufficient to fully determine the kidney quality and predict allograft function. Procurement biopsies can be used to diagnose pre-existing kidney diseases in the donor. On the assumption that older donors are more likely to have undiagnosed chronic kidney disease, assessment by pre implantation biopsy is most common for ECDs. In the USA, 75% of ECD kidneys are biopsied[82] for assessment, a practise that has been linked with high discard rates.

Currently, there are no validated diagnostic tools to evaluate the quality of the graft at retrieval, the degree of injury that the kidney has undergo in the donor

and whether the allograft has the potential to function and recover following transplantation.

Clinicians have to make the decision to accept a donor organ with the knowledge that, in the case of PNF or suboptimal function, there may be serious consequences for the recipient including a return to dialysis and the transplant waiting list with the additional challenge of HLA sensitisation. The type and age of the donor and the function of the kidneys during donor management are some of the factors considered in the decision to accept or decline donor kidneys. Kidney function during donor management can be crudely assessed by using SCr as a surrogate marker or by direct assessment of kidney biopsies using Remuzzi scoring to evaluate the risk of chronic kidney disease or kidney donor profile index (KDPI) to evaluate suitability of the donor.

Remuzzi scoring of kidney biopsies

Remuzzi scoring is an histological assessment of pre-implantation biopsies, grading morphological changes in kidney tissue to cumulatively provide a score. From this score, DBD kidneys are assessed for a baseline chronic kidney disease that could impact long term outcomes. Kidney tissue is assessed for glomerular sclerosis, tubular atrophy, atherosclerosis and interstitial fibrosis and given a score between 0 for no changes and 3 for significant changes in any of these areas. Following evaluation for each tissue component, 0 points would indicate a pristine kidney and a maximum of 12 points would represent significant tissue injury in all four areas. Kidneys with a score between 0-3 are transplanted as single transplants, 4-6 as dual transplants and kidneys scoring 7 and higher are usually discarded[83,84].

The application of Remuzzi scoring to older DBD kidneys has reportedly resulted in a 24% increase in the utilisation of ECD kidneys[83]. Although Remuzzi scoring is widely used in the clinical practise it has significant weaknesses including interpersonal variability in histological interpretation among pathologists, the lack of validation of the scoring on an independent cohort of clinical biopsies and the undesirable extension of CIT for the most susceptible kidneys that go through histological assessment. Additional limitations of histological assessment are:

1) The assumption that these main histological parameters have an equal contribution to the overall injury and function of the kidney in the long term.

2) Variability in biopsy sampling

3) Variability in the quality of the biopsy and the number of glomeruli for assessment

Kidney donor profile index (KDPI)

In the USA, the United National Organ Sharing committee has adopted the determination of KDPI as an assessment tool for their organ allocation system. The KDPI provides a probability of graft failure after transplantation, taking into account donor factors such as age, ethnicity, donor type, height, weight, history of hypertension and diabetes, HCV status, cause of death and terminal SCr level. KDPI scoring is heavily weighted on donor age and the KDPI risk increases by 1% for every additional year for donors older than 50yrs[11]. A KDPI of 80% indicates that the risk of graft failure is higher than for 80% of the donor kidneys for any given population. The utility of KDPI has been challenged because it carries an inherent bias against older but healthy donors whose kidneys have the potential to function well[10]. Also, exclusion of recipient factors or association

donor/recipient matching has led to criticism of the accuracy and usefulness of the KDPI. In the USA, where KDPI is widely used for assessing donor kidneys, the discard rate for ECD kidneys is far higher when compared to the UK or the Eurotransplant zone[85].

1.6 Biomarkers in transplant medicine

The search for biomarkers in transplantation medicine has mainly focused on post-transplant allograft function in the recipient. This stems from the need to monitor and diagnose acute rejection or DGF as soon as possible following implantation and to predict the long term transplantation outcomes with the aim of a more personalised approach to immunosuppression and treatment. However, the relative ease in obtaining clinical samples such as blood and urine from recipients compared to donors may have contributed to the extent of research that has focused on the post-transplantation phase.

It has become apparent that donor kidney quality has a significant and long-lasting impact on transplantation outcomes. This understanding has been achieved through studies on preclinical DBD and DCD models[22,86–88] or registry data analysis of donor demographic and clinical factors and their association to post-transplantation kidney function[41,48]

However, monitoring donor organ quality using surrogate markers of kidney function such as SCr and proteinuria levels during donor management or by histological assessment of procurement biopsy samples has limitations mainly as these methods have low diagnostic sensitivity for injury progression or recovery from injury and lack specificity.

The unique aspect of research into the discovery of biomarkers of kidney quality in donors is that they must be predictive and prognostic of kidney function in a different biological entity, the recipient. This adds an additional level of complexity.

Biomarkers for assessing donor organ quality prior to transplantation have great advantages for the clinicians in that they could:

1) Provide information on whether donor organs are viable for transplantation or should be declined

2) Allow for improved allocation of organs to better match donor and recipient.

3) Provide a measure of the degree of kidney injury either chronic or acute and give an opportunity to manage recipients' early perioperative stages in order to reduce further nephrotoxicity.

4) Provide monitoring tools for novel interventions either during donor management or preservation to achieve kidney resuscitation and repair.

In recent years there has been a considerable effort to identify biomarkers of kidney injury either in the donor or early post-transplantation period predictive of DGF or long term allograft function. To this end, known markers of acute kidney injury (AKI) have been re-evaluated for their utility in the diagnosis of kidney injury during donor management or in early post-transplantation period.

Neutrophil gelatinase-associated lipocalin (NGAL) is a 25kDa iron transporter, protein that is involved in the biological processes of apoptosis, immunity and renal physiology. In injured kidneys NGAL is released from proximal tubular

cells and has been identified as a promising biomarkers of AKI predictive of mortality in critically ill patients[89].

Within the context of organ donation and transplantation, the utility of NGAL has been controversial with some studies identifying it as a promising biomarker for donor kidney quality or allograft dysfunction (DGF or long term) while other studies failing to confirm these findings[90–95].

Hollmen *et al*., have reported that an increased concentration of urine NGAL in deceased donors correlated to biopsy proven kidney damage prior to transplantation but failed to predict the onset of DGF in kidney allografts[96]. In a subsequent study, the same group reported that serum levels of NGAL on the first day post-transplant were correlated strongly with the onset and the duration of DGF[97]. The predictive value of recipient urine NGAL for allograft outcomes 1 year post-transplantation has been reported by Hall *et al*.[98]. Interestingly, Buemi *et al*., reported no correlation between donor plasma and urine levels of NGAL with the onset of DGF. However, when the same group measured the NGAL levels 24 and 48 hours post-transplantation they found that recipient plasma NGAL levels were predictive of DGF occurrence although there was no correlation with urine NGAL values[99].

The shift of cold storage preservation to machine perfusion as a means to improve the quality of ECD grafts has focusedresearch efforts towards exploring the perfusate to identify markers released during the preservation of injured grafts. The European Machine Perfusion Trial was the first machine preservation multicentre trial to demonstrate an improvement in the quality of marginal kidneys. The trial showed reduced DGF rates in perfused kidneys compared to

cold storage and improved 1 year allograft function[100]. Additionally, it was possible to exploit the perfusion parameters and perfusate samples to assess the quality of the perfused kidneys[100,101]. Analysis of the perfusate of 360 kidneys by Moers *et al*., revealed that increased concentrations of N-acetyl-β-glucosaminidase (NAG), heart-type fatty acid binding protein (H-FABP) and glutathione-S-transferase (GST) were associated with a high DGF incidence[101]. A multicentre, prospective study analysed perfusate samples obtained from 775 perfused kidneys was performed by Parikh *et al.,* who showed that increased concentration of NGAL, L-FABP and KIM-1 in combination with high renal resistance was associated with high incidence of DGF and low eGFR at 6 months[102].

Kidney injury molecule–1 (KIM-1) is a type 1 glycoprotein that is upregulated in the epithelium of proximal tubules after kidney injury. The detection of KIM-1 in urine under conditions of kidney injury results from the upregulation of metalloproteinases that subsequently cleave the extracellular domain of KIM-1 releasing it into the urine[103]. The correlation of KIM-1 with acute kidney injury progression has been shown in critically ill patients[104]. Urine levels of KIM-1 in 201 hospitalised patients were predictive of the progression to dialysis and patient death. In the context of kidney transplantation, KIM-1 has been shown to be an independent predictor of graft loss in kidney recipients[105–107]. A study by Nijboer *et al.,* focused on donor tissue and urine analysis and reported that following brain death the expression of KIM-1 was upregulated and urine levels of the protein were increased within 4 hours of brain death in a rodent model prior to any changes observed in SCr levels. Analysis of LD and DBD biopsies and urine samples demonstrated that increased gene expression and urine levels of

KIM-1 were predictive of allograft function 1 year post-transplantation suggesting that it is a useful marker of donor kidney function[108]. These findings were confirmed, at least in part, by Schroppel *et al.,* who showed an increased level of KIM-1 in pre-transplant deceased donor biopsies although the study reported that KIM-1 was not predictive of DGF in allografts[109].

Liver (L) or heart (H) fatty acid binding proteins (FABPs) have been assessed as potential biomarkers of kidney function in donation and transplantation. L-FABP is a carrier protein that binds to intracellularly metabolised lipids that are then re-absorbed into proximal tubules. Upon cellular stress and renal ischaemic injury, high levels of FABP are released into the urine leading to evaluation of L-FABP as a marker of kidney dysfunction[110–112]. Studies have examined the utility of both L- and H-FABP as predictors of the onset of AKI. Jochmans *et al.,* have reported in preclinical studies of perfused porcine kidneys that pre-transplant levels of NGAL, H-FABP were detected in the perfusate with NGAL levels to be associated to kidney ischemia. In a similar study of porcine autotransplant model plasma H-FABP and NGAL early post transplantation were associated with initial graft injury[113–115].

Upregulation of Interleukin-18 (IL-18) mRNA levels in kidney biopsies and increased IL-18 protein levels in urine and plasma have been associated with acute rejection, DGF and 1 year suboptimal allograft function post-transplantation[116–119]. IL-18 is a potent pro-inflammatory regulator of innate immunity promoting maturation of T cells and N-killer cells and stimulates infiltration of macrophages, dendritic cells and B-cells to the site of tissue injury. IL-18 is upregulated in kidney proximal tubules in ischaemia reperfusion models

and biopsy proven kidney dysfunction with a parallel increase of SCr[120,121]. Studies have reported that urine IL-18 levels can predict the onset of AKI in patients who have undergone cardiac surgery and, within the context of transplantation, that alterations of IL-18 levels are predictive of DGF when measured at day 0 post-transplant[117–119].

Additional markers of kidney injury that have shown promising results as predictors of allograft function include clusterin (CLU), osteopondin (OPN) and chitinase (YKL-40).

Clusterin is a glycoprotein with a diverse biological function. CLU isoforms can be either apoptotic or cytoprotective. CLU is expressed from epithelial cells upon injury. Pianta *et al.,* have reported that increased urinary levels of CLU and IL-18 can occur as early as 4 hours post-transplantation and indicate the onset of DGF[122].

OPN has been shown to have a role in promoting inflammation and apoptosis under oxidative stress and plays a role in the development of interstitial fibrosis[123]. Studies in rodent models have shown that increased expression of OPN is associated with interstitial deposition of collagen I and IV, infiltration of macrophages and onset of fibrosis[124]. OPN urine and plasma levels in transplant recipients were associated with acute kidney rejection[125]. Conversely, OPN has also demonstrated cytoprotective properties by reducing peroxide levels under hypoxic conditions[126].

YKL-40 is the product of *chitinase-3-like protein-1* (*CHI3L1*) gene. It is a glycoprotein secreted by a range of cells including inflammatory cells such as macrophages and neutrophils. Increased levels of YKL-40 have been correlated

with anti-apoptotic activity and reparative processes. YKL-40 has been studied as a marker of donor kidney quality and a predictor of allograft recovery in recipients[127–129]. In a recent study by Puthumana *et al.*, the protein level of YKL-40 was assessed in 1301 donors and 2435 ascertained recipients. Higher levels of urinary YKL-40 were detected in donors with AKI and acute tubular necrosis and associated with low incidence of DGF. YKL-40 was measured in the ascertained recipients of these donors. The recipients who developed DGF and had high levels of the protein were correlated with better 6 month function post-transplantation[130].

In contrast with the markers of AKI discussed above, an overview of the literature has revealed limited references to cystatin-c in peri transplantation biomarker research. Cystatin-c has an established role in the diagnosis of AKI as it is associated with injured or dysfunctional proximal tubules, reduced reabsorption and consequent increased levels in urine concentration in patients with AKI. Many studies have shown that cystatin-c complements, or is superior to, SCr in the assessment of kidney function[131]. However, its utility has not been fully explored as a marker of kidney injury pre-transplantation[33].

The 'iron test' for some of the biomarkers discussed above was the prospective multicentre validation study by Reese *et al.* In a study of 1304 donors and 2441 kidney recipients the urine concentration of NGAL, KIM-1, L-FABP and IL-18 were found to be highly associated with donor AKI but had only a weak correlation with DGF and no predictive value for 6 month eGFR post-transplantation. The study also highlighted that the mechanisms and progression of AKI injury might be different in DBDs and DCDs with a different disease progression and long term

outcomes. Finally, the authors stated that a more detailed donor profiling will be more informative on donor kidney quality and will open new avenues for interventions during donor management or preservation. Understanding the mechanisms of injury and repair and developing tools to monitor closely these processes may identify novel biomarkers and targets for intervention[95].

1.7 The role of proteomics in biomarker discovery

Rapid advances in the fields of molecular biology and human genetics with access to the human genome have coincided with advances in mass spectrometry techniques and bioinformatics to create powerful techniques to pursue biomarker research.

Omics technologies, which derive from combined mass spectrometric analysis and bioinformatics to compare spectral data against the human proteome have already improved our understanding of disease mechanisms and have facilitated research towards biomarker discovery. Proteomic studies have expanded our knowledge in many areas such as the study of post-translational modifications of proteins and their relationship to disease states, the secretome of organs or tissues and the degradome of proteins and their association with diseases. In addition, as we are able to analyse more clinical samples and identify more proteins than ever before, the idea of a single protein as a marker has been replaced with the concept of the predictive proteomic profile. In recent developments, the tendency has been not only to explore the entire proteome of tissues of interest but to look closely at smaller subsets such as the peptidome, defined as endogenous small polypeptides, the degradome, defined as protein fragments generated *in vivo* as a result of proteolysis and the secretome, defined

as the proteins secreted from cells or tissues. Analysis of the peptidome has been used to test the hypothesis that the disease process and resultant tissue damage releases endogenous proteases to attack cellular proteins and generate peptides. These peptides could be utilised as clinical biomarkers and contribute to a better understanding of the extent and progression of kidney disease[132,133].

Peptidomic approaches have proven very insightful such as the study by Sigdel *et al.* In this study, a peptidomic profile of urine, identified by mass spectrometry in kidney recipients was associated with acute and chronic rejection after transplantation. In this elegant study almost 250 urine samples were analysed in a case control study design and validated with targeted proteomic analysis. A panel of 35 peptides could cluster the kidney recipients according to risk of acute rejection, developing chronic allograft nephropathy or BK virus nephritis[132].

Another study using a transcriptome profile was by Mas *et al.,*. Authors analysed kidney biopsies obtained at the end of the cold ischaemic period prior to implantation and identified a significant upregulation of immune related genes in the DGF associated kidneys but overall the identified signature had a low predictive utility[134].

In the context of organ transplantation, biomarkers of donor organ quality would preferably be non-invasive, easily detectable in blood or urine with high specificity for the allograft of interest and sensitive enough to be detected early in the donor management process thereby allowing clinicians to intervene and improve the allograft during donor management or organ preservation stages. Moreover, they would need to be easily applicable to suit the clinical challenges of organ donation.

The first step of an -omics based discovery phase usually involves an unbiased analysis of a large number of samples and extensive bioinformatics analysis to shortlist and quantify a panel of proteins. These proteins are subsequently verified by targeted approaches and validated in an independent cohort of samples to assess their sensitivity and specificity. When all these hurdles and challenges have been successfully accomplished it should be possible to consider the practical implementation into clinical practise.

There are many reasons why biomarker studies fail to reach the validation stage. These include a lack of well curated clinical samples in sufficiently large numbers for discovery and validation studies, pre analytical variability in sample quality that introduces bias in all the stages of analysis and insufficient validation in a large cohort of independent samples. In the following chapters these factors will be explored further.

CHAPTER 2

Rationale of DPhil thesis

In **Chapter 1** the clinical challenges of organ donation and transplantation are introduced, resulting from the shortage of donor organs, the changes in donor demographics and the increasing use of extended criteria donors to meet transplant demand. Organs from extended criteria donors present a challenge to clinicians because of the uncertainty of transplantation outcomes associated with donor characteristics such as age or comorbidities that can make organs unsuitable for transplantation. Currently, there is a lack of objective criteria to evaluate donor kidneys, and this can lead to a high donor kidney discard rate. For kidneys, the quality assessment criteria include changes in donor serum creatinine values during donor management, proteinuria and histological assessment of donor kidney biopsies. These criteria have limited value in supporting the decision to decline or accept kidneys as transplants. Objective, evidence based criteria which directly correlate with organ quality are urgently needed. Biomarkers, if selected carefully, are ideal candidates for organ assessment since they are generally amenable to sensitive, rapid diagnostic assays which can be performed in hospital laboratories. However, as I discuss, research on novel biomarkers of donor organ quality has been limited, and in this thesis I seek to address this by using a comprehensive proteomic approach on tissues, urine and blood from kidney donors.

In my thesis, I have used unbiased, label-free quantitative mass spectrometry methodologies in an initial, discovery phase to identify candidate proteins as biomarkers. The principles of label-free mass spectrometry, methods and the analyses used are described in **Chapter 3**. Clinical samples for my analysis were obtained initially from the Prometheus biobank, Groningen, Netherlands and subsequently from the UK QUOD biobank. An overview of the QUOD project and

QUOD biobank, a unique source of well curated samples in addition to clinical and demographic data from donors and recipients, is provided in the same chapter.

The protocols for QUOD sample collection from deceased subjects during donor management were carefully designed to control the potential variability in blood sample collection and processing. Robust and detailed standard operating protocols have been established to safeguard sample integrity for future research, but some variability was inevitable as the samples needed to be taken during anti-social hours, leading to occasional extended periods of storage of blood samples for up to 48 h at ambient temperature before processing. To ensure this did not introduce a potential bias in the experimental analysis of these samples, I investigated the impact of pre- analytical variability of extended storage of whole blood at ambient temperature on the plasma proteome and degradome. The results of these analyses are described in **Chapter 4**.

One of the essential questions I set out to address in my thesis was whether it was feasible to use clinical proteomics to identify and discriminate between donors on the basis of transplantation outcomes. As the QUOD biobank was only established during the first year of my DPhil, there was an insufficient number of clinical samples for the first two years of my studies to investigate this question. Therefore, as described in **chapter 5**, I was able to use serum and urine samples from the Prometheus biobank as part of a collaborative study between our group in Oxford and the University Medical Centre Groningen, The Netherlands. Serum and urine samples from DBDs and DCDs were matched for clinical outcomes, for the incidence of immediate and delayed kidney function post transplantation and

subsequently compared by label-free quantitative mass spectrometry. Living donor samples were analysed simultaneously as a control.

From pre-clinical models it has been shown that brain death adversely impacts abdominal organs[22108,135,136]. However, it remains unknown whether prior to retrieval the donor kidneys can be classified according to their quality and post transplantation function. Confirmation that donor kidneys with suboptimal allograft function are biologically distinct from the good quality donor kidneys will further substantiate our research efforts towards the discovery of predictive biomarkers of donor kidney quality.

To address this key question, I used QUOD kidney samples obtained from deceased donors during donor management. In **chapter 6,** I describe the analysis of QUOD kidney samples from DBDs, aiming to demonstrate whether is possible to discriminate between donor kidneys with good or suboptimal outcomes 12 month post transplantation by comparing the proteomic profile of donor kidney biopsies. The link between 12 month kidney function and long-term graft survival is well established. Therefore, predicting 12 month outcomes prior to transplantation has high clinical relevance. Furthermore, this unbiased approach aimed to generate hypothesis driven research work on the potential biological pathways that are activated to impact donor quality and post transplantation outcomes.

In **Chapter 7**, I have summarised the main findings of my thesis, what I consider clinical relevance of my experimental work and the layout of future studies that may emerge from the work presented here.

In summary, my DPhil thesis has the following research aims:

Aims:

- To assess the pre-analytical variability associated with the processing of whole blood as collected for the QUOD biobank and to identify a baseline proteomic and peptidomic profile to filter candidate protein markers relevant for clinical correlates.
- To determine the feasibility of clinical proteomics to identify novel proteomic signatures in donor blood and urine that may correlate to delayed graft function after kidney transplantation;
- To determine a donor kidney proteomic profile that correlates with one year allograft function and assess which biological pathways may play a role in long-term transplantation outcomes

CHAPTER 3

Methods

3.1 Introduction

The experimental work in this thesis has predominantly used mass spectrometry based methodologies to profile blood, urine and biopsy tissue from kidney donors. Some proteins of particular interest have been further investigated by western blotting to confirm their differential expression in. This chapter describes the methods common to the experimental work described in the subsequent chapters 4-6.

Clinical samples

Blood samples were obtained from healthy volunteers and blood, urine and tissue biopsies from deceased and living donors collected from the Prometheus biobank, University Medical Centre, Groningen, the Netherlands, or the UK QUOD biobank.

3.2 QUality in Organ Donation (QUOD)

The QUOD biobank was established within the strategic research framework of NHSBT for improving donor organ quality, donor organ utilisation and transplantation outcomes for organ recipients[15,137]. A nationwide collection of clinical samples from deceased donors is coordinated by the University of Oxford.

The QUOD initiative is based on a collaboration between scientists and clinicians within transplant centres, academic institutions and NHSBT. Longitudinal blood and urine samples taken throughout the deceased donor management process and abdominal organ tissues taken at organ retrieval are collected and processed then transported and subsequently stored in a central biobank within the University of Oxford. Co-ordination between the QUOD project and the NHSBT Organ Donation and Transplantation (ODT) division enable demographic and clinical data on donors and recipients as well as long-term follow-up data on

transplanted organs to be linked to QUOD samples in an anonymised manner. The collaborative network includes all Specialist Nurses in Organ Donation (SNODs) and health care professionals involved in the National Organ Retrieval Service (NORS) to obtain consent for donor recruitment and provide sample and data collection. Oversight of the QUOD project is provided by the QUOD Steering Committee and the QUOD National Management Team.

To enable collection of clinical samples and donor data from deceased donors in UK hospitals, the QUOD project received specific approval under the extension of the NHSBT Human Tissue Act Research Licence to include the 41 highest donating hospitals in England, Wales and Northern Ireland. Samples are collected from 66 sites in the UK. As of November 1, 2016, samples have been collected from 1860 deceased donors with a consent rate from all UK donors of 95%.

QUOD clinical samples - An overview

Longitudinal blood and urine samples are collected from deceased donors at defined time points during the donation cascade as described in figure 3.1. The sample collection strategy differs between DBDs and DCDs to accommodate the different management processes for these donors. Whilst blood and urine samples collected from DBDs were designed to capture changes due to brain death, the focus in DCDs was to capture the impact of warm ischemia on the quality of abdominal organs.

Following the identification of potential donors in the intensive care unit (ICU), the SNODs approach the donor family to give their consent for donation and participation to QUOD with the collection of donor samples for research. A QUOD

box is provided containing labelled tubes for collection of samples at appropriate time points throughout the donor management and retrieval process. From the consented donors, SNODs collect the donor blood sample, DB2, and donor urine (DU) sample, DU2 and subsequently, the NORs collect DB3 and DU3 at the beginning of the retrieval operation and DB4 and DU4 samples at the end of retrieval. Retrospectively, the QUOD team requests the initial blood and urine samples, DB1 and DU1, that were collected from the hospitals ICUs where donors had been admitted as patients

Single biopsy samples are collected from kidney, liver and spleen. An overview of the timeline for samples are collected from DBDs and DCDs is shown in figure 3.1. All samples after collection and processing are transferred to regional QUOD centres for temporary storage prior to shipping in batches to the QUOD laboratory facility at the University of Oxford for long-term storage. In some cases, samples are processed at the regional centres rather than local sites. Expansion to collect cardiothoracic biopsy samples has been planned.

Ethical approval for research work

Ethical approval for my research work comes under the umbrella of the approved QUOD ethics application for quality in organ donation with reference number 13/NW/0017.

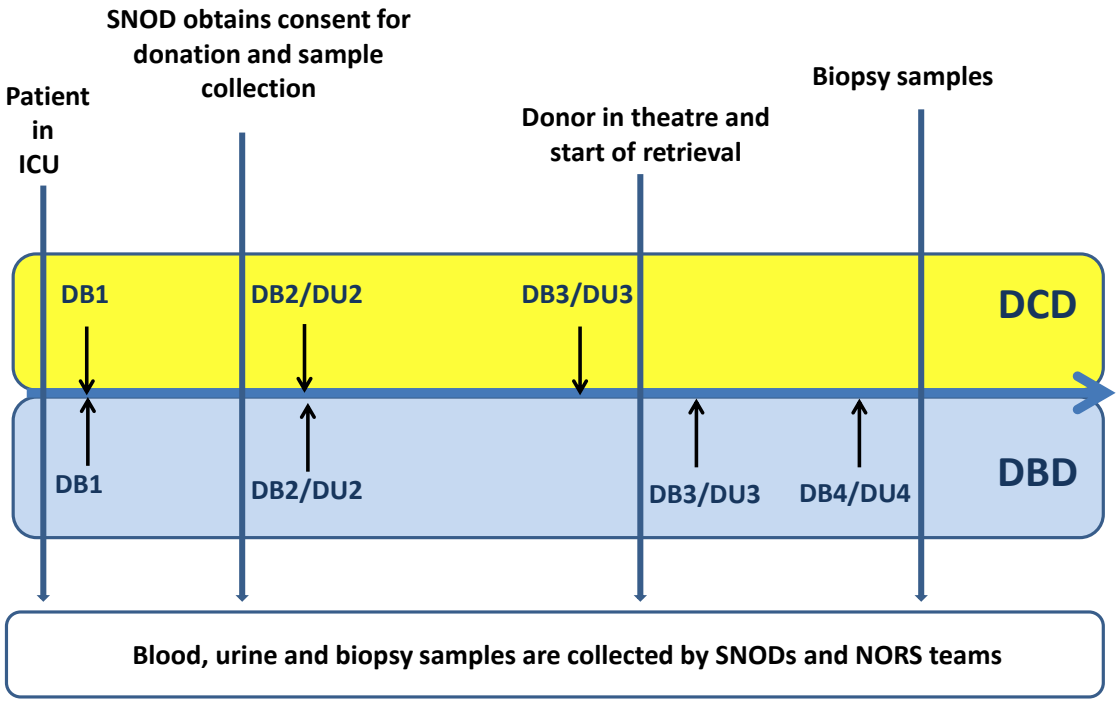

Figure 3.1 Overview of the time points of blood, urine and biopsy sample collection for QUOD

DB: donor blood, DU: donor urine, SNODs: Specialised Nurses in Organ Donation, NORS: National Organ Retrieval Service

3.3 Proteomics and mass spectrometry

The term 'proteome' refers to the whole set of proteins expressed in a biological entity such as blood, urine, tissue or cells. Proteomics is a means to characterise the proteome with methods capable of identifying and quantifying the thousands of proteins within the entity under study.

Mass spectrometry (MS) has emerged as one of the principle proteomic methods to study proteomes. Recent advances in MS technologies and associated developments in bioinformatics have significantly increased both the depth and throughput of proteomic analysis. Whilst the technology has grown rapidly, its application to medical research has at times been significantly hampered by challenges such as clinical sample complexity and biological variability in samples procured for analysis.

Overview of label-free quantitative tandem mass spectrometry (LFQ-MS/MS)

Tandem mass spectrometry (MS/MS) allows automated identification of proteins. Label-free quantitative tandem mass spectrometry (LFQ-MS/MS) allows the sequential relative and absolute quantification of proteins in a set of biological samples. An overview of the workflow of LFQ-MS/MS proteomics is summarised in figure 3.2. Initially, samples were prepared for analysis by concentration of proteins by precipitation[138]. Protein precipitates were resuspended and digested enzymatically to produce peptides. Peptides 7-30 amino acids in length are ideal for LC-MS/MS based peptide and protein identification. Peptide mixtures were separated by liquid chromatography, subjected to desolvation and ionisation by electrospray ionization (ESI) and directly analysed in a tandem mass spectrometer. The acquired MS/MS spectra were then processed by bioinformatics tools to identify and quantify the identified proteins and statistical

tools were employed to shortlist the significantly regulated proteins among the samples.

Data analysis focuses on associations of the identified proteins with relevant meaningful biological pathways and is an indication of the quality of the data. Depending on the complexity of the biological samples, there are challenges that have to be addressed to increase the number of protein identifications. Experimental methods and the challenges associated with the steps are described in further detail below.

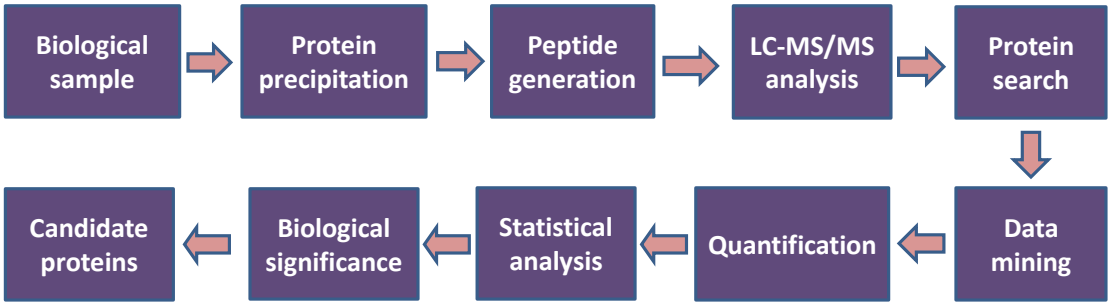

Figure 3.2 Label-Free Quantitative Tandem Mass Spectrometry (LFQ - MS/MS) workflow

The fundamental principle of LFQ-MS/MS proteomics is based on proteolytic digestion of a protein sample into shorter peptides, which are subsequently separated by liquid chromatography (LC) coupled to a tandem mass spectrometer. Samples are analysed by electrospray ionization, and peptide/fragments measured in a tandem mass spectrometer (LC-MS/MS). MS data is subsequently analysed using bioinformatics tools to obtain information about protein composition, relative protein quantification. Such results provide the framework for biological interpretation that lead to shortlisting a list of candidate disease biomarkers.

Overview of liquid chromatography mass spectrometry (LC-MS/MS)

The mass spectrometry pipeline used for the experimental work described in this thesis comprised of LC-MS/MS. Peptide mixtures are separated by reversed phase chromatography on the basis of their charge or hydrophobicity. After separation, peptides are directly injected into the mass spectrometer through a narrow needle held at a high voltage provoking the process of electrospray ionisation in positive mode (ESI+). ESI results in a fine spray of charged droplets that subsequently become smaller until the peptide molecules are completely desolvated and carry a positive charge. In a typical set-up the mass spectrometer (MS) instrument is coupled to the chromatography instrument to allow the separation of the charged peptide ions on the basis of their mass over charge ratio (m/z) in an initial survey scan by the first MS measurement (MS1). With a tandem mass spectrometer, a number of selected ions from the first MS1 scan can be selected for further analysis following dissociation into smaller ions through collision with other molecules (usually an inert gas such as helium or argon), a process known as collision induced dissociation (CID). Fragment ions are then analysed in the second MS (MS2). This step is necessary to break amide between the carbonyl and the nitrogen atoms in the peptide backbone thereby resulting in daughter ions representing C-terminal (y-ions) and N-terminal (b-ions) peptide fragments. The assembly of these b- and y-ion series in MS/MS spectra provides the core information for matching amino acid sequences through probability-based search algorithms such as Mascot, X!Tandem and Sequest[139,140]. This process allows the identification of proteins present in the sample[141,142]. Data from the MS1 and MS2 spectra are also used to obtain relative quantitation information. Many different quantitative methods have been described for use in

combination with mass spectrometry[143]. In this thesis, applied spectral counting[144,145] and label-free quantitation[146] were used.

Dynamic range of the human blood proteome – an analytical challenge

Blood is considered the most complex biological specimen with regard to protein content and the range of protein abundance. Serum albumin is produced by the liver and under physiological conditions has an abundance of 35-50mg/ml or 3.5-5.0 x10^9pg/ml in serum. It is considered the most abundant protein in blood. At the other end of the dynamic range, IL-6 with an abundance of 0-5pg/ml is a marker of inflammation. This gives an approximate dynamic range of 10-12 logs from the most to least abundant proteins. Coverage of this range is beyond the current capabilities of analysis by mass spectrometry[147,148].

In a label-free approach, where all the blood proteins will be subjected to enzymatic digestion for the generation of peptides, the most abundant ions will be favoured disproportionally, leading to an under-representation of peptides derived from low abundance proteins in the MS1 scan phase. The lack of sensitivity in detecting low abundance ions is one of the key limitations in mass spectrometry of biological specimens. Current limits of detection are within the low attomolar range (on column concentration) which translates into a protein detection limit in the ng/ml range in serum or plasma[148–150].

Figure 3.3 shows the dynamic range of blood proteins and the different protein classes that are represented. To improve the detection of lower abundanceproteins, additional blood sample preparation methodologies are used. These include depletion of high abundance proteins and sample fractionation. Both techniques were employed in the experimental work and are described below in more detail.

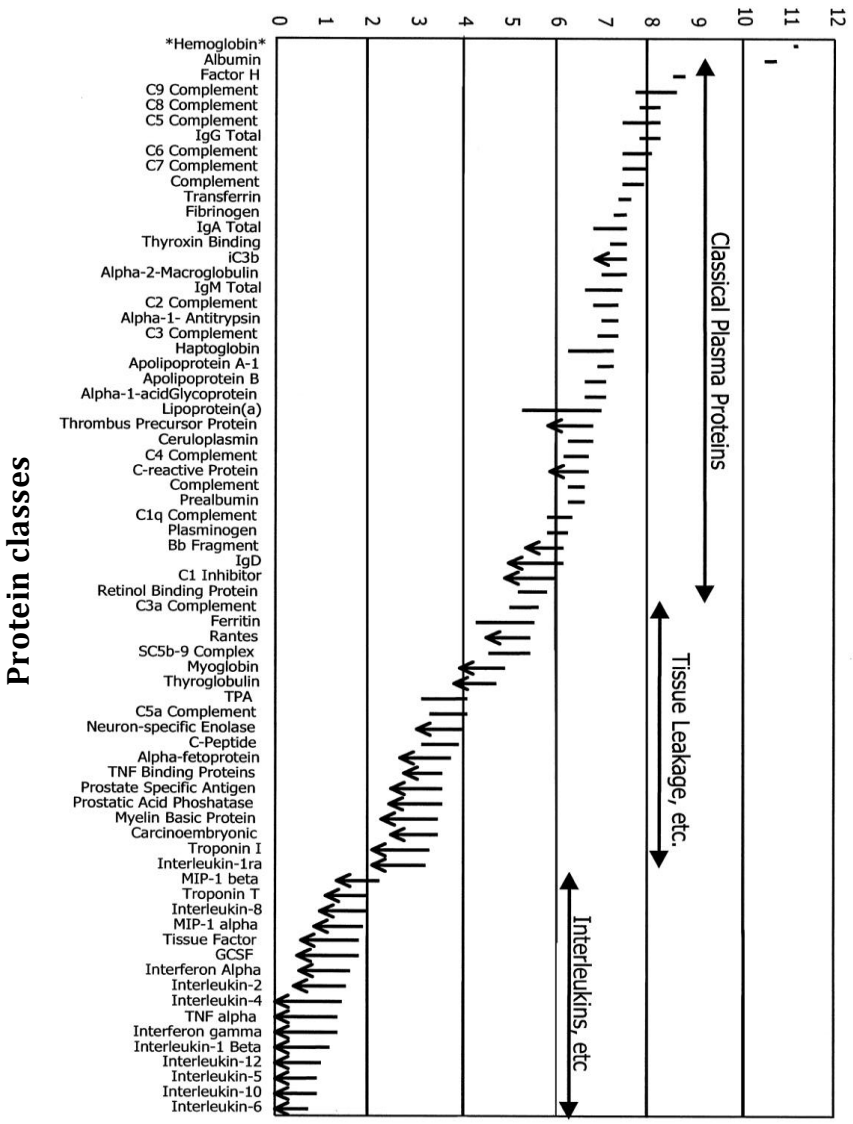

Figure 3.3 Dynamic range of blood proteome[148]
Serum protein abundance is plotted on a log scale spanning 12 orders of magnitude. At the high end (left) are classical plasma proteins such as serum albumin, complement proteins fibrinogen and IgGs (high abundance). Tissue leakage markers such as enzymes and troponins, myoglobin & myelin are clustered in the centre (middle abundance), and metalloproteinases, interleukins and cytokines are clustered to the right (low abundance).

3.4 Mass spectrometry methods

3.4.1 Immunodepletion of the 14 most abundant proteins from plasma

Antibody affinity-based depletion of plasma samples was performed using an Agilent Human top 14 Multiple Affinity Removal System (MARS) coupled to an Ultimate 3000 HPLC system (Thermo Scientific, UK) following the manufacturer's instructions. 80 µl plasma aliquots were centrifuged at 10,000g for 10 min, diluted 4 times in Buffer A (Agilent Technologies, UK) and separated on a MARS column according to the following separation protocol. Protein depletion on the column followed a sequence of isocratic elution steps: 100 % Buffer A for 20 min at 0.125 ml/min followed by 0.7 ml/min for 2.5 min. Flow-through fractions containing the depleted plasma were collected between 7.5 and 14.5 min of each sample run. Each sample was injected four times to obtain a sufficient quantity of protein for further analysis.

3.4.2 Protein precipitation

Flow-through protein fractions of depleted plasma samples were supplemented with sodium deoxycholate to a final concentration of 125 µg/ml followed by 15 min incubation at 22°C. For protein precipitation trichloro-acetic acid (TFA) was added to a final concentration of 6% followed by centrifugation at 12000g at 4°C for 30 min. Sample supernatants containing naturally occurring peptides were collected in new tubes for separate analyses. Protein precipitates were washed with 1ml ice-cold acetone, centrifuged at 12000g for 10 min and pellets resuspended in 50 µl of 6 M urea in 100 mM Tris HCl, pH 7.8. Quantitation of each sample was performed by a BCA protein assay according to the manufacturer's instructions (BCA Protein assay, Thermo Scientific, US).

3.4.3 GeLC-MS/MS proteomic analysis

Another method to increase the detection of lower abundant protein was protein fractionation by gel electrophoresis based liquid chromatography-tandem mass spectrometry (GeLC-MS/MS). Equal amounts of protein (60µg) were suspended in 1x SDS reducing sample buffer and separated by SDS-PAGE on 4-12% Criterion XT bis-tris gels with XT MES running buffer (BioRad, UK). Protein fractionations were visualised by Coomassie Instant Blue (Expedeon Ltd., UK) staining for 10 min followed by de-staining in distilled water. Each gel was divided into three bands using a sterile scalpel and each band subsequently cut into 1-2mm^2 gel pieces and transferred to a labelled tube for further analysis. Gel pieces were de-stained in 50% methanol, 5% acetic acid in Milli-Q-H_2O until transparent, then dehydrated using 200µL acetonitrile for 5 min followed by 1 hr vacuum centrifugation until completely dry. Captured proteins were reduced by addition of 10 mM dithiothreitol (DTT) for 1 hr followed by alkylation with 50 mM iodoacetamide (IAA) for 1 hr then re-dried in a vacuum centrifuge for 2 hr prior to enzymatic digestion. Trypsin digestion was performed overnight at 37°C with gentle mixing. Peptide digests were extracted from the gel matrix using sequential extraction buffers then completely dried in a vacuum centrifugation. Pellets were suspended in 30µl of buffer (98% Milli-Q-H2O, 2% acetonitrile, 0.1% formic acid) and analysed by LC-MS/MS. Desalting was not performed.

3.4.4 In-solution trypsin digestion of plasma and tissue

Peptide tryptic digests were generated from 15 µg aliquots of plasma or tissue as determined by BCA assay (see section 3.4.2 above). Samples were reduced for 1 hr by addition of 200 mM DTT followed by alkylation with 200 mM IAA for 30 min. Trypsin digestion was performed overnight at 37 °C with gentle mixing

using a 1:50 trypsin: protein ratio. Samples were acidified with 1% formic acid (FA) or TFA. Peptide digests were then desalted using Sep-Pak C18 cartridges (Waters, USA) as described below.

3.4.5 In-solution digestion of urine

0.5ml aliquots of urine samples were centrifuged at 12,000g for 15min and then depleted of albumin by the addition of ice cold ethanol to 72% final concentration followed by centrifugation at 12,000g for 30 min at 4°C. Albumin rich supernatant was removed to leave the protein precipitate as a pellet. Precipitated protein was dissolved in 50µl of 6 M Urea, 100 mM Tris HCl, pH 7.8, reduced with 10 mM DTT for 1 hr then alkylated with 50 mM IAA for 1 hr. The urea concentration was reduced to less than 1 mM and the proteins were subjected to trypsin digestion as described for plasma or tissue samples (see 3.4.4 above). Protein digests were desalted as described below.

3.4.6 Desalting of tryptic peptides

Tryptic peptides generated by in–solution digestion were subsequently desalted using SEP-PAK C18 columns (Thermo Scientific SOLA tube SPH-300-010Q) in a vacuum system that was manually regulated to control the flow of the buffers through the columns. C18 columns were first conditioned by buffer B (0.1% TFA with 65% acetronitrile (ACN) and buffer A (0.1 % TFA). Tryptic digests were loaded to the column and first washed with 1 ml buffer A. The peptides were eluted from the column with 500 ml of buffer B and dried by centrifugation under vacuum overnight (Speedvac, ThermoFisher Scientific, UK). The desalted peptides were resuspended in 30 µl of buffer (98 % Milli-Q-H_2O, 2 % ACN, 0.1 % FA), sonicated for 5 min and vortexed for 15 min and stored at -80^{o}C until LC-MS/MS analysis.

3.4.7 PROtein TOpography and Migration Analysis Platform (PROTOMAP)

PROTOMAP analysis involves the comparison of two pooled experimental cohorts. 60µg of protein per pool was denatured and reduced in standard Laemmli buffer with DTT, divided into two equal aliquots and separated by SDS-PAGE (NOVEX, Invitrogen 4-12% gradient, ThermoFisher Scientific, UK). Figure 3.3 provides an overview of the PROTOMAP method. The gel was stained with Coomassie instant blue, and each pooled sample lane was cut into 22 horizontal slices, generating 44 samples overall. Gel pieces were de-stained in a solution of 1 ml 50% methanol, 5% acetic acid in Milli-Q-H_2O solution until transparent, then dehydrated using 200µL ACN for 5 min. Proteins were reduced by addition of 30 µl of 10 mM DTT for 30 min followed by alkylation with 30 µl of 50 mM IAA for 30 min. Gel pieces were dehydrated with 200 µl ACN, resuspended in 30 µl 100 mM ammonium bicarbonate containing 20 ng/µl trypsin and incubated overnight at 37°C with gentle mixing. Peptide digests were extracted from the gel matrix using 50 µl extraction buffer I (50 % ACN, 5 % FA) followed by 50 µl extraction buffer II (85% ACN, 5% FA); the extracted fractions were collected, pooled and dried by vacuum centrifugation.

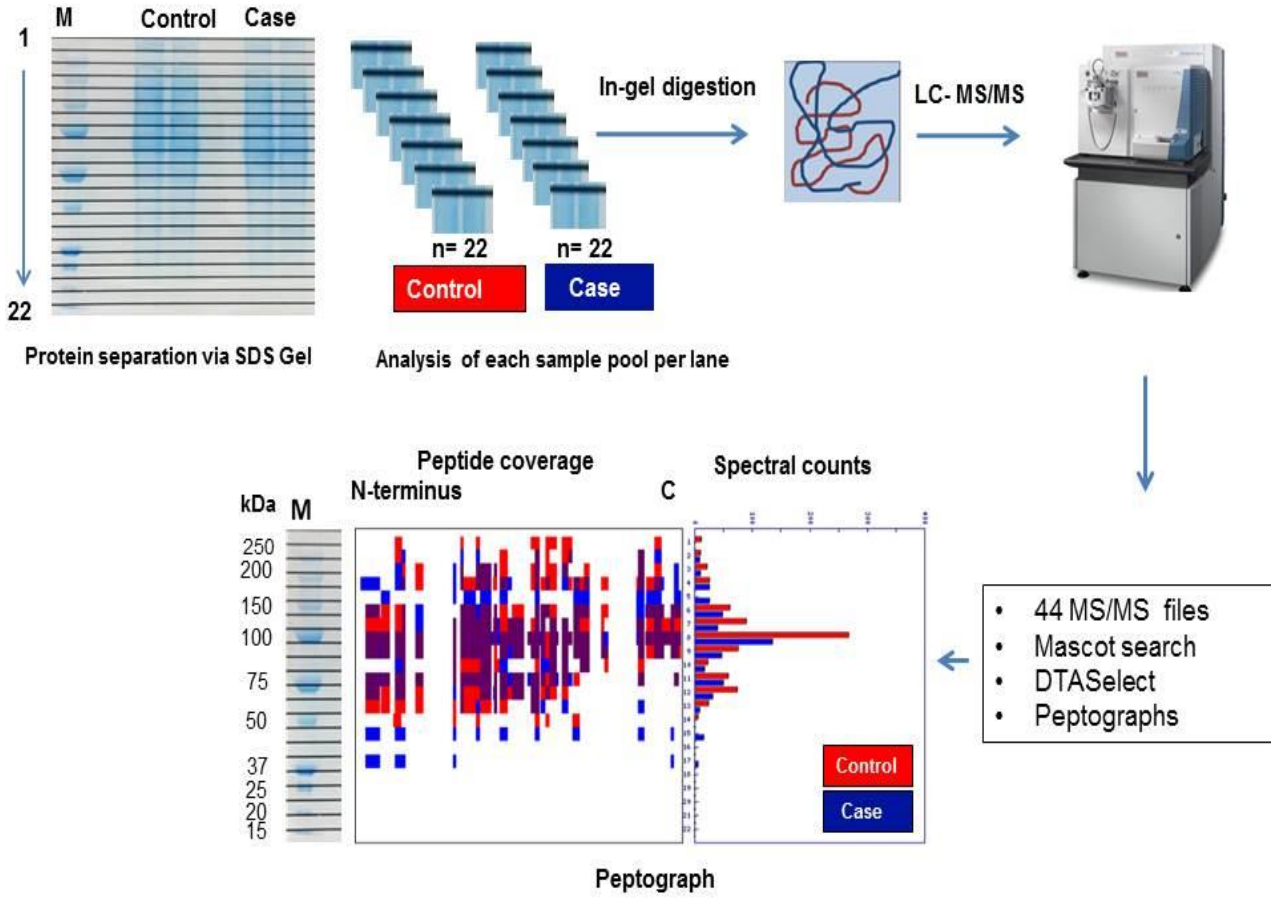

Figure 3.4: Overview of the PROTOMAP method

Protein samples of two conditions (control & case) run on 1-D gel. The gel is subsequently divided into 22 bands per lane (representing one condition each). Each pool per band is cut to create 22 pieces per condition, proteins then subjected to in-solution trypsin digestion and analysed by LC-MS/MS. Raw MS data is analysed by PROTOMAP bioinformatics to generate peptographs. Peptographs consist of two panels and combine information from 1-D gel migration of protein fragments, protein sequence coverage and spectral counts of protein fragments per gel band. The left panel shows the protein sequence coverage from N to C terminus for each band. Peptide sequences represented in red and blue were identified in the control and study pools, respectively, while peptide fragments represented in purple were common to both pooled samples in the same band. The right panel shows the relative quantitation using spectral counts for each protein between the two pools. The red bars represent the 'parent proteins' which are the intact proteins identified in the control samples. Protein degradation is defined by fragments with spectral counts detected in lower bands as compared to the 'parent protein'.

3.5 Data analysis methods

3.5.1 Analysis by mass spectrometry

Desalted peptides were resuspended in 30 µl of buffer (98% Milli-Q-H_2O, 2% ACN, 0.1% FA) and analysed by nano ultra-high performance liquid chromatography tandem mass spectrometry (nUHPLC-MS/MS) using a Thermo LTQ Q Exactive tandem mass spectrometer[151]. Samples were injected and separated by nUHPLC-MS/MS using a Dionex Ultimate 3000 UHPLC (C18 column with a 75 µm × 250 mm, 1.7 µm particle size and eluted with a 2 hr linear gradient at a flow rate of 250nl/min. The UHPLC system was coupled to a Q Exactive tandem mass spectrometer (Thermo Scientific, Germany) for electrospray ionisation. The HPLC consisted of a nanoflow analytical and a capillary loading pump (Agilent 1200 series). Peptides were enriched and separated via nano-LC (0.075 x 150 mm, packed with Zorbax 300SB-C18, 5 µm material, 300 Å pore size) integrated in the HPLC Chip (G4240-62001). Peptides were loaded in the column with 100% solvent A (2% acetonitrile with 0.1% formic acid). A two-step gradient generated at a flow rate of 0.6 µl/min was used for peptide elution. The total run time, including column reconditioning, was 60 min. A full scan was acquired over a range of m/z 400-1700 at 5 spectra per second rate, and MS/MS over m/z 50-1700 at two spectra per second rate selecting the six most abundant double or triple charged precursor ions per cycle. Auto-MS/MS was performed with a total cycle time of 3.3 seconds, as has been described[152],[153]. Spectra were collected from an ion trap mass analyser (LTQ-Orbitrap, Velos, Thermo Fisher Scientific). Samples were analysed in duplicates except where indicated otherwise.

3.5.2 PROGENESIS QI bioinformatics analysis – an overview

Raw MS data were analysed using PROGENESIS LC and the upgraded version QI for Proteomics (QIP) software v3.1.4003.30577 (Nonlinear Dynamics /Waters, UK). The analysis was based on a workflow that involved the following steps, summarised in figure 3.4:

1. ***Import data***: Raw data were imported into the software as MzXML files

2. ***Review alignment***: To quantify multiple LC-MS runs and compare the expression profiles of the identified proteins, the multiple runs were aligned with a reference run which was either chosen automatically by the software or manually. Usually, the manual reference run was a pool of all the analysed by MS/MS samples.

3. ***Filtering:*** To ensure consistency in the comparison of the same ions across all the runs, the software created a map of peptide ions applied to each sample. This allowed comparison of ion intensity between samples for quantification.

4. ***Peak Picking / peptide ion statistics***: Peptide quantitation was performed by ion intensity quantitation across the LC/MS runs.

5. ***Identify peptides***: Peptide Mascot search was performed against the human databases (Uniprot or Swissprot, released 2015) using the Mascot search engine. The search was carried out according to the default search that includes carbamidomethylation on cysteines as fixed modification and deamidation (glutamine) and oxidation (methionine) as variable modifications. One missed cleavage and 10ppm/0.5Da mass deviations for MS and MS/MS ions were allowed. To calculate the false discovery rate (FDR), Mascot compared the total number of spectra matched to the proteins with a decoy search. The proteins

imported into PROGENESIS for quantification had FDR<1% and a protein score >20. Only proteins with at least two peptides were included in the protein data set for further analysis.

6. ***Review proteins/protein statistics:*** For label-free protein quantitation, Mascot results were inserted into the LC-Progenesis program. A final list of the identified proteins with ANOVA p values, fold changes between the lowest and highest mean intensities for each protein were displayed. Principle component analysis and expression profiles were generated according to the experimental design as seen in figure 3.4 under the tab 'protein statistics'.

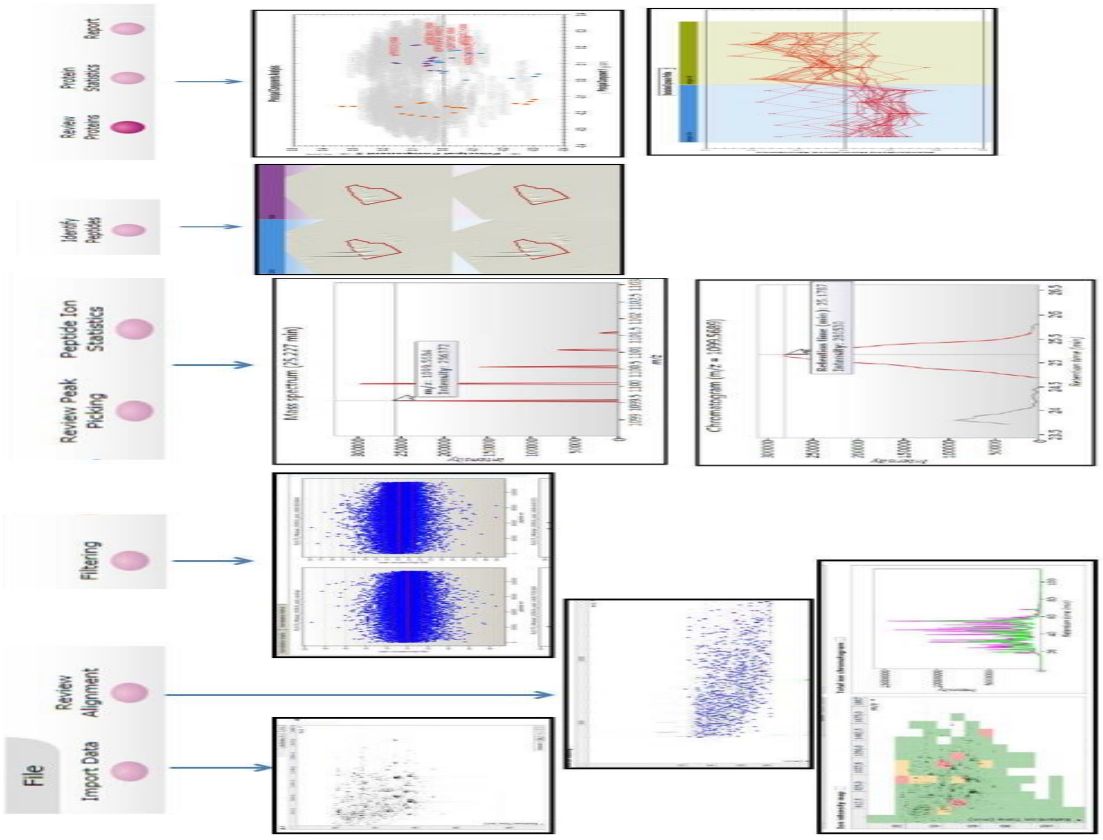

Figure 3.5 Summary workflow for PROGENESIS QI for Proteomics
(QIP software v3.1.4003.30577, Nonlinear Dynamics). MS data processing includes several steps, such as i) importing MS data, ii) MS1 data alignment, iii) database searches and importing protein identifications, iv) MS data normalisation for quantification. The software allows for the examination of peptide peak assignments and quantitation to check the quality of accuracy of quantitation.

3.5.3 Central Proteomic Facilities Pipeline (CPFP)

Apart from PROGENESIS, MS data were processed and identified proteins quantified using an 'in house' bioinformatics tool pipeline, CPFP[144,145]. Raw data were converted to Mascot generic (mgf) files using msconvert [154] and subsequently submitted to CPFP for searches using OMSSA and X!TANDEM. Searches were performed against the human Swissprot database. The parameters used for the search were: instrument chosen was Orbitrap, trypsin as the enzyme used for the digestion, one missed cleavage. The accepted tolerance for the precursor was 50 ppm and 0.1 Da for the fragment. The search was extended to include 1+, 2+ and 3+ charge state, fixed modification for cysteine carbamidomethyl and variable modification for asparagine and glutamine deamidation, and methionine oxidation. The label free analysis was carried out using the normalized spectral index. Normalised spectral index quantitation (SINQ) is based on the sum of the intensity of matched fragments for all spectra that define a protein[74,75]. SINQ values and sequence coverage scores were exported to an Excel file (Microsoft, USA) for further analysis.

3.5.4 PROTOMAP bioinformatics

The PROTOMAP workflow integrates protein migration patterns on SDS–PAGE electrophoresis with peptide sequence coverage and spectral counts acquired by LC-MS/MS analysis. The results were visualised as peptographs (figure 3.4)[155]. Raw data were converted to Mascot generic files using msconvert[154], searched with Mascot and further analysed as described by Niessen *et al.*[156]. Specifically, MS/MS spectra data were searched using Mascot v2.5.1 against the UniProt *Homo sapiens* Reference proteome (retrieved 15/10/2014).

Mascot results were exported as DTASelect at a FDR threshold of 1% and analysed using the PROTOMAP perl scripts obtained from http://www.scripps.edu/cravatt/protomap/.

3.5.5 Hierarchical clustering analysis

Hierarchical clustering analysis (HCA) classifies samples without *a priori* knowledge of the biological relevance of the experimental cohorts and is based only on relative protein abundance. HCA is a robust statistical method to analyse extensive data sets obtained from a small number of subjects[157]. In the following chapters, HCA was used to identify associations between analysed subjects from proteomic data. For the analysis of the proteomic sets, clustering and data visualisation were performed using PermutMatrix software[158]. Protein abundance values derive either from PROGENESIS or CPFP relative quantitation were entered in the online open access bioinformatics software PermuMatrix[158].

HCA is based on the dissimilarity calculation which is the comparative distance between compared samples when all the identified features are considered (protein abundance). Hierarchical clustering was performed using Euclidean distance and the single linkage (closest neighbour linkage) as default algorithms. As the PermutMatrix software cannot perform HCA with missing data, missing abundance data were imputed. For a given protein, missing abundance data were imputed with the mean value of protein expression for all the runs in the same cohort. Data were imputed when only 40% of individual samples had missing data. The proteins with missing values for more than 40% of samples per cohort for a specific protein were excluded from the analysis.

3.6 Study design

Experimental groups were defined on the basis of recipient outcomes following a case control study design. To identify changes in the kidney or blood proteomic signatures associated with donor quality, the extreme clinical outcomes were considered such as the onset of delayed graft function compared to immediate function (chapter 5) or good kidney function 3 and 12 months post-transplantation compared to suboptimal function (chapter 6). A cohort of clinical samples obtained from living donors was included as controls representing optimal transplantation outcomes. As donor type, donor age and CIT are strongly associated with transplantation outcomes, as discussed in chapter 1, it was important to ensure that experimental groups were as homogenous as possible with regard to these characteristics although this posed a logistical challenge in recruiting sufficient samples per cohort for the study.

The overall experimental design is summarised in figure 3.6. A selection of samples was used for the discovery phase via an untargeted proteomic analysis. Statistical and bioinformatics analysis as described above, led to a list of candidate proteins that were further validated by western blotting as described in chapter 6.

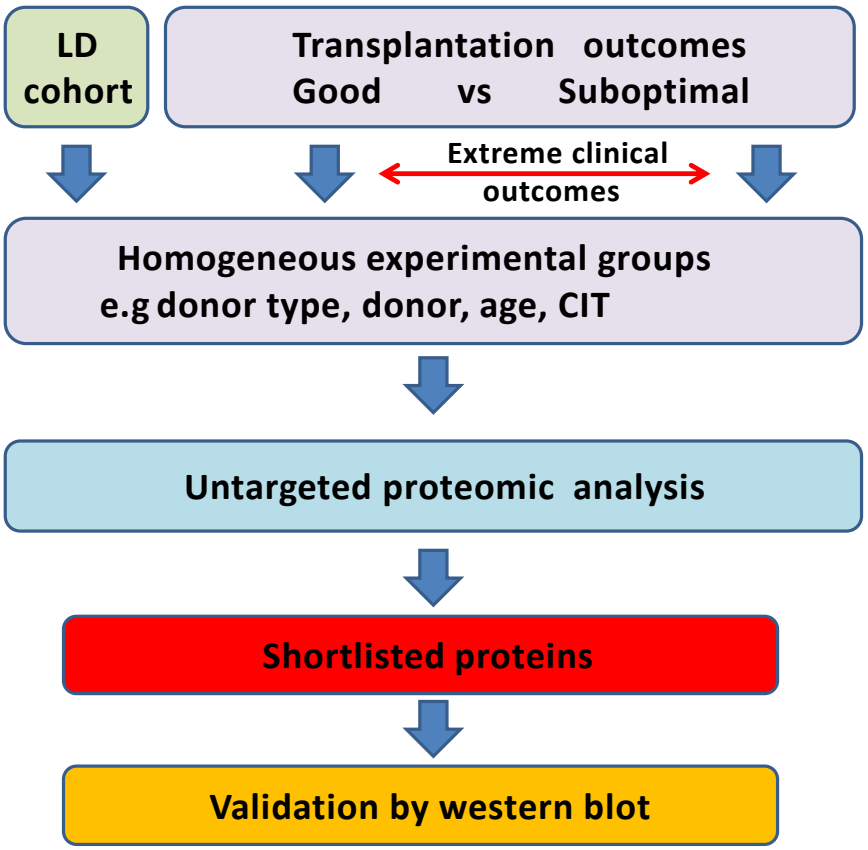

Figure 3.6 Overview of the study design

The samples were selected on the basis of transplantation outcomes and, in parallel, a cohort of living donor samples were analysed. Samples were selected from donors with similar demographic and clinical characteristics such as donor/recipient age, donor type, cold ischemia time (CIT). Samples were analysed by untargeted proteomics and the differentially regulated proteins were validated by western blotting. This approach was followed in chapters 5&6.

Pooled versus individual samples for proteomics analysis

Comparative proteomic analysis can be carried out on individual samples or on pooled samples with similar clinical characteristics. There are advantages and disadvantages to either approach. Experiments using mass spectrometry are expensive to conduct and MS instrument time is often at a premium. Pooling samples with similar properties can reduce the cost and amount of instrument time needed to conduct the study. Furthermore, analysis of pooled samples can even out the biological heterogeneity between samples and enhance the identification of proteins common among the samples. As new instruments are very sensitive it is still possible to identify a large number of proteins of interest. However, with pooled samples it can be more difficult to discriminate between disease-related signals and the background noise created by variability between individuals. Analysis of individual samples can allow significant changes in protein profiles to be more easily associated with individual, clinical and demographic characteristics of the analysed donor group but at greater cost and instrument time. The more samples analysed the greater the statistical significance of changes. A compromise approach is to use a pooled approach for the discovery phase then conduct a validation on significant proteins of interest using individual samples. The experimental work adopted in this thesis was to use a combination of pooled and individual sample analysis were possible, as described in more detail in chapters 5 and 6.

CHAPTER 4

Plasma proteome and degradome alterations during blood storage

4.1 Introduction

The QUality in Organ Donation (QUOD) program, as described previously, is an initiative to collect blood, urine and abdominal organ tissues from solid organ donors during donor management to provide an invaluable bioresource to study the quality of organs for transplant. The QUOD biobank collects samples from transplant centres throughout the UK. The QUOD national management team designed a robust protocol with pre-determined optimal time points for collection of samples from the donor in the period leading up to organ donation. Adherence to the protocol necessitated taking some samples during antisocial hours when rapid processing of samples was not a priority and it was considered likely that some samples could remain unprocessed for up to 48 hrs. This variability in sample processing, although rare, was identified as a potential weakness which could cause problems with comparative analyses at a later date.

Eliminating sample variability was considered particularly important to reduce false-positive discovery of potential biomarkers[159,160]. In biomarker discovery and validation studies, where high sensitive methods such as mass spectrometry are used, there are many variables that could influence the outcome of these studies introducing unintended bias[161,162]

Storage of blood samples at ambient temperature (AT) was the preferred option between procurement and processing to avoid activation of the cellular components in blood such as platelets and neutrophils. However, further work was needed to investigate the effect of storage at up to 48 hrs at AT on the plasma proteins and the extent of endogenous proteolysis which could occur under these conditions.

The work described in this chapter was an investigation on the impact to the proteome and degradome of plasma when whole blood remained at ambient temperature (AT) for a variable time period between 30 min and 48 hrs.

4.2 Hypothesis and aims

When whole blood is stored at ambient temperature (AT) plasma proteins may be enriched, in part from activation of the cellular parts of blood, or become depleted by the activity of endogenous proteases. If endogenous proteases degrade plasma proteins they will produce peptides, these peptides constitute the degradome. The aim of this study was to investigate the plasma proteome and degradome when whole blood remained at AT for variable periods between 30 min and 48hrs (30min, 8hr, 24hr and 48hr) prior to centrifugation and isolation of plasma. The selected time points of 30 min to 48 hrs were chosen as the minimum and maximum time QUOD blood samples were likely to remain at AT prior to centrifugation due collection out of hours or at weekends.

4.3 Methods

Sample collection and processing

Blood from healthy volunteers was collected, processed and analysed following the experimental protocol shown in figure 4.1. 40 ml blood was collected from 5 healthy individuals in EDTA gel vacutainer plasma gel separator tubes (BD, Vacutainer® PPTTM Plastic tube with BD Pearlescent White HemogardTM Closure) according to the University of Oxford research consent policy[163]. Blood was collected by peripheral venepuncture using a 20-gauge needle and mixed with EDTA by gently inverting the EDTA tubes, then stored at AT for 30 min, 8 hrs, 24 hrs, or 48 hrs (figure 4.1). For the purpose of this study, AT was defined as 22 $\pm$ 2°C, and the protocols for preparation of all the samples were the same for each participant. Subsequently, plasma was isolated by centrifugation of samples at 1500g for 15 min at 22°C. Plasma was aliquotted and stored at -80°C awaiting analysis. No haemolysis was observed in any of the blood samples before or after blood centrifugation or during the period of 48 hrs at AT.

Experimental plan

Individual plasma samples, stored as whole blood at AT (22°C ± 2°) for 30 min, 8 hrs, 24 hrs and 48 hrs, were analysed by LC-MS/MS to identify changes in the proteomic profile of plasma proteins across the time points from 30 min to 48 hrs (figure 4.1). The extent of endogenous proteolysis was assessed by two experimental approaches:

i) Analysis of smaller, soluble peptide fragments remaining in the supernatant following pelleting of the intact plasma proteins across all the time points

ii) PROTOMAP analysis on pooled samples (n=5) of the two extreme conditions of AT storage, 30 min and 48hrs. The experimental workflow is shown in figure 4.1.

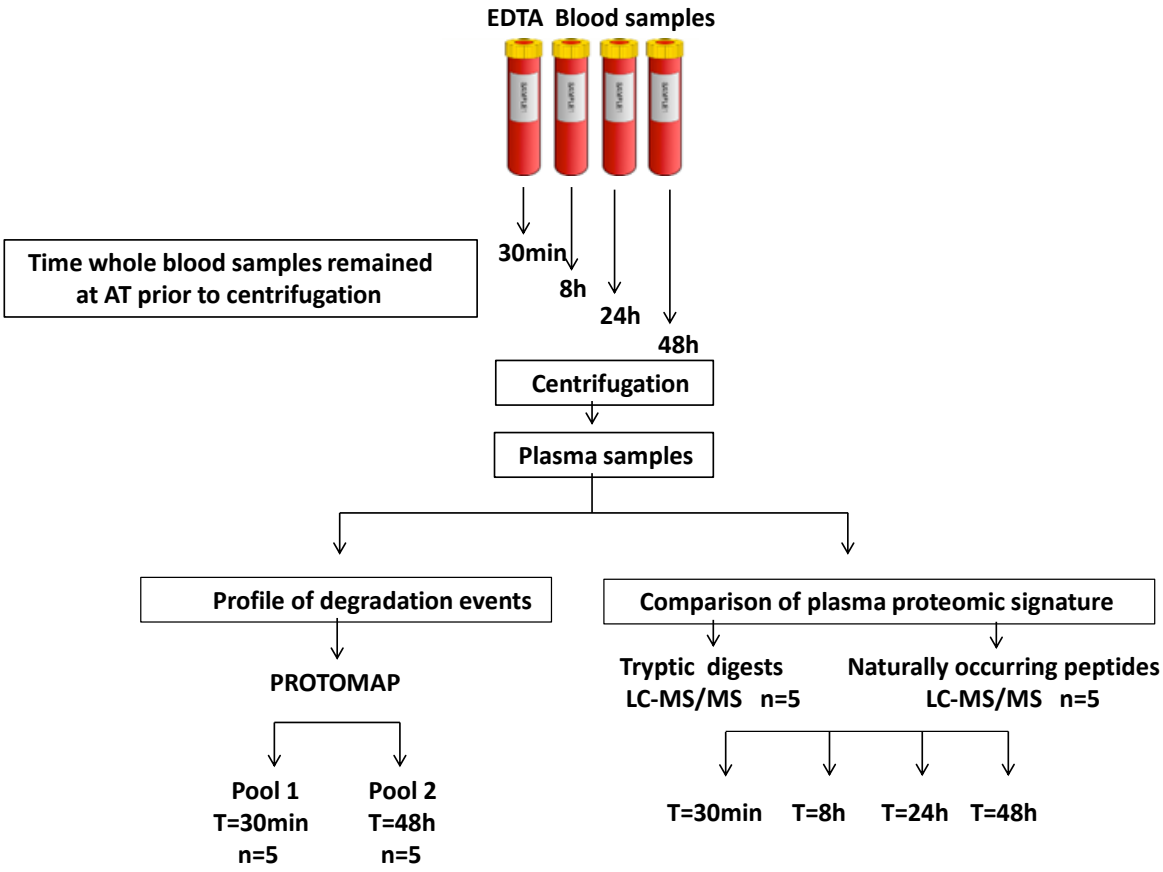

Figure 4.1 Experimental workflow

4 EDTA blood tubes were collected from 5 healthy volunteers and kept at AT for T=30min, 8hrs, 24hrs & 48hrs prior to centrifugation and plasma preparation. Alteration of plasma proteomic signatures across the four time points was compared by LC-MS/MS (tryptic digests). Comparison of naturally occurred peptides in blood for all storage conditions was performed by LC-MS/MS (non-tryptic digests). Profiling of degradation events of pooled plasma samples (n=5) was performed using PROTOMAP analysis of the two extreme storage conditions.

Label free quantitative MS/MS analysis of tryptic and naturally occurred peptides

Plasma samples were immunodepleted to remove the 14 most abundant plasma proteins according to the method described in chapter 3.4.1.

Proteins were precipitated and recovered as a pellet by centrifugation then subjected to tryptic digestion using an in-solution digestion protocol. Peptides were desalted and re suspended in FA for MS/MS analysis (tryptic digests, figure 4.1).

The supernatant was also retained for analysis since this contained the naturally occurring peptides. The naturally occurring peptides were desalted using Sep-Pak C18 cartridges, resuspended in FA and analysed by MS/MS. All the relevant protocols are described in detail in chapter 3.4.

PROTOMAP analysis

To profile protein degradation events occurring in whole blood exposed to AT for different times, a PROteolytic TOpography and Migration Analysis Platform, (PROTOMAP) study was carried out by the method described in chapter 3.4.7. Immunodepleted plasma samples were used to create two plasma pools as shown in figure 4.2. Pool 1 contained plasma samples that had been prepared from whole blood by centrifugation after 30 min following blood collection and Pool 2 contained plasma samples prepared 48hrs after collection.

Tryptic and non- tryptic digests LC-MS/MS data analysis

Tryptic and non-tryptic digests were analysed by LC-MS/MS as described in chapter 3.5.1 and raw data were analysed and quantified using Progenesis QI for Proteomics (QIP) software v3.1.4003.30577 (Nonlinear Dynamics) as described in chapter 3.5.2.

Statistical comparison of protein abundance changes observed between the four time points of whole blood centrifugation (T=30min and T= 8hrs, 24hrs, and 48hrs) was performed using a one-way ANOVA F-test within the Progenesis QI software (calling significant changes at $p \leq 0.05$).

PROTOMAP data analysis

As shown in figure 4.2 the PROTOMAP analysis was performed to profile the degradome events occurred when whole blood was stored for 48 hrs in AT in comparison to 30 min. The protocol is described in chapter 3.4.7.

The peptographs consist of two panels; the left hand side panel shows the peptide sequences represented in red and blue for 30 min and 48 hrs samples respectively. Peptide fragments in purple were common to both experimental conditions in the same band. The right hand panel shows the relative quantitation using spectral counts for each protein between the two pools. The red bars represent the parent proteins which are the intact proteins identified in the plasma samples prepared after centrifugation at 30min while blue bars represent the spectral counts of proteins in the samples centrifuged after storage for 48hrs. Protein degradation was defined by the presence of fragments with spectral counts detected in lower bands when compared to the parent protein.

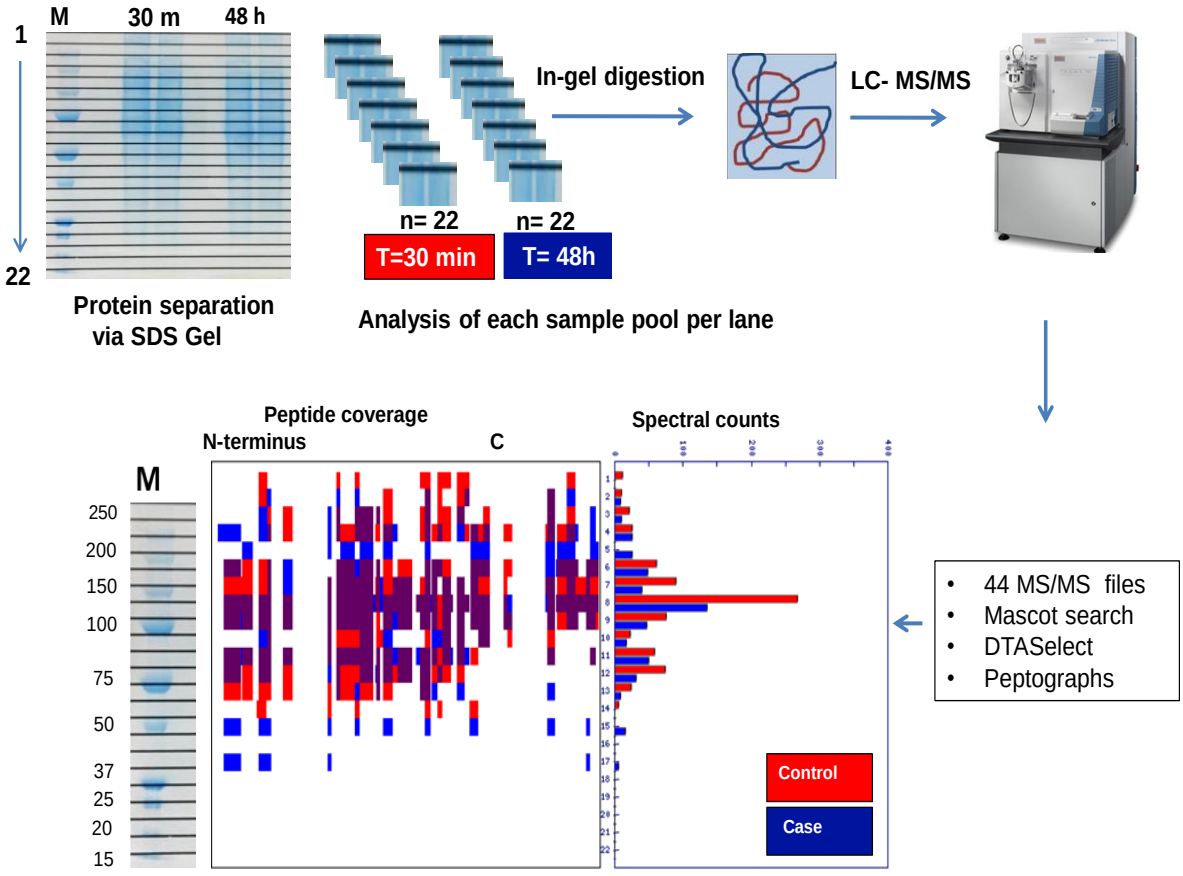

Figure 4.2 PROTOMAP workflow

The 30 min (Pool 1, n=5) and 48 hrs samples (Pool 2, n= 5) were separated by 1-D SDS-PAGE and proteins visualised by Coomassie blue staining. The gel was subsequently divided into 22 bands per lane (representing one condition each). Each pool per band was cut to create 22 pieces per condition, proteins were subjected to trypsin digestion and analysed by LC-MS/MS. Raw MS data was analysed by PROTOMAP bioinformatics to generate peptographs.

Western blotting

Depleted plasma samples containing 20 µg of protein were denatured at 95°C for 5 minutes in Laemmli buffer, loaded onto and separated by 4–12% pre-cast SDS-PAGE gels (Bio-Rad, USA), followed by immunoblotting onto PVDF membranes (Merck Millipore, USA) using standard protocols. Membranes were incubated overnight at 4°C with monoclonal rabbit anti-C4B (1µg/ml, Abcam Ab168358) or goat polyclonal anti thrombospondin-1 (1.2µg/ml, R&D systems AF3074). 1:5000 dilution of Dye-800-conjugated anti-goat or -rabbit IgG (Li-Cor, USA) was used as secondary antibodies for detection. Bands were visualised using an Odyssey CLx system (Li-Cor).

4.4 Results

Label free quantitative MS/MS analysis produced a reference list of proteomic and peptidomic alterations in whole blood when stored in AT between 30 min and 48 hrs[164,165]. Remarkably few changes in the plasma proteome were seen (table 4.1). This suggests that storage of whole blood at ambient temperature does not impact significantly on proteome integrity for up to 48hrs.

Plasma proteomic signatures of blood stored at* AT *for variable time periods

To establish how the plasma proteome and degradation profile was affected by leaving whole blood at AT for a period between 30min and 48hrs, whole blood from 5 individuals was stored at AT for 30 min, 8hrs, 24hrs and 48hrs prior to plasma preparation and analysis by LC-MS/MS (figure 4.1). Interestingly, analysis revealed no obvious trend of change in the majority of protein levels with respect to time (at least 2 unique peptides and > 95%confidence in protein identification) (figure 4.3A). When the significantly regulated proteins (ANOVA p ≤0.05) between T=30min and later centrifugation conditions were considered, only 18 proteins with increased levels were observed (table 4.1& 4.S1). Eight proteins increased within the first 8hrs following blood collection and the rest at a later stage. With the exception of profilin-1 which increased by seven-fold after 48hrs and Ankyrin by two-fold, all the rest of the proteins were altered by less than two-fold (table 4.1 & 4.S1). Among the shortlisted proteins with altered levels of concentration were thrombospondin-1 and cystatin C and proteins that associated with the complement and coagulation cascade.

Table 4.1 Proteomic signature of susceptible plasma proteins at AT

	LFQ LC-MS/MS			PROTOMAP analysis
		Fold change		
Protein description	***T= 8h vs T=30m***	***T= 24h vs T=30m***	**T= 48h vs T=30m**	**T= 48h vs T=30m**
Fibrinogen gamma chain	*1.4*	*1.3*	1.2	No Degradation
Apolipoprotein A-I	*1.3*	*1.3*	1.3	No Degradation
Profilin-1	*1.1*	*2.0*	7.1	No Degradation
DNA polymerase epsilon catalytic subunit A	*1.2*	*1.2*	1.2	No Degradation
Coiled-coil domain-containing protein 11	*1.2*	*1.3*	1.3	No Degradation
Coagulation factor XIII B chain	*1.2*	*1.2*	1.2	No Degradation
Heat shock protein 70 kDa	*1.3*	*1.3*	1.2	No Degradation
Dedicator of cytokinesis protein 7	*1.5*	*1.5*	1.4	No Degradation
Cystatin-C	*1.3*	*1.3*	1.3	No Degradation
Uncharacterized protein C2orf53	*1.8*	*1.9*	1.7	No Degradation
Complement C1q subcomponent subunit B	*1.3*	*1.3*	1.3	No Degradation
Leukocyte immunoglobulin-like receptor	*1.2*	*1.4*	1.4	No Degradation
MCM domain-containing protein 2	*1.6*	*1.7*	1.7	No Degradation
Ankyrin repeat domain- protein 54	*2.2*	*2.3*	2.2	No Degradation
Thrombospondin-1[b]	*1.2*	*1.3*	1.4	Partially degraded
Coagulation factor XI[c]		*N/E*		Partially degraded
Complement C1r[c]		*N/E*		Partially degraded
Actin[c]		*N/E*		Partially degraded
Complement C3[c]		*N/E*		Partially degraded
Complement C4B[c]		*N/E*		Partially degraded
Talin-1[c]		*N/E*		Partially degraded
Apolipoprotein B-100[c]		*N/E*		Partially degraded
Complement C5[c]		*N/E*		Partially degraded
Ceruloplasmin[c]		*N/E*		Partially degraded
Alpha-1 antichymotrypsin[c]		*N/E*		Partially degraded
Inter alpha trypsin inhibitor[c]		*N/E*		Partially degraded
Kallistratin[c]		*N/E*		Partially degraded
Corticosteroid-binding globulin[c]		*N/E*		Partially degraded
Serum paraoxonase[c]		*N/E*		Partially degraded
Fibronectin[c]		*N/E*		Partially degraded
Plasmonogen like protein A[c]		*N/E*		Partially degraded
Complement C2[c]		*N/E*		Partially degraded
Fibrinogen alpha chain[c]		*N/E*		Partially degraded
Extracellular matrix protein-1[c]		*N/E*		Partially degraded
Collagen alpha 3[c]		*N/E*		Partially degraded
Protein disulphide isomerase A3[c]		*N/E*		Partially degraded

[a] *The shaded part of the table shows proteins identified and quantified by PROGENESIS QI and compared across all time points (ANOVA P≤0.05). Raw data is included in Table 4S1.*
N/E indicates that the abundance of these proteins was not significantly changed as measured by LFQ LC-MS/MS but fragments from these proteins were generated as identified in the lower molecular weight range by PROTOMAP analysis.
[b] *Thrombospondin was markedly increased between T=30 min and later time points in addition to the generation of proteolytic fragments observed in T=48hrs samples.* [C] *Indicates PROTOMAP results. MS data has been deposited and is widely available at the PRIDE repository (PXD004205 and 10.6019/PXD004205).*

Naturally occurring peptides

Plasma samples from the same 5 individuals were analysed as described in figure 4.1 for changes in the natural occurring plasma peptides. Only minor changes were observed in peptides assigned to 140 plasma proteins. There was a significant increase in proteolytic peptides derived from nine proteins after 48hrs. These were Rho-GDP-dissociation inhibitor, serum deprivation-response protein, vasodilator stimulated phosphoprotein, complement C4A and the cytoskeletal proteins thymosin beta-4, vinculin, importin and filamin, myosin-9. (figure 4.3C, D).

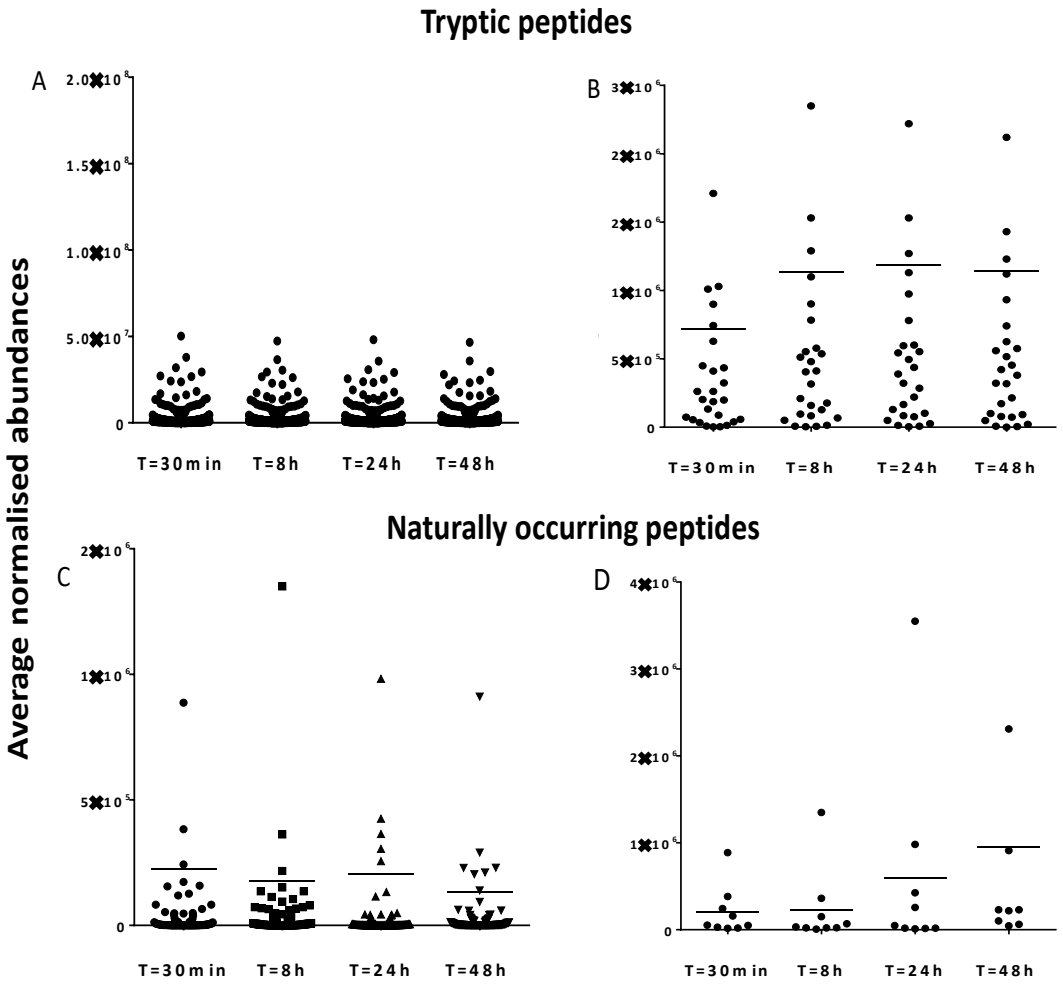

Figure 4.3 Effect of blood storage on plasma proteome and peptidome signatures

*(**A**) Abundance levels of all proteins identified at the indicated times (table 4.S1).*

*(**B**) Abundance levels of significantly regulated proteins (ANOVA $p \leq 0.05$).*

*(**C**) Abundance levels of 140 naturally occurring peptides (peptidome) in plasma observed at the indicated times.*

*(**D**) Abundance levels of nine naturally occurring peptides in plasma that are significantly regulated among the time points (ANOVA $p \leq 0.05$).*

PROTOMAP analysis of whole blood stored at ambient temperature

PROTOMAP analysis was applied to further investigate proteolytic fragments of plasma proteins in whole blood stored at AT. Five pooled plasma samples derived from the whole blood storage conditions of 30 min and 48 hrs were compared and analysed (figure 4.1). The PROTOMAP method compares two conditions (control vs experimental), hence the requirement for pooling[155] (figure 4.2). The PROTOMAP analysis identified 820 unique proteins and generated 2,300 individual peptographs. Notably, only 52 proteins revealed changes between the T=30m and T=48hrs plasma pools, representing less than 7% of the total 820 unique proteins identified. Shortlisted proteins showed patterns of degradation or enrichment, and their selection was based on either:

i) increased spectral counts of fragments that were found in lower gel bands i.e., had a lower molecular mass than the intact protein.

ii) enrichment or unique identification at 48hrs.

From the 52 proteins, 20 were enriched in plasma and 32 showed breakdown products indicating likely proteolysis. Examples of peptographs from these two groups are shown in figures 4.4, 4.5 & 4.6. Peptographs of S100A8, S100A9, annexin A1, platelet glycoprotein 4 and profilin-1 demonstrated enrichment of these proteins at 48hrs as they were identified at the expected molecular mass of 10kDa, 13kDa, 38kDa, 75kDa and 15kDa respectively, for each protein (figure 4.4A). Plasminogen like protein A showed a fragment at around 20kDa in 48hrs blood sample (figure 4.5). Talin-1 showed increased fragmentation of the intact protein (>250kDa) over time with breakdown intermediates observed at 140kDa, 30-40kDa and 15-22kDa at 48hrs (figure 4.4B).

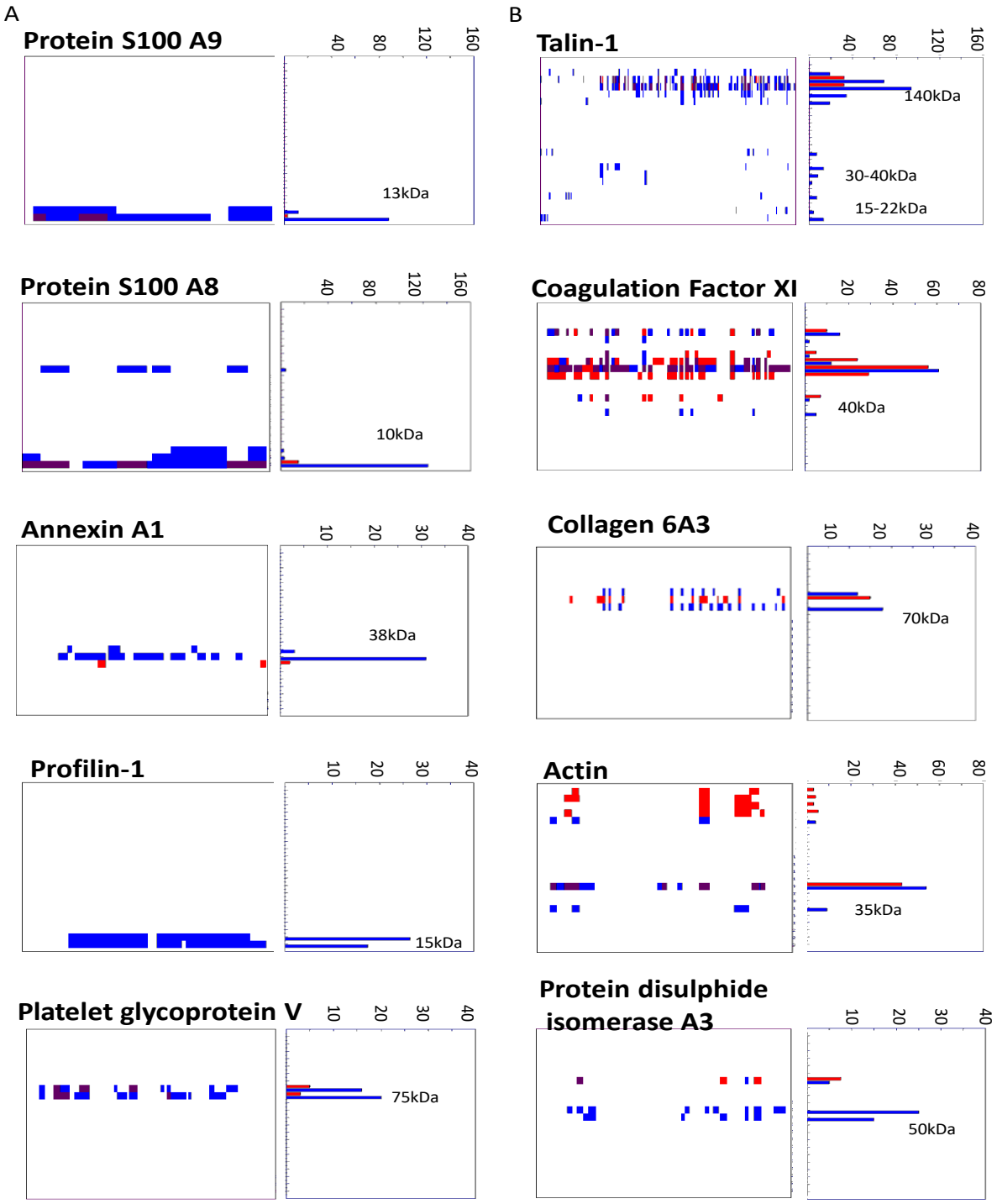

Figure 4.4 PROTOMAP showing enrichment or degradation of plasma proteins as a result of variable blood storage

*(**A**) Protein S100 A9, S100 A8, annexin A1, profiling-1 and platelet glycoprotein V levels are enriched after 48 hrs of blood storage (blue bars) compared to 30 min (red bars). (**B**). Prolonged blood storage indicates partial degradation of talin-1, coagulation factor XI, complement collagen 6A3, actin and protein disulphide*

isomerase-3 as exemplified by their corresponding peptographs (red bars – 30 min; blue bars – 48 hrs blood storage at ambient temperature).

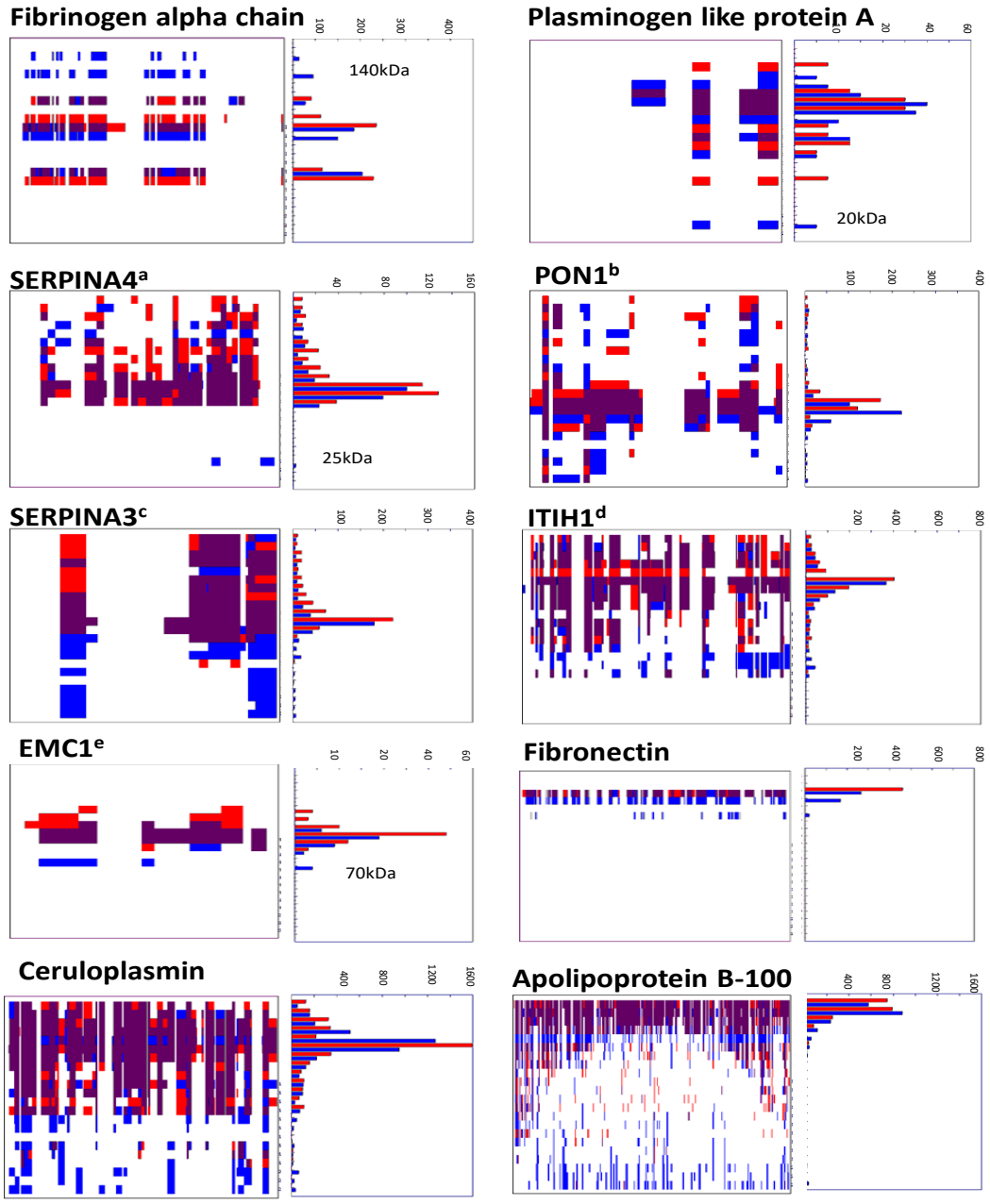

Figure 4.5 PROTOMAP showing plasma protein degradation as a result of variable blood storage

Prolonged blood storage results in partial degradation of some plasma proteins, shown in their corresponding peptographs (red bars – 30 min; blue bars – 48 hrs blood storage at ambient temperature). [a]Corticosteroid-binding globulin, [b]Serum paraoxonase, [c]Alpha-1 antichymotrypsin, [d]Inter aplha trypsin inhibitor,[e] Extracellular matrix protein-1

Coagulation factor XI (CFXI) and complement C3 showed no protein enrichment but the appearance of degradation fragments (Figure 4.4B & 4.6). Alterations to complement proteins are indicated by the peptographs in figure 4.6. A combination of generation of unique protein fragments in lower molecular weight bands and enrichment of certain fragments after 48hrs was demonstrated for all the complement proteins presented in figure 4.6. C5 and C3 showed enrichment of fragments around 80kDa and 50KDa respectively (indicated by green arrows, figure 4.6). C1r and C2 showed clear fragmentation patterns with the generation of fragments in lower molecular weight bands 50kDA and 80kDa respectively (yellow arrows, figure 4.6).

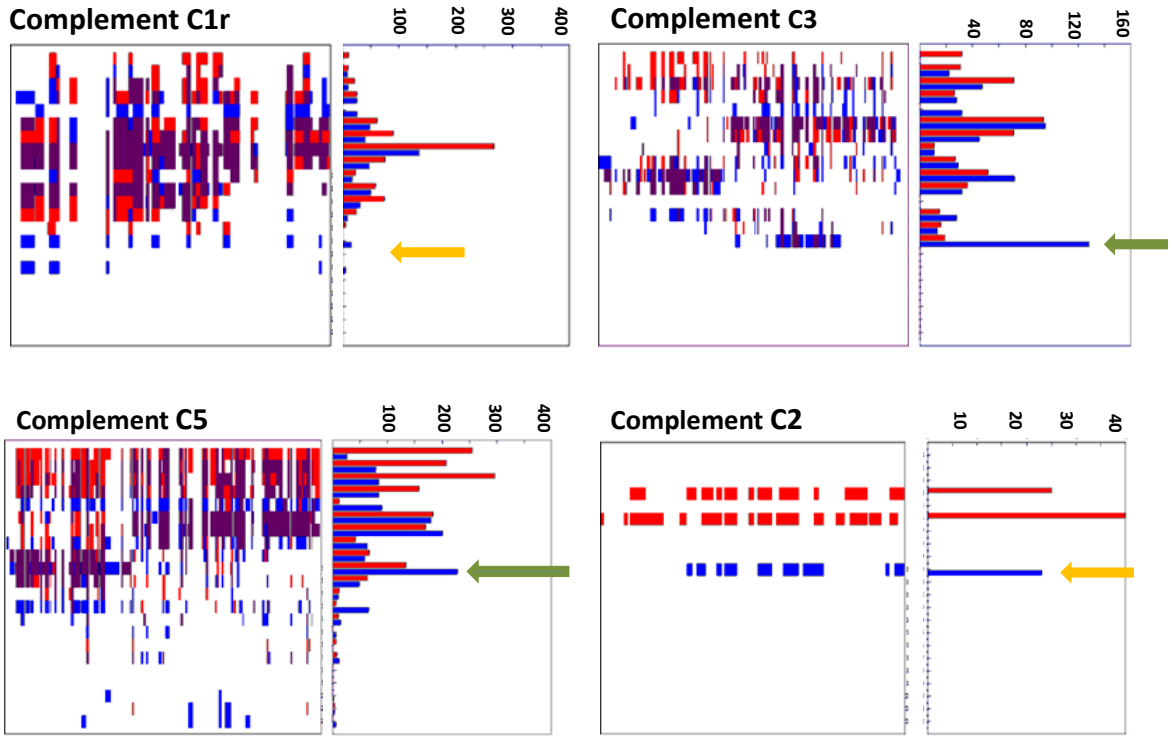

Figure 4.6 PROTOMAP showing enrichment or degradation of plasma proteins as a result of variable blood storage

Complement proteins C1r, C3, C2 and C5 exhibit enrichment for certain fragments (green arrows) and generation of protein fragments (yellow arrows) as a result of degradation as shown by the profile by their corresponding peptographs (Red bars – 30 min; blue bars – 48 hrs blood storage at ambient temperature).

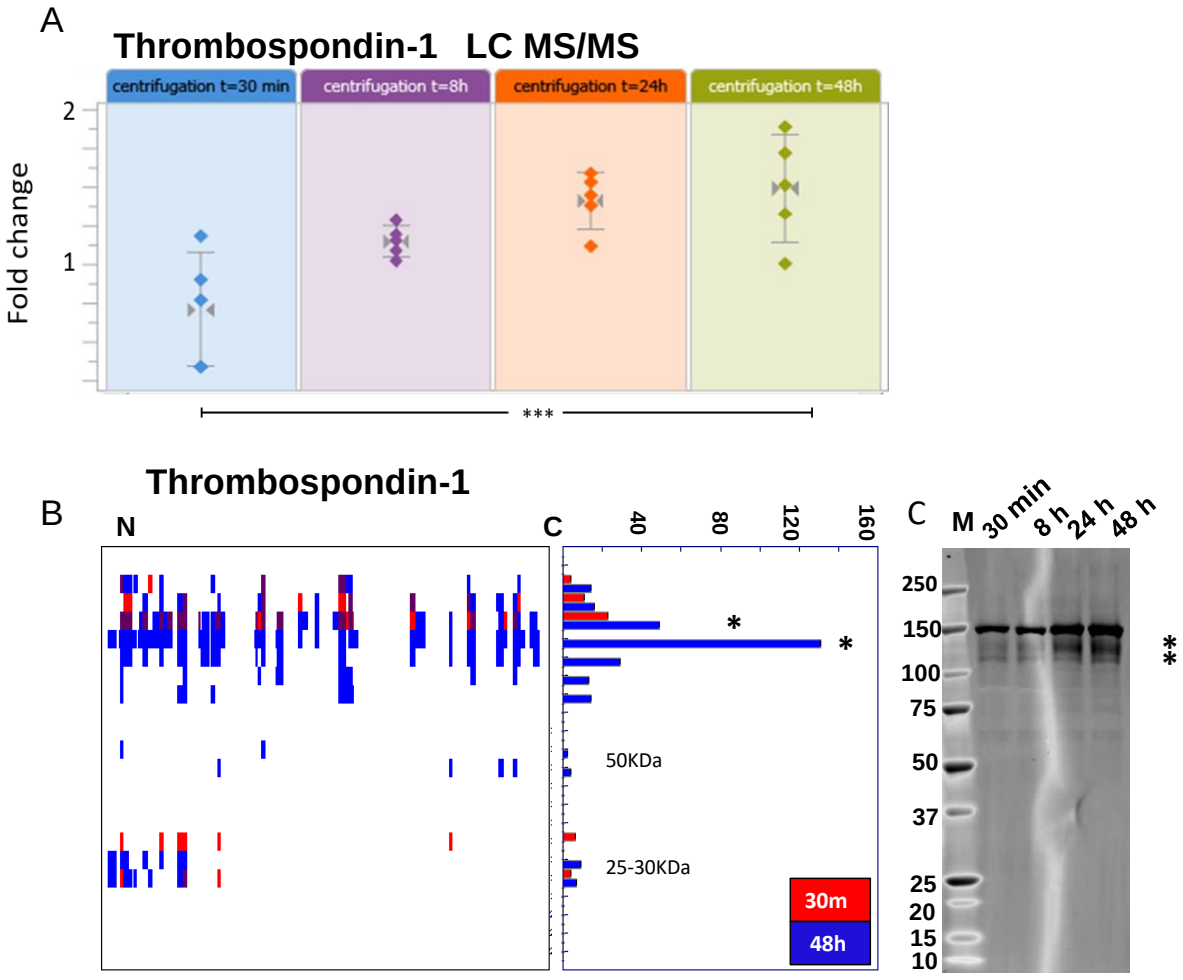

Figure 4.7 Prolonged blood storage affects TSP-1 protein levels and causes protein degradation

(***A***) *Gradual increase of TSP-1 protein levels as indicated by label-free quantitative mass spectrometry analysis of tryptic peptides, indicating a 1.4-fold change after 48 hrs of blood storage ($p<0.001$).* (***B***) *TSP-1 protein degradation patterns as observed by the PROTOMAP peptograph (red bars – 30 min; blue bars – 48 hrs) and confirmed by western blot analysis at the indicated times. The stars indicated in the PROTOMAP peptograph correspond to the bands in the 120-150 kDa region observed in the western blot, suggesting an increase in protein levels as well as partial degradation.*

Confirmation of protein fragmentation by western blot

Protein degradation profiled by PROTOMAP was confirmed by western blotting for thrombospondin-1 (TSP-1) and complement C4B. TSP-1 increased gradually to a maximum fold of 1.4 in the T=48hrs compared against the T=30 min sample as shown by LC-MS/MS analysis (figure 4.7A). PROTOMAP analysis showed an increase level of intact protein (~150kDa) and the appearance of protein fragments within the 80 to 150kDa range and an N-terminal proteolytic fragment of ~25kDa (figure 4.7B). Western blot validation of plasma TSP-1 for all four conditions indicated a gradual increase in TSP-1 protein levels correlating with the time of blood storage at AT (figure 4.7B). The predicted size of intact TSP-1 was 133kDa. However, PROTOMAP and blotting revealed a storage time-dependent accumulation of protein species in the range of 120 to 150 kDa, most likely due to increased cellular secretion and proteolytic processing.

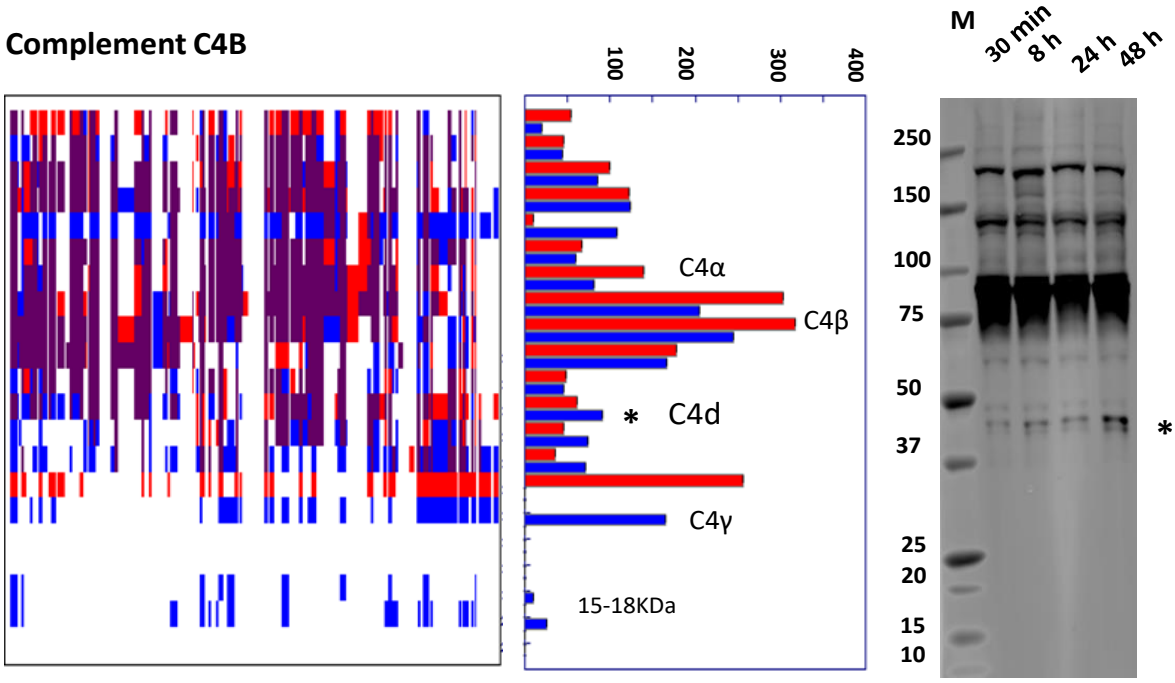

Figure 4.8 Minimal proteolysis of complement C4B upon blood storage
Blood sample pools centrifuged after 30 min and 48 h of storage at ambient temperature were analysed by PROTOMAP (red bars – 30 min; blue bars – 48 hrs) and anti-complement C4B western blotting. The 40kDa fragment highlighted with a star (*) was increased as shown by the PROTOMAP peptograph, corresponding to a degradation intermediate also detected by western blotting. This fragment corresponds to C4d component. Two more fragments of lower MW were increased in the PROTOMAP peptograph, corresponding to ~18 and ~30kDa.

C4B complement protein was identified in plasma at ~200kDa with predominant fragments at 100kDa and 75kDa corresponding to α chain and β chain, respectively[166]. No difference in the level of these proteins was observed between 30 min and 48hrs storage with western blot analysis (figure 4.8). Notably, a cluster of fragments between 35-40kDa potentially corresponding to the C4d complement protein[166] was gradually increased with storage time as confirmed by western blot analysis (figure 4.8). The C4B peptograph indicates the generation of two more C4B derived fragments at ~30kDa that might correspond to C4 γ chain and an additional fragment at ~15kDa[166], which were not detected by blotting. Combined, these results indicated partial proteolytic processing of a small sub-fraction of members of the complement cascade upon blood storage (figure 4.6 & 4.8).

4.5 Discussion

Blood is the most common clinical sample collected in biobanks. The purpose of this study was to optimise the quality of clinical samples whilst establishing a UK biobank in organ donation and transplantation (QUOD) collecting biomaterial from more than 60 hospital sites including out-of-hours and at week-ends[137]. Here, different blood storage times were assessed as a pre-analytical factor that could impact on proteomic analysis and introduce a bias on selection of candidate proteins in biomarker discovery studies. Despite a general tendency in bio-banking to store whole blood in hypothermic temperatures of around 4°C prior to sample processing, the QUOD protocols stipulated that whole blood samples should remain at AT prior to plasma preparation. The rationale behind this was to minimize platelet and leucocyte activation and the subsequent release of cytosolic proteins and enzymes that could constitute a potential source of bias or alter the integrity of plasma proteins[161]. Remarkably, when we compared samples stored between 30 min and 48 hrs less than 4% of the identified 430 proteins were found to be altered. The majority of the altered proteins were of cellular origin. Amongst them was cystatin-c (CysC), a non-glycosylated, low molecular weight protein continuously secreted by all nucleated cells (table 4.1 & 4.S1). CysC is freely filtered from blood into kidney glomeruli and provides an estimation of glomerular filtration rate. CysC is a well-described biomarker of kidney function[167,168]. In the first eight hours of blood storage, the levels of CysC had already increased by 1.3 fold, suggesting an initial stimulation that caused cellular secretion irrelevant of disease or other physiological changes.

The limited impact of AT in plasma proteome dynamics was consistent with the study by Aguilar-Mahecha *et al.,* reporting minimal variability on medium to high

abundant plasma proteins when whole blood remained at *AT* for up to 6 hrs as opposed to storage and processing at 4°C[169]. Also, in the same study, no benefit in protein stability was found when blood tubes containing proteinase inhibitors were used for whole blood remaining at AT up to 6 hrs. In the present study, as shown in figure 4.3, when naturally occurring peptides in plasma by LC-MS/MS were analysed, fragments from a small number of proteins were identified, even after 48hrs storage.

Proteolysis is an intrinsic homeostatic phenomenon in blood, and for the consideration of proteolytic protein fragments to be potential biomarkers, the degree of plasma proteolysis due to collection and storage conditions was investigated. The plasma peptidome (derived from protein degradation) has been a source of novel biomarkers for human diseases including transplantation[170–173]. PROTOMAP analysis was applied to assess plasma proteolysis. Two extreme conditions, 30 min and 48hrs, were selected to demonstrate the full effect of proteolysis, reflecting blood specimens collected in the clinic and remaining at AT over prolonged times or weekends prior to diagnostic analysis. To provide insights into proteolysis dynamics, SDS-PAGE based fractionation prior to LC-MS/MS analysis extended the number of plasma proteins identified to 820. For 20 proteins, enrichment and the appearance of protein isoforms that were uniquely identified in the 48hrs pool were observed and 22 proteins exerted a clear proteolysis profile (figure 4.4 & 4.5 & 4.6). Thrombospondin-1 (TSP-1) was identified in both, LC-MS/MS and PROTOMAP analysis (figure 4.7A&B). A gradual increase in TSP-1 levels was observed between 30 min, 8hrs, 24hrs and 48hrs and also confirmed by western blotting (figure 4.7B). TSP-1, a 450kDa matricellular protein, is one of the main

constituents of alpha granules released from platelets following activation. Upon release, TSP-1 undergoes proteolysis to generate several fragments in the 140-, 75-, 50- and 25kDa range[174]. PROTOMAP analysis revealed an increase in the 150kDa fragment with additional fragments in the range of 50 – 150kDa. Notably, a 28kDa N-terminal fragment was found to be moderately enriched in the 48 hrs condition (figure 4.7). This N-terminal peptide may be a heparin binding domain that derives from serine-dependent proteolysis within the platelet α granules[174–177]. This heparin binding peptide subsequently migrates to the platelet membrane to interact with the actin cytoskeleton and fibrin to stabilise platelet aggregates during platelet activation. It is currently unknown whether the release of this fragment was the result of degranulation due a low degree of platelet activation or whether it has been shed in plasma from platelet membranes. Changes in circulating levels of TSP-1 fragments have been considered as potential biomarkers of tumour cell metastasis, inflammation, haemostasis and thrombosis[178–180]. Pre-analytical variability of TSP-1 as described here may provide a baseline for more accurate diagnostic assessment in plasma samples.

PROTOMAP also detected proteolytic fragments of the complement proteins C1r, C3, C4B and C5 (figure 4.6 & 4.8). Activation of platelets, even to a low degree, can activate and propagate the complement system[181]. Similarly, the circulation of complement fragments in plasma can trigger platelet activation. Potential triggers of platelet activation can be particles that are released or shed from white cells such as neutrophils or simply from the sheer stress to blood extracted from the vascular system during collection.

4.6 Conclusion

This study revealed remarkably few changes in plasma proteome dynamics, suggesting that within the clinical setting with the many challenges associated with QUOD sample collection whole blood that remains at ambient temperature undergoes limited alterations and the integrity of samples is maintained. In addition, a baseline proteomic signature was defined that could be used for the selection of proteins as potential biomarkers of donor organ quality. As protein fragments can be considered as markers of donor organ quality mapping the degradome profile of plasma samples stored for up to 48hrs at AT has shown that only limited plasma protein degradation takes place. Therefore, it gives reassurance that those products of degradation identified as candidate biomarkers result from predictable changes to blood physiology and do not arise from the way samples are stored prior to processing.

CHAPTER 5

Donor serum and urine proteomic signatures differentiate between immediate and delayed graft function

5.1 Introduction

The persistent shortage of donor organs for transplantation has resulted in long waiting lists for life saving transplants and has urged the transplantation community to utilise donor organs that previously would have not been considered suitable. To reduce morbidity and mortality for patients waiting for a transplant the deceased donor pool has been expanded to include so-called 'marginal donors', which include organs from donors after circulatory death (DCD) or older donors after brain death (DBD). Allografts transplanted from these donors have suboptimal outcomes compared to standard criteria donors (SCD) following transplantation[44,182–184].

Despite the need for higher donation rates the UNOS registry data shows that 43% of kidneys obtained from ECDs (chapter 1, figure 1.4) are discarded in the USA due to the uncertainty of kidney function and graft survival following transplantation[85]. Early kidney dysfunction in the recipient manifests itself as Primary Non Function (PNF) or Delayed Graft Function (DGF) requiring dialysis treatment within the first week post transplantation and may result in complications, prolonged hospitalisation and increased risk of chronic allograft dysfunction over the long-term. The incidence of both PNF and DGF is significantly increased in the recipients of kidneys obtained from ECDs and DCDs and donor age has been shown to be a strong independent predictor for DGF development[30,185].

Following transplantation, 24-50% of recipients of deceased donor kidneys develop DGF which makes it a common post-transplant complication[65,186]. The impact of DGF on the graft survival and long term allograft function has been

debated extensively. The incidence of DGF is higher in recipients receiving kidneys from DCDs compared to DBDs (49% and 24% respectively)[41]. Interestingly, the recipients who receive DBD kidneys and develop DGF are more likely to have significantly reduced kidney function 12 months post-transplantation and reduced graft survival 5 years post-transplantation compared to recipients who do not develop DGF[66,67]. Conversely, recipients of DCD kidneys who develop DGF have no long term adverse outcomes when compared to recipients whose kidneys function immediately post-transplantation. The observed differences between deceased donor subgroups suggest that diverse biological mechanisms determine the onset and recovery from DGF and long term allograft function[51,66,67,187].

The onset of DGF following engraftment is a form of acute kidney failure that results from a multifactorial sequence of biological events that are triggered by the process of donation and transplantation. As discussed in chapter 1, the development of ischaemia during donor management and organ procurement is further propagated by cold preservation and the maximum extent of injury occurs when the kidney is perfused with warm recipient blood. Ischaemia reperfusion injury (IRI) plays a key role in the development and progression of DGF[29,35].

The pathophysiological changes which arise from brain death in DBDs and an anoxic period during storage at hypothermic temperatures results in metabolic dysfunction with resultant mitochondria dysregulation and progressive oxidative stress. The generation of reactive oxygen species from mitochondria dysregulation provokes an inflammatory response with the release of pro-

inflammatory cytokines such as tumour necrosis factor α (TNFα) and *Interleukins* IL-6, IL-8 and IL-1β that further promote damage to cellular components triggering apoptotic processes and necrosis[23,135,188–190]. Upregulation of adhesion molecules such as ICAM-1, V-CAM, P-selectin, E-selectin with consequent invasion of leukocytes, macrophages and neutrophils into interstitial or proximal tubular cells promote allograft immunogenicity and kidney ischaemia[189,191].

The process of IRI is complex with a range of inflammatory mediators such as T cells, B-cells, antigen presenting dendritic cells (DC), complement activation and endothelium injury occurring in kidney compartments. Loverre *et al*., examined the role of different subtypes of DC (myeloid and plasmacytoid) in the development of DGF. Increased numbers of myeloid dendritic cells (injury promoting cells) were detected in the tubulointerstitial area of allograft kidneys after acute rejection and in kidney biopsies of recipients with DGF while the tolerance promoting plasmacytoids were not significantly increased. The study concluded that myeloid DCs were increasing immunogenicity and activating the innate immune system which, in turn, could elicit an adaptive immunoresponse leading to acute graft rejection[187].

Donor related factors such as pre-existing chronic kidney disease and donor age could predispose DBD kidneys to injury during CIT and IRI thus increasing susceptibility to developing DGF with lower graft survival[192].

To date, there are no robust and clinically relevant markers to predict DGF and the extent of kidney injury associated to DGF.

Research into identification of new biomarkers has suggested the potential utility of NGAL, IL-18 and L-FABP and, most recently, clusterin protein to diagnose and

monitor DGF. However, published studies have been conducted on small sample cohorts and the lack of validation in prospective studies has meant that none of these candidate biomarkers have yet to be properly tested or implemented into clinical practise[116,193–195].

This chapter explores the feasibility of a clinical proteomics approach to provide a detailed assessment of kidney quality at the point of retrieval and to identify the kidneys that will develop DGF in the recipient.

As a first step in this process, a study was designed to compare the proteomic profiles of serum and urine samples obtained from DBD and DCD donors whose kidneys had either functioned immediately or had delayed function after transplantation.

Study limitations

All the samples for this study were from the PROMETHEUS bio-resource, University Medical Centre, Groningen (UMCG), The Netherlands. This study was conceived as a pilot study to test the feasibility of the experimental approach and therefore only a limited number of samples were analysed for each experimental group. Serum samples were pooled for the initial proteomic work. After completion of the experimental work and subsequent analysis, a request to the UMCG for additional demographic and follow-up clinical data on the recipients revealed that errors had occurred in the initial classification of the samples associated with either IF or DGF. As pooled serum samples had been analysed it was not possible to remove erroneous assigned samples from the data set and reanalyse the results. However, urine proteomic analysis had been performed on individual samples and data from these samples were then reanalysed. The

limited availability of clinical samples at this stage of my project meant that it was not possible to repeat this work or to further confirm the proteomic findings by blotting or ELISA immunoassay.

5.2 Hypothesis and aims

This work in this chapter set out to tests the two following hypotheses:

i) That it is possible, on the basis of a serum proteomic profile, to discriminate between living donors (LD) and deceased donors

ii) Using a non-biased approach, it was possible to identify alterations in the donor serum and urine proteome that could correlate with the onset of delayed graft function in the transplanted kidney, defined as the need for dialysis within the first week after transplantation.

5.3 Methods

Sample groups

Serum and urine samples were obtained from three donor groups, LD (n=10), DBD (n=10) and DCD (n=10) as shown in figure 5.1. All LD kidneys functioned immediately post-transplantation and acted as the control group. DBD and DCD kidneys were subdivided into DGF post-transplant (n=5) and IF (n=5).

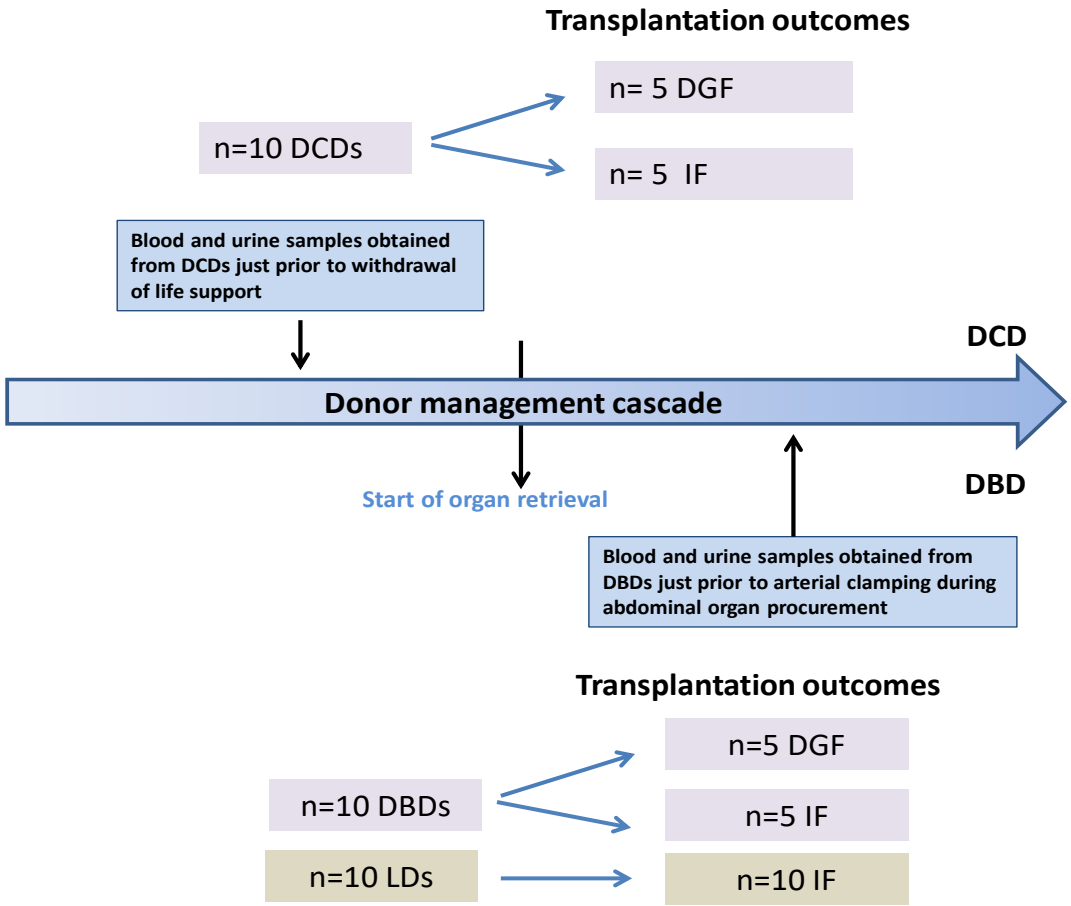

Figure 5.1 Experimental groups analysed in this study
Samples were collected from DCDs prior to withdrawal of life support while samples from DBDs and LDs were collected just prior to arterial clumping during kidney procurement. DFG: delayed graft function in the recipient; IF: immediate function in the recipient.

Donor sample characteristics

Donor serum and urine samples were obtained from the PROMETHEUS bio-resource, University Medical Centre Groningen, The Netherlands. Donor and recipient demographic and clinical baseline data characteristics are summarised in table 5.1. To define whether the association of transplantation outcomes was independent of the donor and recipient age, Student t-test statistical analysis was performed, with a statistical significant level defined as $p \leq 0.05$ (table 5.1).

Table 5.1: **Donor demographics and clinical characteristics**

Donor variables	DBD (DGF) (n=5)	DBD (IF) (n=5)	p- value	DCD (DGF) (n=5)	DCD (IF) (n=5)	p- value	LD (IF) (n=10)
Age (yrs)*	33.8 ± 8.7	42.8 ± 10.2	P=0.52	57.2 ± 2.3	41.6± 9.4	P=0.14	40± 10.5
Gender (M:F)	1:4	1:4		2:3	2:3		4:6
Cause of death (%):							
CVA	2	3		2	3		
Trauma	2	1		1	1		
Other	1	1		2	1		

*indicates mean +/- SD

P values comparing the mean age of donors in each outcome cohort obtained using Student t-test. Baseline statistical difference was defined as $p \leq 0.05$.

Experimental design

Three different proteomic experiments were performed in this study. The experimental design is shown in figure 5.2. The first experiment was a proteomic comparison of serum obtained from three donor type; LDs, DBDs and DCDs. (figure 5.2A). The second experiment was a comparison of pooled donor serum samples on the basis of DGF or IF following kidney transplantation (figure 5.2B). The third experiment was a comparison of individual urine samples within each donor type (DBD, DCD) on the basis of DGF vs IF.

Serum proteomic analysis was conducted by GeLC-MS/MS, described in chapter 3.4.3, to achieve protein fractionation and allow the detection of lower abundant proteins (figure 5.3). As discussed in chapter 3.3 and figure 3.3, serum is a protein rich medium with a range of protein abundances that extends 12 orders of magnitude. GeLC-MS/MS included a 1-D SDS-PAGE protein separation protocol and subsequent division of the gel into three bands to generate three samples for analysis for each initial clinical sample (figure 5.2B). As LC-MS/MS analysis is expensive and this was intended as a pilot study, costs were reduced by pooling small number of samples with the same characteristics (figure 5.2A & B). Furthermore, a pooling approach has as a consequence of 'levelling out' biological heterogeneity between clinical samples while signals common across pools are enhanced. Compared to plasma or serum, urine contains fewer high abundant proteins. Consequently, the urine proteome is less complex. This enabled donor urine samples to be analysed by LC-MS/MS as individual samples without pre-fractionation. The most abundant protein, albumin, was depleted prior to LC-MS/MS analysis using a chemical depletion protocol as described in chapter 3.4.5. The experimental design is shown in figure 5.2C.

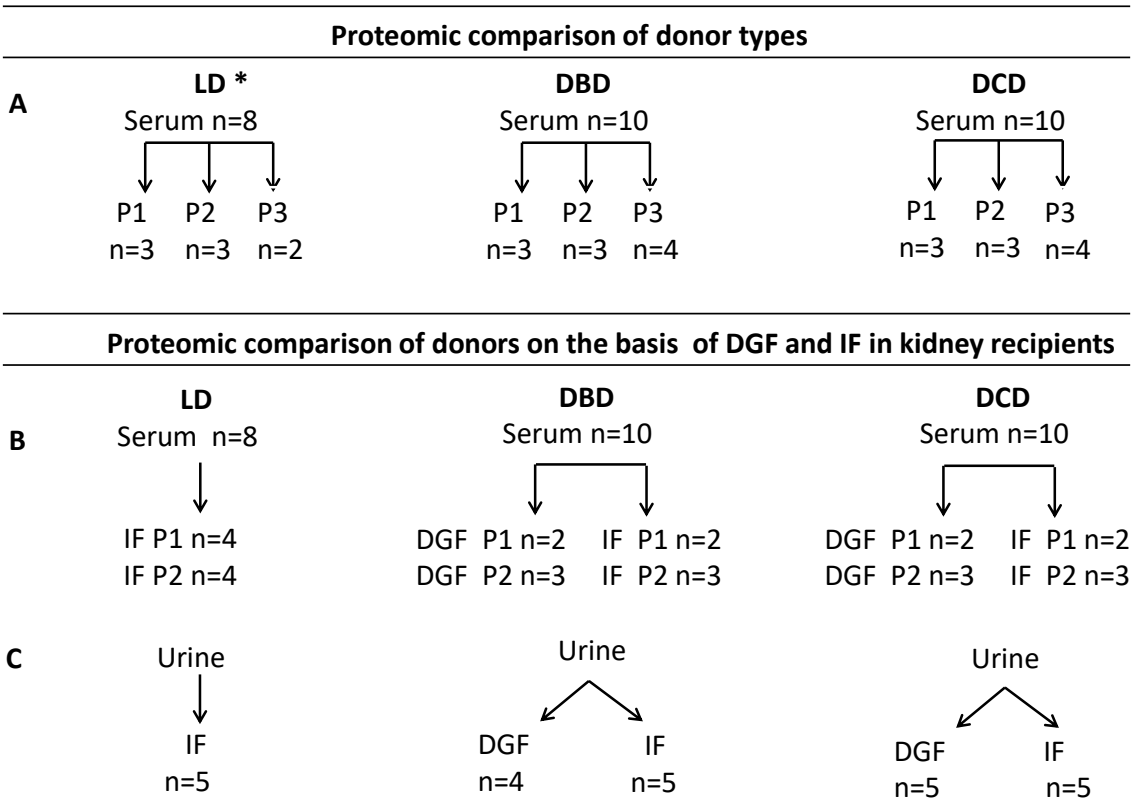

Figure 5.2 Experimental design

(A) *Proteomic comparison of serum obtained from three donor types. Serum samples from LDs (n=8), DBDs (n=10) and DCDs (n=10) were combined to create three pools within each donor type P1, P2 and P3.* ***(B)*** *Donor serum proteomic comparison on the basis of DGF or IF following kidney transplantation. Serum samples from LDs (n=8), DBDs (n=10) and DCDs (n=10) were grouped according to the incidence of DGF or IF in kidney recipients. Samples within each subgroup were combined to generate two pools P1 and P2 for mass spectrometry analysis. LD serum samples were associated only with IF.* ***(C)*** *Donor urine proteomic comparison on the basis of DGF or IF following kidney transplantation. Urine samples from the same donors were grouped according to the incidence of DGF or IF post transplantation and analysed individually. There were only four urine samples from DBD donors whose kidneys developed DGF.*

*n=10 LD samples were received from PROMETHEUS biobank but two samples were found to be haemolysed and not included in this study; therefore n=8 were analysed.

Proteomic comparison of serum samples from living and deceased donors

Serum samples from three donor groups LD (n=8), DBD (n=10) and DCD (n=10) were obtained from the PROMETHEUS biobank. Although 10 LD samples were obtained, two were haemolysed so only 8 serum samples were used (figure 5.2A). Serum samples were immunodepleted to remove the 14-most abundant proteins to increase the sensitivity of detection for low abundant proteins as described in chapter 3.4.1 (figure 5.3A). Following immunodepletion, three pooled samples P1, P2 & P3 were generated from each donor cohort to a total volume of 150µl (figure 5.2 A). For LD (n=8) P1 & P2 were generated by pooling three serum samples (50µl/ sample) and P3 by pooling two (75µl/ sample) while for the DBD (n=10) and DCD (n=10) samples, P1 & P2 were formed by pooling three serum samples (50µl/ sample) and P3 by pooling four (37.5µl/ sample). Protein precipitation was performed and the pellets were solubilised in 1x SDS reducing sample buffer (chapter 3.4.2). Equal amounts of protein per pooled sample were separated by SDS- PAGE to allow consistency in the comparison and relative quantitation of ion intensity between samples (figure 5.3B).

Protein fractionates were visualised by Coomassie Instant Blue staining and the gel was divided into three bands. Each band was analysed separately. Captured proteins were reduced and alkylated prior to tryptic digestion. Peptide digests were extracted from the gel matrix and analysed by LC-MS/MS (Thermo LTQ Orbitrap Velos) (chapter 3.4.3 and 3.5.1).

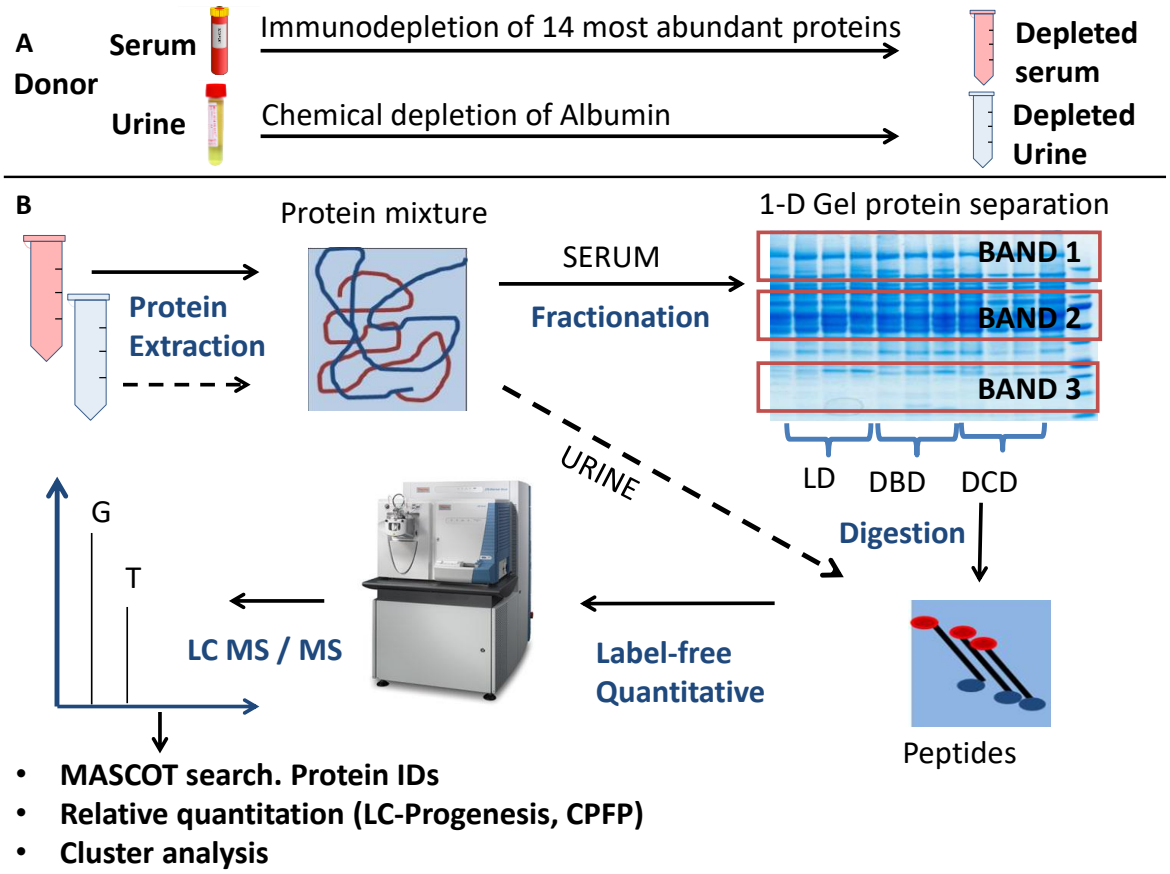

Figure 5.3 Serum and urine proteomic workflow and bioinformatics analysis

(A) *Serum samples were immunodepleted to remove the 14 most abundant proteins. Urine samples were chemically depleted to remove albumin (protocols are described in Chapter 3.4)* ***(B)*** *Proteins were precipitated from the depleted serum and urine samples. Precipitates were fractionated by 1-D gel electrophoresis, visualised by staining the gels with Coomassie Instant Blue and divided into three bands. Each band was analysed separately. Captured proteins were reduced and alkylated prior to tryptic digestion. Peptide digests were extracted from the gel matrix and analysed by LC-MS/MS in duplicates (Thermo LTQ Orbitrap Velos). The urine protein precipitates were trypsin digested and analysed by LC-MS/MS in duplicate. Analysis of the data is described in the method protocol.*

Proteomic comparison of serum and urine samples from donors on the basis of DGF and IF post-transplantation

Comparison of serum of donors whose kidneys either developed DGF or functioned immediately (DBD: DGF (n=5), IF (n=5), DCD: DGF (n=5), IF (n=5), LD: IF (n=8)) was performed as described in figures 5.1 and 5.2B. For all the experimental cohorts two pooled samples were formed, P1 & P2 (figure 5.2B). P1 was generated by combining two samples and P2 by combining three. LD pools were formed by combining four samples per pool. Serum proteomic comparison of DGF and IF within the DBD and DCD cohort was performed by GeLC-MS/MS (chapter 3.4.3 and 3.5.1) (figure 5.1B, 5.2 & 5.3). LDs were used as a control group. Overall, there were four incorrectly allocated samples, one in each outcome DGF & IF in both DBD and DCD groups. The impact, therefore, would be to decrease any observable differences in the analyses between DGF and IF in the deceased donors.

Urine samples were obtained from the same donors as above and analysed individually using the in-solution digestion protocol described in chapter 3.4.5. Five urine samples per transplantation outcome (DGF or IF) were analysed for each donor type with the exception of DGF associated samples within the DBD cohort as urine was available only from four donors (figure 5.2C).
Equal volumes of urine per sample were processed. Following depletion of albumin, urine, protein precipitation precipitates were digested with trypsin using an in-solution protocol and analysed by LC-MS/MS (chapter 3.4.1).

Bioinformatics analysis

Raw MS data obtained from the serum GeLC-MS/MS analysis were processed using PROGENESIS-LC software (version3.1.4003.30577) and CPFP bioinformatics as described in chapter 3.5.3 and 3.5.4. MS/MS spectra were searched against the IPI human database using MASCOT allowing one missed cleavage and 20ppm/0.5Da mass deviations for MS and MS/MS ions with a discovery false rate (FDR) of less than 1%. Only proteins that were defined with at least two peptides were included in the protein data set for further analysis.

Statistical comparison of protein abundance changes were made in the following experimental groups: DBD versus LD and DCD versus LD in the first experimental analysis and DGF versus IF in DBDs and DGF versus IF in DCDs in the second analysis. P values for statistical comparison were obtained by the PROGENESIS-LC software using a two sample ANOVA test. When CPFP analysis was performed the statistical comparison between pools was performed using unpaired t-test samples. $P \leq 0.05$ was considered the cut off for statistical significance. Relative protein quantitation data sets obtained from both CPFP and PROGENESIS-LC were used to provide a more comprehensive list of proteins.

Proteins with at least a two-fold change in abundance and with $p \leq 0.05$ significance between donor groups (pools or individual urine samples) were selected for further analysis.

Supervised HCA analysis included all the proteins significantly regulated among the experimental groups (fold change ≥ 2, $p \leq 0.05$, ANOVA) using the PermutMatrix software[158] with Euclidean distance and the complete linkage as default algorithms. Pathway analysis was performed using STRING

bioinformatics http://string-db.org/cgi/network.pl software using the significant regulated proteins. STRING bioinformatics compares a list of shortlisted proteins against curated databases and maps them onto existing canonical pathways providing the most likely direct associations with other proteins that participate in the same pathway. The analysis calculates a confidence score which indicates the probability that the observed protein – protein interactions has occurred by chance. The lower the false discovery rate (FDR) is the higher the probability that the protein – protein interaction and the assigned pathways are true.

Urine LC-MS/MS raw data were processed and proteins identified and quantified using an 'in-house' bioinformatics tool pipeline CPFP[144]. The reason for using CPFP only for urine MS data is that it was not possible to align the chromatograms of the different mass spectrometer runs of the samples by PROGENESIS-LC due to the varied protein content of the donor urine samples. CPFP software calculates the normalised spectral index quantitation (SINQ) based on the sum of the intensity of matched fragments for all spectra that define a protein[144,145].

Unsupervised HCA was performed for the individual urine samples using the same parameters as described previously in the serum proteomic analysis. As the number of the shortlisted significant proteins in urine proteomic analysis was small supervised HCA was not performed. HCA analysis is described in chapter 3.5.5.

5.4 Results

Serum proteomic comparison between living and deceased donors

The serum proteomic comparison of LD versus deceased donors resulted in the identification of 301 proteins with at least two unique peptides identified in the analysis and FDR <1%. . 107 proteins were significantly altered ($p \leq 0.05$; ANOVA). 85 proteins showed at least a two-fold change in their abundance between LDs and deceased, 50 of these proteins with increased levels in LDs and 35 with increased levels in deceased donors (figure 5.4, table S5.1). Supervised HCA per gel band of the 85 proteins that were statistically regulated with at least two-fold change in abundance showed that the proteomic signatures of DBD and DCD cohorts were similar and distinctive from LD (figure 5.4). It was interesting to observe that some proteins were identified in more than one band. This may have been caused by the presence of isoforms, protein degradation resulting in protein fragments or the process of cutting across protein bands when dividing the gel resulting in some proteins being present in adjacent gel pieces.

From the 85 statistically significantly proteins, 6 proteins were associated to blood coagulation, 4 proteins to signalling pathways, 3 to plasminogen cascade, 7 to complement activation cascade and 6 to cell death.

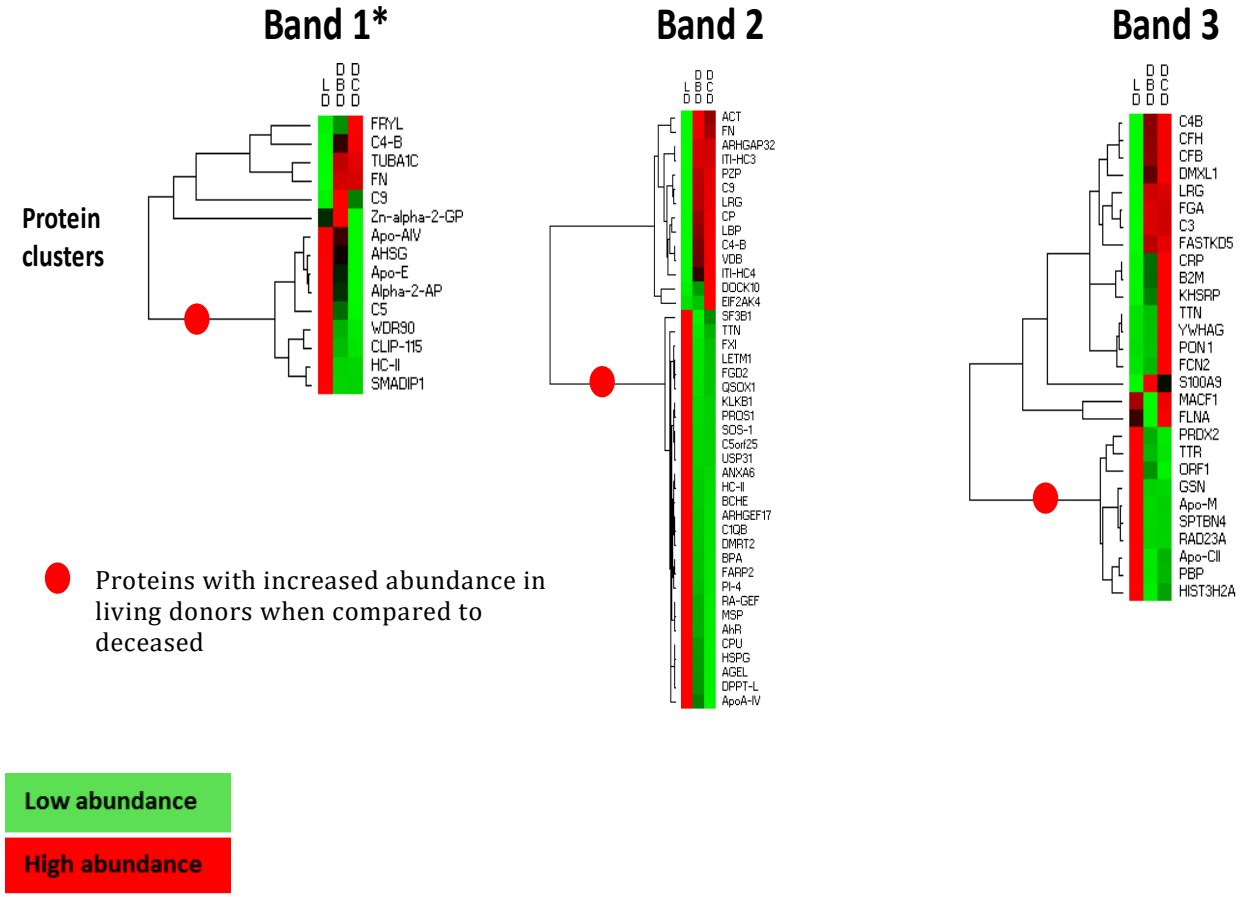

Figure 5.4 Serum proteomic signatures associated with three donor types: LD, DBD and DCD

Supervised HCA of all significantly ($p \leq 0.05$, ANOVA) regulated proteins with at least two fold change in their abundance (up-regulated and down regulated) among the three donor types.

**Bands refer to protein gels bands of GeLC-MS/MS analysis. Red represents high and green low abundance of the identified proteins. HCA algorithm: complete linkage and Euclidean distance.*

HCA: hierarchical clustering analysis

Comparison of proteomic profiles of serum samples from DBD donor kidneys with DGF or IF

DGF was compared with IF in DBDs by proteomic analysis of pooled serum. Profiles from LDs, who all had IF, were used as controls. Overall, 640 proteins were identified. Unsupervised HCA of all the 640 proteins is shown in figure S5.1. 130 proteins were at least two fold significantly regulated (up- and down-regulated) in the DGF related samples compared to IF or LD samples ($p \leq 0.05$, ANOVA). Supervised analysis of the 130 significantly regulated proteins was performed for each gel band and showed that there was a higher degree of similarity between proteomic signatures of LD and DBDs with IF than between these two groups and DBDs with DGF (figure 5.5). 116 proteins were significantly up-regulated by at least two fold in DGF when compared to IF (table S5.2). Of these 116 proteins, five were associated cytoprotective pathways, two uniquely assigned to the DGF subgroup (table 5.2). 44 proteins were assigned to cell death pathways with 11 unique to the DGF subgroup (table 5.3). Eight proteins were assigned to the glycolytic pathway (figure 5.7).

String pathway analysis was applied to identify the most probable direct associations between the significantly regulated proteins in each pathway. String analysis of all the 130 proteins indicated that among the predominant activated pathways were the response to cellular stress (figure 5.6, n=56 proteins; FDR:$9E10^{-13}$), regulation of MAPK and JNK cascades (figure S5.2, n=14 proteins; FDR: $4E10^{-5}$), glycolytic pathway (figure 5.7, n=8 FDR: $5E10^{-15}$).

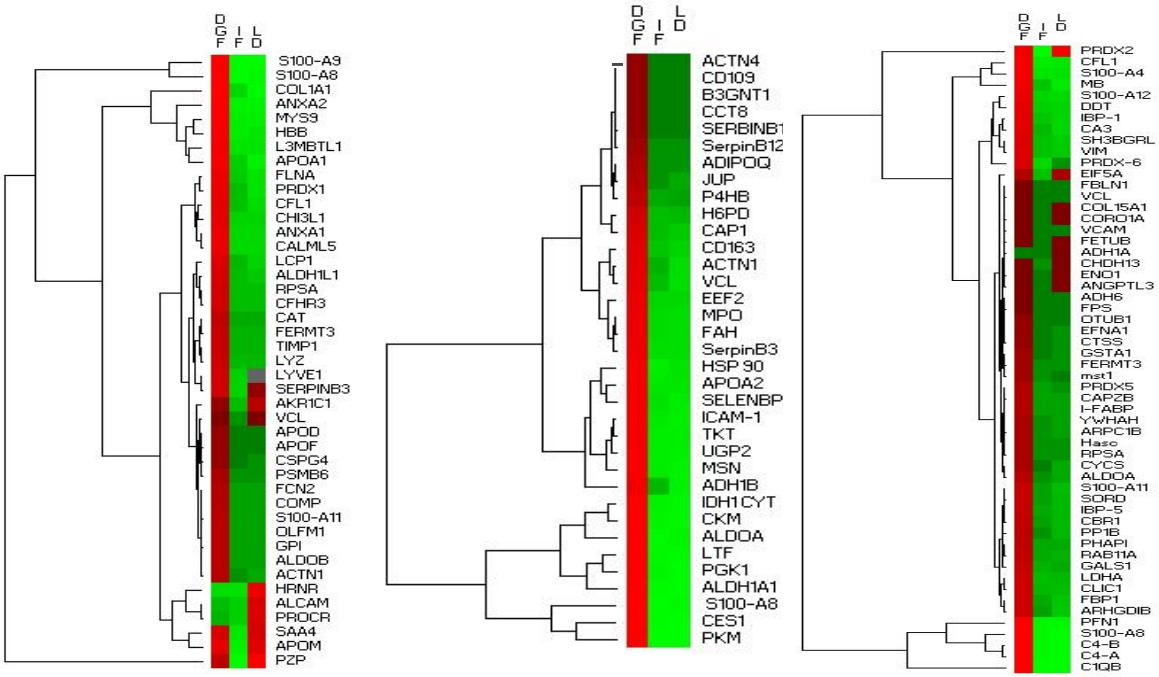

Figure 5.5 DBD serum proteomic signatures associated with DGF and IF in kidney recipients

Supervised HCA of 130 significantly (fold≥2, p ≤0.05, ANOVA) regulated proteins in DBD subgroups, DGF and IF, and LDs in each gel band as analysed by GeLC-MS/MS. Red represents high and green low abundance of the identified proteins Relative protein abundance values were obtained from the analysis using bioinformatics software PROGENESIS-LC.

Table 5.2 **Cytoprotective proteins enriched in DGF associated DBD serum samples**

Entrez Gene name	Description	Fold Change (DGF vs IF)
CAT	Catalase	DGF
TXN	Thioredoxin	DGF
PRDX2	Peroxiredoxin 2	3.80
PRDX1	Peroxiredoxin 1	3.00
PRDX5	Peroxiredoxin 6	2.30

(p ≤0.05, ANOVA); DGF in the fold change column indicates proteins uniquely identified in the DBD-DGF kidneys.

Table 5.3 Proteins enriched in DGF associated DBD serum samples assigned to cell death pathways

Entrez Gene name	Description	Fold Change (DGF vs IF)
IGF2R	Cation-Independent mannose-6 phosphate receptor	DGF
ANXA2	Annexin A2	DGF
FERMT3	Fermitin family homologue 3	DGF
ALDH1A1	Apolipoprotein A-I	DGF
MSN	Myosin	DGF
SERPINE1	Plasminogen activator Inhibitor 1	DGF
GPI	Glucose-6-phosphate isomerase	DGF
PEBP1	Phosphatidylethanolamine-binding protein 1	DGF
VCAM1	Vascular cell adhesion protein 1	DGF
ANXA1	Annexin 1	DGF
FBLN1	Fibulin-1	DGF
CYCS	Cytochrome -C	DGF
S100A9	Protein S100A9	35.13
PYCARD	Apoptosis associated peck like protein containing CARD	17.18
HBB	Hemoglobin subunit beta	12.98
MYH9	Myosin 9	11.71
THBS1	Thrombospondin 1	9.46
LGALS3	Galectin-3	6.00
PPIA	Peptidyl-propyl cis trans isomerase A	5.15
SERPINB3	Serpin B3	4.60
FLNA	Filamin A	4.45
CFL1	Cofilin 1	4.35
YWHAZ	14-3-3 protein zeta/ protein kinase inhibitor	4.18
IGFBP1	Insulin - like growth factor binding protein 1	3.98
NME2	Nucleoside diphosphate kinase B	3.76
S100A4	Protein S100A4	3.61
HNRNPA1	Heterogeneous nuclear ribonucleoprotein A1	3.11
F2	Prothrombin	3.11
TAGLN2	Tansgelin 2	2.99
GSTP1	Glutathione-s-transferase	2.97
LGALS1	Galectin 1	2.93
NGAL	Neutrophil gelatinase associated lipocalin	2.88
FETUB	Fetuin B	2.71
S100A8	Protein S100A8	2.60
MST1	Hepatocyte growth factor like protein	2.54
HRG	Histidine rich glycoprotein	2.45
ADIPOQ	Adiponectin	2.39
ENO1	Alpha enolase	2.26
LDHA	L lactate dehydrogenase alpha chain	2.26
AGT	Angiotensinogen	2.23
APOB	Apolipoprotein B100	2.21
MIF	Macrophage migration inhibitory factor	2.15
SH3BGRL3	SH3 Domain binding glutamic acid rich like protein 3	2.13
IGFBP5	Insulin like growth factor binding protein 5	2.12

($p \leq 0.05$, ANOVA); DGF in the fold change column indicates proteins uniquely identified in the DBD-DGF kidneys.

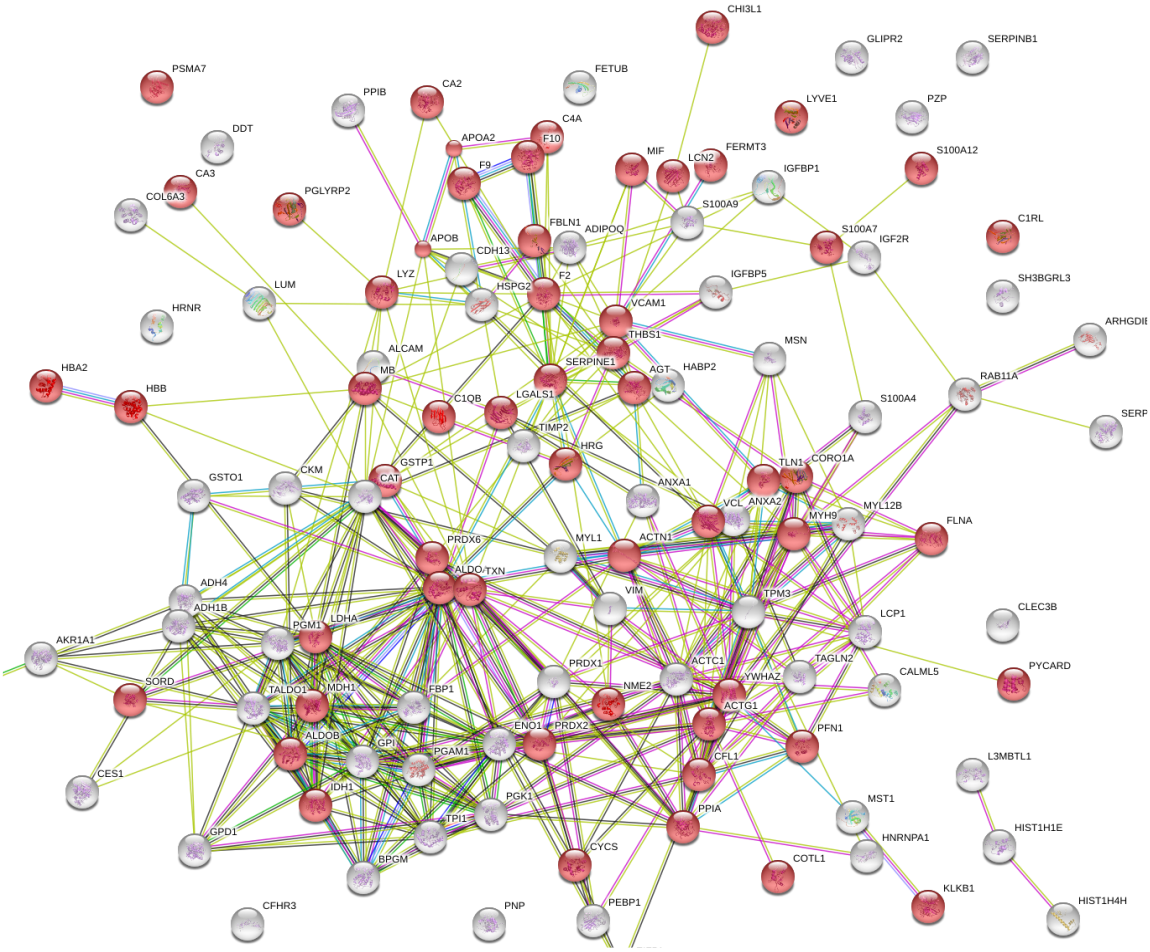

Figure 5.6 Response to cellular stress pathway

String analysis of 130 proteins significantly regulated proteins between DGF compared to IF associated serum samples in DBDs. The red sheres represent the proteins that were assigned to response to cellular stress pathway (n=56; FDR:9E10^{-13})

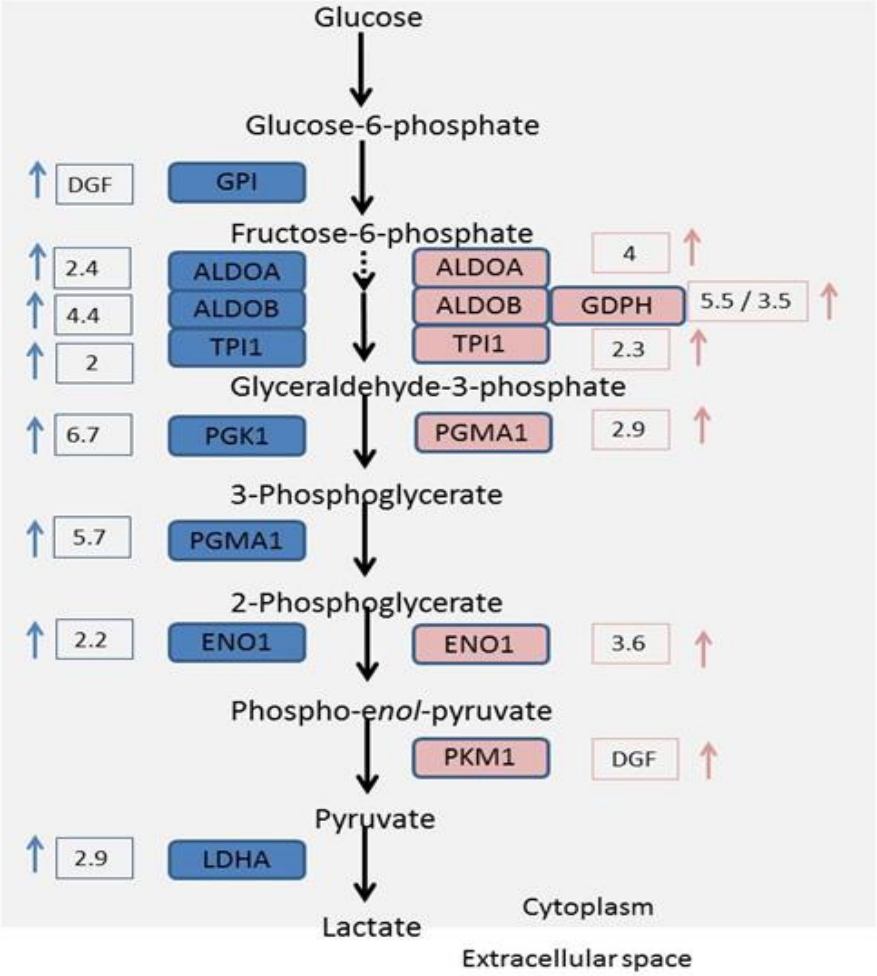

Figure 5.7 Glucose flux through the glycolytic pathway
A schematic re-presentation of all the identified glycolytic enzymes with the fold change of expression in DGF vs IF in DBD and DCD donor samples. The blue & red arrows indicate the identified glycolytic proteins with an increased expression in DGF compared to IF with the fold change indicated in the boxes. The enzymes listed on the left side and denoted in blue were identified in DBDs and on the right, in red, in DCDs.

Comparison of proteomic profiles of serum samples from DCD donor kidneys with DGF or IF

DGF was compared with IF in DCDs by proteomic analysis of pooled serum. Profiles from LDs, who all had IF, were used as controls. 89 proteins in DCDs were at least two fold up-regulated in the DGF subgroup compared to IF or LD subgroups (DGF vs IF $\geq$2 fold change, DGF vs LD $\geq$2 fold change $p \leq 0.05$, ANOVA, table S5.3). 44 proteins were identified only in the DGF subgroup. Fourteen proteins were assigned to the cell death pathway, in comparison to 45 proteins in the DBD-DGF subgroup, and eight to the glycolysis pathway (figure 5.7). Supervised HCA was performed for the significantly regulated proteins identified in each gel band amongst the experimental groups. There were a limited number of proteins that were upregulated in the IF group (as indicated by the predominant green colour in IF column in figure 5.8). Both DGF and LD groups were characterised by a signature of up-regulated proteins with a small overlap as was apparent in all three bands (figure 5.8).

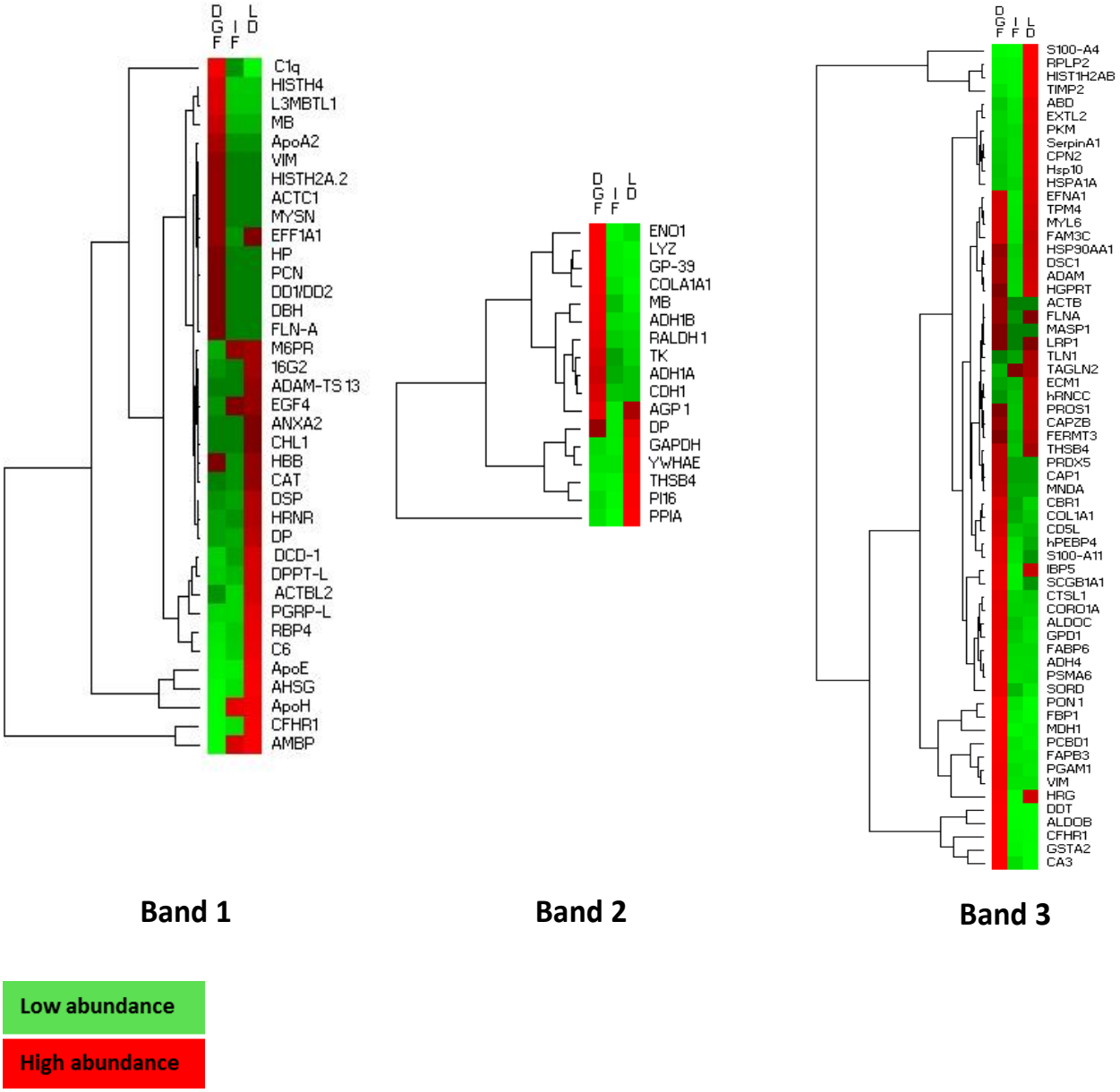

Figure 5.8 DCD serum proteomic signatures associated with DGF and IF in kidney recipients

Supervised HCA of all significantly regulated proteins (fold≥2; p≤0.05, ANOVA) in DCD subgroups (DGF and IF) and LDs in each gel band as analysed by GeLC-MS/MS. Red represents high and green low abundance of the identified proteins.

Proteomic analysis of donor urine samples

24 urine samples were obtained from the same LD, DBD and DCD donors at the same time as the serum samples as previously described (figure 5.2C). Samples were grouped according to DGF or IF outcome and were analysed individually by label-free MS/MS (figure 5.3). Comparison of the DBD and DCD samples (DGF versus IF and LD) by unsupervised HCA showed limited discrimination on the basis of a proteomic signature (figure 5.9A & B). HCA showed a high biological variability and although the dendograms showed the formation of clusters, only limited discrimination of donor samples on the basis of the onset of DGF was seen.

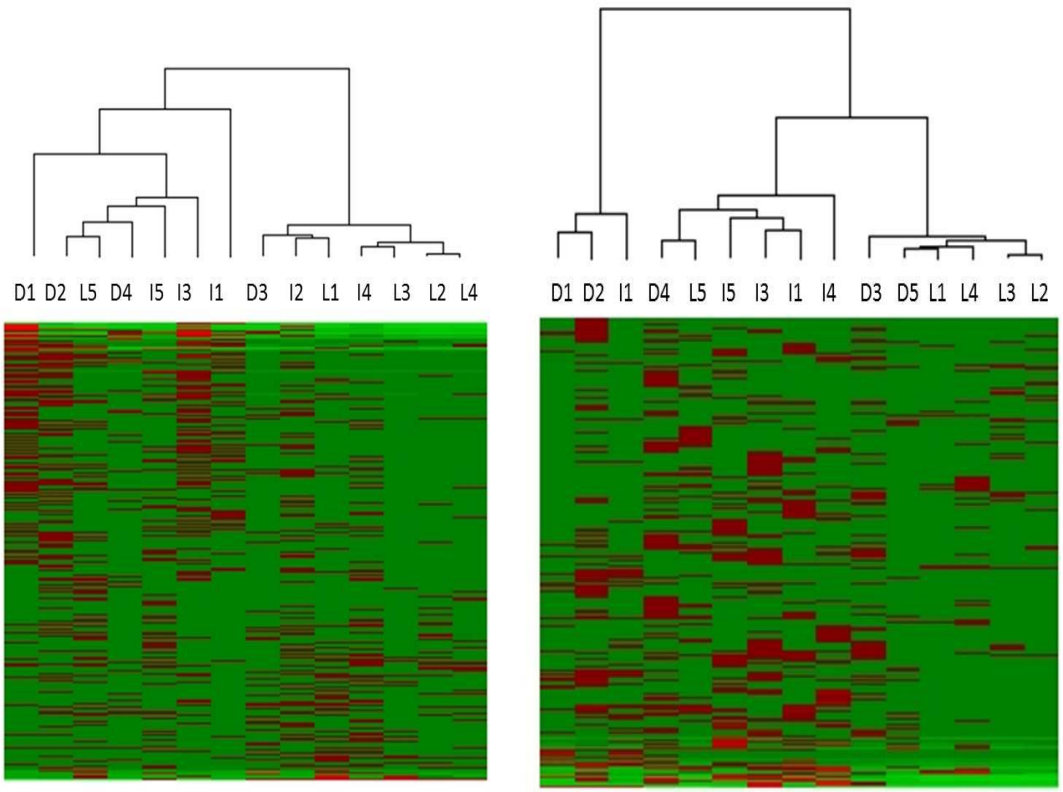

A. DBD (DGF vs IF) & LD

B. DCD (DGF vs IF) & LD

Figure 5.9 HCA of donor urine proteomic signatures according to transplantation outcome in kidney recipients

Unsupervised HCA of proteins identified in the proteomic analysis of individual urine samples (DGF vs IF vs LD). D: DGF associated urine samples. I: IF associated urine samples and L: LD urine samples. Panel ***(A)*** *represents DBDs and* ***(B)*** *DCDs*

120 proteins were regulated between DBD-DGF, DBD-IF and LDs. The shortlisted proteins were identified in at least 3 out of 5 analysed individual samples in the deceased (DGF and IF) subgroup. On this basis, 10 proteins were identified only in the DBD (DGF and IF) samples, so not in LD urine samples. These proteins are listed in table 5.4. In addition, some proteins were present in all the donor samples with increased levels in DBD-DGF but not statistically significantly different between DGF and IF (table S5.4). If this experiment was to be repeated, normalisation against a better variable than urine volume may yield clearer comparable data.

136 proteins were regulated between DCD-DGF, DCD-IF and LDs. 18 proteins were uniquely identified in the DCD (DGF and IF) samples and absent from all the LD urine samples. These proteins are listed in table 5.5. From the remaining proteins only two were statistical significant with up-regulation of expression in DGF (table S5.5). These were actin and pepsin-A3.

Table 5.4 **Proteins identified uniquely in DBD (DGF & IF) when compared to LDs**

Protein description
Isoform 2B of Desmocollin-2
Lipopolysaccharide-binding protein
Lysozyme C
Napsin-A
Carbonic anhydrase 1
Collagen alpha-1(I) chain
Cystatin-M
Dermatopontin
Dystroglycan
Isoform 2 of Vascular cell adhesion protein 1

Raw data S5.5 is listed in table S5.4

Table 5.5 **Proteins identified uniquely in DCD (DGF & IF) when compared to LDs**

Protein description
Carbonic anhydrase 1
Collagen alpha-1(I) chain
Collagen alpha-2(I) chain
Cystatin-M
Dermatopontin
Dystroglycan
Fatty acid-binding protein, heart
Glia maturation factor beta
Glia maturation factor gamma
Heat shock protein beta-6
Insulin-like growth factor-binding protein 1
Isoform 2 of Vascular cell adhesion protein 1
Isoform 2 of V-set and immunoglobulin domain-containing protein 4
Isoform 2B of Desmocollin-2
Isoform 3 of Immunoglobulin superfamily member 8
Isoform Alpha of Poliovirus receptor-related protein 2
Lithostathine-1-alpha
Lysozyme C
Myocilin

Raw data is listed in table S5.5

5.5 Discussion

This pilot study was designed to test the feasibility of clinical proteomics to identify alterations in the serum and urine proteomes that were associated with donor type and onset of DGF.

A comparison of the donor proteomic signatures from DCD, DBD and LD serum samples revealed that the proteomic profiles of DBDs and DCDs were distinctly different from LDs (figure 5.4). Therefore, this preliminary analysis showed it was possible to distinguish deceased from living donors using serum label-free quantitative proteomics.

In serum pools, 50 proteins were present at significantly higher levels in LDs compared to deceased donors and 35 proteins were present at significantly higher levels in deceased donors compared to LDs. However, examination of the biological function of the proteins did not identify any correlation to specific biochemical pathways that could account for the changes (table S5.2 and figure 5.4). Complement and coagulation proteins were increased in both experimental groups. The reason for this is unclear. One possible explanation is that activation of complement and coagulatory pathways reflect the profound pathophysiological changes occurring during brain injury and brain stem death in deceased donor groups whereas in living donors it results from systemic changes occurring during anaesthesia and surgery.

After the preliminary comparison of deceased and living donors, the proteomic signatures of deceased donors were compared to see if it was possible to differentiate between donors on the basis of kidney transplantation outcomes.

Pooled serum samples from DCD and DBD donors who donated kidneys that either developed DGF or IF post-transplantation were compared against each other with LD as a gold standard control. As shown in figures 5.5 & 5.8, proteomic analysis of serum from DBD and DCD donors could clearly distinguish between donors with kidneys with immediate function in the recipient or develop DGF post-transplant. HCA analysis showed that the proteomic signatures of living donors, all with functioning kidneys post-transplant, were closely related to the signatures of DBDs with IF (figure 5.5) but not associated with the signatures of DCDs with IF (figure 5.8).

With respect to DGF, when the significantly regulated proteins in all groups were analysed ($p \leq 0.05$, ANOVA), the DGF proteomic signatures in DBDs were distinctly different from those of IF and LD (figure 5.5). A more detailed analysis of the proteomic signatures showed 116 proteins that had significantly increased expression or were uniquely present in serum of DBDs with DGF outcomes (figure 5.5 and table S5.3). These proteins are associated with pathways involved in metabolic dysregulation, inflammation, cytoprotection, complement activation, cell death, cellular response to stress and apoptosis. Based on this analysis, it can be hypothesised that the DGF proteomic signature identified in DBDs reflects the severity of the systemic pathophysiological changes that may occur in the donor following brain stem death and subsequent donor management prior to organ retrieval. As discussed in chapter 1, brain death results in profound changes to the normal functions of the body including haemodynamic instability leading to hypoperfusion and cellular hypoxia, hormonal and metabolic changes that promote activation of pathways of apoptosis and cellular death in a time dependent manner[20].

The proteomic profiles of serum from deceased donors pointed to the presence of metabolic dysregulation with an increased abundance of eight glycolytic enzymes at a systemic level (figure 5.7) suggesting a switch from aerobic to glycolytic metabolism in many cell types and tissues. Consistent with this, a recent transcriptome study of kidney biopsies obtained from the same LD, DBD & DCD donors analysed in this study showed the up-regulation of mRNA expression of the same glycolytic genes[196].

Increased abundance of glycolytic proteins in conjunction with cell death and ROS scavenger molecules suggested an elevated ROS production. Oxidative stress and energy starvation can lead to permeabilization of outer mitochondrial membranes which allows migration of pro-apoptotic cofactors, such as cytochrome C, to the cytosol triggering caspase- dependent apoptosis[197,198]. Cytochrome C was among the proteins uniquely identified in DGF associated samples in DBD serum samples (table 5.3, table S5.2). Pathway analysis of all the regulated proteins $p \leq 0.05$ indicated that the leading role of Mitogen Activated Protein kinase (MAPK) and c-Jun amino terminal kinase (JNK) (figure S5.2). MAPK and JNK are two major stress-related protein kinases also involved in renal diseases and IRI, as shown in pre-clinical studies, and inhibition of JNK following brain death prolongs graft survival in Lewis rats[199,200].

In DBD donors, proteomic signatures associated with DGF (figure 5.5) showed an increase in proteins with a cytoprotective function (table 5.2). These may act, at least in part, as a counterbalance of the detrimental pathophysiological changes following brain death[201–203]. However, it is important to note that the proteomic analyses were performed on donor blood serum so the signatures reflect

systemic rather than kidney specific pathophysiological changes. Proteomic analyses of donor kidney biopsies would be needed to demonstrate if these changes were also found in the kidney.

Although the proteomic signatures in DCD serum revealed the activation of the glycolytic pathway to a similar degree as in DBDs, the extent of activation of cell death pathways and cytoprotective mechanisms was less pronounced in DCDs when compared to DBDs. It is possible that the different time points that procurement of serum and urine samples in DBDs compared to DCDs (figure 5.1) may explain these differences.

To confirm that the differentially regulated proteomic signatures observed in DGF related donor serum was indicative of a predisposition to a reduced donor kidney function post-transplantation, individual urine samples from the same donors were analysed. Urine, as a direct product of the functioning kidney, acts as a proximal bio fluid with a lower complexity compared to serum[148].

HCA of proteomic profiles of urine samples indicated a high biological variability amongst donors and no discrimination between deceased donors associated with DGF or IF or LDs was observed (figure 5.9). Urine samples were normalised on the basis of urine volume for analysis and this may have distorted the relative amounts of proteins present in each sample. It is unknown how diabetes insipidus during donor management may have impacted on the urine of the samples since the severity will differ between individual donors introducing a bias in urine sampling. As there was great variability between the protein contents of the analysed urine samples one can hypothesise that it has been a significant source of variability in this analysis. This is a difficult problem to

overcome as urine output can vary widely during donor management dependant on the hydration state of the donor. An alternative approach would be to normalise against the ratio of albumin to total protein for different donors or on urine creatinine concentration prior to analysis[204].

Despite these study limitations it was possible to shortlist some proteins for further examination based on being identified in the deceased urine samples in DBDs and DCDs and being absent from all the LD urine samples (table 5.4, table 5.5). Confirmation that these proteins could be used as biomarkers will depend on confirmatory data on a larger sample set as from the current analysis it was not possible to identify any significant association to DGF when compared to IF.

Acute kidney injury marker neutrophil gelatinase-associated lipocalin (NGAL) was differentially increased in abundance in the serum of the DGF subgroup in DBD[205]. In urine, detection of vascular cell adhesion molecule-1 (VCAM-1), H-fatty acid binding protein lysozyme (FABP3), lysozyme (LYS) and insulin growth factor binding protein -1 (IGFBP-1) have been associated with acute kidney injury and kidney dysfunction as has been reported from previous studies[206–210]. Similarly, collagen I alpha chain fragments (COLIA1, COLIA2) were uniquely identified in urine samples of DBDs and DCDs suggesting an early onset of kidney fibrosis[211,212] although their association to kidney function and post transplantation outcomes has to be examined in future studies.

As discussed in this chapter and in the introductory chapter, donor characteristics such as donor type and donor age have an impact in the development of DGF. However, it is important to consider that only a minority of donors who donated both kidneys as allografts, both kidneys will develop DGF.

Louvar *et al.,* in a study of 19,461 recipient pairs of the same donor, reported that only 10% of recipient pairs with the same donor both developed DGF and 29% of pair recipients with one developed DGF[59]. In view of this, more consideration is needed whether the choice of DGF as the clinical phenotype is a robust experimental end point for this analysis.

5.6 Conclusions

This pilot study demonstrated that the application of clinical proteomics using an unbiased approach can be very informative and provide a snapshot of the alterations in the blood and urine of donors associated with transplantation outcomes.

Following completion of the analysis it was discovered that there was incorrect classification of four serum samples to the wrong transplantation outcome. However, as the serum analysis were performed on pooled samples it was not possible to reanalyse the data. The expectation is that differences between the two groups would be less pronounced than they would have otherwise been so that key differences observed between the samples would still be of value. That said, the samples cohorts were small and any significant variability between samples would impact on the data so any conclusions must be drawn with caution. The work in this chapter has indicated some general biological pathways that may prevail in the different donor types. The next step will be to confirm some of the findings on a large, independent cohort of samples to see if the different expression profiles observed in blood and urine are maintained.

Future studies on donor clinical samples that are grouped on the basis of transplantation outcomes should consider the recipient outcomes of concordant donor kidneys during sample selection. Furthermore, a combination of clinical

phenotypes such as the onset of DGF in addition to suboptimal allograft function 3 or 12 months post transplantation would increase the confidence that the donor blood, urine or tissue proteomic alterations correlate with biological changes that impact on donor kidney quality and could be predictive of transplantation outcomes.

CHAPTER 6

Donor kidney tissue proteomic profiles correlate with long-term transplantation outcomes

6.1 Introduction

Kidney transplantation is a lifesaving treatment for end stage kidney disease that confers considerable benefits to recipients in terms of survival and quality of life. However, the shortage of donor organs and the high risk of death while on waiting list have led to the increased utilisation of donor organs that are less than ideal. These organs are obtained from either older DBDs, or unstable during donor management DBDs or DCDs, as discussed in chapter 1, and it is anticipated that some of these allografts will have suboptimal outcomes following transplantation[85,213,214].

The clinician, faced with the offer of a kidney from a marginal donor requires objective criteria to decide on the suitability of the kidney for transplantion. These clinical challenges entail difficult decisions from clinicians who have to balance the risk of patients dying while waiting for a transplant against the uncertainty of outcomes from suboptimal transplants[44,182]. In the setting of donor organ retrieval and organ allocation, where all these decisions are made, the tools to assess and quantify the risks are lacking.

The utilisation of diagnostic tools to assess donor organs would be increasingly necessary for the evaluation of organs from younger donors who due to life style choices are at increased risk of type 2 diabetes, cardiovascular and kidney diseases.

Advancements in chemistry and engineering have resulted in the development of novel and powerful analytical technologies such as transcriptomics, proteomics, peptidomics, metabolomics and has made profiling and integration of large data sets both affordable and reliable in research laboratories. Integration of -omics

technologies such as proteomics and peptidomics (protein fragments generated by endogenous proteolysis) with clinical and demographic data provides a powerful approach to the discovery of clinically relevant proteomic profiles that correlate to clinical endpoints. In recent years researchers have begun to apply –omics technologies to assess kidney quality in the recipient.

Nankivell et al., in a study published in New England Journal of Medicine in 2003 tested the hypothesis that the development of chronic allograft nephropathy within the first 12 months following transplantation impacts the long term graft function and survival. The authors concluded that incremental and progressive subclinical injury causes irreversible kidney damage that leads to declining kidney function with high risk of graft loss[215]. In an attempt to predict progressive kidney allograft injury, the prospective study by Connell *et al.,* in 2016, applied transcriptomic profiling of biopsies from kidney allografts at 3 months post-transplant. The study concluded that the diagnosis of subclinical alterations in the allograft kidneys at 3 months was feasible, based on a 13 gene signature, which would reliably predict which recipients would have suboptimal allograft function or graft loss at 12 and 24 months post transplantation[216]. This was an important study which showed that an –omics approach was diagnostically useful and, moreover, that a panel of identifiers (proteins or genes) may be required for diagnosis rather than single genes or proteins.

The pilot proteomic study described in chapter 5 showed that it was feasible to detect differences in the blood proteome between donors whose kidneys will either function immediately or develop DGF in the recipient. When blood from deceased donors who offered kidneys that developed DGF was compared with

deceased donors with immediate kidney function and LD kidneys clear alterations in serum proteome were detected. These systemic changes in donor blood revealed increased levels of proteins associated with apoptosis, inflammation and, in contrast, cytoprotective pathways.

One of the main research questions stemmed from the study described in chapter 5 was to determine whether donor kidneys at the time of retrieval are predisposed to either suboptimal or good function post transplantation. The aim of this current chapter was to use advanced mass spectrometry techniques to explore deeper the donor kidney biopsy proteome to identify kidney profiles that correlate to long-term allograft function in the recipient.

6.2 Hypothesis and aims

The study described in this chapter was designed to explore the question whether donor kidneys that have suboptimal function in the recipient are biologically distinct from those that function well 12 months after transplantation.

The rationale behind this study was based on the following assumptions:

- Donor kidney injury can predispose allografts to suboptimal function
- Current assessment methods and surrogate markers are not sophisticated or sensitive enough to identify subclinical injury in the donor kidneys that can lead to suboptimal allograft function in the long-term.
- Donor kidney injury and inflammation will result in specific biochemical changes to kidney tissues which could correlate with the degree of kidney injury.

Based on these rationales, the study was designed with the following objectives:

1. Perform proteomic analyses of kidney biopsies to test whether or not it is possible to discriminate, prior to transplantation, donor kidneys with suboptimal or good long-term function in the recipient.

2. Identify and characterise dysregulated biological processes in the donor kidneys associated with suboptimal or good function in the recipients.

3. To use PROTOMAP for the identification of protein degradation patterns that correlate with donor kidney quality and transplantation outcomes.

The experimental work described in this chapter was performed utilising kidney biopsies from the QUOD biobank (described in chapter 3.2). This was the first research study performed with QUOD samples.

6.3 Methods

Study samples

Deceased kidney biopsy samples were obtained from the QUOD biobank as detailed in section 3.2.

Kidney biopsies were obtained from the upper pole of kidney cortex at the back table after retrieval using a 23mm needle biopsy gun according to QUOD standard operating protocols. Each biopsy specimen was divided in two segments; one was stored in RNAlater and subsequent stored in the gas phase above liquid nitrogen, the other in formalin, then embedded in a paraffin block for histological analysis.

Sample selection

Donor kidney biopsy samples were selected on the basis of recipient transplantation outcomes. The NHSBT Organ Donation and Transplantation

(NHSBT ODT) database was interrogated to identify pairs of recipients from the same donor with 3 months post-transplantation follow-up clinical data. At the time of analysis, no further follow-up data was available but at a later stage 12 month eGFR follow-up values were obtained. Baseline donor and recipient demographic characteristics were considered to create as homogeneous groups as possible as shown in table 6.1.

Kidney biopsy samples were obtained from 38 DBD donors at organ retrieval and selected on the basis of post-transplantation outcomes of both kidney recipients (n=76) with the same donor (figure 6.1). Only donors who had provided two kidneys as single transplants were selected for analysis and both transplanted kidneys from the same donor had the same outcome in the recipients, sub-optimal (SO; n=38) or good outcomes (GO; n=38) (figure 6.1).

The 38 recipients of donor kidneys with SO had a mean eGFR 33.4 +/-9.8ml/min at the 3 months follow-up and the 38 recipients of donor kidneys with GO at a 3 months follow-up had a mean eGFR of 62.5 +/-10.2 ml/min (figure 6.1).

19 donors were recruited from each outcome and only one biopsy sample was analysed from each donor.

Within the SO cohort all 19 recipients who received the kidney from which a biopsy was analysed in this study had developed DGF and had a mean 3month follow-up eGFR 29.8 +/- 7ml/min. DGF was defined as the need for dialysis the first week post-transplantation after excluding urine obstruction and hyperkalaemia. Within the GO cohort, all 19 recipients who received the kidney from which a biopsy was analysed had all functioned immediately after

transplantation and the recipients had a mean eGFR 65.1 +/- 8 ml/min after 3 months.

There was no significant difference between the mean donor age, recipient age and CIT between the two cohorts. Donor and recipient demographic and clinical characteristics are summarised in table 6.1.

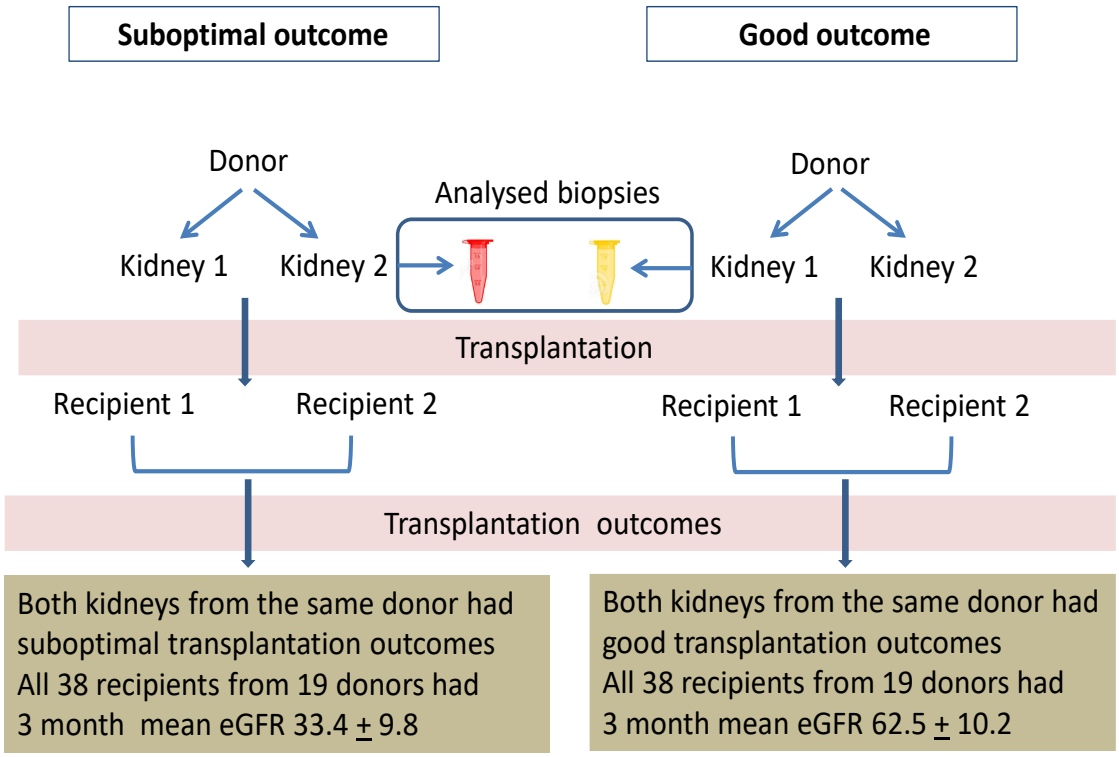

Figure 6.1 Kidney biopsy sample selection
Analysed biopsy samples were selected on the basis of transplantation outcomes and two experimental groups (suboptimal and good) were created on the basis of 3 month post transplantation kidney function. Selected donors offered both kidneys as single transplants, each with the same outcome although analysed biopsies were obtained from only one kidney.

Table 6.1 Donor and recipient demographic and clinical characteristics

	Suboptimal Outcome (n=19)	Good Outcome (n=19)	*P* Value
Donor characteristics			
Age (yr)*	56 ± 13	54 ± 11	0.5
Gender (%)			
Male	10 (53)	7 (37)	0.5
Race (%)			
White	18 (95)	16 (84)	0.6
Other	1 (5)	3 (16)	
Cause of death (%)			0.6
Intracranial heamorhage	10 (53)	10 (53)	
Hypoxic brain injury	4 (21)	2 (10)	
Other	5 (26)	7 (37)	
AKIN classification (%)			0.5
No AKIN	16 (85)	15 (79)	
1	1 (5)	3 (16)	
2	1 (5)	1 (5)	
3	1 (5)	0	
Remuzzi score[a] (%)			0.5
0- 3	13 (68)	15 (79)	
4-8	1 (5)	1 (5)	
Recipient characteristics			
Age (yr)*	50.1 ± 13.5	48.4 ± 13.6	0.5
Gender (%)			
Male	13 (68)	13 (68)	1
Race (%)			
White	15 (79)	10 (53)	0.17
Other	4 (21)	9 (47)	
HLA mismatches (%)			0.22
1	3 (16)	3 (16)	
2	5 (26)	7 (37)	
3	11 (58)	7 (37)	
4		2 (10)	
CIT (h)			1
0- 12	6 (31)	6 (31)	
12-26	13 (69)	13 (69)	
Post transplantation Kidney function (mean eGFR ml/min)*			<0.0001
3 month	29.8 ± 7	65.1 ± 8	
12 month	35.9 ± 6	73.0 ± 18	

**mean +/- SD of n=19 recipients per outcome of the donor kidneys analysed in this study*

[a] *Missing values: 14/19 donors for the suboptimal group and 16/19 donors in good outcome group had enough glomeruli for Remuzzi scoring assessment*

Donor Acute kidney Injury (AKIN) assessment

Donor acute donor injury (AKIN) classification was performed by calculating the fold change in SCr levels from terminal to baseline at donor admission in intensive care[217]. Clinical data regarding donor SCr was obtained from NHSBT. Fold change <1.5-2 was defined as AKIN 1, changes between ≤ 2-3 as AKIN 2 and change ≥ 3 as AKIN 3[217].

Remuzzi scoring

Remuzzi scoring of kidney biopsies was carried out by Dr A Klooster (University of Groningen, The Netherlands). Kidney paraffin sections (4μm) were de-waxed, rehydrated and stained with 0.5% periodic-acid for 5 min, rinsed with distilled water, placed in Schiffs reagent for 15 min then washed for 5 min in tap-water. The slides were counter-stained with Mayer's haematoxylin and washed in tap water for 5 min.

Evaluation of donor biopsies for chronic kidney disease (CKD) using Remuzzi scoring was performed retrospectively. Biopsies from 30 donors were successfully scored while biopsies from 8 donors had less than 7 glomeruli and were considered insufficient for scoring. Remuzzi scoring assessment was performed blindly to the donor identity or transplantation outcomes.

Proteomics analysis

Five biopsy samples per subgroup were analysed by label-free quantitative (LFQ) liquid chromatography tandem mass spectrometry (LC-MS/MS) as described in chapter 3.4.4 (figure 3.2A). In brief, kidney biopsy samples were lysed in 300 µL of RIPA buffer (150 mM NaCl, 1.0% NP-40, 0.5% sodium deoxycholate, 1% SDS, 50 mM Tris, pH 8.0) containing protease (Roche, USA) and phosphatase inhibitor cocktail (Sigma, UK). Homogenization was performed on a beads beater at 6500 rpm for 40 seconds with immediate transfer to ice. Protein quantitation was performed by BCA as described in chapter 3.4.2 and equal amounts of protein per sample were first digested to tryptic peptides and subsequently analysed by LC-MS/MS according to the protocol described in chapter 3.5.1. Raw MS data were analysed as previously described using the CFPF platform for protein identification and quantitation described in chapter 3.5.3.

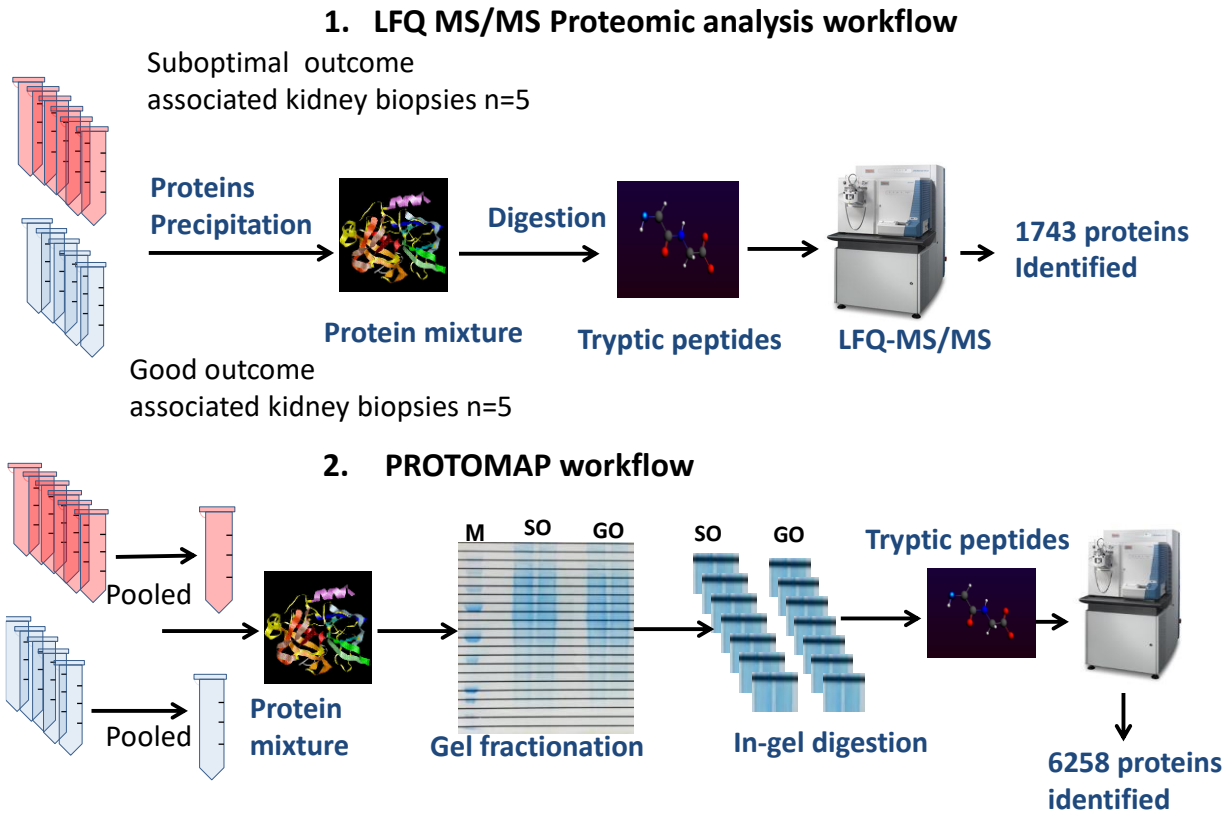

Figure 6.2 Experimental workflow

(1) Initially n=10 individual kidney biopsies (n=5 samples per transplantation outcome) were analysed by label free quantitative tandem mass spectrometry (LFQ-MS/MS). Biopsy samples homogenates were precipitated, proteins were enzymatically digested to tryptic peptides that analysed by mass spectrometry. Bioinformatic analysis resulted in the identification of 1743 proteins (FDR<1%) (2.) To identify protein degradation patterns that are associated with transplantation outcomes PROTOMAP analysis was applied. Biopsy samples homogenates were pooled. Precipitated proteins were fractionated by gel electrophoresis. The gel was divided into 22 horizontal bands per sample lane. Captured proteins were digested to tryptic peptide fragments that were subsequently extracted from the gel and analysed by tandem mass spectrometry. Bioinformatic analysis resulted in the identification of 6258 proteins.(3). Western blot validation analysis was performed in an independent cohort of DBD kidney biopsies n=28 (n=14 biopsy samples per transplantation outcome). SO: suboptimal outcome, GO: good outcome.

Statistical analysis

Statistical comparison of the protein abundance changes observed between GO and SO was performed using non-parametric Mann Whitney test, in which p ≤0.05 was set as the threshold of significance (GraphPad Prism version 7). Proteins with a change in abundance that was statistically significant and that had non-zero values in at least three out of five donor samples per group defined a candidate proteomic signature and were included in the analysis.

Some proteins identified as significantly expressed in kidneys associated with SO or GO outcome by proteomic analysis were later validated on an independent cohort of kidney biopsies by western blot. The protocol for western blotting is described below. To measure expression levels of proteins on blots, a semi-quantitative densitometric analysis normalised by β-actin was carried out. Statistical comparison was performed using non-parametric Mann Whitney statistical test accepting as significant baseline p ≤0.05. Western blot results were presented as scatter plots with a horizontal line indicating the mean values of protein abundance.

To assess whether the association of transplantation outcomes was independent of the donor demographic and clinical variables and recipient demographic factors as listed in table 6.1, statistical analysis of categorical data was performed with chi squared or Fisher's exact test.

Hierarchical clustering analysis

Unsupervised and supervised hierarchical clustering analysis (HCA) was performed as previously described in chapter 3.5.3 using PermutMatrix[158]. Abundance values of all 1743 identified proteins were used for the unsupervised HCA while abundance values for 214 statistically significant proteins ($p \leq 0.05$) were used to perform supervised HCA.

Pathway analysis

To assess whether the kidney proteomic signatures associated with transplantation outcomes were biologically meaningful, pathway analysis was performed using STRING open access http://string-db.org/cgi/network.pl bioinformatics on the 214 proteins significantly dysregulated between the two groups ($p \leq 0.05$)[218,219]. Protein names were uploaded onto the search window of the software with the selected organism being *Homo sapiens* to reflect that the acquired proteins derived from human clinical samples. STRING bioinformatics provides the most probable protein –protein associations and the biological pathways defined from these interactions. The analysis calculates a confidence score which indicates the probability that the observed protein – protein interactions has occurred by chance. The lower the score the higher the probability that the protein – protein interactions and the assigned pathways are true.

The nodes presented in red spheres are the proteins that are assigned in the pathway of interest.

PROTOMAP analysis

The two experimental conditions (suboptimal vs good outcome) were compared to identify degradation patterns associated with transplantation outcomes. Five biopsy samples per clinical outcome (suboptimal vs good) were pooled to one sample and analysed by PROTOMAP (figure 6.2) as described in chapter 3.4.7. Briefly, the two pooled kidney biopsy samples were subjected to SDS-PAGE. The gel was stained by Coomassie Blue to visualise the proteins and divided into 22 horizontal bands per lane (each lane represented one condition). Each pool per band was cut to create 22 pieces. Proteins captured in gel pieces were subjected to in-solution digestion and tryptic peptides were analysed by LC-MS/MS. Raw data were analysed by PROTOMAP bioinformatics to generate peptographs. Peptographs consist of two panels as described in figure 3.4; chapter 3. Peptographs combine information from 1-D gel migration of protein fragments, protein sequence coverage and spectral counts of protein fragments per gel band. The left panel shows the protein sequence coverage from N to C terminus for each band. Peptide sequences represented in red and blue were identified in the good outcome and suboptimal outcome cohorts, respectively, while peptide fragments represented in purple were common to both pooled samples in the same band. The right panel shows the relative quantitation using spectral counts for each protein between the two pools. The red bars represent the 'parent proteins' which were the intact proteins identified in the control samples. Protein degradation was defined by fragments with spectral counts detected in lower bands as compared to the 'parent protein'.

Western blotting

Western blotting was performed on an independent cohort of n=28 biopsy samples (n=14 kidney biopsies per transplantation outcomes). 15 µg kidney extract samples were denatured at 95°C for 5 minutes in Laemmli buffer and loaded onto 8–12% pre-cast SDS-PAGE gels (Bio-Rad, USA). Proteins separated by SDS-PAGE were transferred to hydrophobic PVDF membranes (Merck Millipore, USA) in transfer buffer (25 mM Tris, 192 mM glycine and 10% methanol) overnight. PVDF membranes were blocked for 1 hr in TBST buffer (25 mM Tris, pH 7.5, 0.15 M NaCl, 0.05% Tween 20) containing 5% milk. Membranes were incubated for overnight at 4°C with anti-TRX1 (ab26320, 1:1000), anti-PRX3 (ab73349, 1:1000), anti-Catalase (ab16731, 1:1000), anti-GST (ab53940, 1:3000)(Abcam, UK), anti-STAT-1 (mab14901, 1:1000) and anti-PDGFRα (af307na, 1:800) (R&D Systems, USA). Rabbit monoclonal anti -β-actin served as a loading control (ab8227, 1:5000) (Abcam). Membranes were washed for 30 min with 5 changes of wash buffer and then incubated at room temperature for 1 hr in blocking buffer containing a 1:5000 dilution of Dye-800-conjugated anti-mouse, -rabbit, or -goat secondary antibody (Li-Cor, USA). Bands were visualised on an Odyssey CLx (Li-Cor). Detected signal was quantified and normalized to the β-actin signal on the same blot.

6.4 Results

Comparison of proteomic signatures of DBD kidney biopsies associated with either good or sub-optimal outcome in the recipient

LFQ-MS/MS analysis was conducted on the 10 donor kidney biopsy samples, five biopsies from kidneys with suboptimal and five with good outcome at 3 months post-transplant. 1743 unique proteins were identified with a false discovery rate (FDR) <1%. Further analysis identified 214 proteins with abundance levels significantly altered between the two groups ($p \leq 0.05$). A volcano plot comparing the magnitude of the change in protein abundance and the statistical significance of these changes between the two groups (GO vs SO) revealed that 132 proteins of the 214 proteins had significantly increased levels in the SO associated kidneys compared to GO and 67 were more than 2 fold increased in SO than in GO (figure 6.3). There were 17 proteins that were identified only in SO outcome and 3 only in GO and these proteins were not mapped in the volcano plot as the software maps proteins that were identified in both experimental groups.

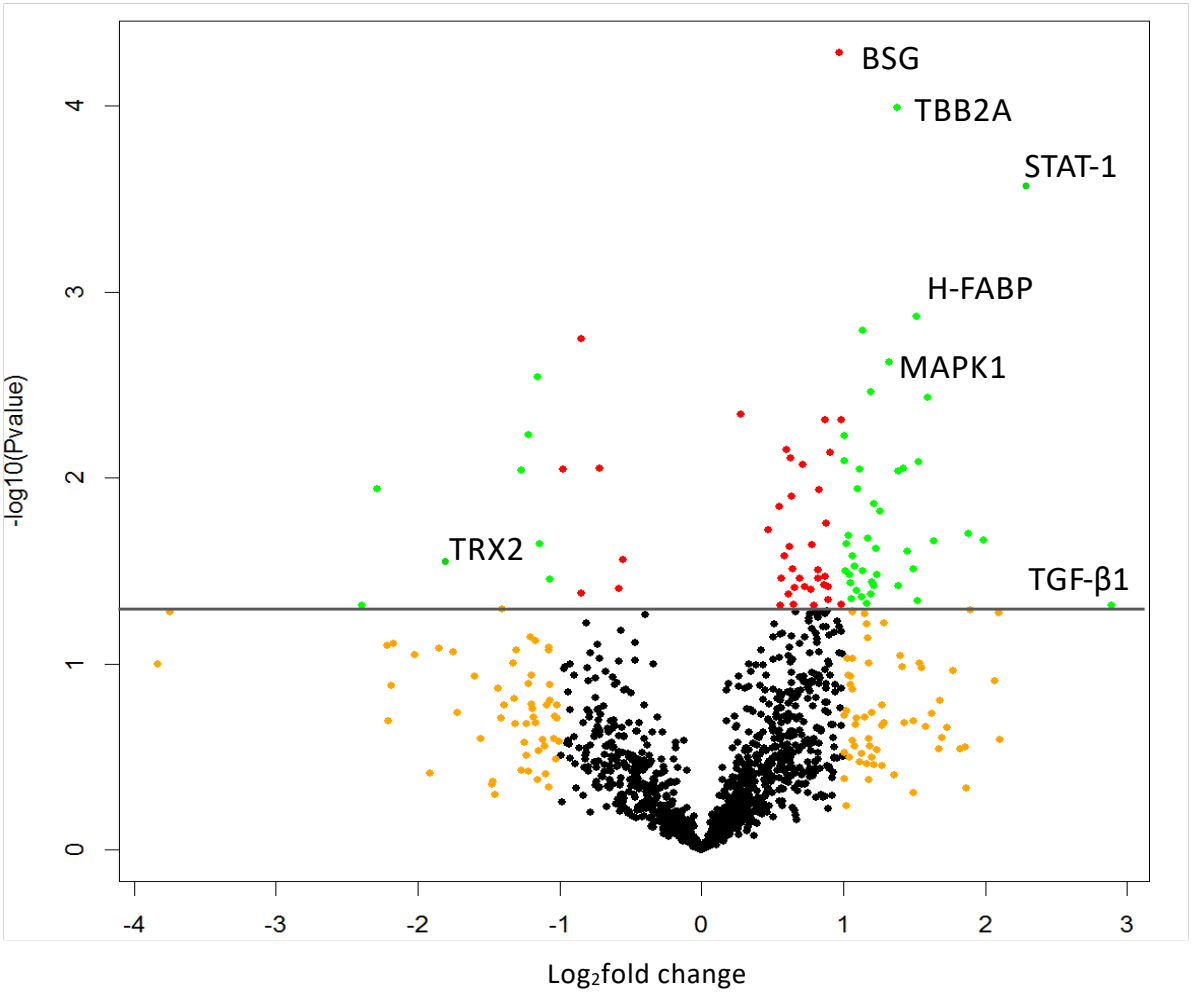

Figure 6.3 Volcano plot showing the distribution of proteins in suboptimal and good outcome associated kidney samples in terms of relative fold change of protein abundance and statistical significance

Volcano plot showing the distribution of the proteins identified by LFQ-LC-MS/MS according to log_2 fold changes (axis-x) and $-log_{10}$ t-test (axis-y). Black dots represent the proteins with ≤2 fold change and p ≥0.05, yellow dots represent the proteins with ≥2 fold change and p≥ 0.05, red dots represent proteins with ≤ 2 fold change and p≤0.05 and green dots represent ≥ 2 fold change and p≤0.05. The line indicates the threshold of p≤0.05.

To explore the uniformity of data within each group and to investigate the degree of closeness between the two groups, HCA was performed as described in chapter 3.5.3. On the basis of similarity between individual samples, unsupervised HCA placed four out of five donor kidneys within the same outcome cohort in adjacent positions (figure 6.4). Supervised HCA using the proteomic signature of the most statistically significant 214 proteins segregated the 10 biopsy samples into two clearly distinct groups, GO or SO, according to 3 months post-transplantation outcome (figure 6.5A).

After the proteomic work had been completed, 12 month eGFR values of the kidney recipients became available. This enabled the 3 month and 12 month follow-up clinical data to be compared for the analysed biopsies. The 12 month eGFR values, shown in figure 6.5B, were broadly similar to 3 month values. Two kidneys, S1 & S2 had improved eGFR values but still were within the SO cohort. One SO kidney had progressed to graft failure and no value was obtained from one GO associated kidney (G1).

A comparison of eGFR values at 12 months against the supervised HCA analysis shows that the donor kidneys with the most extreme eGFR values at 3 and 12 month post-transplantation were clustered furthest apart. Conversely, S1 & S2 with improved eGFR values compared to 3 months values clustered closest to the kidneys associated with GO. For kidneys associated with GO, those that clustered furthest to the right (G2, G4, G3) had consistently good function at 3 and 12 months (figure 6.5B). Although the number of biopsies analysed was small, these results suggest it may be possible not only to predict suboptimal or good outcomes in the recipient but to sub-categorise SO kidneys into those that will

continue to have suboptimal function after 12 months and those to which a degree of recovery could occur.

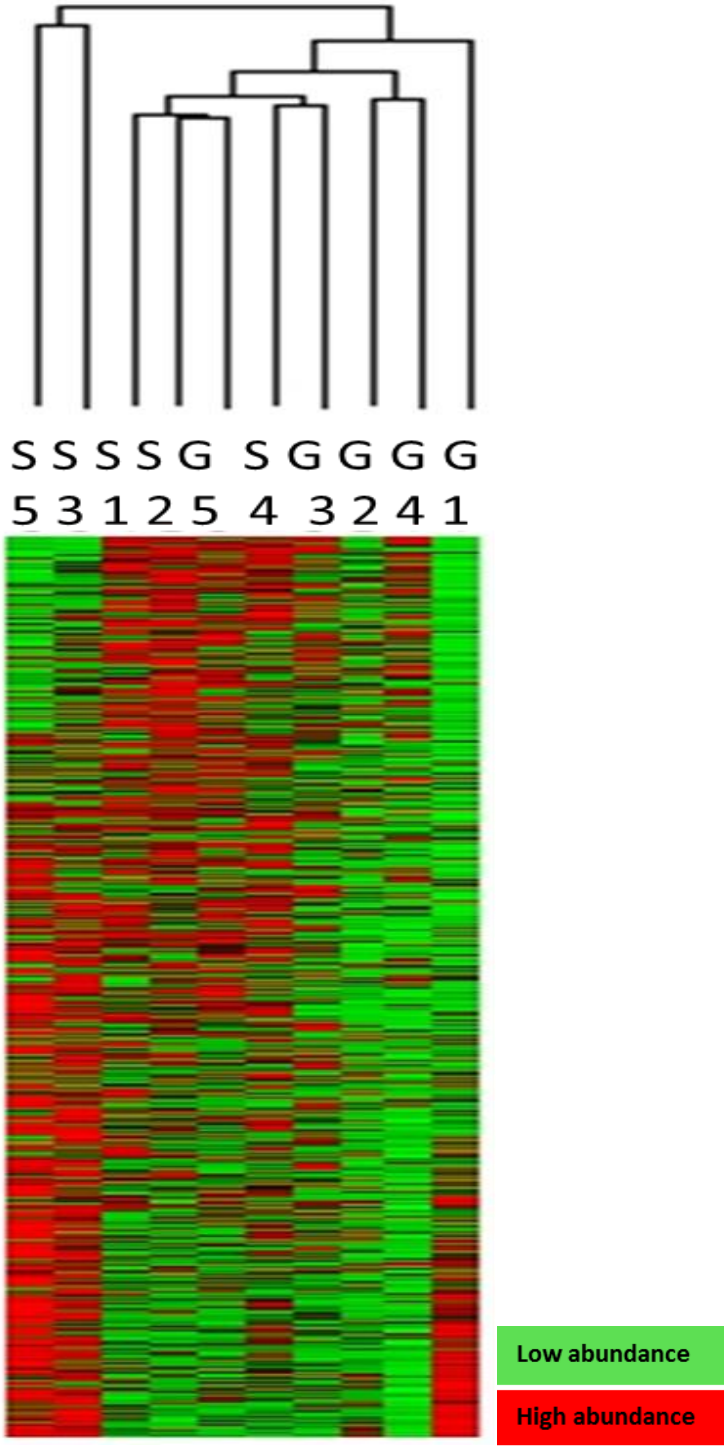

Figure 6.4 Unsupervised HCA of donor kidney biopsies associated with suboptimal or good outcome in the recipient

S: suboptimal outcome, G: good outcome. S1-5: donor kidney biopsies with suboptimal function in the recipient and G1-5: donor kidney biopsies with good function in the recipient.

A

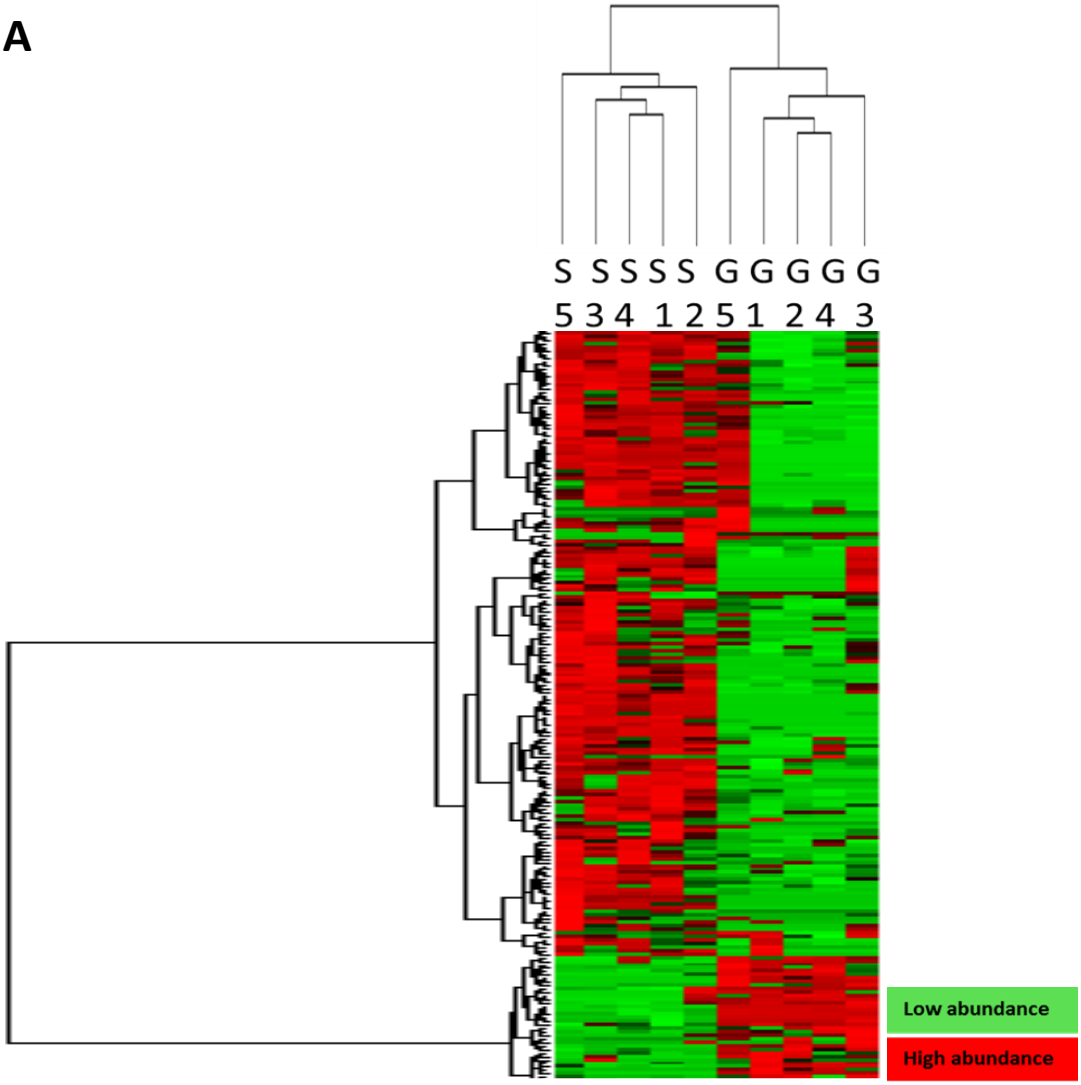

B

	Suboptimal outcome					Good outcome				
eGFR ml/min	S5	S3	S4	S1	S2	G5	G1	G2	G4	G3
3 month	24	31	29	27	28	50	54	65	62	70
12 month	28	31	GF	48	40	65	MV	66	72	75

Figure 6.5 Supervised HCA and associated transplantation outcomes of donor kidney biopsies associated with suboptimal or good outcome in the recipient

A. *Supervised HCA segregated individual donor kidneys in two distinct groups according to 3 month kidney function post transplantation.* ***B.*** *Association between the HCA derived dendrogram to recipient kidney function detected at 3 and 12 month post transplantation as defined by eGFR. . GF: graft failure, MV: missing value. S1-5: Individual donor kidneys with suboptimal outcomes. G1-5: Individual donor kidneys with good outcomes.*

Pathway analysis

Pathway analysis performed in the 214 significantly regulated proteins indicated that 67 identified proteins were involved in regulation of cellular metabolic processes (FDR: $2x10^{-3}$) (figure 6.6), 26 proteins were cellular stress response proteins (FDR: $2x10^{-3}$) (table 6.3 and figure 6.7), 40 proteins were involved in cellular catabolic processes (FDR: $2.27x10^{-5}$) (figure S6.1) and 40 proteins were involved in cell surface receptor signalling pathways (FDR: $3\ 10^{-3}$) (figure S6.2). Among the predominant Kyoto encyclopaedia of genes and genomes (KEGG) identified pathways was the metabolic dysregulation pathway with 67 associated proteins (FDR:$7.13x10^{-6}$)(table 6.2 and figure 6.6), the tight junction pathway with 40 associated proteins (FDR: $3x10^{-3}$) and the proteasome pathway with 9 proteins (FDR: $1x10^{-2}$).

Table 6.2 Proteins associated with KEGG metabolic pathway

Protein	Description	Fold change		
		Sub/Good	Good/Sub	p values
OCAD1	OCIA domain-containing protein 1	Sub only	0.00	Sub only
DDX6	Probable ATP-dependent RNA helicase DDX6 1 SV=2	Sub only	0.00	Sub only
SHPK	Sedoheptulokinase	Sub only	0.00	Sub only
PPP5	Serine/threonine-protein phosphatase 5 PPP5C1	Sub only	0.00	Sub only
SMD2	Small nuclear ribonucleoprotein Sm D2 SNRPD21	Sub only	0.00	Sub only
SF3B3	Splicing factor 3B subunit 3 SF3B34	Sub only	0.00	Sub only
OCLN	Isoform 2 of Occludin OCLN	Sub only	0.00	Sub only
RS27	40S ribosomal protein S27 RPS27	17.76	0.06	ND
STAT1	Signal transducer and activator of transcription 1-alpha/beta	6.94	0.14	3.00E-04
FKBP3	Peptidyl-prolyl cis-trans isomerase FKBP3 FKBP31	6.19	0.16	ND
S10A8	Protein S100-A8 S100A81	4.65	0.22	4.84E-03
PEF1	Peflin PEF11	3.92	0.26	ND
IPYR	Inorganic pyrophosphatase PPA12	3.68	0.27	1.05E-02
RLA2	60S acidic ribosomal protein P2 RPLP21	3.03	0.33	3.57E-03
PFKAP	ATP-dependent 6-phosphofructokinase, platelet type OS=Homo sapiens	2.87	0.35	3.45E-02
PGM2	Phosphoglucomutase-2 PGM24	2.83	0.35	5.03E-02
FAS	Fatty acid synthase FASN	2.83	0.35	ND
AT2A2	Sarcoplasmic/endoplasmic reticulum calcium ATPase 2 ATP2A2	2.61	0.38	9.04E-03
AMPE	Glutamyl aminopeptidase ENPEP	2.60	0.38	1.85E-02
SYEP	Bifunctional glutamate/proline--tRNA ligase EPRS5	2.39	0.42	1.21E-02
PDLI5	PDZ and LIM domain protein 5 PDLIM55	2.31	0.43	ND
DHB4	Peroxisomal multifunctional enzyme type 2 HSD17B4	2.17	0.46	5.22E-03
MP2K2	Dual specificity mitogen-activated protein kinase kinase 2 MAP2K21	2.13	0.47	ND
AOFA	Amine oxidase [flavin-containing] A MAOA1	2.08	0.48	4.94E-02
RL3	60S ribosomal protein L3 RPL32	2.05	0.49	1.89E-02
SND1	Staphylococcal nuclease domain-containing protein 1 SND11	2.03	0.49	1.70E-02
CX6B1	Cytochrome c oxidase subunit 6B1 COX6B12	2.01	0.50	3.78E-03
KINH	Kinesin-1 heavy chain KIF5B1	1.98	0.50	4.37E-03
NDUS2	NADH dehydrogenase [ubiquinone] iron-sulfur protein 2, mitochondrial NDUFS22	1.91	0.52	4.44E-02
IGHG3	Ig gamma-3 chain C region IGHG32	1.87	0.54	4.86E-03
RL5	60S ribosomal protein L5 RPL5	1.85	0.54	3.03E-02
RL8	60S ribosomal protein L8 RPL82	1.85	0.54	3.19E-02
CATD	Cathepsin D CTSD1	1.83	0.55	4.77E-03
TCPA	T-complex protein 1 subunit alpha TCP11	1.78	0.56	4.42E-02
SUCB2	Succinyl-CoA ligase [GDP-forming] subunit beta, mitochondrial OS	1.77	0.56	1.15E-02
RS18	40S ribosomal protein S18	1.76	0.57	3.67E-02
TENS1	Tensin-1 TNS12	1.76	0.57	2.56E-02
TCPZ	T-complex protein 1 subunit zeta CCT6A	1.72	0.58	1.38E-02
F10A1	Hsc70-interacting protein ST132	1.70	0.59	2.79E-02
APEX1	DNA-(apurinic or apyrimidinic site) lyase APEX12	1.62	0.62	3.24E-02
HSPB1	Heat shock protein beta-1 HSPB12	1.57	0.64	4.61E-02
RS9	40S ribosomal protein S9 RPS9	1.55	0.64	1.11E-02
QCR6	Cytochrome b-c1 complex subunit 6, mitochondrial UQCRH2	1.53	0.65	2.14E-02
NNTM	NAD(P) transhydrogenase, mitochondrial NNT	1.51	0.66	5.40E-03
QCR2	Cytochrome b-c1 complex subunit 2, mitochondrial OS=Homo sapiens	1.47	0.68	2.62E-02
HOGA1	4-hydroxy-2-oxoglutarate aldolase, mitochondrial HOGA11	0.68	1.47	2.43E-02
QCR7	Cytochrome b-c1 complex subunit 7 UQCRB2	0.67	1.49	2.13E-02
ATPO	ATP synthase subunit O, mitochondrial ATP5O1	0.61	1.64	6.65E-03
PROSC	Proline synthase co-transcribed bacterial homolog protein PROSC1	0.58	1.73	2.06E-02
RL7A	60S ribosomal protein L7a RPL7A2	0.57	1.75	4.12E-02
DPP2	Dipeptidyl peptidase 2 DPP7	0.56	1.80	2.85E-03
PA2G4	Proliferation-associated protein 2G4 PA2G4	0.48	2.10	3.73E-02
DDB1	DNA damage-binding protein 1 DDB11	0.46	2.16	ND
PAPLN	Papilin;PAPLN;ortholog	0.45	2.21	4.96E-02
MT1H	Metallothionein-1H MT1H1	0.43	2.33	1.32E-02
H2A1C	Histone H2A type 1-C HIST1H2AC	0.42	2.41	5.78E-03
ITIH2	Inter-alpha-trypsin inhibitor heavy chain H2 ITIH2 PE=	0.40	2.47	ND
TRX-2	Thioredoxin reductase-2	0.37	3.36	4.00E-02
FKBP2	Peptidyl-prolyl cis-trans isomerase FKBP2 FKBP22	0.26	3.89	ND
MIOX	Inositol oxygenase MIOX1	0.24	4.25	ND
GRPE1	GrpE protein homolog 1, mitochondrial GRPEL12	0.22	4.50	3.96E-03
ASNA	ATPase ASNA1 ASNA12	0.00	Good only	Good only
CH3L1	Chitinase-3-like protein 1 CHI3L12	0.00	Good only	Good only

ND (not defined) indicates that there were only one abundance value from this protein in one of the subgroups and at least three values in the other subgroup so the t test value could not be accurately defined.

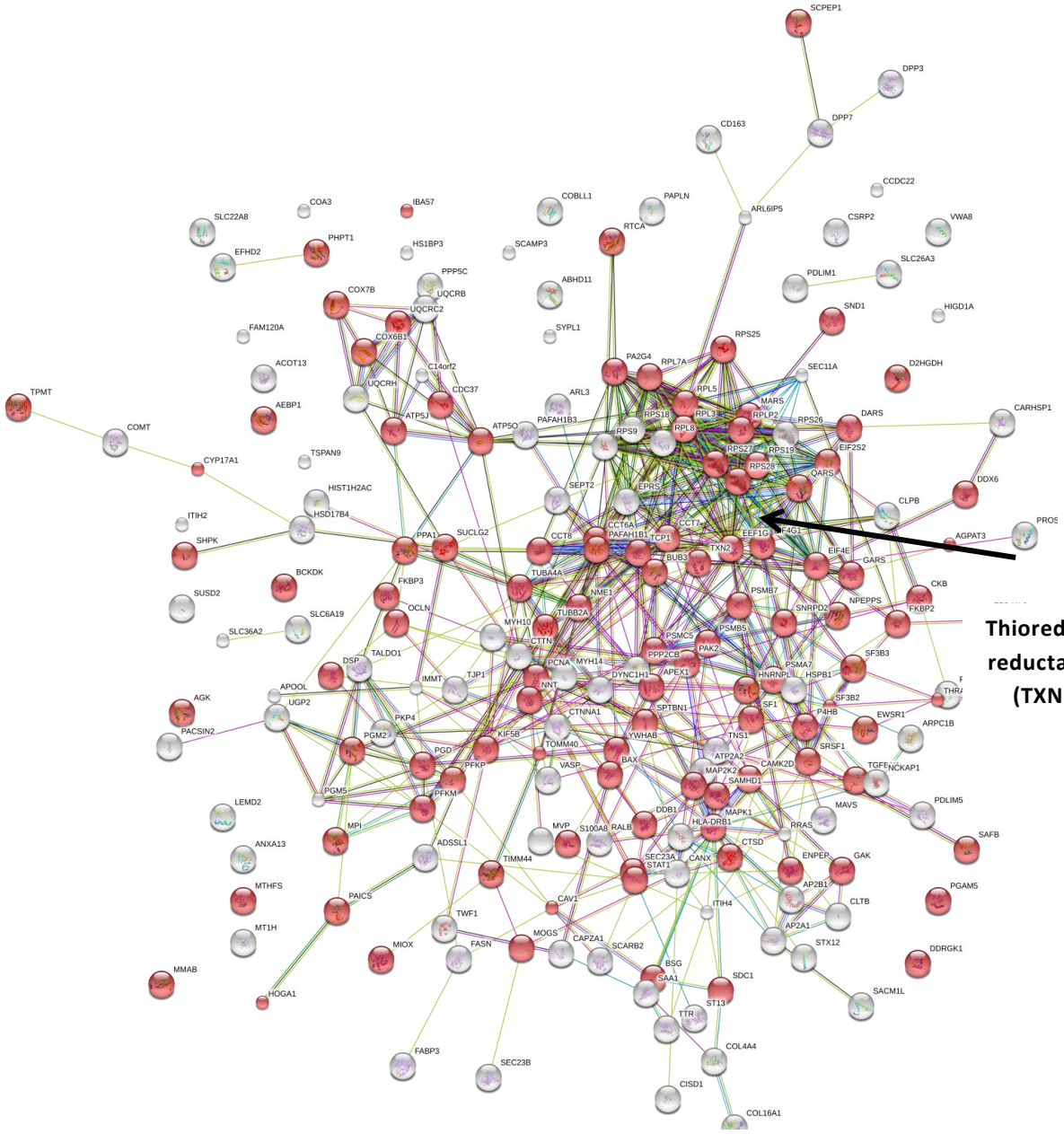

Figure 6.6 Proteins associated with cellular metabolic process pathways
String bioinformatics analysis showing the 67 proteins identified and associated with metabolic pathways with FDR 2x10^{-3} from the proteins that were statistically significant in their regulation between the SO & GO subgroups (214 proteins). The red spheres represent the subset of proteins associated with the cellular response to stress; the grey spheres represent the remaining proteins. Thioredoxin reductase-2 has a central position in the metabolic pathway according to the string analysis and is indicated by the blue arrow. Proteins details are provided in table 6.2.

Table 6.3 Protein associated with the cellular response to stress pathway

Protein	Description	Fold change Sub/Good	Fold change Good/Sub	p values
RS27	40S ribosomal protein S27	17.76	0.06	ND
TGFI1	Transforming growth factor beta-1-induced transcript 1 protei	7.42	0.13	4.53E-02
STAT1	Signal transducer and activator of transcription 1-alpha/beta	6.94	0.14	3.00E-04
S100A8	Protein S100-A8	4.65	0.22	4.84E-03
FAS	Fatty acid synthase	2.83	0.35	ND
FABPH	Fatty acid-binding protein, heart	2.68	0.37	7.38E-03
PSMB7	Proteasome subunit beta type-7	2.44	0.41	3.68E-02
PSMA7	Isoform 2 of Proteasome subunit alpha type-7	2.33	0.43	7.48E-03
MP2K2	Dual specificity mitogen-activated protein kinase kinase 2	2.13	0.47	ND
MAPK1	Mitogen-activated protein kinase 1	2.11	0.47	3.55E-02
SAA1	Serum amyloid A-1 protein	2.11	0.47	ND
KINH	Kinesin-1 heavy chain	1.98	0.50	4.37E-03
BASI	Isoform 2 of Basigin	1.96	0.51	2.09E-05
RS25	40S ribosomal protein S25	1.84	0.54	1.65E-02
CALX	Isoform 2 of Calnexin	1.81	0.55	3.93E-02
RS28	40S ribosomal protein S28	1.77	0.57	2.83E-02
RS18	40S ribosomal protein S18	1.76	0.57	3.67E-02
F10A1	Hsc70-interacting protein	1.70	0.59	2.79E-02
APEX1	DNA-(apurinic or apyrimidinic site) lyase	1.62	0.62	3.24E-02
SAMH1	Deoxynucleoside triphosphate triphosphohydrolase SAMHD1	1.60	0.62	ND
HSPB1	Heat shock protein beta-1	1.57	0.64	4.61E-02
RS19	40S ribosomal protein S19	1.50	0.67	2.51E-02
PSMC5	Isoform 2 of 26S protease regulatory subunit 8	1.47	0.68	1.39E-02
EF1G	Elongation factor 1-gamma	1.64	0.61	8.40E-03

ND (not defined): indicates that there were only one abundance value from this protein in one of the subgroups and three values in the other subgroup so the t test value could not be accurately defined.

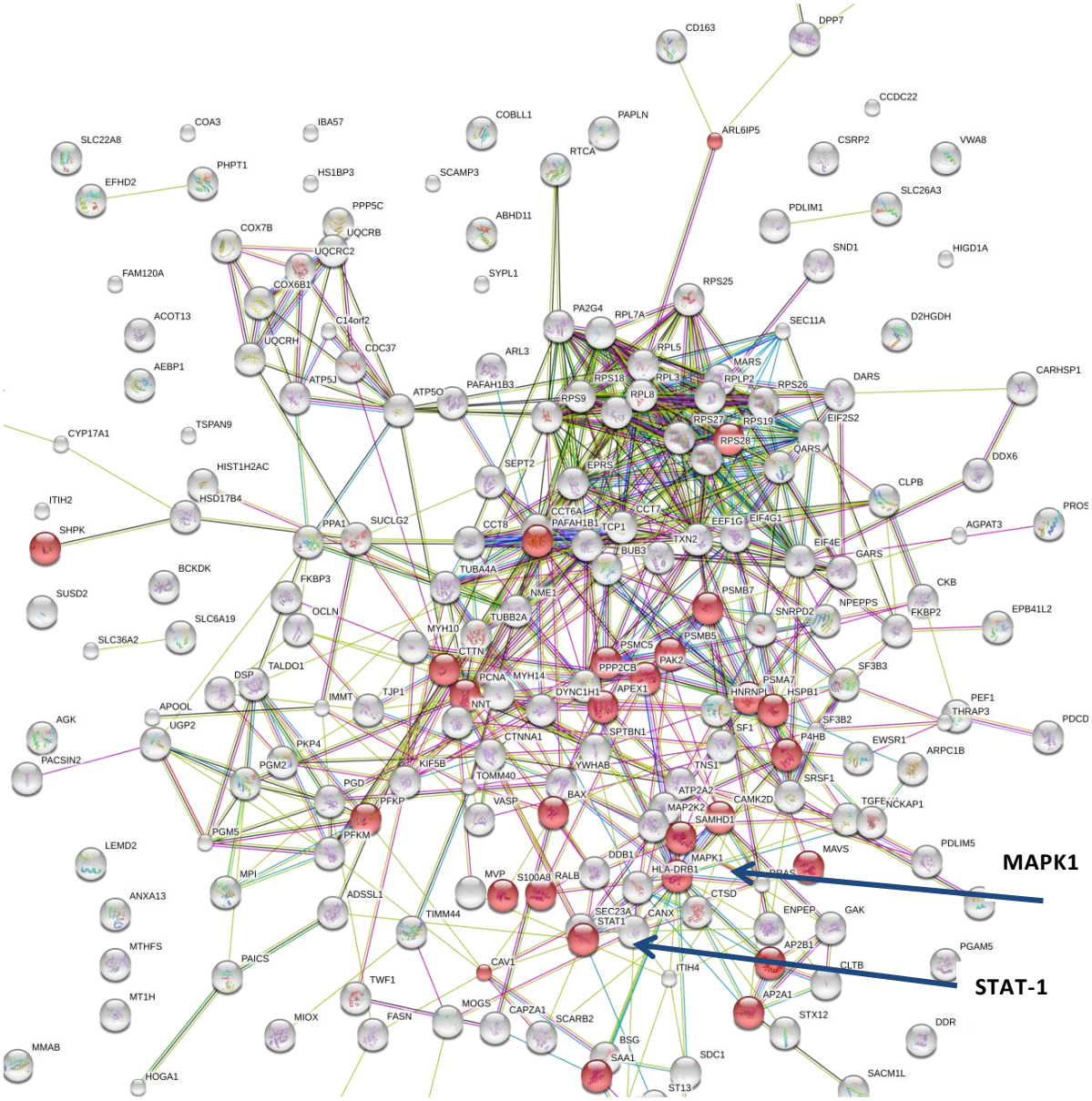

Figure 6.7 Proteins associated with cellular response to stress stimuli
Analysis was as described in figure 6.6. 26 proteins were identified and associated in this pathway with FDR 2 10^{-3}. String analysis includes only the proteins that were statistically significant regulated between the SO & GO subgroups (214 proteins). The red spheres represent the proteins associated with cellular response to stress processes. The rest of the spheres represent the proteins identified by LC-MS/MS. STAT-1 and MAPK-1 are key signalling molecules of stress induced signalling pathways and are highlighted with arrows. Proteins details are provided in table 6.3.

Interplay between injury and cytoprotective pathways

As shown in table 6.3 and figure 6.7, pathway analysis identified some key mediators of cellular stress pathways among the 26 proteins significantly increased in the kidneys that had suboptimal function post-transplantation. Among these proteins were the signal transduction proteins MAPK-1, TGF-β1 and STAT-1. The levels of both TGF-β1 (p=0.04) and STAT-1 (p=0.0003) increased by 7 fold in the kidneys in SO compared to GO kidneys and the levels of MAPK-1 increased by 2.1 fold (p=0.03) (table 6.3 & figure 6.7).

Evidence of endothelia cell activation was suggested by the highly significant increased abundance of basigin (BSG) in the kidneys with suboptimal function (1.96 fold; p=0.0001). Similarly, the increased abundances of heart-fatty acid binding protein (H-FABP) (2.7 fold; p=0.007) (figure 6.8) suggested enhanced kidney dysfunction and the proteasome subunit type 7 (2.5 fold; p=0.05) suggested enhanced catabolic activity in the SO associated donor kidneys (figure 6.8).

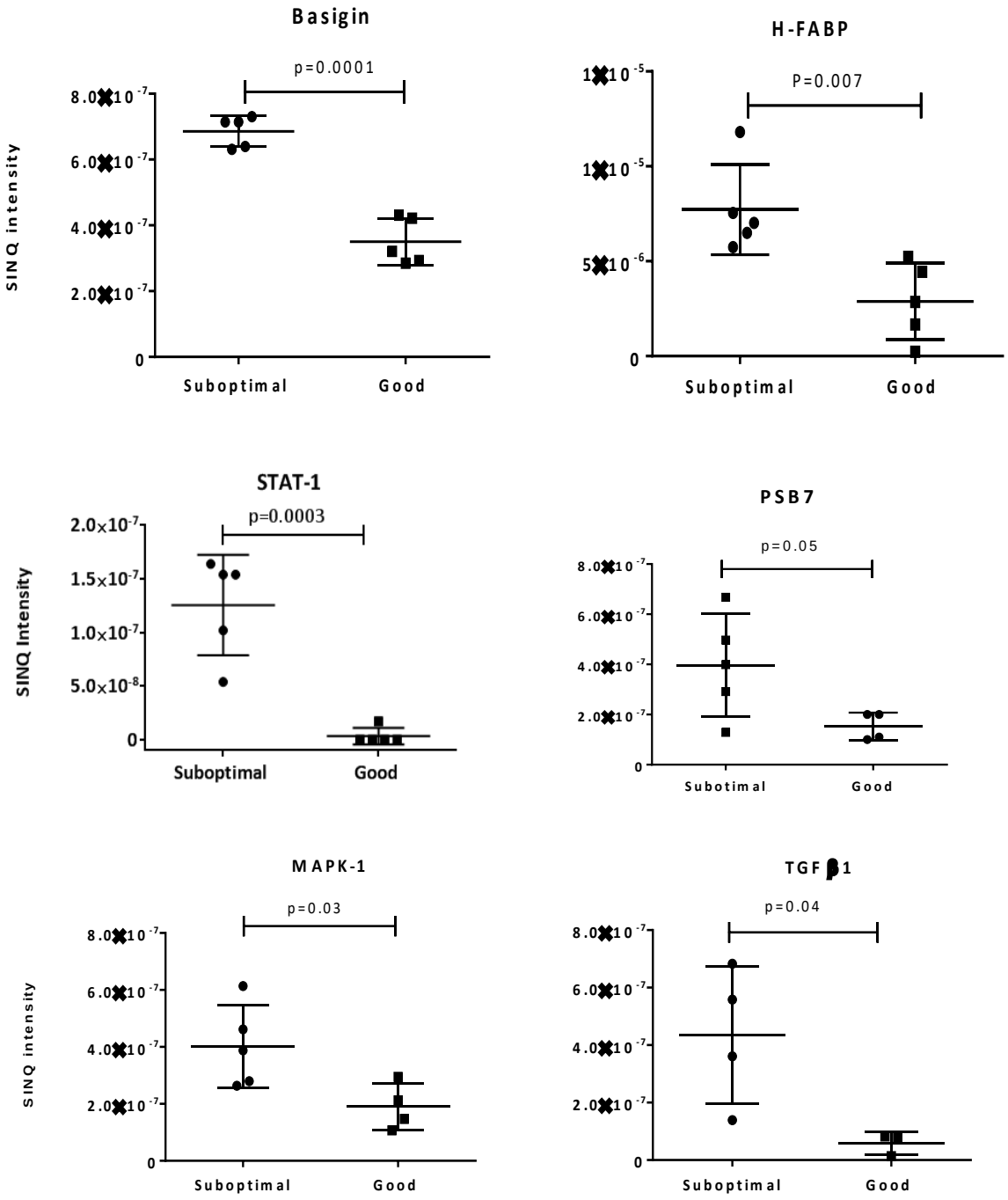

Figure 6.8 Proteins associated with kidney injury in donor kidney biopsies with suboptimal outcomes

Quantitative mass spectrometry revealed increased abundance of signal transduction proteins in donor kidney biopsies associated with suboptimal compared to good transplantation outcomes (measured by spectral index quantitation – SINQ). Levels of signal transduction and activator of translational-1 (STAT-1), mitogen activated protein kinase-1 (MAPK-1), proteasome subunit B type 7 (PSB7), transforming growth factor-β (TGF-β), basigin and heart-fatty acid binding protein (H-FABP) are shown.

STAT-1 was identified in all the analysed SO associated kidney biopsies in addition to demonstrating the most significant change amongst the two experimental groups (figure 6.8). Therefore, STAT-1 was chosen for further investigation by western blot to see if this enhanced expression could be demonstrated in an independent cohort of SO associated biopsies. 28 kidney biopsies, 14 SO and 14 GO associated, were analysed by western blot and probed with anti-STAT-1 (figure 6.9). Densitometric quantification values were normalised against β-actin values. The combined densitometric values confirmed the significant increased expression of STAT-1 in the SO compared to GO associated kidneys (2.8 fold change; p=0.02) (figure 6.9).

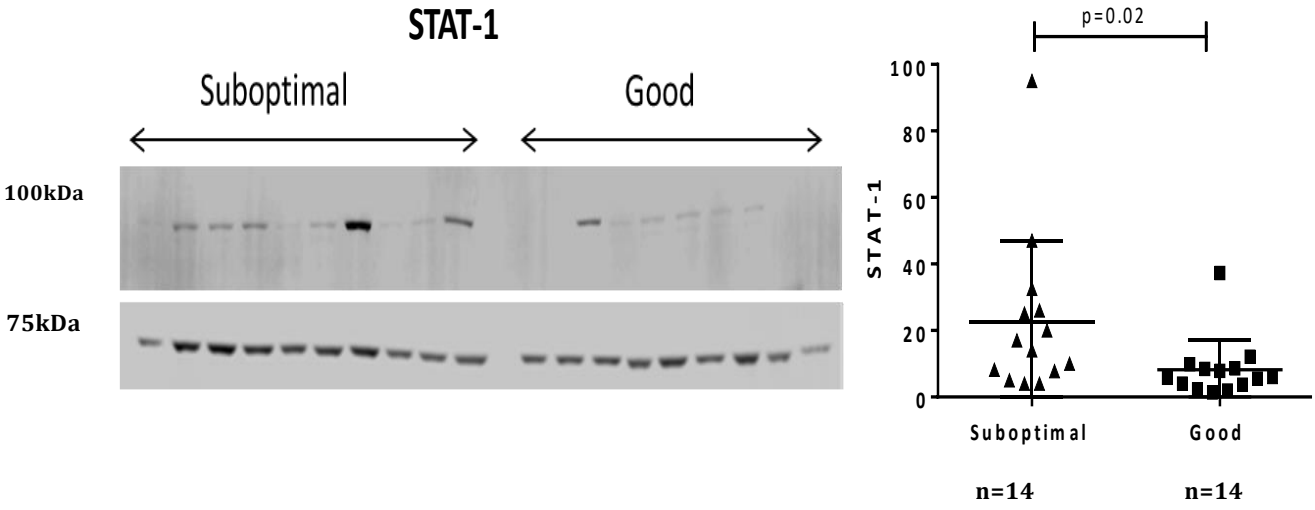

Figure 6.9 Comparison of STAT-1 protein in suboptimal and good outcome associated kidney biopsies

Western blot of STAT-1 (MW:88kDa) (left panel) and densitometric quantification of β-actin normalised intensities values (right panel) was performed on an independent cohort of n=28 donor kidney biopsy samples. The raw western blot data of n=28 kidney biopsy samples is presented in figure S6.4

The increased expression of the pro-fibrotic mediator TGF-β1 in the kidneys of SO (figure 6.8) suggested a potentially increased occurrence of fibrosis in SO compared to GO kidneys. To test this possibility, platelet derived growth factor receptor α (PDGFRα) was analysed by western blotting (figure 6.10B). PDGFRα was of particular interest for two reasons. Firstly, PDGFRα exerts a synergetic role with TGF-β1 in the onset and propagation of fibrosis. Secondly, an increased expression of PDGFRα was observed in the PROTOMAP analysis of biopsies from SO associated kidneys (figure 6.10A). Blotting confirmed significantly increased levels of PDGFRα in the SO associated kidneys compared to GO associated kidneys ($p=0.01$) (figure 6.10B & C).

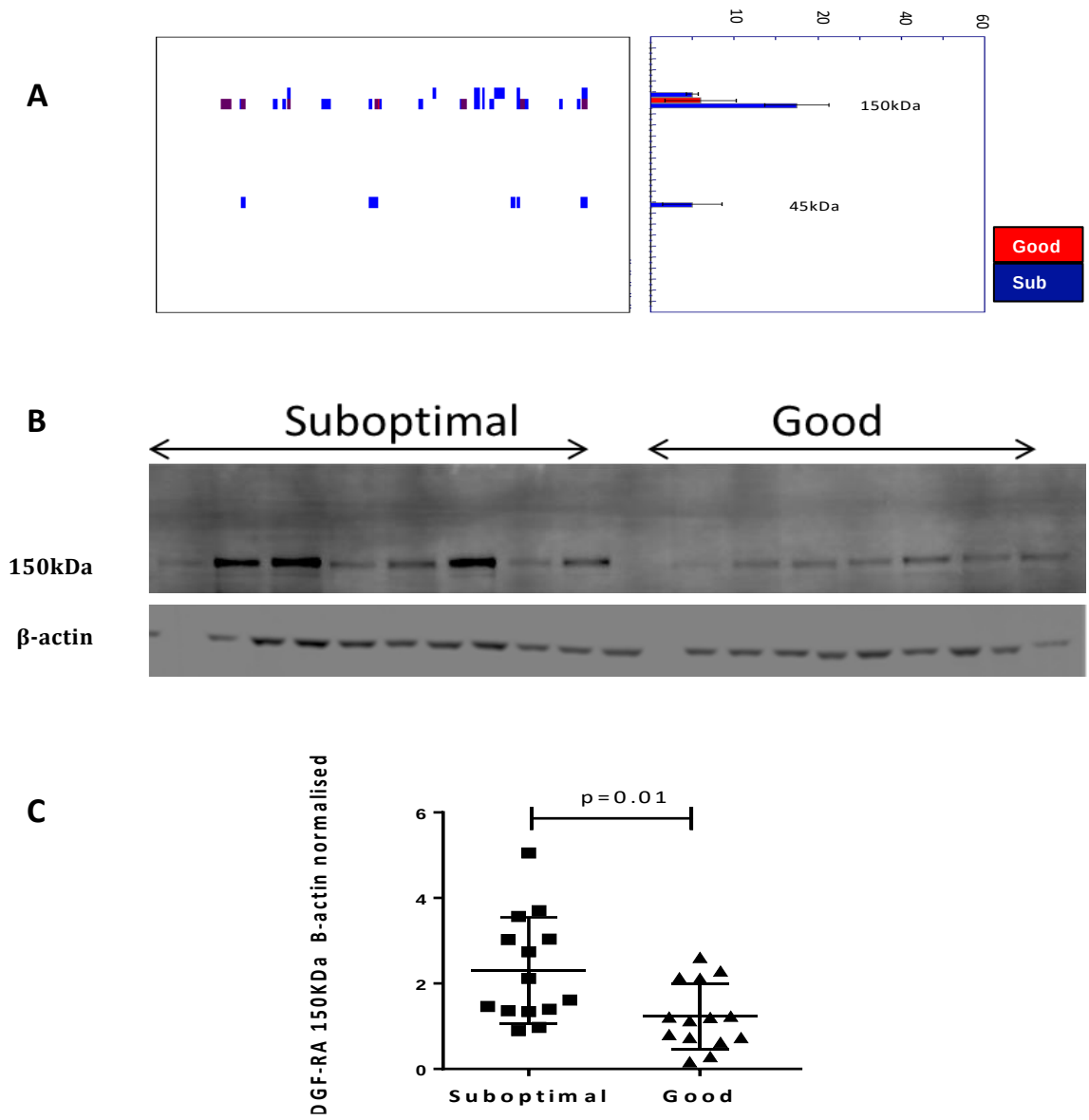

Figure 6.10 Platelet derived growth factor receptorα (PDGFRα) analysis
A. *Degradomics analysis by PROTOMAP revealed by a PDGFRα peptograph, shows enrichment of the parent protein (150KDa) and the appearance of a 45kDa fragment present in the suboptimal associated kidneys but not good outcome kidneys. The analysis was on pooled n=5 biopsy samples per transplantation outcome. Red bars represent MS spectral counts observed for the pooled kidney biopsy samples with GO, while the blue bars show the counts for the pooled biopsy samples with SO.* ***B****. Western blot analysis of an independent cohort of n= 28 biopsy samples (n=14 SO & n=14 GO), β-actin western blot was used for normalisation of the PDGFRα analysis. The western blot of all the samples can be seen in figure S6.3.* ***C****. Densitometric analysis normalised to β-actin shows a significant difference in PGDFRα 150 kDa levels observed between the two subgroups.*

In contrast to the injury associated proteins with increased levels of expression in the SO kidneys, proteomic analysis of GO associated kidneys showed increased levels of key antioxidant and cytoprotective proteins such as thioredoxin reductase-2 (Trx2), (3.36 fold increase, p=0.04). To further investigate the increased antioxidant protein expression of GO associated kidneys, key antioxidant proteins of the thioredoxin group and glutathione metabolism system were investigated by western blot. 28 biopsy samples (14 GO associated and 14 SO associated) were probed with antibodies to thioredoxin 1 (Trx1), glutathione-S-transferase (GST), peroxiredoxin-3 (Prx3) and catalase (figure 6.11 and S6.4). Band intensity values were estimated by densitometric analysis. Blotting confirmed that Trx1 (p=0.005), GST (p=0.02) and Prdx3 (p=0.04) had significantly increased levels in the GO associated kidneys compared to SO kidneys. Catalase however, was not significantly different between the two groups.

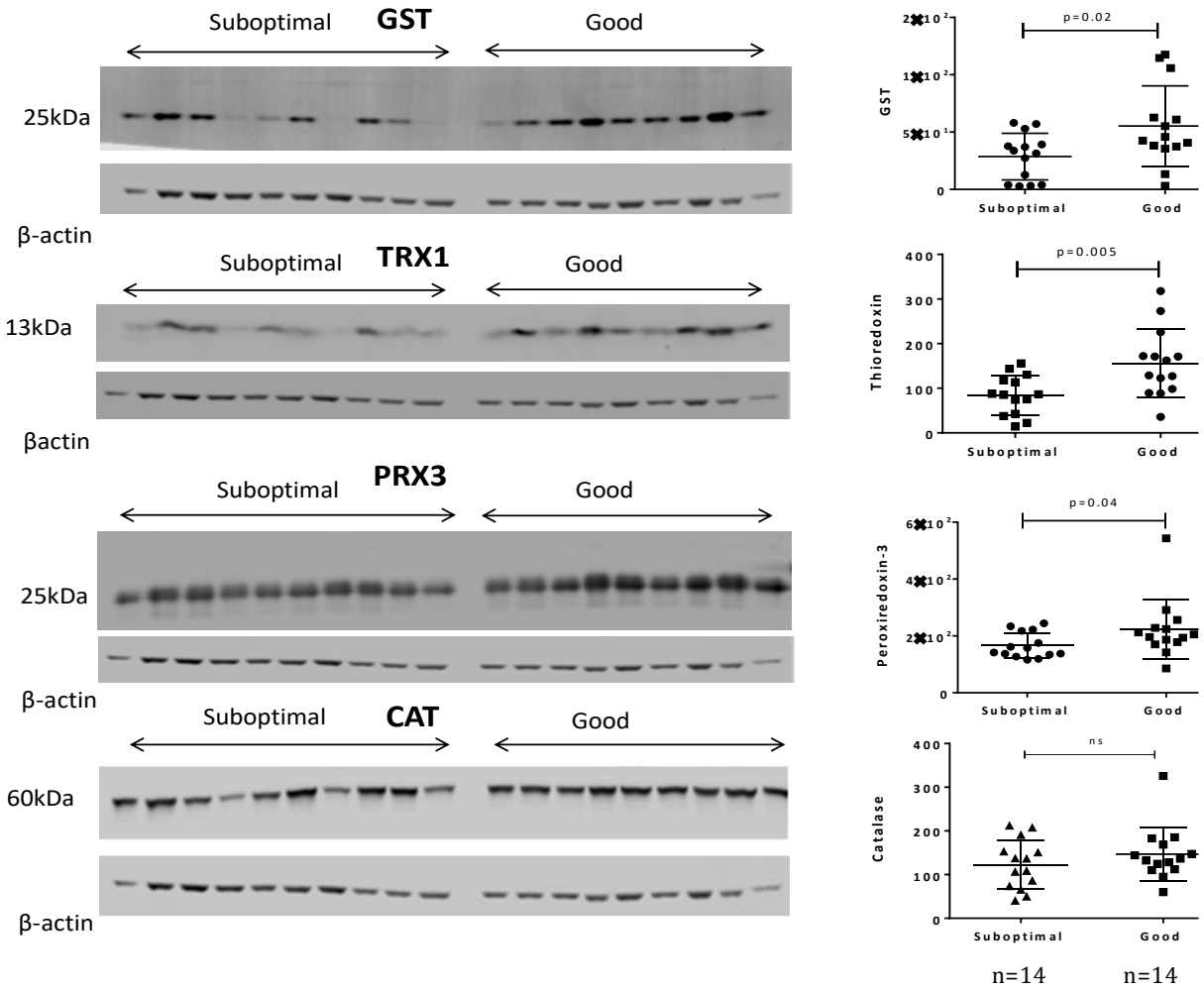

Figure 6.11 Western blot and densitometric analysis of proteins associated with cytoprotective and antioxidant pathways in SO and GO kidney biopsies
Western blot validation analysis and densitometry based quantification of β-actin normalised intensities of key antioxidant proteins of the thioredoxin group and glutathione metabolism system. Thioredoxin 1 (Trx1; MW: 13kDa), glutathione S transferase (GST; MW:26), peroxiredoxin -3 (Prx3; MW:25kDa) and Catalase (CAT; MW:60kDa) were analysed on an independent cohort of donor biopsy samples (n=28; 14 good (GO), 14 suboptimal (SO)). The western blots for all samples is shown figure S6.4. ns: not significant

Alterations in the degradome profile of key kidney cytoskeletal proteins and their association to suboptimal allograft function 3 and 12 months post transplantation

The initial LFQ-MS/MS proteomic data and pathway analysis suggested that 30 significantly regulated proteins were associated with catabolic processes, indicating that there is enhanced proteolytic activity in donor kidney biopsies (FDR: 2.27 10-5; figure S6.1). To test this, a PROTOMAP analysis was performed to explore differences in protein degradation patterns and to visualise proteins degradation intermediates resulting from the action of endogenous proteases. Using PROTOMAP, two conditions (SO vs GO) were compared resulting in the identification of 6258 proteins. Peptographs for each of these proteins were assessed visually to identify proteins that shown evidence of proteolysis. Figure 6.12 presents a selection of peptographs showing patterns of protein degradation. Their selection was based on:

i) increased spectral counts of fragments that had migrated at a lower molecular mass in SO (blue bars) as compared to GO (red bars),

ii) enrichment of the intact protein or protein fragments in the SO group and

iii) biological relevance, with an emphasis on cytoskeletal proteins involved in the glomerular filtration barrier

Most notably, degradation of a number of proteins was observed that have a vital role in sustaining the structure of healthy podocytes, the slit diaphragm and connections to glomerular basement membrane (GMB).

All the proteins and their corresponding peptographs shown in figures 6.12 demonstrated either, an enrichment of the parent protein in one of the two

experimental groups (for example, alpha actninin-4) or, the generation lower molecular mass of protein fragments compared to the parent protein.

Utrophin showed fragmentation of the intact protein (>390kDa) in both cohorts with the generation of fragments observed at around 210 kDa and at a lower molecular mass two fragments identified only in the SO group (blue bars) at around 180-190kDa. This lower fragment lacked the N-terminal component of the full length protein (figure 6.12).

Laminin subunit beta-2 showed C-terminal fragments of the 200 kDa, parent protein at around 40-50kDa only seen in SO group (figure 6.12).

Talin-2 showed increased fragmentation of the intact protein (>250kDa) with breakdown intermediates observed at 200-170 kDa, 60kDa and 40kDa in both groups. However, a 25kDa C-terminal fragment was observed only in SO associated samples (figure 6.12).

Peptographs of the proteins integrin alpha-1 and alpha actinin-1 showed that both proteins had undergone proteolysis with the generation of lower molecular weight fragments at around 185 and 150kDa respectively (figure 6.12).

Collagen proteins alpha 1 chain III exhibited fragmentation across all the gel bands with the generation of SO associated fragments at around 10kDa. Alpha 1 chain (XVIII) showed a distinct pattern that was outcome specific. With the expected molecular weight at around 179 kDa, there were protein fragments at 75 to 25 kDa seen only in the GO samples and two clusters of fragments, one around 100-120 kDa and another at around 20-15kDa seen only in SO samples (figure 6.12).

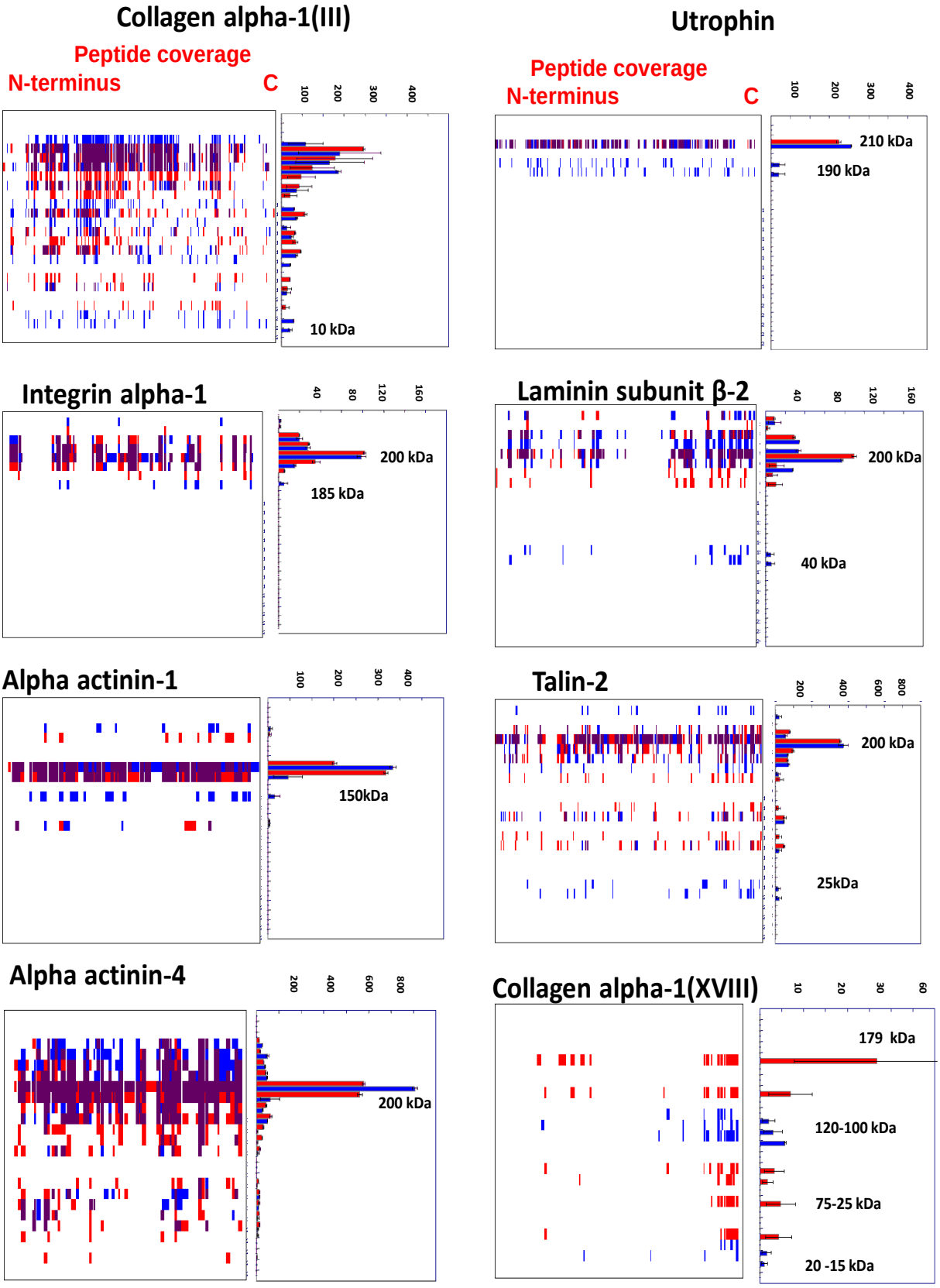

Figure 6.12 Peptographs of selected proteins identified by PROTOMAP analysis

Good Sub

Finally, figure 6.13 shows the peptograph of the calpain 1 catalytic subunit with protein enrichment of the parent protein at 80kDa and the generation of a fragment at around 20kDa molecular mass seen only in the SO samples.

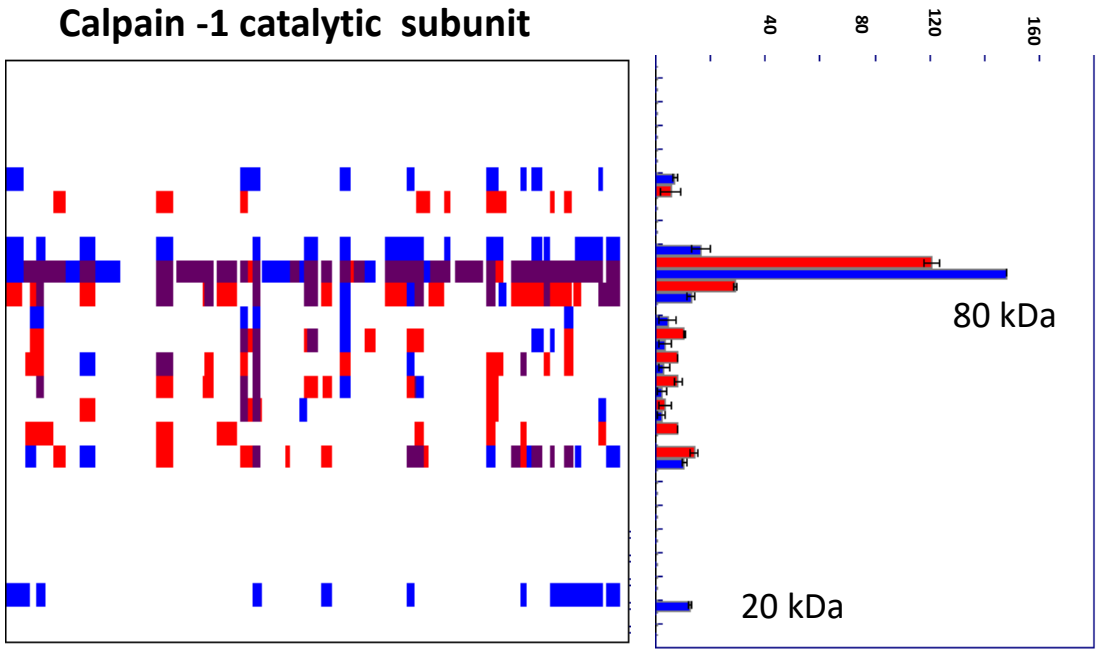

Figure 6.13 Peptograph of calpain-1 catalytic subunit
Peptograph of calpain 1 catalytic subunit showing protein enrichment in the kidneys with suboptimal allograft function (blue bars) at 80kDa and the generation of a unique protein fragment at around 20kDa.

6.5 Discussion

The lack of more refined diagnostic tools to assess donor kidney quality has led to a high rate of kidneys deemed unsuitable for transplantation but also to acceptance of marginal donor organs that resulted in a poor long-term outcome. Tools to assist clinical decisions on whether to accept or decline kidneys for transplant are needed to support the clinical decision at time of offering. Furthermore, as techniques are developed to resuscitate organs or mitigate ischaemic damage by perfusion prior to transplantation, the same tools could be used to develop and monitor these protocols.

Proteomic analysis of donor kidney biopsies can predict post-transplantation outcome

This study has shown that it is possible to differentiate, at the time of retrieval, donor kidneys which will go on to have a suboptimal outcome in the recipient from those with a good long-term transplantation outcome based solely on the proteomic signatures of biopsy tissue. The initial recruitment of donors and selection of biopsies was based on three month follow-up data since 12 month follow-up data was not available. However, the 12 month follow-up eGFR data later confirmed the initial predicted assignment of transplantation outcomes. A comparison of the proteomic signature between the GO and SO associated biopsies revealed an increased level of mediators of tissue injury in SO associated kidneys and increased levels of cytoprotective proteins in GO kidneys. This suggests that different physiological processes are active in the two kidney cohorts and that activation of either injury or repair pathways may be primary determinants of kidney function post-transplantation (figures 6. 5A & B, 6.9, 6.10 & 6.11).

Remuzzi scoring or AKIN classification of kidney biopsies and post-transplantation outcomes

AKIN classification of deceased donors and Remuzzi scoring of kidney biopsy tissue are two methods currently used to assess donors and marginal kidneys for their suitability for donation and as transplants. As shown in table 6.1, Remuzzi scoring and AKIN classification of the kidney samples analysed in this study failed to discriminate between donor kidneys with SO and GO outcomes. However, a proteomic profile of the samples identified 214 differentially expressed proteins that, taken together, could discriminate between the SO & GO associated samples (figure 6.5A&B).

The criteria for donor samples selected for this study were stringent in that the donors had donated both kidneys to two recipients and both recipients had the same transplantation outcome. This was to ensure that the observed differences between the experimental groups were most likely to arise from donor organ quality. Furthermore, for kidneys within the SO cohort multiple clinical end points were considered, such as the onset of DGF and allograft function indicated by eGFR values at 3 months post-transplantation. 12 month follow-up data showed that there was a modest improvement in eGFR values within the SO group compared to 3 month follow-up values, from a mean eGFR 29.8± 7.0 to a mean eGFR 35.9± 6.0 ml/min but all kidney recipients at 12 months were still classified as chronic kidney disease (CKD) stage 3b as defined by MDRD[220]. Transplanted kidneys classified as CKD stage 3b have an increased risk of progression to stages 4 and 5 and a high prevalence of graft failure as recently published by Clayton *et al.,* [223].

The sustained reduced allograft function observed in the recipients of SO kidneys used in this suggested the presence of an on-going pathology such as subclinical inflammation and injury that adversely affects the transplantation outcome, as previously reported[216,222]. Further evidence to support the impact of donor kidney quality on the suboptimal allograft function can be drawn from the pathway analysis of the proteomic data of donor kidneys. This highlighted the dynamic interactions of metabolic, cellular stress, inflammatory and catabolic pathways. In contrast, donor kidneys associated with good transplantation outcomes 3 and 12 months post-transplant had an increased expression of cytoprotective proteins (figures 6.9, 6.10, 6.11).

Increased expression of apoptotic and pro-fibrotic mediators in kidneys associated with suboptimal outcomes

The enrichment of proteins of cellular stress and metabolic dysregulation with parallel increased levels of pro-fibrotic and apoptotic protein levels in SO associated biopsies (figure 6.6 & 6.7) agreed with previous findings in a rodent brain death model by Akhtar *et al*[22]. Using a proteomics and metabolomics integrative approach, the authors observed metabolic dysregulation, mitochondrial dysfunction and generation of ROS species.

The dynamic relationship between ROS and TGF-β has been extensively examined *in vitro* and *in vivo*[223–225]. The proteomic data showed significant increased levels of TGF-β1 in DBD kidneys with SO compared to GO (figure 6.8). TGF-β1 mediates ROS production and suppresses antioxidant activity causing an imbalance in redox homeostasis that further promotes oxidative stress. This potent fibrogenic mediator has a key role in the onset and progression of fibrosis in all organs

(figure 6.14). Animal model studies have shown that blocking TGF-β1 limits or prevents the progression of fibrosis[226].

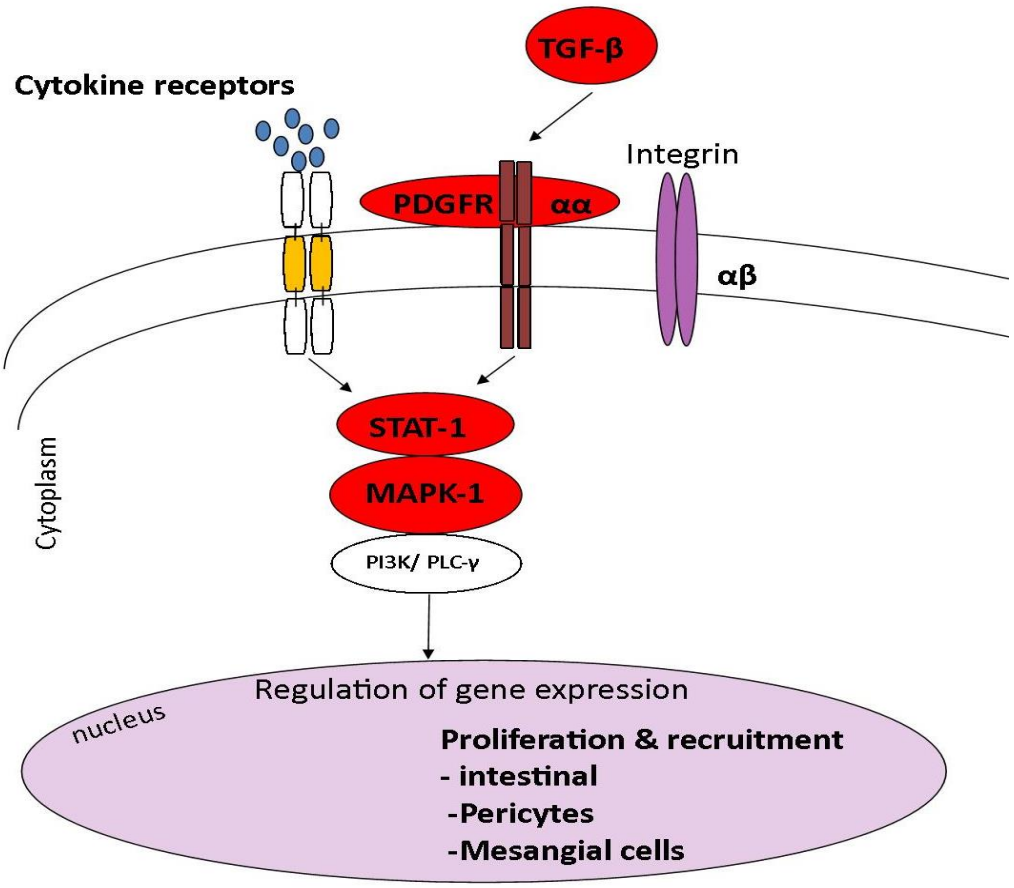

Figure 6.14 TGF-β1 and PDGFRα signalling in kidney glomeruli network formation and fibrosis[227]

Activation of PDGFRα leads to the recruitment of pericytes (mesangial cells) in the kidney glomerulus and is usually required for normal formation of a branched network of capillaries in kidney glomeruli. This pathway appears to be activated under pro-fibrotic conditions. Red indicated the pro-fibrotic and signalling proteins identified with increased expression levels in donor kidneys with suboptimal transplantation outcomes when compared to good function associated kidneys. The described model of PDGFR signalling has been modified from Boor et al., Nature Reviews Nephrology, 2010[227].

Considering the key role of TGF-β1 in the progression of kidney injury, it was not surprising that the significant increased protein levels of TGF-β1 correlated with increased levels of PDGF Rα in the same SO cohort (figure 6.8, 6.10 & 6.14). Activation of PDGF receptors can be achieved by alternative mediators to PDGF ligands and one of these is TGF-β. PDGFRα is one of the two receptors in the PDGF family and although all PDGF factors play a vital role in healthy kidney development, PDGF Rα contributes in promoting kidney fibrosis through a maladaptive process of wound healing[228–230]. Furthermore, the synergistic action of TGF-β and PDGFRα can promote the differentiation of pericytes and recruitment of fibroblasts and myofibroblasts causing irreversible changes to the extracellular matrix and with fibrosis and damage to renal tubules[223,226,231–233] (figure 6.14). As key players in both the development or negative regulation of kidney fibrosis, blocking their chemoattractant action with targeted interventions has been reported to reduce fibrosis in many studies[234–240].

As early as 1996, Yamamoto *et al.,* demonstrated in a rat model how activation of PDGF receptors promoted downstream signalling of STAT-1 activation and transcription of genes that propagate inflammation and apoptosis[241]. Since that paper, this association has been demonstrated in many models of fibrosis and atherosclerosis including, most recently, by He *et al.,* using an atherosclerosis model where activation of PDGF receptors led to STAT-1 phosphorylation in a JAK1/2 dependent process in vascular smooth muscle cells (VSMCs), whereas deletion reduced inflammation and atherosclerosis in VSMCs[242–245].

These observations are consistent with the proteomic and western blot data described in this chapter showing an increased expression in PDGFRα and STAT-

1 in SO associated donor kidneys (figures 6.9 &6.10). During this study it was not possible to explore whether these proteins were phosphorylated or not, mainly due to limited availability of biopsy material for additional experiments. Therefore, these results can only suggest that the increased levels of STAT-1 results from upstream activation of signalling pathways triggered by the high abundance of inflammatory cytokines activating their cognate receptors. Thus STAT-1 may be a marker of pro-apoptotic gene expression and kidney injury in DBDs[189,211,246,247]. The parallel increased expression of STAT-1 and MAPK-1 levels could indicate an orchestrated activation of JAK/STAT and mitogen-activated protein kinase (MAPK)/p38 pathways that drive transcription of genes leading to inflammation and apoptosis. In turn, this results in an enhanced immunogenic state prior to retrieval that can be aggravated during cold preservation and at time of reperfusion of the allograft resulting in kidney injury and long term kidney impairment, as has been previously reported[199,248].

The most common causes of brain death in organ donors in the UK are intracranial haemorrhage or hypoxic brain death. As discussed in chapter 1, brain death leads to profound systemic changes, including haemodynamic instability, hormonal imbalance, systemic circulation of chemokines and cytokines, all of these with an adverse impact on cardio-thoracic and abdominal organs[19]. One of the main consequences of these systemic changes is the infiltration of inflammatory cells into donor organs, the expression of danger associated molecular patterns (DAMPs) and metabolic disturbances including depletion of adenosine triphosphate (ATP)[31,191,249].

In this study, all analysed deceased donor kidneys obtained from DBDs had similar clinical and demographic characteristics (table 6.1). In an attempt to explain the diversity in transplantation outcomes, consideration needs to be given to the genetic make-up of each donor and lifestyle choices that could have impacted on kidney function and contributed, in the aftermath of brain death, to the onset of irreversible damage in some kidneys, whilst in other kidneys the capacity of recovery has remained.

Antioxidant proteins increased in kidneys with GO

Excessive production of ROS has important implications on redox homeostasis and on cell signalling events that promotes apoptosis and cell death. As a counterbalance, antioxidant cellular mechanisms - enzymatic or not - are activated under conditions of oxidative stress to reinstate a healthy cellular environment[31,250,251].

Combined, proteomic and western blot analysis showed that increased levels of key antioxidant factors were distinctly associated with good kidney function suggesting that the ability to remove or neutralise oxidant molecules makes these DBD kidneys less susceptible to ischaemia.

ROS regulation is achieved by oxidation-reduction reactions with the involvement of thiol groups in proteins resulting in the modulation of tyrosine or serine-threonine phosphorylation of target proteins[252]. Two cellular redox systems play key role in these processes: the thioredoxin and glutathione systems. The thioredoxin system includes thioredoxin (Trx), thioredoxin reductase (TrxR) and thioredoxin peroxidases (Prx) while the glutathione system includes glutathione (GST), glutathione reductase (GSTR), glutathione

peroxidase(GSTP) [253] (figure 6.11). TrxRs are named for their ability to reduce oxidized thioredoxins as a process of ROS elimination[252,253].

This study demonstrated a parallel significant increase of Trx1, TrxR, Prx3 and GST protein levels in in GO associated kidneys suggesting the activation of redox signalling pathways downstream of the generation of intracellular ROS. Activation of redox pathways may point to a key protective role in kidneys that will function well in the recipient, by reducing or negating the harmful effects of ROS generation from ischaemic damage. Trx1 is selectively expressed in the cortex of human kidneys and localised mainly in the proximal tubules and, to a lesser extent in distal tubules. It is either secreted into the cytosol or translocated to the nucleus upon activation and promotes gene expression[254]. In ischaemia/reperfusion injury (I/R) animal models, Trx1 and Prx3 were both increased immediately after reperfusion in the segments most vulnerable to ischaemia with high metabolic activity and low oxygen supply as reported by Kasuno *et al.,*[255]. However, overexpression of human Trx1 had a protective impact following I/R in those localised areas of the nephron[256]. This cytoprotective capacity of Trx1 has been tested in a lung transplantation model where priming donor lungs with Trx1 before transplantation limited NF-kB activation, inflammatory cell infiltration and reduced the extent of I/R injury in allografts[257].

GST antioxidant activity has a role to protect mitochondria through a process of detoxification of products of oxidative stress or lipid peroxidation[258,259]. A number of previous studies have shown the role of GST as a biomarker of kidney injury, indicating a multifaceted role under metabolic dysregulation and

conditions of oxidative stress. An isoform of GST, pi-GST, has been measured in perfusate during machine perfusion of deceased-donor kidneys and has been independently associated with DGF[260].

The results indicate that it may be possible, by recording the antioxidant activity of certain ROS scavengers, to discriminate between DBD kidneys that will recover and function well from those where mechanisms leading to injury and apoptosis result in fibrosis and subsequent limited capacity for recovery post-transplantation. A summary of the potentially competing cytoprotective and apoptotic pathways that may occur in DBD kidneys is shown in figure 6.15.

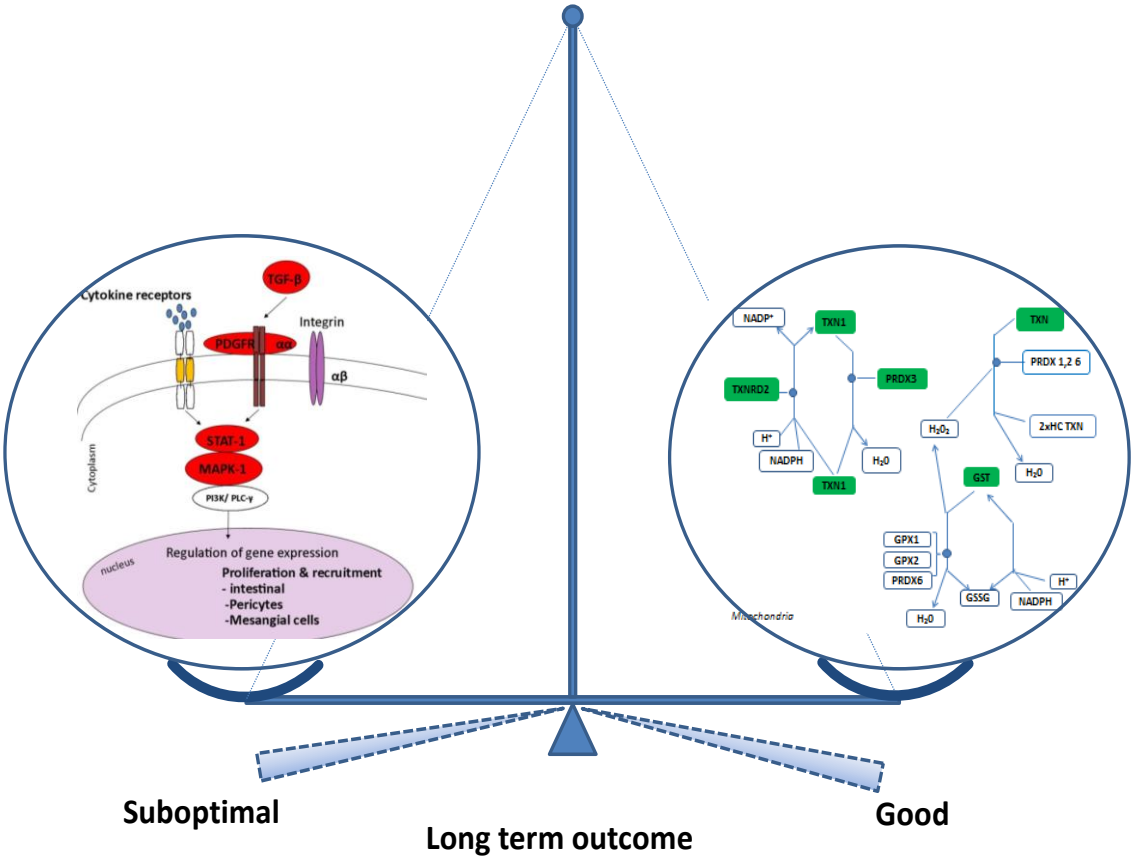

Figure 6.15 Kidney transplantation outcomes depend on a balance of donor kidney injury and cytoprotection

On the left, red indicates increased levels of proteins associated with PDGFRα signalling in donor kidneys that may promote subclinical injury to kidney allografts and suboptimal function 12 months post transplantation. On the right, green indicates increased levels of proteins altered in the kidney proteome that are part of the thioredoxin and glutathione system. These pathways promote cytoprotection and ROS elimination in donor kidneys and may contribute to good transplantation outcomes.

PROTOMAP analysis revealed elevated levels of protein degradation fragments in kidneys with suboptimal outcomes

As discussed above, the pathway analysis of the LFQ proteomic data indicated that enhanced catabolic activity was highly likely in the donor kidneys that had suboptimal function. To explore this in a more systematic fashion, it was reasoned that a mass spectrometry approach tailored to assessing protein degradation (degradomics) would be useful. Several technologies have been developed for this purpose including Terminal Amine Isotopic Labelling of Substrates (TAILS) [261] PRotein TOpography and Migration Analysis Platform (PROTOMAP)[155] or pulsed stable isotope labelling of amino acids in cell culture (pSILAC)[262]. The PROTOMAP approach was used to measure degradation of the serum proteome upon variable blood storage (chapter 4). Since this method provides a comprehensive map of observable protein degradation intermediates, a PROTOMAP analysis was performed to assess evidence for protein degradation with a focus on cytoskeletal and scaffolding proteins that support the glomerular filtration function.

The integrity of the cellular and structural architecture of the glomerulus and the glomerular filtration barrier define the healthy or disease state of the kidneys and its function. The glomerular filtration barrier is formed by closely linked podocyte foot processes and endothelia cells separated by the glomerular filtration membrane [263], as illustrated in figure 6.16.

The structure of the podocyte foot architecture encompasses the podocytes anchored in the GBM, interconnected through the slit diaphragm with a unique cytoskeleton that reveals a precise and distinct cellular structure. This structure carries out the blood filtration function by regulating which molecules will cross this barrier into the urine on the basis of their size[264] (figure 6.16B).

Multiple components play a role in the interconnection of podocytes to GBM and in sustaining the integrity of glomerular filtration barrier. Scaffolding macromolecules such as actins, laminins and collagens, termed focal adhesions, link the podocytes to the GBM. A schematic representation of the podoctyte-GBM interactions is shown in figure 6.16.

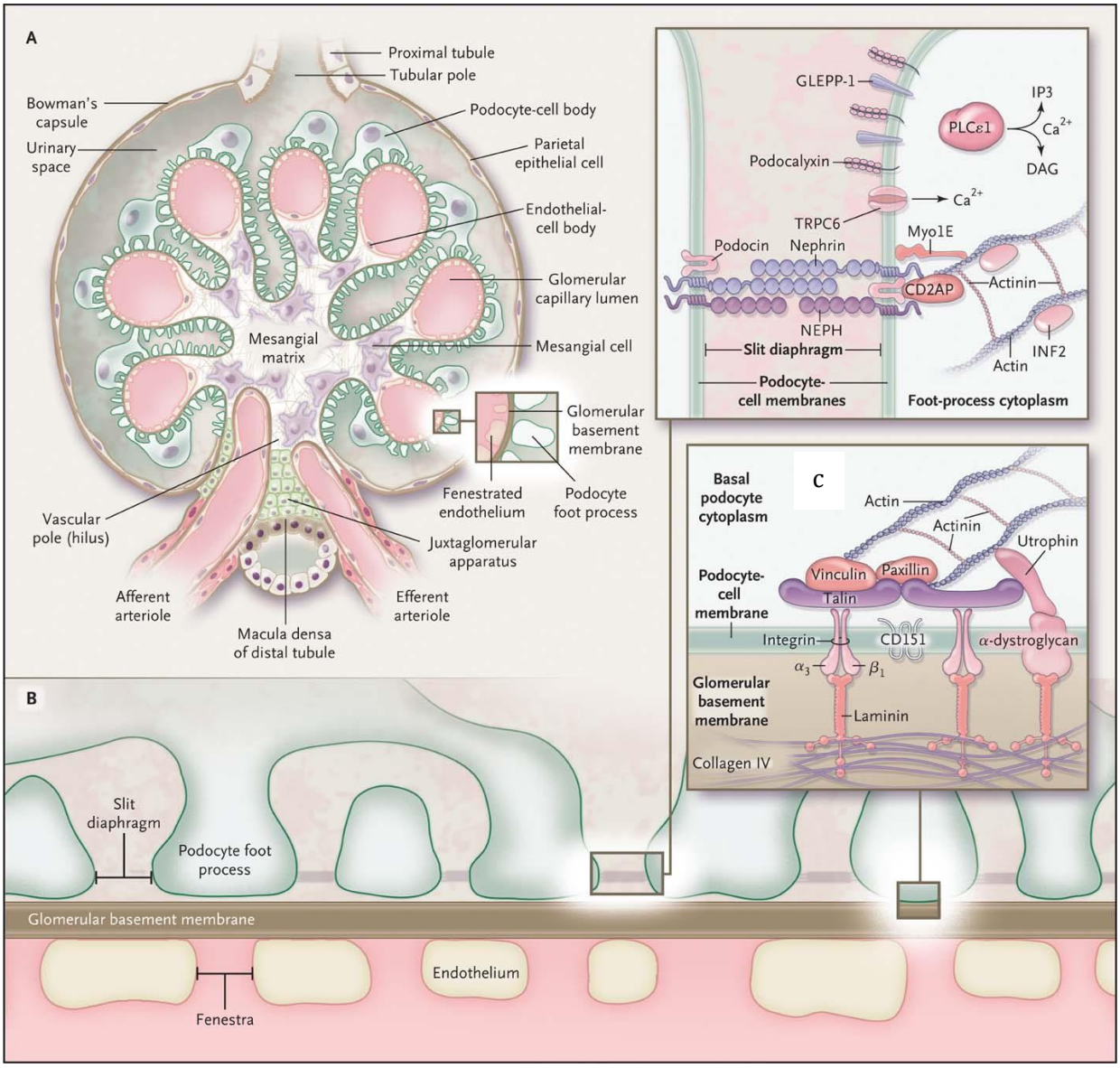

Figure 6.16 Morphology and molecular structure of the glomerulus, the glomerular filtration barrier, and podocytes with the slit diaphragm[263]
A. *Morphology of the glomerulus and the important structures that provide structural support to the glomerular filtration membrane.* ***B.*** *Glomerular filtration barrier.* ***C.*** *Proteins that have a significant role in sustaining the structure of podocytes and slit diaphragm.*

PROTOMAP analysis revealed that some of these structural and scaffolding proteins playing a vital role in the integrity of the glomerular filtration barrier were partially degraded in sub-optimal kidneys, as discussed below.

Laminin β2 (LAMβ2) is one of the key focal adhesion molecules in the podocyte –GBM architecture. The importance of LAMβ2 within the actin cytoskeleton network in maintaining the integrity of filtration barrier has been identified by the correlation of known mutations in the *LAMβ2* gene to nephrotic syndromes (Pearson syndrome) and the occurrence of clinical phenotypes such as proteinuria[265]. Degradome analysis showed the generation of a C-terminal fragment in the SO cohort at a lower molecular mass around 40kD as compared to the parent protein with a molecular mass of 200kDa (figure 6.12). Evidence for the integral role of the C-terminal β2 chain of laminin – integrin interactions comes from the study of Taniguchi *et al*., suggesting that the C-terminal region of laminin β chain plays a role in modulating the binding affinity of laminin to integrins in basement membranes[266].

Transmembrane anchoring proteins that include integrins, α-dystroglycan and heparin sulphate proteoglycans provide, in concert with focal adhesion molecules, the scaffolding structure to enable podocytes to adhere to the GBM to withstand the flow and pressure from the blood filtration process and act as intracellular signal transmitters to podocytes[267]. Figure 6.16 shows that two molecules involved in the scaffolding complex, utrophin and talin, connect actin and actinin in the podocyte cytoplasm to laminins in the GBM. PROTOMAP analysis demonstrated that both utrophin and talin-2 had undergone partial proteolysis in SO biopsies, resulting in the generation of fragments at a lower molecular mass (figure 6.12). Proteolytic cleavage of utrophin has been extensively studied within the context of muscular dystrophy, and

calpain-1is an intracellular enzyme that hydrolyses the intact utrophin protein to generate a fragment of 190kDa[268]. This is in agreement with the fragment uniquely observed in the PROTOMAP analysis in SO kidneys (figure 6.12). The fragmentation of utrophin led to examination of calpain 1 or 2 expression in the PROTOMAP dataset to see if any specific association with SO kidneys could be identified. The PROTOMAP data showed that there was an increased expression of the catalytic subunit of calpain-1 but not calpain -2, in SO compared to GO samples with the generation of a lower fragment at around 20kDa only found in the SO cohort (figure 6.13). Calpains are serine proteases that are activated when intracellular Ca^{2+} levels are increased under inflammatory conditions and in tissue injury, particular in neurons[269–271]. Brain stem death with subsequent systemic changes result in abdominal organ hypoperfusion as discussed in chapter 1. Under hypoxic conditions with subsequent cellular energy depletion, intracellular mechanisms regulated by ATP are disrupted. These changes cause Na^{+}/K^{+} ATP dependent membrane depolarization with intracellular Ca^{2+} overload and proteases, such as calpains to be activated [272,273]. Upon activation, calpain-1 is cleaved to generate a smaller fragment around 25kDa[273]. The active catalytic subunit described by Moldoveanu *et al*., agrees with the fragment size identified by the PROTOMAP analysis described in figure 6.13. Within the context of kidney physiology, increased levels of calpains in the kidney cortex of a rodent model have been shown to propagate a state of inflammation with the infiltration of inflammatory cells[274]. Based on the peptograph data, it appears that the observed 20kDa fragment (figure 6.13) agrees with the previous reports [227] consistent with an elevated activated calpain-1 species found in SO kidneys. It will be interesting to further explore the correlation of calpain activation with allograft function post-transplantation, in particular by discovering other potential calpain-1 substrates.

Talin-2 was among the integrin proteins identified with SO specific protein fragments fragments at around 25kDa (figure 6.12). Previous work in mice had demonstrated that talin is degraded by calpain -2 activation leading to podocyte foot effacement, glomerular injury and proteinuria[267,275]. Calpain-2 cleaves talin-2 to release fragments that would include fragments of 20-25kDa[275] as observed in the talin-2 peptograph of figure 6.12. Western blot validation would be the appropriate method to confirm these observations in donor kidney biopsies.

Among the known basement membrane heparin sulphate proteoglycans (HSP) are agrin, netrin, perlecan and collagen alpha-1 chain XVIII. Agrin and netrin are localized in the GBM and were included in the PROTOMAP dataset but no differences were seen between the two cohorts (results not shown). However, collagen alpha-1 chain XVIII is localized to mesangial cells that surround the glomerular capillaries and PROTOMAP analysis showed the generation of specific fragments for each experimental cohort (SO vs GO) (figure 6.12). The complex interactions and interconnections of HSPs with other components of glomerulus and GBM and the association to clinical phenotypes like proteinuria in glomerular diseases has been the research focus of numerous studies.

A comprehensive review[276] by Raats, Born and Berden examined the extent and mechanisms of dysregulation of the glomerular glycans and degradation of cytoskeletal proteins in conjunction with generation of ROS and the infiltration of immune cells[276]. Experimental work carried out by the same group has shown that ROS release proteases that can degrade HSP in a rat model and lead to alterations in the GBM and onset of albuminuria. Furthermore, the depletion of hydroxyl radicals with ROS scavenger agents ameliorated the clinical phenotypes observed[277].

Another group of scaffolding proteins is the alpha actinins which interact with various cytoskeletal proteins such as F-actin, modulate cell adhesion by crosslinking to actin filaments and provide a mechanism for cell signaling to support the structural integrity of the GBM. PROTOMAP analysis of alpha-actinin 4 demonstrated increased protein levels in the kidneys with SO compared to GO (figure 6.12). Dysregulation of α-actinin-4, mainly resulting from gene *ACTN4* mutations, has been described in early nephrotic syndromes[278,279].

The combined proteomic and PROTOMAP data supported the hypothesis that kidneys with a suboptimal outcome had suffered injury to glomerulus causing proteolysis, most probably from activation of apoptotic pathways. As the data from the PROTOMAP analysis was derived from pooled samples it is important to confirm these findings on a larger, independent cohort of individual donor kidney biopsies.

Limitations of the study

Kidneys consist of diverse and highly specialized clusters of cells that create a very heterogeneous tissue composition. Dissecting podocyte or slit diaphragm specific protein expressions and detecting changes in expression under oxidative stress is not yet possible with techniques in commonly use, although laser capture microdissection of glomeruli and mass spectrometry analysis has yielded promising results[280]. Determination of the changes occurring in specific structures of the kidney will help us to assess the susceptibility of specific proteins and help characterize the biological mechanisms responsible for long term suboptimal allograft function.

To perform the comparative quantitative analysis, kidney biopsy samples have been normalized on the basis of total protein levels. From the Remuzzi scoring analysis it was evident that there were biopsies with a low number of glomeruli and that is a pre-

analytical element that was difficult to control. Ideally, it would be preferable to normalize the kidney biopsy samples according to the same number of glomeruli prior to comparison.

The collection of biopsy samples from the donors according to the QUOD protocols requires biopsies to be obtained from the cortex but sampling errors and variability in sampling could have an impact on the analysis arising from differences in the proportion of medulla and cortex in the biopsy.

Increasing the number of individual samples for analysis and further validation on a large, independent samples cohort could compensate for pre-analytical variability between samples.

6.6 Conclusions

Summarising, this study has provided evidence of a discriminative proteomic profile that can distinguish between donor kidneys associated with suboptimal function and susceptible to developing post-transplant CKD, and those donor kidneys that have potential to recover and obtain good function 12 months after transplantation. Next, I was able to confirm in a small panel of proteins that early subclinical onset of injury and alterations to cytoskeletal proteins of podocytes and GBM are associated with suboptimal long-term allograft function.

This work suggests that the balance between injury and survival mechanisms is an important determinant of outcome and kidney allograft function. Further studies are needed to unravel the 'ratios' of injury and repair that may predict marginal, suboptimal or good outcome prior to transplantation.

CHAPTER 7

Discussion

7.1 Summary of research findings

In the introductory chapter I discussed that the success of transplantation has created an imbalance between the patients waiting for life saving transplants and the number of organs offered for transplantation. To bridge this gap clinicians are accepting organs from less than ideal donors. Utilising high risk organs has benefits when the risk of dying while waiting for a transplant is taken into consideration. However, for kidneys, many potentially useable organs are declined because there are no reliable and objective criteria to assess their long term function in the recipient.

The current demand for kidney transplants is growing with an aging population and increasing rates of disease such as diabetes and obesity associated with poor lifestyle choices. At the same time the donor base is also ageing with many of the same co-morbidities as recipients so better assessment tools for donor organ quality are urgently needed. Assessment tools in current use include monitoring serum creatinine levels and proteinuria during donor management or histological assessment of procurement biopsy samples. These methods are of low sensitivity and lack specificity.

My thesis has provided strong evidence that, at the point of retrieval, donor kidneys are biologically distinct, and on the basis of a proteomic signature, it is possible to identify those that will have suboptimal outcomes from the donor kidneys that will have a good function 1 year post-transplantation. Moreover, hierarchical clustering analysis of the donor kidney proteomic profiles indicated that individual donor kidneys can be stratified on the basis of eGFR values at 1 year post-transplantation. However, the number of samples analysed was small

and these results will need to be confirmed in a larger study. This work was done on kidney biopsies and it would be of value to explore whether similar donor stratification can be achieved by analysis of donor blood or urine since this would remove the need to biopsy the kidney.

In chapter 6, I compared the proteomic profiles obtained from kidneys from DBD donors with suboptimal or good outcomes in recipients at 3 and 12 months post-transplant. The discriminative proteomic profile was biological meaningful. Accumulated evidence from combined proteomics, PROTOMAP and western blot analysis showed that prior to procurement, pro-fibrotic, apoptotic and catabolic pathways were enriched in the DBD kidneys with suboptimal function 1 year after transplantation. Conversely, cytoprotective pathways were active in the DBD kidneys with good allograft function. That dissimilar biochemical pathways should prevail in donor kidneys with such divergent short and long term outcomes is not surprising. The observed differences in the tissue proteome agree with established pathophysiological changes reported in preclinical and experimental models.

The biopsy tissue provided a snapshot of the biological processes that were active at the point of kidney retrieval and provided evidence that the proteome in kidneys differed between suboptimal and good outcomes. PROTOMAP analysis provided a tool to further explore a subset of the kidney tissue proteome, the tissue degradome. The rationale for believing that the degradome was worth exploring was that gross pathophysiological changes resulting from oxidative stress, apoptosis and ischaemia would promote catabolic processes and protein degradation, inducing damage to kidney cell structure and the molecular

integrity of glomerular filtration membrane. The results obtained clearly showed that suboptimal kidneys had an enriched degradome profile compared to good outcome kidneys. Proteolytic fragments from podocyte cytoskeleton and the glomerular basement membrane were found suggesting that suboptimal kidneys had suffered irreversible glomerular damage that predisposed these kidneys to suboptimal function. The presence of proteolytic fragments seen only, or at significantly greater levels, in suboptimal kidneys suggests that these could be candidate biomarkers of kidney quality. Further investigation on a larger cohort of biopsies would be required to confirm these findings. Western blots analysis of the degradome may be particularly informative as both the intact protein and proteolytic fragments could be monitored at the same time.

Evidence of glomerular damage suggests that some degraded proteins may be found in the urine of suboptimal kidneys. Therefore, profiling the proteome and degradome of donor urine may yield potential biomarkers of donor kidney quality.

Kidney biopsies are only available at explantation and procurement is an invasive procedure. The ultimate clinical goal will be the development of non-invasive tools for donor kidney assessment. Collection of blood and urine is minimally invasive so if a diagnostic assay of donor quality can be developed from these material samples this would meet this goal. Furthermore, blood and urine can be procured at any stage of the donor management process enabling donors to be screened well before kidney retrieval. Not only would this reduce the likelihood of unsuitable kidneys being offered to recipients but permit pharmaceutical or

mechanical interventions during donor management to see if damage to kidney could be prevented or reversed.

My doctoral research included a comparative analysis of donor blood and urine samples from LD, DBD and DCD donors. This work is described in chapter 5. Proteomic analysis showed that it was feasible to detect alterations in donor blood and urine proteomes that were associated both to donor type, deceased or living and the onset of DGF. The serum proteomic profile of living donors was significantly distinct from deceased donors. Furthermore, when deceased donor samples were grouped on the basis of the onset of DGF in the recipient, proteomic signatures could differentiate between donors whose kidneys developed DGF from those allografts that functioned immediately post-transplant. Although there are specific limitations, as described in chapter 5, I intend to analyse longitudinal plasma samples from the same donors whose biopsies were analysed in chapter 6. This will be a discovery phase for a plasma proteomic signature discriminative of donor kidney quality and predictive of allograft function. The planned experimental work will be performed on clinical samples collected and stored in the QUOD biobank.

A potential confounding factor in the discovery of blood based disease-specific molecular signatures is the variability that can arise in the collection, processing and storage of clinical blood samples prior to analysis. Consequently, potentially novel protein markers of disease have failed the 'iron test' of validation and implementation into clinical practice as the differences seen in early experiments arose from pre-analytical variability in samples rather than the disease under investigation. My contribution to the establishment of the QUOD biobank was an

important element of my early doctoral work and will be vital in providing samples to pursue and validate candidate biomarkers identified by proteomic profiling of kidney donors, work I described in chapters 5 & 6. One unavoidable element of sample collection identified in the QUOD protocol was a variable period, up to 48 hrs, of storage at ambient temperature before processing. It was important to understand how the plasma proteome was affected by this storage period to assess the extent of pre-analytical variability. A reference list of proteins and peptides that were significantly altered when whole blood is stored in AT was defined[164,165]. This proteomic and degradome signature will guide the selection of candidate blood based biomarkers using QUOD samples by excluding the proteins that are either released from the cellular parts of whole blood or are susceptible to endogenous proteases and are degraded while whole blood remains in AT prior to plasma preparation.

7.2 Future studies

Taking into account the main observations derived from my experimental work my thesis has laid the foundations to further pursue the discovery of biomarkers of donor kidney quality and investigate how novel interventions can resuscitate "high risk" donor kidneys.

Developing diagnostics of donor kidney quality

Longitudinal analysis blood and urine samples from the QUOD biobank by clinical proteomics in a discovery cohort will examine the possibility of defining a blood and urine based proteomic signature that correlates to long term kidney function. Further validation in an independent cohort of samples will assess the sensitivity and specificity of a panel of proteins to predict 1 year post transplantation

function. The long term nature of the QUOD project means that follow-up clinical data will continue to be collected on recipients and will be available for researchers. When five-year data becomes available it will be possible to re analyse the identified proteomic data to further shortlist proteins that have a robust correlation to long term function.

To move closer to a diagnostically valuable assay, future work should include a prospective study using the QUOD infrastructure to evaluate the utility of the validated signatures to assist in the decision whether to transplant or decline donor kidneys.

Rescuing organs through interventions during donor management or dynamic preservation

It is reasonable to propose that stimulating the cytoprotective pathways and suppressing or ameliorating the harmful cytotoxic processes may change the fate of donor kidneys predisposed to suboptimal function. Opportunities for interventions could be during donor management or, most importantly, during preservation, which will allow targeted conditioning of each organ according to the need.

To understand better the opportunities to intervene during donor management it will be of interest to monitor the level of antioxidant proteins during the period of brain death, defined as the interval from brain death confirmation to kidney procurement. It is possible that lengthy donor management periods cause the depletion of cellular reserves needed to initiate cytoprotection and a targeted therapy could be devised to overcome this depletion.

Future experimental work could focus on exploiting the modulation of redox pathways by pharmacological ROS scavenging agents in-*vitro* and brain death preclinical models to test the feasibility of these interventions prior to clinical trials.

Following the completion of my DPhil I will continue my research work on the identification of novel biomarkers of donor kidney quality predictive of transplantation outcomes using clinical samples from the QUOD biobank. I have received approval from the QUOD steering committee to analyse longitudinal plasma samples (chapter 3, figure 3.1) from the same donors whose kidney biopsies I analysed in chapter 6. The experimental work will involve proteomic analysis of plasma samples from donors from whom both kidneys have been transplanted and either had suboptimal or good outcome 1 year post-transplantation. Following the completion of the proteomic analysis I am planning to validate a shortlisted panel of proteins on an independent cohort of plasma samples to assess the sensitivity and specificity of a protein panel to predict kidney allograft function at 1 year.

As the PROTOMAP analysis provided evidence of degradation of GBM proteins I am planning to validate these selected proteins discussed in chapter 6 on an independent cohort of donor kidney biopsy samples. Furthermore, I am aiming to explore the hypothesis that fragments from these degraded proteins can be detected in the donor urine and investigate further their utility as potential biomarkers of donor kidney quality predictive of transplantation outcomes.

CHAPTER 8

Appendices

8.1. Funding that supported this work

NHS Blood and Transplant Trust fund TF031 awarded to Professor Ploeg, Professor Scott and Maria Kaisar

European FP 7 COPE awarded to Professor Ploeg

8.2 Publications from my DPhil work

1. **Kaisar M**, van Dullemen LFA, Thézénas ML, Charles PD, Ploeg RJ KB: Plasma Biomarker Profile Altered Through Variable Blood Storage. Clin Chem 2016, 62:1272–1277.

2. **Kaisar M**, van Dullemen LFA, Thézénas ML, Akhtar MZ, Huang H, Rendel S, Charles PD, Fischer R, Ploeg RJ and. Kessler MB Plasma Degradome Affected by Variable Storage of Human Blood. Clin Proteomics, Sept 2016 13:26

3. **Kaisar M**, Leon F.A. van Dullemen[+], M Zeeshan Akhtar[+], Marie-Laëtitia Thézénas, Honglei Huang, Nicholas A. Watkins, Benedikt M. Kessler & Rutger J. Ploeg: Deceased Donor Kidney Proteomic Profiles Correlate to 12 month allograft function post transplantation (submitted to JASN).

4. **Kaisar M**[+], M Zeeshan Akhtar[+], Rendel S, Brailsford C, Collet D, Neuberger J, Watkins NA and Ploeg RJ on behalf of the QUOD Consortium: Transplantation Medicine: QUality in Organ Donation (QUOD) (Manuscript in preparation, to be submitted to *Transplantation*).

8.3 Publications related to my DPhil (2013-2016)

1. Jochmans I, Akhtar MZ, Nasralla D, Kocabayoglu P, Boffa C, **Kaisar M**, Brat A, O'Callaghan J, Pengel LHM, Knight S, Ploeg R: Past, present and future of dynamic

kidney and liver preservation and resuscitation. Am J Transplant 2016, 16:2545-2555.

2. Akhtar MZ, Huang H*, **Kaisar M*,** Lo Faro ML, Robolledo R, Morten K, Heather LC, Dona A, Leuvenink HG, Fuggle S V, Kessler BM, Pugh CW, Ploeg RJ: Using an integrated -omics approach to identify key cellular processes that are disturbed in the kidney following brain death. Am J Transplant 2015, 16: 1-25. (* equal contribution)

3. Honglei Huang, Leon FA van Dullemen, Mohammed Z Akhtar, Letitia M Lo Faro, Zhanru Yu, Alessandro Valli, Anthony Dona, Marie-Laëtitia Thézénas, Roman Fischer, **Maria Kaisar**, Henri GD Leuvenink, Rutger J Ploeg and Benedikt M Kessler: Lipid metabolism modulation is associated with molecular injury and kidney dysfunction in a rat ischaemia model (submitted to AJT).

8.4 Participation in Conferences with oral presentations

1. "Molecular markers as diagnostic tools of donor organ quality and predictors of transplantation outcome".

Maria Kaisar; Honglei Huang; Zeeshan M Akhtar; Henri GD Leuvenink; Climent CasalsPascual; Benedikt M Kessler; Rutger J Ploeg. **Best abstract category, ESOT, August 2013, Vienna, Austria.**

2. "Characterising the serum and urine proteome of organ donors to identify molecular signatures associated with function after kidney transplantation**".**

Maria Kaisar; Honglei Huang; Zeeshan M Akhtar; Henri GD Leuvenink; Benedikt M Kessler; Rutger J Ploeg. **EDTCO, Oct 2014, Budapest, Hungary.**

3. "Molecular markers as diagnostic tools of donor organ quality and predictors of transplantation outcome".

Maria Kaisar; Honglei Huang; Zeeshan M Akhtar; Benedikt M Kessler, Rutger J Ploeg. **17th British Transplant Society, February 2014, Glasgow UK.**

4."Use of proteomic signatures in donor serum and urine to differentiate between immediate function and delayed graft function after kidney transplantation".

Maria Kaisar; Honglei Huang; Zeeshan M Akhtar; Benedikt M Kessler, Rutger J Ploeg. **ESOT, September 2015, Brussels, Belgium.**

5. "Activated cytoprotective mechanisms in DBD donor kidneys correlate with kidney function in transplant recipients: A study using clinical samples from the UK QUOD Biobank".

Maria Kaisar; Leon V Dullemen; Zeeshan M Akhtar; Honglei Huang; Benedikt M Kessler, Rutger J Ploeg. **18th British Transplant Society, February 2016, Glasgow, UK.**

6. **"**Activated cytoprotective mechanisms in DBD donor kidneys correlate with kidney function in transplant recipients: A study using clinical samples from the UK QUOD Biobank".

Maria Kaisar; Leon V Dullemen; Zeeshan M Akhtar; Honglei Huang; Benedikt M Kessler, Rutger J Ploeg. **American Transplant Congress 2016, June 2016, Boston USA.**

7. **"**Activated cytoprotective mechanisms in DBD donor kidneys correlate with kidney function in transplant recipients: A study using clinical samples from the UK QUOD Biobank".

Maria Kaisar; Leon V Dullemen; Zeeshan M Akhtar; Honglei Huang; Benedikt M Kessler, Rutger J Ploeg. **European Conference on Donor Health and Management, July 2016, Cambridge UK.**

8. "Proteomic profiles of donor kidney biopsies obtained at retrieval correlate to allograft function at 1 year post transplantation"

Maria Kaisar; Leon V Dullemen; Zeeshan M Akhtar; Honglei Huang; Benedikt M Kessler, Rutger J Ploeg. **Best six abstract category. To be presented 19th British Transplant Society, March 2017, Harrogate, UK.**

8.5 Invited talk

1. "Biomarkers of Donor Kidney Quality as Predictors of Transplantation Outcomes"

Maria Kaisar; Clinical and R&D conference NHS Blood and Transplant. The King's Fund, September 2016, London UK.

8.6 Successful grant applications

1. NHS Blood and Transplant Trust Fund (TF031), September 2012, £50,000

Applicants: Professor Rutger Ploeg, Professor Marion Scott, Maria Kaisar

2. Oxford Transplant Foundation, September 2016, £5,000.

Applicant: Maria Kaisar

3. European Innovation and Technology (EIT) PhD Transition Fellowship, September 2016, €15,000.

Applicant: Maria Kaisar

REFERENCES

1. Zalai, D., Szeifert, L. & Novak, M. Psychological Distress and Depression in Patients with Chronic Kidney Disease. *Semin. Dial.* **25,** 428–438 (2012).
2. Merrill, J. P., Murray, J. E., Harrison, J. H. & Guild, W. R. Landmark article Jan 28, 1956: Successful homotransplantation of the human kidney between identical twins. By John P. Merrill, Joseph E. Murray, J. Hartwell Harrison, and Warren R. Guild. *JAMA* **251,** 2566–71 (1984).
3. Morris, P. J. Transplantation--a medical miracle of the 20th century. *N. Engl. J. Med.* **351,** 2678–80 (2004).
4. Leigh, W. Sir Michael Francis Addison Woodruff (1911-2001) FRS DSc MD MS FRCS. *J. Med. Biogr.* **19,** 21–5 (2011).
5. NHS Blood and Transplant. *Organ Donation and Transplantation Activity Report 2014/15*. *NHS Blood and Transplant* (2015).
6. NHS Blood and Transplant. *Kidney Activity*. *NHS Blood and Transplant* (2015).
7. Hill, C. J. & Fogarty, D. G. Changing trends in end-stage renal disease due to diabetes in the United kingdom. *J. Ren. Care* **38 Suppl 1,** 12–22 (2012).
8. Chronic kidney disease prevalence model. *Public Heal. Engl.* (2014).
9. Rao, P. S. & Ojo, A. The alphabet soup of kidney transplantation: SCD, DCD, ECD--fundamentals for the practicing nephrologist. *Clin. J. Am. Soc. Nephrol.* **4,** 1827–31 (2009).
10. Reese, P. P., Harhay, M. N., Abt, P. L., Levine, M. H. & Halpern, S. D. New Solutions to Reduce Discard of Kidneys Donated for Transplantation. *J. Am. Soc. Nephrol.* **27,** 973–80 (2016).
11. Lee, a. P. K. & Abramowicz, D. Is the Kidney Donor Risk Index a step forward in the assessment of deceased donor kidney quality? *Nephrol. Dial. Transplant.* 1–6 (2014). doi:10.1093/ndt/gfu304
12. Hall, I. E. *et al.* Associations of Deceased Donor Kidney Injury With Kidney Discard and Function After Transplantation. *Am. J. Transplant.* **15,** 1623–1631 (2015).
13. Callaghan, C. J. *et al.* The discard of deceased donor kidneys in the UK. *Clin. Transplant.* **28,** 345–53 (2014).
14. Massie, A. B. *et al.* Survival benefit of primary deceased donor transplantation with high-KDPI kidneys. *Am. J. Transplant* **14,** 2310–6 (2014).
15. NHS Blood and Transplant. Taking Organ Transplantation to 2020.
16. Bos, E. M., Leuvenink, H. G. D., van Goor, H. & Ploeg, R. J. Kidney grafts from brain dead donors: Inferior quality or opportunity for improvement? *Kidney Int.* **72,** 797–805 (2007).
17. Ranasinghe, A. M. & Bonser, R. S. Endocrine changes in brain death and transplantation. *Best Pract. Res. Clin. Endocrinol. Metab.* **25,** 799–812 (2011).
18. Watts, R. P., Thom, O. & Fraser, J. F. Inflammatory signalling associated with brain dead organ donation: from brain injury to brain stem death and posttransplant ischaemia reperfusion injury. *J Transpl.* **2013,** 521369 (2013).
19. Bugge, J. F. Brain death and its implications for management of the potential organ donor. *Acta Anaesthesiol. Scand.* **53,** 1239–1250 (2009).

20. Schuurs, T. a. *et al.* Time-dependent changes in donor brain death related processes. *Am. J. Transplant.* **6,** 2903–2911 (2006).
21. Nagareda, T. *et al.* Clinicopathology of kidneys from brain-dead patients treated with vasopressin and epinephrine. *Kidney Int.* **43,** 1363–70 (1993).
22. Akhtar, M. Z. *et al.* Using an integrated -omics approach to identify key cellular processes that are disturbed in the kidney following brain death. *Am. J. Transplant* (2015). doi:10.1111/ajt.13626
23. Westendorp, W. H., Leuvenink, H. G. & Ploeg, R. J. Brain death induced renal injury. *Curr. Opin. Organ Transplant.* **16,** 151–156 (2011).
24. Bradley, J. a, Pettigrew, G. J. & Watson, C. J. Time to death after withdrawal of treatment in donation after circulatory death (DCD) donors. *Curr. Opin. Organ Transplant.* **18,** 133–9 (2013).
25. British, T. & Society, T. United kingdom guidelines - Transplantation from donors after deceased circulatory death. *Br. Transplant. Soc.* (2013).
26. Akoh, J. a. Kidney donation after cardiac death. *World J. Nephrol.* **1,** 79 (2012).
27. van den Eijnden, M. M. E. D. *et al.* Effect of brain death and non-heart-beating kidney donation on renal function and injury: an assessment in the isolated perfused rat kidney. *Exp. Clin. Transplant.* **1,** 85–95 (2003).
28. Thuillier, R. *et al.* Benefits of active oxygenation during hypothermic machine perfusion of kidneys in a preclinical model of deceased after cardiac death donors. *J. Surg. Res.* **184,** 1174–81 (2013).
29. Ponticelli, C. Ischaemia-reperfusion injury: A major protagonist in kidney transplantation. *Nephrol. Dial. Transplant.* **29,** 1134–1140 (2014).
30. Cavaillé-Coll, M. *et al.* Summary of FDA workshop on ischemia reperfusion injury in kidney transplantation. *Am. J. Transplant.* **13,** 1134–1148 (2013).
31. Eltzschig, H. K. & Eckle, T. Ischemia and reperfusion—from mechanism to translation. *Nat. Med.* **17,** 1391–1401 (2011).
32. Serkova, N., Fuller, T. F., Klawitter, J., Freise, C. E. & Niemann, C. U. H-NMR-based metabolic signatures of mild and severe ischemia/reperfusion injury in rat kidney transplants. *Kidney Int.* **67,** 1142–51 (2005).
33. Snoeijs, M. G. J. *et al.* Tubular epithelial injury and inflammation after ischemia and reperfusion in human kidney transplantation. *Ann. Surg.* **253,** 598–604 (2011).
34. Lee, S.-Y., Shin, J.-A., Kwon, H. M., Weiner, I. D. & Han, K.-H. Renal ischemia-reperfusion injury causes intercalated cell-specific disruption of occludin in the collecting duct. *Histochem. Cell Biol.* **136,** 637–47 (2011).
35. Karim, A. S. *et al.* Nox2 Is a Mediator of Ischemia Reperfusion Injury. *Am. J. Transplant* **15,** 2888–99 (2015).
36. Damman, J. *et al.* Crosstalk between complement and Toll-like receptor activation in relation to donor brain death and renal ischemia-reperfusion injury. *Am. J. Transplant* **11,** 660–9 (2011).
37. Karthik K. Tennankore1, 2, S. Joseph Kim3, 4 & Ian P.J. Alwayn5 and Bryce A. Kiberd1, 2. Prolonged warm ischemia time is associated with graft failure and mortality after kidney transplantation.
38. Denic, A., Glassock, R. J. & Rule, A. D. Structural and Functional Changes With the Aging Kidney. *Adv. Chronic Kidney Dis.* **23,** 19–28 (2016).
39. Abdel-Rahman, E. M. & Okusa, M. D. Effects of aging on renal function and regenerative capacity. *Nephron. Clin. Pract.* **127,** 15–20 (2014).

40. Abdelhafiz, A. H., Brown, S. H. M., Bello, A. & El Nahas, M. Chronic kidney disease in older people: physiology, pathology or both? *Nephron. Clin. Pract.* **116,** c19–c24 (2010).
41. Summers, D. M. *et al.* Analysis of factors that affect outcome after transplantation of kidneys donated after cardiac death in the UK: a cohort study. *Lancet* **376,** 1303–11 (2010).
42. Ojo, A. O. *et al.* Survival in recipients of marginal cadaveric donor kidneys compared with other recipients and wait-listed transplant candidates. *J. Am. Soc. Nephrol.* **12,** 589–97 (2001).
43. Merion, R. M. *et al.* Deceased-donor characteristics and the survival benefit of kidney transplantation. *JAMA* **294,** 2726–33 (2005).
44. Metzger, R. A. *et al.* Expanded criteria donors for kidney transplantation. *Am. J. Transplant* **3 Suppl 4,** 114–125 (2003).
45. Terasaki, P. I., Cecka, J. M., Gjertson, D. W. & Takemoto, S. High Survival Rates of Kidney Transplants from Spousal and Living Unrelated Donors. *N. Engl. J. Med.* **333,** 333–336 (1995).
46. Resende, L. *et al.* Impact of donor age on renal allograft function and survival. *Transplant. Proc.* **41,** 794–6 (2009).
47. Martínez-Vaquera, S. *et al.* Outcomes in renal transplantation with expanded-criteria donors. *Transplant. Proc.* **45,** 3595–8 (2013).
48. Summers, D. M. *et al.* Effect of donor age and cold storage time on outcome in recipients of kidneys donated after circulatory death in the UK: a cohort study. *Lancet* **381,** 727–34 (2013).
49. Kayler, L. K., Srinivas, T. R. & Schold, J. D. Influence of CIT-induced DGF on kidney transplant outcomes. *Am. J. Transplant* **11,** 2657–64 (2011).
50. Aubert, O. *et al.* Long term outcomes of transplantation using kidneys from expanded criteria donors: prospective, population based cohort study. *BMJ* **351,** h3557 (2015).
51. Summers, D. M. *et al.* Kidney donation after circulatory death (DCD): state of the art. *Kidney Int.* (2015). doi:10.1038/ki.2015.88
52. El-Zoghby, Z. M. *et al.* Identifying Specific Causes of Kidney Allograft Loss. *Am. J. Transplant.* **9,** 527–535 (2009).
53. Dahmane, D. *et al.* Retrospective follow-up of transplantation of kidneys from 'marginal' donors. *Kidney Int.* **69,** 546–52 (2006).
54. Yarlagadda, S. G., Klein, C. L. & Jani, A. Long-term renal outcomes after delayed graft function. *Adv. Chronic Kidney Dis.* **15,** 248–56 (2008).
55. Yarlagadda, S. G., Coca, S. G., Formica, R. N., Poggio, E. D. & Parikh, C. R. Association between delayed graft function and allograft and patient survival: a systematic review and meta-analysis. *Nephrol. Dial. Transplant* **24,** 1039–47 (2009).
56. Tapiawala, S. N. *et al.* Delayed graft function and the risk for death with a functioning graft. *J. Am. Soc. Nephrol.* **21,** 153–61 (2010).
57. Boom, H., Mallat, M. J., de Fijter, J. W., Zwinderman, A. H. & Paul, L. C. Delayed graft function influences renal function but not survival. *Transplant. Proc.* **33,** 1291 (2000).
58. Wu, W. K., Famure, O., Li, Y. & Kim, S. J. Delayed graft function and the risk of acute rejection in the modern era of kidney transplantation. *Kidney Int.* (2015). doi:10.1038/ki.2015.190
59. Louvar, D. W. *et al.* 'Nature versus nurture' study of deceased-donor pairs

in kidney transplantation. *J. Am. Soc. Nephrol.* **20,** 1351–8 (2009).
60. Marcén, R. *et al.* Delayed graft function does not reduce the survival of renal transplant allografts. *Transplantation* **66,** 461–6 (1998).
61. Siedlecki, a., Irish, W. & Brennan, D. C. Delayed graft function in the kidney transplant. *Am. J. Transplant* **11,** 2279–96 (2011).
62. Troppmann, C. *et al.* Delayed graft function in the absence of rejection has no long-term impact. A study of cadaver kidney recipients with good graft function at 1 year after transplantation. *Transplantation* **61,** 1331–7 (1996).
63. Troppmann, C. *et al.* Delayed graft function, acute rejection, and outcome after cadaver renal transplantation. The multivariate analysis. *Transplantation* **59,** 962–8 (1995).
64. McLaren, A. J. *et al.* Delayed graft function: risk factors and the relative effects of early function and acute rejection on long-term survival in cadaveric renal transplantation. *Clin. Transplant.* **13,** 266–72 (1999).
65. Ojo, A. O., Wolfe, R. A., Held, P. J., Port, F. K. & Schmouder, R. L. Delayed graft function: risk factors and implications for renal allograft survival. *Transplantation* **63,** 968–74 (1997).
66. Mallon, D. H., Summers, D. M., Bradley, J. A. & Pettigrew, G. J. Defining Delayed Graft Function after Renal Transplantation: Simplest Is Best. *Transplantation* **0,** 1–5 (2013).
67. Nagaraja, P. *et al.* Influence of delayed graft function and acute rejection on outcomes after kidney transplantation from donors after cardiac death. *Transplantation* **94,** 1218–23 (2012).
68. Mengel, M., Husain, S., Hidalgo, L. & Sis, B. Phenotypes of antibody-mediated rejection in organ transplants. *Transpl. Int.* **25,** 611–22 (2012).
69. Lamb, K. E., Lodhi, S. & Meier-Kriesche, H.-U. Long-term renal allograft survival in the United States: a critical reappraisal. *Am. J. Transplant* **11,** 450–62 (2011).
70. Dharnidharka, V. R., Lamb, K. E., Zheng, J., Schechtman, K. B. & Meier-Kriesche, H.-U. Lack of significant improvements in long-term allograft survival in pediatric solid organ transplantation: A US national registry analysis. *Pediatr. Transplant.* **19,** 477–83 (2015).
71. Marcén, R. & Dal Canton, A. Glomerular filtration rate: utility for assessing long-term renal allograft outcomes in kidney allograft recipients. *J. Nephrol.* **26,** 1009–24
72. Sigdel, T. K. *et al.* The identification of novel potential injury mechanisms and candidate biomarkers in renal allograft rejection by quantitative proteomics. *Mol. Cell. Proteomics* **13,** 621–31 (2014).
73. Sigdel, T. K. *et al.* Non-HLA antibodies to immunogenic epitopes predict the evolution of chronic renal allograft injury. *J. Am. Soc. Nephrol.* **23,** 750–63 (2012).
74. Gonzales, M. M., Bentall, A., Kremers, W. K., Stegall, M. D. & Borrows, R. Predicting Individual Renal Allograft Outcomes Using Risk Models with 1-Year Surveillance Biopsy and Alloantibody Data. *J. Am. Soc. Nephrol.* (2016). doi:10.1681/ASN.2015070811
75. Yang, C. W., Li, C. & Yang, C. W. The pathogenesis and treatment of chronic allograft nephropathy. *Nat. Rev. Nephrol* **5,** 513–519 (2009).
76. Yao, G. *et al.* A systematic review and economic model of the clinical and

cost-effectiveness of immunosuppressive therapy for renal transplantation in children. *Health Technol. Assess.* **10,** iii–iv, ix–xi, 1-157 (2006).
77. Butler, J. A., Roderick, P., Mullee, M., Mason, J. C. & Peveler, R. C. Frequency and impact of nonadherence to immunosuppressants after renal transplantation: a systematic review. *Transplantation* **77,** 769–76 (2004).
78. Denhaerynck, K. *et al.* Prevalence, consequences, and determinants of nonadherence in adult renal transplant patients: a literature review. *Transpl. Int.* **18,** 1121–1133 (2005).
79. Chapman, J. R., O'Connell, P. J. & Nankivell, B. J. Chronic renal allograft dysfunction. *J. Am. Soc. Nephrol.* **16,** 3015–26 (2005).
80. Resende, L. *et al.* First year renal function as a predictor of kidney allograft outcome. *Transplant. Proc.* **41,** 846–8 (2009).
81. Kasiske, B. L., Israni, A. K., Snyder, J. J. & Skeans, M. A. The relationship between kidney function and long-term graft survival after kidney transplant. *Am. J. Kidney Dis.* **57,** 466–75 (2011).
82. Shapiro, R., Halloran, P. F., Delmonico, F. L. & Bromberg, J. S. The 'Two, One, Zero' Decision: What to Do with Suboptimal Deceased Donor Kidneys. *Am. J. Transplant.* **10,** 1959–1960 (2010).
83. Remuzzi, G. *et al.* Long-term outcome of renal transplantation from older donors. *N. Engl. J. Med.* **354,** 343–52 (2006).
84. Remuzzi, G. *et al.* Early experience with dual kidney transplantation in adults using expanded donor criteria. Double Kidney Transplant Group (DKG). *J. Am. Soc. Nephrol.* **10,** 2591–2598 (1999).
85. Tanriover, B. *et al.* Kidneys at higher risk of discard: expanding the role of dual kidney transplantation. *Am. J. Transplant* **14,** 404–15 (2014).
86. Hossain, M. A. *et al.* HSP70, Peroxiredoxin-3 and -6 are upregulated during renal warm ischaemia in a donation after circulatory death model. *J. Proteomics* **108,** 133–45 (2014).
87. Maathuis, M. H. J., de Groot, M., Ploeg, R. J. & Leuvenink, H. G. D. Deterioration of Endothelial and Smooth Muscle Cell Function in DCD Kidneys After Static Cold Storage in IGL-1 or UW. *J. Surg. Res.* **152,** 231–237 (2009).
88. Kosmoliaptsis, V. *et al.* Baseline Donor Chronic Renal Injury Confers the Same Transplant Survival Disadvantage for DCD and DBD Kidneys. *Am. J. Transplant* **15,** 754–63 (2015).
89. Obermüller, N., Geiger, H., Weipert, C. & Urbschat, A. Current developments in early diagnosis of acute kidney injury. *Int. Urol. Nephrol.* **46,** 1–7 (2014).
90. Sureshkumar, K. K. & Marcus, R. J. Urinary biomarkers as predictors of long-term allograft function after renal transplantation. *Transplantation* **90,** 688–9 (2010).
91. Heyne, N. *et al.* Urinary neutrophil gelatinase-associated lipocalin accurately detects acute allograft rejection among other causes of acute kidney injury in renal allograft recipients. *Transplantation* **93,** 1252–7 (2012).
92. Buemi, A. *et al.* Is plasma and urine neutrophil gelatinase-associated lipocalin (NGAL) determination in donors and recipients predictive of renal function after kidney transplantation? *Clin. Biochem.* **47,** 68–72 (2014).
93. Nejat, M. *et al.* Some biomarkers of acute kidney injury are increased in pre-renal acute injury. *Kidney Int.* **81,** 1254–1262 (2012).

94. Juan C Ramirez-Sandoval, Jonatan Barrera-Chimal, Perla E Simancas, Alejandro Rojas-Montano, Ricardo Correa-Rotter, N. A. B. Urinary neutrophil gelatinase-associated lipocalin predicts graft loss after acute kidney injury in kidney transplant. **5804,** 1–7 (2013).
95. Reese, P. P. *et al.* Associations between Deceased-Donor Urine Injury Biomarkers and Kidney Transplant Outcomes. *J. Am. Soc. Nephrol.* (2015). doi:10.1681/ASN.2015040345
96. Hollmen, M. E. *et al.* Deceased donor neutrophil gelatinase-associated lipocalin and delayed graft function after kidney transplantation: a prospective study. *Crit. Care* **15,** R121 (2011).
97. Hollmen, M. E., Kyllönen, L. E., Merenmies, J. & Salmela, K. T. Serum neutrophil gelatinase-associated lipocalin and recovery of kidney graft function after transplantation. *BMC Nephrol.* **15,** 123 (2014).
98. Hall, I. E. *et al.* Association between peritransplant kidney injury biomarkers and 1-year allograft outcomes. *Clin. J. Am. Soc. Nephrol.* **7,** 1224–33 (2012).
99. Buemi, A. *et al.* Is plasma and urine neutrophil gelatinase-associated lipocalin (NGAL) determination in donors and recipients predictive of renal function after kidney transplantation? *Clin. Biochem.* **47,** 68–72 (2014).
100. Moers, C., Pirenne, J., Paul, A. & Ploeg, R. J. Machine perfusion or cold storage in deceased-donor kidney transplantation. *N. Engl. J. Med.* **366,** 770–1 (2012).
101. Moers, C. *et al.* The value of machine perfusion perfusate biomarkers for predicting kidney transplant outcome. *Transplantation* **90,** 966–973 (2010).
102. Chirag R. Parikh, MD, PhD1, 2, 3 Isaac E. Hall, MD, MS1, 2 Ronik S. Bhangoo, MD4 Joseph Ficek, MA, MS1 Peter L. Abt, MD5 Heather Thiessen-Philbrook, MMath1 Haiqun Lin, PhD1 Milan Bimali, MS1 Patrick T. Murray, MD6 Veena Rao, PhD1 Bernd Schröppel, MD7, 8 M, M. Associations of perfusate biomarkers and pump parameters with delayed graft function and deceased-donor kidney allograft function. - PubMed - NCBI. at <http://www.ncbi.nlm.nih.gov/pubmed/26695524>
103. Ichimura, T., Brooks, C. R. & Bonventre, J. V. Kim-1/Tim-1 and immune cells: shifting sands. *Kidney International* **81,** 809–811 (2012).
104. Du, Y. *et al.* Urinary biomarkers to detect acute kidney injury in the pediatric emergency center. *Pediatr. Nephrol.* **26,** 267–74 (2011).
105. Vaidya, V. S. *et al.* Kidney injury molecule-1 outperforms traditional biomarkers of kidney injury in preclinical biomarker qualification studies. *Nat. Biotechnol.* **28,** 478–485 (2010).
106. Moore, E., Bellomo, R. & Nichol, a. Biomarkers of acute kidney injury in anesthesia, intensive care and major surgery: from the bench to clinical research to clinical practice. *Minerva Anestesiol* **76,** 425–440 (2010).
107. Arthur, J. M. *et al.* Evaluation of 32 urine biomarkers to predict the progression of acute kidney injury after cardiac surgery. *Kidney Int.* **85,** 431–8 (2014).
108. Nijboer, W. N. *et al.* Kidney injury molecule-1 is an early noninvasive indicator for donor brain death-induced injury prior to kidney transplantation. *Am. J. Transplant* **9,** 1752–9 (2009).
109. Schröppel, B. *et al.* Tubular expression of KIM-1 does not predict delayed

function after transplantation. *J. Am. Soc. Nephrol.* **21,** 536–42 (2010).
110. Oezkur, M. *et al.* Preoperative serum h-FABP concentration is associated with postoperative incidence of acute kidney injury in patients undergoing cardiac surgery. *BMC Cardiovasc. Disord.* **14,** 117 (2014).
111. Siew, E. D. *et al.* Distinct injury markers for the early detection and prognosis of incident acute kidney injury in critically ill adults with preserved kidney function. *Kidney Int.* **84,** 786–94 (2013).
112. Asada, T. *et al.* Impact of clinical context on acute kidney injury biomarker performances: differences between neutrophil gelatinase-associated lipocalin and L-type fatty acid-binding protein. *Sci. Rep.* **6,** 33077 (2016).
113. Jochmans, I., Lerut, E., van Pelt, J., Monbaliu, D. & Pirenne, J. Circulating AST, H-FABP, and NGAL are Early and Accurate Biomarkers of Graft Injury and Dysfunction in a Preclinical Model of Kidney Transplantation. *Ann. Surg.* **254,** 784–792 (2011).
114. De Vusser, K. *et al.* Telomere length, cardiovascular risk and arteriosclerosis in human kidneys: an observational cohort study. *Aging (Albany. NY).* **7,** 766–75 (2015).
115. Jochmans, I., Monbaliu, D. & Pirenne, J. Neutrophil gelatinase-associated lipocalin, a new biomarker candidate in perfusate of machine-perfused kidneys: A porcine pilot experiment. *Transplant. Proc.* **43,** 3486–3489 (2011).
116. Lee, E. Y., Kim, M. S., Park, Y. & Kim, H.-S. Serum Neutrophil Gelatinase-Associated Lipocalin and Interleukin-18 as Predictive Biomarkers for Delayed Graft Function After Kidney Transplantation. *J. Clin. Lab. Anal.* **26,** 295–301 (2012).
117. Hall, I. E. *et al.* IL-18 and urinary NGAL predict dialysis and graft recovery after kidney transplantation. *J. Am. Soc. Nephrol.* **21,** 189–97 (2010).
118. Parikh, C. R. *et al.* Urinary IL-18 is an early predictive biomarker of acute kidney injury after cardiac surgery. *Kidney Int.* **70,** 199–203 (2006).
119. Parikh, C. R. *et al.* Urine NGAL and IL-18 are Predictive Biomarkers for Delayed Graft Function Following Kidney Transplantation. *Am. J. Transplant.* **6,** 1639–1645 (2006).
120. McCullough, P. A. *et al.* Diagnosis of acute kidney injury using functional and injury biomarkers: workgroup statements from the tenth Acute Dialysis Quality Initiative Consensus Conference. *Contrib. Nephrol.* **182,** 13–29 (2013).
121. Tsigou, E., Psallida, V., Demponeras, C., Boutzouka, E. & Baltopoulos, G. Role of new biomarkers: functional and structural damage. *Crit. Care Res. Pract.* **2013,** 361078 (2013).
122. Pianta, T. J. *et al.* Clusterin in kidney transplantation: novel biomarkers versus serum creatinine for early prediction of delayed graft function. *Transplantation* **99,** 171–9 (2015).
123. Irita, J. *et al.* Osteopontin deficiency protects against aldosterone-induced inflammation, oxidative stress, and interstitial fibrosis in the kidney. *Am. J. Physiol. Renal Physiol.* **301,** F833-44 (2011).
124. Okada, H. *et al.* Osteopontin expressed by renal tubular epithelium mediates interstitial monocyte infiltration in rats. *Am. J. Physiol. - Ren. Physiol.* **278,** (2000).
125. Wang, J. *et al.* Osteopontin level correlates with acute cellular renal

allograft rejection. *J. Surg. Res.* **182,** 161–165 (2013).
126. Xie, Y. *et al.* Expression, roles, receptors, and regulation of osteopontin in the kidney. *Kidney Int.* **60,** 1645–57 (2001).
127. Schmidt, I. M. *et al.* Chitinase-like protein Brp-39/YKL-40 modulates the renal response to ischemic injury and predicts delayed allograft function. *J. Am. Soc. Nephrol.* **24,** 309–19 (2013).
128. Hector, A. *et al.* The chitinase-like protein YKL-40 modulates cystic fibrosis lung disease. *PLoS One* **6,** (2011).
129. Lee, C. G. *et al.* Role of chitin and chitinase/chitinase-like proteins in inflammation, tissue remodeling, and injury. *Annu. Rev. Physiol.* **73,** 479–501 (2011).
130. Puthumana, J. *et al.* YKL-40 Associates with Renal Recovery in Deceased Donor Kidney Transplantation. *J. Am. Soc. Nephrol.* ASN.2016010091 (2016). doi:10.1681/ASN.2016010091
131. Masson, I. *et al.* KDIGO Guidelines and Kidney Transplantation: Is the Cystatin-C Based Recommendation Relevant? *Am. J. Transplant* **15,** 2211–4 (2015).
132. Sigdel, T. K. *et al.* Mining the human urine proteome for monitoring renal transplant injury. *Kidney Int.* **89,** 1244–52 (2016).
133. Quintana, L. F. *et al.* Urine proteomics to detect biomarkers for chronic allograft dysfunction. *J. Am. Soc. Nephrol.* **20,** 428–35 (2009).
134. Mas, V. R. *et al.* Pretransplant transcriptome profiles identify among kidneys with delayed graft function those with poorer quality and outcome. *Mol Med* **17,** 1311–1322 (2011).
135. Schuurs, T. a. *et al.* Distinct transcriptional changes in donor kidneys upon brain death induction in rats: Insights in the processes of brain death. *Am. J. Transplant.* **4,** 1972–81 (2004).
136. Nijboer, W. N., Moers, C., Leuvenink, H. G. D. & Ploeg, R. J. How important is the duration of the brain death period for the outcome in kidney transplantation? *Transpl. Int.* **24,** 14–20 (2011).
137. https://www.nds.ox.ac.uk/research/quod.
138. Wessel, D. & Flügge, U. I. A method for the quantitative recovery of protein in dilute solution in the presence of detergents and lipids. *Anal. Biochem.* **138,** 141–3 (1984).
139. Perkins, D. N., Pappin, D. J. C., Creasy, D. M. & Cottrell, J. S. Probability-based protein identification by searching sequence databases using mass spectrometry data. *Electrophoresis* **20,** 3551–3567 (1999).
140. Sadygov, R. G., Cociorva, D. & Yates, J. R. Large-scale database searching using tandem mass spectra: Looking up the answer in the back of the book. *Nat. Methods* **1,** 195–202 (2004).
141. Mann, M. Mass tool for diagnosis. *Nature* **418,** 731–2 (2002).
142. Ferguson, P. L. & Smith, R. D. Proteome Analysis by Mass Spectrometry*. *Annu. Rev. Biophys. Biomol. Struct.* **32,** 399–424 (2003).
143. Coombs, K. M. Quantitative proteomics of complex mixtures. *Expert Rev. Proteomics* **8,** 659–677 (2011).
144. Trudgian, D. C. *et al.* CPFP: A central proteomics facilities pipeline. *Bioinformatics* **26,** 1131–1132 (2010).
145. Trudgian, D. C. *et al.* Comparative evaluation of label-free SINQ normalized spectral index quantitation in the central proteomics facilities pipeline.

Proteomics **11,** 2790–2797 (2011).
146. Neilson, K. A. *et al.* Less label, more free: Approaches in label-free quantitative mass spectrometry. *Proteomics* **11,** 535–553 (2011).
147. Corthals, G. L., Wasinger, V. C., Hochstrasser, D. F. & Sanchez, J. C. The dynamic range of protein expression: a challenge for proteomic research. *Electrophoresis* **21,** 1104–15 (2000).
148. Anderson, N. L. & Anderson, N. G. The human plasma proteome: history, character, and diagnostic prospects. *Mol. Cell. Proteomics* **1,** 845–67 (2002).
149. Anderson, N. G., Matheson, A. & Anderson, N. L. Back to the future: The human protein index (HPI) and the agenda for post-proteomic biology. *Proteomics* **1,** 3–12 (2001).
150. Anderson, N. L. *et al.* A human proteome detection and quantitation project. *Mol. Cell. Proteomics* **8,** 883–6 (2009).
151. Fischer, R. *et al.* Discovery of candidate serum proteomic and metabolomic biomarkers in ankylosing spondylitis. *Mol. Cell. Proteomics* **11,** M111.013904 (2012).
152. Ternette, N. *et al.* Inhibition of mitochondrial aconitase by succination in fumarate hydratase deficiency. *Cell Rep.* **3,** 689–700 (2013).
153. Huang, H. *et al.* Discovery and validation of biomarkers to guide clinical management of pneumonia in African children. *Clin. Infect. Dis.* **58,** 1707–15 (2014).
154. Kessner, D., Chambers, M., Burke, R., Agus, D. & Mallick, P. ProteoWizard: open source software for rapid proteomics tools development. *Bioinformatics* **24,** 2534–6 (2008).
155. Dix, M. M., Simon, G. M. & Cravatt, B. F. Global Mapping of the Topography and Magnitude of Proteolytic Events in Apoptosis. *Cell* **134,** 679–691 (2008).
156. Niessen, S., Hoover, H. & Gale, A. J. Proteomic analysis of the coagulation reaction in plasma and whole blood using PROTOMAP. *Proteomics* **11,** 2377–2388 (2011).
157. Ji, H. & Liu, X. S. Analyzing 'omics data using hierarchical models. *Nat. Biotechnol.* **28,** 337–40 (2010).
158. Caraux, G. & Pinloche, S. PermutMatrix: a graphical environment to arrange gene expression profiles in optimal linear order. *Bioinformatics* **21,** 1280–1 (2005).
159. Li, X.-J. *et al.* An integrated quantification method to increase the precision, robustness, and resolution of protein measurement in human plasma samples. *Clin. Proteomics* **12,** 3 (2015).
160. Karczmarski, J. *et al.* Pre-analytical-related variability influencing serum peptide profiles demonstrated in a mass spectrometry-based search for colorectal and prostate cancer biomarkers. *Acta Biochim. Pol.* **60,** 417–25 (2013).
161. West-Nørager, M. *et al.* Unravelling in vitro variables of major importance for the outcome of mass spectrometry-based serum proteomics. *J. Chromatogr. B. Analyt. Technol. Biomed. Life Sci.* **847,** 30–7 (2007).
162. Villanueva, J. *et al.* Correcting common errors in identifying cancer-specific serum peptide signatures. *J. Proteome Res.* **4,** 1060–72
163. http://www.admin.ox.ac.uk/uohs/policies-guidance/blood/". No Title. at <http://www.admin.ox.ac.uk/uohs/policies-guidance/blood/">

164. Kaisar M, van Dullemen LFA, Thézénas ML, Charles PD, Pleog RJ, K. B. Plasma Biomarker Profile Altered Through Variable Blood Storage. *Clin. Chem.* **62,** 1272–1277 (2016).
165. Kaisar M, van Dullemen LFA, Thézénas ML, Akhtar MZ, Huang H, Rendel S, Charles PD, Fischer R, P. R. and. K. M. Plasma Degradome Affected by Variable Storage of Human Blood. *Clin. Proteomics* **In press,** (2016).
166. Andoh, A. *et al.* Molecular characterization of complement components (C3, C4, and factor B) in human saliva. *J. Clin. Immunol.* **17,** 404–7 (1997).
167. Onopiuk, A., Tokarzewicz, A. & Gorodkiewicz, E. Cystatin C: a kidney function biomarker. *Adv. Clin. Chem.* **68,** 57–69 (2015).
168. Vanmassenhove, J., Vanholder, R., Nagler, E. & Van Biesen, W. Urinary and serum biomarkers for the diagnosis of acute kidney injury: an in-depth review of the literature. *Nephrol. Dial. Transplant* **28,** 254–73 (2013).
169. Aguilar-Mahecha, A., Kuzyk, M. a., Domanski, D., Borchers, C. H. & Basik, M. The effect of pre-analytical variability on the measurement of MRM-MS-based mid- to high-abundance plasma protein biomarkers and a panel of cytokines. *PLoS One* **7,** e38290 (2012).
170. Sigdel, T. K., Klassen, R. B. & Sarwal, M. M. Interpreting the proteome and peptidome in transplantation. *Adv. Clin. Chem.* **47,** 139–69 (2009).
171. Li, Y. Y. *et al.* Circulating proteolytic products of carboxypeptidase N for early detection of breast cancer. *Clin. Chem.* **60,** 233–42 (2014).
172. Merchant, M. L. *et al.* Plasma kininogen and kininogen fragments are biomarkers of progressive renal decline in type 1 diabetes. *Kidney Int.* **83,** 1177–84 (2013).
173. Mullen, W., Delles, C. & Mischak, H. Urinary proteomics in the assessment of chronic kidney disease. *Curr. Opin. Nephrol. Hypertens.* **20,** 654–61 (2011).
174. Starlinger, P. *et al.* Thrombospondin-1: a unique marker to identify in vitro platelet activation when monitoring in vivo processes. *J. Thromb. Haemost.* **8,** 1809–19 (2010).
175. Dardik, R. & Lahav, J. Functional changes in the conformation of thrombospondin-1 during complexation with fibronectin or heparin. *Exp. Cell Res.* **248,** 407–14 (1999).
176. Tan, K. *et al.* The structures of the thrombospondin-1 N-terminal domain and its complex with a synthetic pentameric heparin. *Structure* **14,** 33–42 (2006).
177. Damas, C., Vink, T., Nieuwenhuis, H. K. & Sixma, J. J. The 33-kDa platelet alpha-granule membrane protein (GMP-33) is an N-terminal proteolytic fragment of thrombospondin. *Thromb. Haemost.* **86,** 887–93 (2001).
178. Bonnefoy, A. & Legrand, C. Proteolysis of subendothelial adhesive glycoproteins (fibronectin, thrombospondin, and von Willebrand factor) by plasmin, leukocyte cathepsin G, and elastase. *Thromb. Res.* **98,** 323–32 (2000).
179. Resovi, A., Pinessi, D., Chiorino, G. & Taraboletti, G. Current understanding of the thrombospondin-1 interactome. *Matrix Biol.* **37,** 83–91 (2014).
180. Jeanne, A., Schneider, C., Martiny, L. & Dedieu, S. Original insights on thrombospondin-1-related antireceptor strategies in cancer. *Front. Pharmacol.* **6,** 252 (2015).
181. del Conde, I. Platelet activation leads to activation and propagation of the complement system. *J. Exp. Med.* **201,** 871–879 (2005).

182. Moers, C., Leuvenink, H. G. D. & Ploeg, R. J. Non-heart beating organ donation: overview and future perspectives. *Transpl. Int.* **20,** 567–75 (2007).
183. Hwang, J. K. *et al.* Long-term outcomes of kidney transplantation from expanded criteria deceased donors at a single center: comparison with standard criteria deceased donors. *Transplant. Proc.* **46,** 431–6 (2014).
184. Pramod Nagaraja, Gareth W. Roberts, Michael Stephens, Szabolcs Horvath, Jana Fialova, Rafael Chavez, Argiris Asderakis, and Z. K. *et al.* Influence of delayed graft function and acute rejection on outcomes after kidney transplantation from donors after cardiac death. *Transplantation* **99,** 226–31 (2012).
185. Schröppel, B. & Legendre, C. Delayed kidney graft function: from mechanism to translation. *Kidney Int.* **86,** 251–8 (2014).
186. Perico, N., Cattaneo, D., Sayegh, M. H. & Remuzzi, G. Delayed graft function in kidney transplantation. *Lancet* **364,** 1814–1827 (2004).
187. Loverre, A. *et al.* Ischemia-reperfusion injury-induced abnormal dendritic cell traffic in the transplanted kidney with delayed graft function. *Kidney Int.* **72,** 994–1003 (2007).
188. Park, S. W., Chen, S. W. C., Kim, M., D'Agati, V. D. & Lee, H. T. Human heat shock protein 27-overexpressing mice are protected against acute kidney injury after hepatic ischemia and reperfusion. *Am. J. Physiol. Renal Physiol.* **297,** F885-94 (2009).
189. Bouma, H. R., Ploeg, R. J. & Schuurs, T. a. Signal transduction pathways involved in brain death-induced renal injury. *Am. J. Transplant.* **9,** 989–997 (2009).
190. McDaniel, D. O. *et al.* Early expression profile of inflammatory markers and kidney allograft status. *Transplant. Proc.* **45,** 1520–1523 (2013).
191. Nijboer, W. N. *et al.* Effects of brain death on stress and inflammatory response in the human donor kidney. *Transplant. Proc.* **37,** 367–9
192. Matignon, M. *et al.* Arteriolar Hyalinization Predicts Delayed Graft Function in Deceased Donor Renal Transplantation. *Transplantation* **86,** 1002–1005 (2008).
193. van den Akker, E. K. *et al.* Neutrophil Gelatinase-Associated Lipocalin, but Not Kidney Injury Marker 1, Correlates with Duration of Delayed Graft Function. *Eur. Surg. Res.* **55,** 319–327 (2015).
194. Cantaluppi, V. *et al.* Neutrophil Gelatinase Associated Lipocalin Is an Early and Accurate Biomarker of Graft Function and Tissue Regeneration in Kidney Transplantation from Extended Criteria Donors. *PLoS One* **10,** e0129279 (2015).
195. Pajek, J. *et al.* Non-inferiority of creatinine excretion rate to urinary L-FABP and NGAL as predictors of early renal allograft function. *BMC Nephrol.* **15,** 117 (2014).
196. Damman, J. *et al.* Hypoxia and Complement-and-Coagulation Pathways in the Deceased Organ Donor as the Major Target for Intervention to Improve Renal Allograft Outcome. *Transplantation* **0,** 1 (2014).
197. Peng, J. *et al.* Hyperglycemia, p53, and mitochondrial pathway of apoptosis are involved in the susceptibility of diabetic models to ischemic acute kidney injury. *Kidney Int.* **87,** 137–50 (2015).
198. Dalleau, S., Baradat, M., Guéraud, F. & Huc, L. Cell death and diseases related

to oxidative stress: 4-hydroxynonenal (HNE) in the balance. *Cell Death Differ.* **20,** 1615–30 (2013).
199. Kyriakis, J. M. & Avruch, J. Mammalian MAPK signal transduction pathways activated by stress and inflammation: a 10-year update. *Physiol. Rev.* **92,** 689–737 (2012).
200. Kanellis, J. *et al.* JNK signalling in human and experimental renal ischaemia/reperfusion injury. *Nephrol. Dial. Transplant.* **25,** 2898–2908 (2010).
201. Wood, Z. A., Schröder, E., Robin Harris, J. & Poole, L. B. Structure, mechanism and regulation of peroxiredoxins. *Trends Biochem. Sci.* **28,** 32–40 (2003).
202. Godin, N. *et al.* Catalase overexpression prevents hypertension and tubular apoptosis in angiotensinogen transgenic mice. *Kidney Int.* **77,** 1086–97 (2010).
203. Satoh, M. Benefits of catalase overexpression in renal proximal tubular cells. *Kidney Int.* **77,** 1060–1062 (2010).
204. Bansal, N. *et al.* Urine Injury Biomarkers and Risk of Adverse Outcomes in Recipients of Prevalent Kidney Transplants: The Folic Acid for Vascular Outcome Reduction in Transplantation Trial. *J. Am. Soc. Nephrol.* **27,** 2109–21 (2016).
205. Bolignano, D. *et al.* Neutrophil Gelatinase-Associated Lipocalin (NGAL) and Progression of Chronic Kidney Disease. *Clin. J. Am. Soc. Nephrol.* **4,** 337–344 (2009).
206. Krolewski, A. S. *et al.* Early progressive renal decline precedes the onset of microalbuminuria and its progression to macroalbuminuria. *Diabetes Care* **37,** 226–34 (2014).
207. Koo, T. Y. *et al.* Pre-transplant Evaluation of Donor Urinary Biomarkers can Predict Reduced Graft Function After Deceased Donor Kidney Transplantation. *Medicine (Baltimore).* **95,** e3076 (2016).
208. Worthmann, K. *et al.* Urinary excretion of IGFBP-1 and -3 correlates with disease activity and differentiates focal segmental glomerulosclerosis and minimal change disease. *Growth Factors* **28,** 129–138 (2010).
209. Liu, W. J. *et al.* Urinary proteins induce lysosomal membrane permeabilization and lysosomal dysfunction in renal tubular epithelial cells. *Am. J. Physiol. Renal Physiol.* **308,** F639-49 (2015).
210. Damman, J. & Seelen, M. a. Mannan binding lectin: a two-faced regulator of renal allograft injury? *Kidney Int.* **83,** 191–3 (2013).
211. Poosti, F. *et al.* Selective delivery of IFN-γ to renal interstitial myofibroblasts: a novel strategy for the treatment of renal fibrosis. *FASEB J.* **29,** 1029–42 (2015).
212. Ling, X. B. *et al.* Integrative urinary peptidomics in renal transplantation identifies biomarkers for acute rejection. *J. Am. Soc. Nephrol.* **21,** 646–53 (2010).
213. Collins, M. G., Chang, S. H., Russ, G. R. & McDonald, S. P. Outcomes of transplantation using kidneys from donors meeting expanded criteria in Australia and New Zealand, 1991 to 2005. *Transplantation* **87,** 1201–9 (2009).
214. Singh, R. P. *et al.* Kidney transplantation from donation after cardiac death donors: lack of impact of delayed graft function on post-transplant

outcomes. *Clin. Transplant.* **25,** 255–64
215. Nankivell, B. J. *et al.* The natural history of chronic allograft nephropathy. *N. Engl. J. Med.* **349,** 2326–33 (2003).
216. O'Connell, P. J. *et al.* Biopsy transcriptome expression profiling to identify kidney transplants at risk of chronic injury: a multicentre, prospective study. *Lancet (London, England)* **388,** 983–93 (2016).
217. Ricci, Z., Cruz, D. N. & Ronco, C. Classification and staging of acute kidney injury: beyond the RIFLE and AKIN criteria. *Nat. Rev. Nephrol.* **7,** 201–8 (2011).
218. von Mering, C. *et al.* STRING: known and predicted protein-protein associations, integrated and transferred across organisms. *Nucleic Acids Res.* **33,** D433-7 (2005).
219. Szklarczyk, D. *et al.* STRING v10: protein-protein interaction networks, integrated over the tree of life. *Nucleic Acids Res.* **43,** D447-52 (2015).
220. Levey, A. S. *et al.* A more accurate method to estimate glomerular filtration rate from serum creatinine: a new prediction equation. Modification of Diet in Renal Disease Study Group. *Ann. Intern. Med.* **130,** 461–70 (1999).
221. Clayton, P. A., Lim, W. H., Wong, G. & Chadban, S. J. Relationship between eGFR Decline and Hard Outcomes after Kidney Transplants. *J. Am. Soc. Nephrol.* 1–7 (2016). doi:10.1681/ASN.2015050524
222. Naesens, M. *et al.* Subclinical inflammation and chronic renal allograft injury in a randomized trial on steroid avoidance in pediatric kidney transplantation. *Am. J. Transplant* **12,** 2730–43 (2012).
223. Liu, R.-M. & Desai, L. P. Reciprocal regulation of TGF-β and reactive oxygen species: A perverse cycle for fibrosis. *Redox Biol.* **6,** 565–77 (2015).
224. Djamali, A., Vidyasagar, A., Adulla, M., Hullett, D. & Reese, S. Nox-2 is a modulator of fibrogenesis in kidney allografts. *Am. J. Transplant* **9,** 74–82 (2009).
225. Jenkins, R. H., Martin, J., Phillips, A. O., Bowen, T. & Fraser, D. J. Transforming growth factor β1 represses proximal tubular cell microRNA-192 expression through decreased hepatocyte nuclear factor DNA binding. *Biochem. J.* **443,** 407–16 (2012).
226. Zhong, X., Chung, A. C. K., Chen, H.-Y., Meng, X.-M. & Lan, H. Y. Smad3-mediated upregulation of miR-21 promotes renal fibrosis. *J. Am. Soc. Nephrol.* **22,** 1668–81 (2011).
227. Boor, P., Ostendorf, T. & Floege, J. Renal fibrosis: novel insights into mechanisms and therapeutic targets. *Nat. Rev. Nephrol.* **6,** 643–56 (2010).
228. Boor, P., Ostendorf, T. & Floege, J. PDGF and the progression of renal disease. *Nephrol. Dial. Transplant* **29 Suppl 1,** i45–i54 (2014).
229. Eitner, F. *et al.* PDGF-C expression in the developing and normal adult human kidney and in glomerular diseases. *J. Am. Soc. Nephrol.* **14,** 1145–53 (2003).
230. Floege, J., Eitner, F. & Alpers, C. E. A new look at platelet-derived growth factor in renal disease. *J. Am. Soc. Nephrol.* **19,** 12–23 (2008).
231. Eddy, A. A. Overview of the cellular and molecular basis of kidney fibrosis. *Kidney Int. Suppl.* **4,** 2–8 (2014).
232. Richter, K., Konzack, A., Pihlajaniemi, T., Heljasvaara, R. & Kietzmann, T. Redox-fibrosis: Impact of TGFβ1 on ROS generators, mediators and functional consequences. *Redox Biol.* **6,** 344–52 (2015).

233. Daehn, I. *et al.* Endothelial mitochondrial oxidative stress determines podocyte depletion in segmental glomerulosclerosis. *J. Clin. Invest.* **124,** 1608–21 (2014).
234. Chen, Y.-M. Y.-T. *et al.* Platelet-derived growth factor receptor signaling activates pericyte-myofibroblast transition in obstructive and post-ischemic kidney fibrosis. *Kidney Int.* **80,** 1170–81 (2011).
235. Hudkins, K. L. *et al.* Exogenous PDGF-D is a potent mesangial cell mitogen and causes a severe mesangial proliferative glomerulopathy. *J. Am. Soc. Nephrol.* **15,** 286–98 (2004).
236. Li, X. *et al.* PDGF-C is a new protease-activated ligand for the PDGF alpha-receptor. *Nat. Cell Biol.* **2,** 302–9 (2000).
237. Kishioka, H. *et al.* Effects of PDGF A-chain antisense oligodeoxynucleotides on growth of cardiovascular organs in stroke-prone spontaneously hypertensive rats. *Am. J. Hypertens.* **14,** 439–45 (2001).
238. Floege, J. *et al.* Infusion of platelet-derived growth factor or basic fibroblast growth factor induces selective glomerular mesangial cell proliferation and matrix accumulation in rats. *J. Clin. Invest.* **92,** 2952–62 (1993).
239. Yuan, A., Lee, Y., Choi, U., Moeckel, G. & Karihaloo, A. Chemokine receptor Cxcr4 contributes to kidney fibrosis via multiple effectors. *Am. J. Physiol. Renal Physiol.* **308,** F459-72 (2015).
240. Martin, I. V *et al.* Platelet-derived growth factor (PDGF)-C neutralization reveals differential roles of PDGF receptors in liver and kidney fibrosis. *Am. J. Pathol.* **182,** 107–17 (2013).
241. Yamamoto, H., Crow, M., Cheng, L., Lakatta, E. & Kinsella, J. PDGF receptor-to-nucleus signaling of p91 (STAT1 alpha) transcription factor in rat smooth muscle cells. *Exp. Cell Res.* **222,** 125–30 (1996).
242. Vignais, M. L., Sadowski, H. B., Watling, D., Rogers, N. C. & Gilman, M. Platelet-derived growth factor induces phosphorylation of multiple JAK family kinases and STAT proteins. *Mol. Cell. Biol.* **16,** 1759–69 (1996).
243. He, C. *et al.* PDGFRβ signalling regulates local inflammation and synergizes with hypercholesterolaemia to promote atherosclerosis. *Nat. Commun.* **6,** 7770 (2015).
244. Paukku, K. *et al.* Platelet-derived growth factor (PDGF)-induced activation of signal transducer and activator of transcription (Stat) 5 is mediated by PDGF beta-receptor and is not dependent on c-src, fyn, jak1 or jak2 kinases. *Biochem. J.* **345 Pt 3,** 759–66 (2000).
245. Choudhury, G. G., Marra, F., Kiyomoto, H. & Abboud, H. E. PDGF stimulates tyrosine phosphorylation of JAK 1 protein tyrosine kinase in human mesangial cells. *Kidney Int.* **49,** 19–25 (1996).
246. Jenkins, B. J. Transcriptional regulation of pattern recognition receptors by Jak/STAT signaling, and the implications for disease pathogenesis. *J. Interferon Cytokine Res.* **34,** 750–8 (2014).
247. Al-Lamki, R. S. & Mayadas, T. N. TNF receptors: signaling pathways and contribution to renal dysfunction. *Kidney Int.* **87,** 281–296 (2015).
248. Sengul, S., Zwizinski, C. & Batuman, V. Role of MAPK pathways in light chain-induced cytokine production in human proximal tubule cells. *Am. J. Physiol. Renal Physiol.* **284,** F1245-54 (2003).
249. Nongnuch, A., Panorchan, K. & Davenport, A. Brain-kidney crosstalk. *Crit. Care* **18,** 225 (2014).

250. Chouchani, E. T. *et al.* Ischaemic accumulation of succinate controls reperfusion injury through mitochondrial ROS. *Nature* **515,** 431–5 (2014).
251. Gorrini, C., Harris, I. S. & Mak, T. W. Modulation of oxidative stress as an anticancer strategy. *Nat. Rev. Drug Discov.* **12,** 931–47 (2013).
252. Thioredoxin reductase. - PubMed - NCBI. at <http://www.ncbi.nlm.nih.gov/pubmed/10657232>
253. Hanschmann, E.-M., Godoy, J. R., Berndt, C., Hudemann, C. & Lillig, C. H. Thioredoxins, glutaredoxins, and peroxiredoxins--molecular mechanisms and health significance: from cofactors to antioxidants to redox signaling. *Antioxid. Redox Signal.* **19,** 1539–605 (2013).
254. Netto, L. E. S. & Antunes, F. The Roles of Peroxiredoxin and Thioredoxin in Hydrogen Peroxide Sensing and in Signal Transduction. *Mol. Cells* **39,** 65–71 (2016).
255. Kasuno, K., Nakamura, H., Ono, T., Muso, E. & Yodoi, J. Protective roles of thioredoxin, a redox-regulating protein, in renal ischemia/reperfusion injury. *Kidney Int.* **64,** 1273–82 (2003).
256. Advani, A. *et al.* Expression, localization, and function of the thioredoxin system in diabetic nephropathy. *J. Am. Soc. Nephrol.* **20,** 730–41 (2009).
257. Hu, H. *et al.* Priming donor lungs with thioredoxin-1 attenuates acute allograft injury in a rat model of lung transplantation. *J. Heart Lung Transplant.* **27,** 1142–9 (2008).
258. Suvakov, S. *et al.* Glutathione S-transferase A1, M1, P1 and T1 null or low-activity genotypes are associated with enhanced oxidative damage among haemodialysis patients. *Nephrol. Dial. Transplant* **28,** 202–12 (2013).
259. Walsh, J. *et al.* Identification and quantification of the basal and inducible Nrf2-dependent proteomes in mouse liver: biochemical, pharmacological and toxicological implications. *J. Proteomics* **108,** 171–87 (2014).
260. Hall, I. E. *et al.* Glutathione S-transferase iso-enzymes in perfusate from pumped kidneys are associated with delayed graft function. *Am. J. Transplant.* **14,** 886–896 (2014).
261. Doucet, A., Kleifeld, O., Kizhakkedathu, J. N. & Overall, C. M. in 273–287 (2011). doi:10.1007/978-1-61779-148-2_18
262. Schwanhäusser, B., Gossen, M., Dittmar, G. & Selbach, M. Global analysis of cellular protein translation by pulsed SILAC. *Proteomics* **9,** 205–209 (2009).
263. D, V. D., Kaskel, F. J. & Falk, R. J. Focal Segmental Glomerulosclerosis. *N Engl J Med* **25365,** 2398–411 (2011).
264. Mundel, P. & Shankland, S. J. Podocyte biology and response to injury. *J. Am. Soc. Nephrol.* **13,** 3005–15 (2002).
265. Perico, L., Conti, S., Benigni, A. & Remuzzi, G. Podocyte–actin dynamics in health and disease. *Nat. Rev. Nephrol.* **12,** 692–710 (2016).
266. Taniguchi, Y. *et al.* The C-terminal Region of Laminin Chains Modulates the Integrin Binding Affinities of Laminins. *J. Biol. Chem.* **284,** 7820–7831 (2009).
267. Calderwood, D. a, Campbell, I. D. & Critchley, D. R. Talins and kindlins: partners in integrin-mediated adhesion. *Nat. Rev. Mol. Cell Biol.* **14,** 503–17 (2013).
268. Courdier-Fruh, I. & Briguet, A. Utrophin is a calpain substrate in muscle cells. *Muscle Nerve* **33,** 753–759 (2006).
269. Castillo, M. R. & Babson, J. R. Ca(2+)-dependent mechanisms of cell injury in

cultured cortical neurons. *Neuroscience* **86,** 1133–44 (1998).
270. Iwata, A. *et al.* Traumatic axonal injury induces proteolytic cleavage of the voltage-gated sodium channels modulated by tetrodotoxin and protease inhibitors. *J. Neurosci.* **24,** 4605–13 (2004).
271. Wang, K. K. W., Larner, S. F., Robinson, G. & Hayes, R. L. Neuroprotection targets after traumatic brain injury. *Curr. Opin. Neurol.* **19,** 514–9 (2006).
272. Peng, T.-I. & Jou, M.-J. Oxidative stress caused by mitochondrial calcium overload. *Ann. N. Y. Acad. Sci.* **1201,** 183–188 (2010).
273. Moldoveanu, T. *et al.* A Ca(2+) switch aligns the active site of calpain. *Cell* **108,** 649–60 (2002).
274. Peltier, J. *et al.* Calpain Activation and Secretion Promote Glomerular Injury in Experimental Glomerulonephritis: Evidence from Calpastatin-Transgenic Mice. *J Am Soc Nephrol* **17,** 3415–3423 (2006).
275. Bate, N. *et al.* Talin contains a C-terminal calpain2 cleavage site important in focal adhesion dynamics. *PLoS One* **7,** e34461 (2012).
276. C.J. ILSE RAATS, JACOB VAN DEN BORN, and J. H. M. B. Glomerular heparan sulfate alterations: Mechanisms and relevance for proteinuria.
277. Raats, C. J. I., Bakker, M. A. H., Van Den Born, J. & Berden, J. H. M. Hydroxyl Radicals Depolymerize Glomerular Heparan Sulfate in Vitro and in Experimental Nephrotic Syndrome*.
278. Zhao, X., Hsu, K.-S., Lim, J. H., Bruggeman, L. A. & Kao, H.-Y. α-Actinin 4 potentiates nuclear factor κ-light-chain-enhancer of activated B-cell (NF-κB) activity in podocytes independent of its cytoplasmic actin binding function. *J. Biol. Chem.* **290,** 338–49 (2015).
279. Henderson, J. M., Alexander, M. P. & Pollak, M. R. Patients with ACTN4 mutations demonstrate distinctive features of glomerular injury. *J. Am. Soc. Nephrol.* **20,** 961–8 (2009).
280. Satoskar, A. A. *et al.* Characterization of glomerular diseases using proteomic analysis of laser capture microdissected glomeruli. *Mod. Pathol.* **25,** 709–21 (2012).

Data Appendix

Table S4.1 List of all proteins identified in the proteomic analysis

			Average normalised abundance				Fold Change		
Accessior	Description	Anova (p)*	Centrifugation T=30 min	Centrifugation T=8h	Centrifugation T=24h	Centrifugation T=48h	8h vs 30m	24h vs 30mir	48h vs 30m
Q4G0Z9	MCM domain-containing protein 2	8.30E-07	205000	332000	342000	347000	1.62	1.67	1.69
P02768	Serum albumin	1.01E-05	10100000	17900000	19000000	18300000	1.77	1.88	1.81
Q07864	DNA polymerase epsilon catalytic subunit A	1.28E-05	628000	783000	780000	741000	1.25	1.24	1.18
P07737	Profilin-1	2.86E-05	12900	14300	25900	92200	1.11	2.01	7.15
Q96N67	Dedicator of cytokinesis protein 7	6.08E-04	1030000	1530000	1530000	1430000	1.49	1.49	1.39
Q96M91	Coiled-coil domain-containing protein 11	8.62E-04	744000	902000	974000	932000	1.21	1.31	1.25
P07996	Thrombospondin-1	1.41E-03	449000	537000	601000	625000	1.20	1.34	1.39
P02746	Complement C1q subcomponent subunit B	2.50E-03	1660000	2160000	2140000	2110000	1.30	1.29	1.27
Q53SZ7	Uncharacterized protein C2orf53	2.57E-03	262000	480000	495000	454000	1.83	1.89	1.73
P02647	Apolipoprotein A-I	2.00E-02	434000	553000	553000	559000	1.27	1.27	1.29
Q6NXT1	Ankyrin repeat domain-containing protein 54	2.00E-02	57400	128000	130000	124000	2.23	2.26	2.16
P05160	Coagulation factor XIII B chain	3.00E-02	965000	1200000	1180000	1170000	1.24	1.22	1.21
O75019	Leukocyte immunoglobulin-like receptor subfamily A member 1	3.00E-02	54300	67700	76500	73800	1.25	1.41	1.36
P02679	Fibrinogen gamma chain	4.00E-02	1710000	2350000	2220000	2120000	1.37	1.30	1.24
P01876	Ig alpha-1 chain C region;	4.00E-02	34000	83100	84000	78100	2.44	2.47	2.30
P01034	Cystatin-C	4.00E-02	38600	50800	49800	48900	1.32	1.29	1.27
P01834	Ig kappa chain C region;	5.00E-02	203000	412000	437000	421000	2.03	2.15	2.07
P11021	78 kDa glucose-regulated protein	5.00E-02	1010000	1290000	1270000	1230000	1.28	1.26	1.22
Q8IUH4	Palmitoyltransferase ZDHHC13	5.00E-02	1730000	1500000	1580000	1490000	0.87	0.91	0.86
P01619	Ig kappa chain V-III region B6	6.00E-02	2022.75	3676	3845.89	4375.64	1.82	1.90	2.16
P00738	Haptoglobin	8.00E-02	133000	209000	220000	214000	1.57	1.65	1.61
P02775	Platelet basic protein	8.00E-02	199000	177000	285000	322000	0.89	1.43	1.62
P07951	Tropomyosin beta chain	8.00E-02	700000	851000	940000	943000	1.22	1.34	1.35
P06753	Tropomyosin alpha-3 chain	8.00E-02	705000	858000	938000	931000	1.22	1.33	1.32
P54108	Cysteine-rich secretory protein 3	9.00E-02	73400	95700	102000	99900	1.30	1.39	1.36
Q86U86	Protein polybromo-1;	1.00E-01	3080000	3550000	3630000	3610000	1.15	1.18	1.17
P02776	Platelet factor 4; S	1.00E-01	8573.19	7584.43	13700	21300	0.88	1.60	2.48
P31949	Protein S100-A11	1.20E-01	14.45	0	274.09	574.75	0.00	18.97	39.78
P01859	Ig gamma-2 chain C region;	1.50E-01	262000	405000	389000	380000	1.55	1.48	1.45
P06702	Protein S100-A9	1.60E-01	17300	19100	96400	136000	1.10	5.57	7.86
P01861	Ig gamma-4 chain C region;	1.70E-01	411000	512000	544000	516000	1.25	1.32	1.26
P00558	Phosphoglycerate kinase 1	1.70E-01	3400000	3070000	3190000	3030000	0.90	0.94	0.89
Q16322	Potassium voltage-gated channel subfamily A member 10	1.70E-01	132000	103000	97800	99300	0.78	0.74	0.75
P00736	Complement C1r subcomponent	1.80E-01	3060000	2740000	2790000	2610000	0.90	0.91	0.85
O15481	Melanoma-associated antigen B4	2.00E-01	822000	712000	765000	741000	0.87	0.93	0.90
Q8IWN7	Retinitis pigmentosa 1-like 1 protein;	2.30E-01	1750000	1900000	2020000	1990000	1.09	1.15	1.14
Q14532	Keratin, type I cuticular Ha2	2.30E-01	1500000	1560000	1760000	1780000	1.04	1.17	1.19
Q12860	Contactin-1; AltName	2.30E-01	68700	56200	66100	65500	0.82	0.96	0.95
P01009	Alpha-1-antitrypsin	2.40E-01	387000	405000	436000	413000	1.05	1.13	1.07
O75882	Attractin	2.70E-01	995000	896000	843000	825000	0.90	0.85	0.83
P03951	Coagulation factor XI	3.00E-01	433000	392000	406000	402000	0.91	0.94	0.93
P05109	Protein S100-A8	3.00E-01	34700	31400	57700	80800	0.90	1.66	2.33
Q5T013	Putative hydroxypyruvate isomerase	3.00E-01	1090000	1260000	1140000	1120000	1.16	1.05	1.03
P14618	Pyruvate kinase PKM	3.00E-01	342000	304000	317000	324000	0.89	0.93	0.95
P35908	Keratin, type II cytoskeletal 2 epidermal	3.10E-01	565000	495000	498000	474000	0.88	0.88	0.84
P00915	Carbonic anhydrase 1	3.40E-01	1670000	1900000	1840000	1750000	1.14	1.10	1.05
Q6TDU7	Protein CASC1	3.80E-01	706000	644000	610000	558000	0.91	0.86	0.79
Q02985	Complement factor H-related protein 3	4.10E-01	519000	508000	460000	459000	0.98	0.89	0.88
P50406	5-hydroxytryptamine receptor 6	4.10E-01	139000	142000	117000	112000	1.02	0.84	0.81
Q8IXR9	Uncharacterized protein C12orf56	4.30E-01	982000	1110000	1130000	1020000	1.13	1.15	1.04
P25815	Protein S100-P	4.50E-01	10300	10500	13100	13600	1.02	1.27	1.32
P02787	Serotransferrin	4.60E-01	854000	963000	973000	922000	1.13	1.14	1.08
Q9NQ79	Cartilage acidic protein 1	4.60E-01	13500	12100	15600	15600	0.90	1.16	1.16
Q13103	Secreted phosphoprotein 24	4.70E-01	147000	132000	118000	111000	0.90	0.80	0.76
Q14168	MAGUK p55 subfamily member 2	4.70E-01	610000	648000	662000	665000	1.06	1.09	1.09
Q9H939	Proline-serine-threonine phosphatase-interacting protein 2	4.70E-01	1290000	1210000	1350000	1350000	0.94	1.05	1.05
Q9NQI0	Probable ATP-dependent RNA helicase DDX4	4.70E-01	926000	1060000	1010000	903000	1.14	1.09	0.98
Q9NR34	Mannosyl-oligosaccharide 1,2-alpha-mannosidase IC	4.70E-01	103000	85900	105000	102000	0.83	1.02	0.99
Q04756	Hepatocyte growth factor activator	4.80E-01	1070000	939000	1020000	998000	0.88	0.95	0.93
P15923	Transcription factor E2-alpha	4.80E-01	738000	851000	797000	697000	1.15	1.08	0.94
P06396	Gelsolin	4.90E-01	10500000	9650000	10100000	9960000	0.92	0.96	0.95
Q9Y490	Talin-1	4.90E-01	5690000	5240000	5300000	5340000	0.92	0.93	0.94
Q6YHU6	Thyroid adenoma-associated protein	4.90E-01	4720000	4840000	5220000	5140000	1.03	1.11	1.09
Q6UVK1	Chondroitin sulfate proteoglycan 4	4.90E-01	1710000	1650000	1720000	1600000	0.96	1.01	0.94
P17936	Insulin-like growth factor-binding protein 3	5.00E-01	143000	125000	136000	131000	0.87	0.95	0.92
Q5VZM2	Ras-related GTP-binding protein B	5.00E-01	374000	313000	370000	353000	0.84	0.99	0.94
P02654	Apolipoprotein C-I	5.20E-01	286000	234000	243000	326000	0.82	0.85	1.14
P48741	Putative heat shock 70 kDa protein 7	5.20E-01	999000	915000	925000	898000	0.92	0.93	0.90
P02753	Retinol-binding protein 4	5.30E-01	2800000	3030000	3330000	2780000	1.08	1.19	0.99
P00746	Complement factor D	5.30E-01	57500	50900	53900	56100	0.89	0.94	0.98
P23142	Fibulin-1	5.40E-01	689000	632000	710000	736000	0.92	1.03	1.07

Q8IZJ4	Ral-GDS-related protein	5.40E-01	608000	484000	546000	613000	0.80	0.90	1.01
P12259	Coagulation factor V	5.60E-01	7530000	6920000	7020000	6750000	0.92	0.93	0.90
Q9Y2V7	Conserved oligomeric Golgi complex subunit 6	5.60E-01	930000	844000	872000	834000	0.91	0.94	0.90
P61626	Lysozyme C	5.70E-01	106000	98000	94800	106000	0.92	0.89	1.00
P55056	Apolipoprotein C-IV	5.70E-01	57000	51700	51200	50200	0.91	0.90	0.88
Q9Y2K3	Myosin-15	5.80E-01	6180000	5810000	5860000	5740000	0.94	0.95	0.93
P0DJI8	Serum amyloid A-1 protein	5.80E-01	4916.99	6706.49	9214.87	14700	1.36	1.87	2.99
P63104	14-3-3 protein zeta/delta	5.80E-01	101000	86700	81600	90600	0.86	0.81	0.90
Q6ZTQ3	Ras association domain-containing protein 6	5.80E-01	2230000	2070000	2290000	2110000	0.93	1.03	0.95
P04220	Ig mu heavy chain disease protein	5.90E-01	33500	51000	48500	45500	1.52	1.45	1.36
O94901	SUN domain-containing protein 1	5.90E-01	5210000	4930000	4750000	4680000	0.95	0.91	0.90
Q03591	Complement factor H-related protein 1	6.00E-01	2340000	2150000	2150000	2200000	0.92	0.92	0.94
Q9H8V3	Protein ECT2	6.00E-01	1820000	1670000	1610000	1610000	0.92	0.88	0.88
P02790	Hemopexin	6.10E-01	50200000	47300000	48100000	46600000	0.94	0.96	0.93
P37802	Transgelin-2	6.10E-01	2380000	2590000	2610000	2480000	1.09	1.10	1.04
P23528	Cofilin-1	6.10E-01	266000	238000	247000	260000	0.89	0.93	0.98
P00338	L-lactate dehydrogenase A chain	6.10E-01	1230000	1110000	1100000	1070000	0.90	0.89	0.87
Q8IZF0	Sodium leak channel non-selective protein	6.20E-01	1150000	1070000	1080000	1060000	0.93	0.94	0.92
O75626	PR domain zinc finger protein 1	6.20E-01	477000	398000	390000	381000	0.83	0.82	0.80
P02649	Apolipoprotein E	6.30E-01	3660000	3560000	3590000	3330000	0.97	0.98	0.91
Q15195	Plasminogen-like protein A	6.30E-01	238000	214000	226000	225000	0.90	0.95	0.95
Q96PV7	Protein FAM193B;	6.30E-01	283000	240000	257000	276000	0.85	0.91	0.98
Q9BYX7	Putative beta-actin-like protein 3	6.40E-01	464000	411000	426000	462000	0.89	0.92	1.00
P02766	Transthyretin	6.50E-01	110000	125000	120000	96800	1.14	1.09	0.88
P07195	L-lactate dehydrogenase B chain	6.50E-01	211000	197000	205000	218000	0.93	0.97	1.03
P02745	Complement C1q subcomponent subunit A	6.60E-01	719000	808000	769000	744000	1.12	1.07	1.03
O00391	Sulfhydryl oxidase 1	6.60E-01	4450000	4070000	3970000	3860000	0.91	0.89	0.87
Q8WVM7	Cohesin subunit SA-1	6.60E-01	2500000	2250000	2330000	2430000	0.90	0.93	0.97
P04217	Alpha-1B-glycoprotein	6.70E-01	9040000	8660000	8780000	8380000	0.96	0.97	0.93
P05154	Plasma serine protease inhibitor	6.70E-01	138000	115000	122000	152000	0.83	0.88	1.10
P00742	Coagulation factor X	6.70E-01	946000	1030000	992000	953000	1.09	1.05	1.01
P43121	Cell surface glycoprotein MUC18	6.70E-01	3310000	2870000	3070000	3010000	0.87	0.93	0.91
Q96CF2	Charged multivesicular body protein 4c	6.70E-01	375000	361000	359000	335000	0.96	0.96	0.89
P02765	Alpha-2-HS-glycoprotein	6.80E-01	24200000	22200000	23300000	22000000	0.92	0.96	0.91
Q04695	Keratin, type I cytoskeletal 17	6.80E-01	1760000	1590000	1770000	1620000	0.90	1.01	0.92
Q9Y5Y7	Lymphatic vessel endothelial hyaluronic acid receptor 1; Short=LYV	6.80E-01	6220000	6560000	6680000	6820000	1.05	1.07	1.10
P01011	Alpha-1-antichymotrypsin	6.90E-01	10600000	10200000	10100000	9790000	0.96	0.95	0.92
Q9UK55	Protein Z-dependent protease inhibitor	6.90E-01	6220000	6560000	6670000	6810000	1.05	1.07	1.09
P01877	Ig alpha-2 chain C region	6.90E-01	200000	227000	230000	224000	1.14	1.15	1.12
P02763	Alpha-1-acid glycoprotein 1	6.90E-01	110000	136000	111000	105000	1.24	1.01	0.95
P19652	Alpha-1-acid glycoprotein 2	6.90E-01	115000	146000	123000	115000	1.27	1.07	1.00
Q96AY3	Peptidyl-prolyl cis-trans isomerase FKBP10	6.90E-01	420000	407000	388000	357000	0.97	0.92	0.85
P07360	Complement component C8 gamma chain	7.00E-01	839000	761000	801000	773000	0.91	0.95	0.92
Q9Y4G6	Talin-2	7.00E-01	4250000	3840000	4050000	4060000	0.90	0.95	0.96
Q38SD2	Leucine-rich repeat serine/threonine-protein kinase 1	7.00E-01	4570000	4160000	4070000	3970000	0.91	0.89	0.87
Q15166	Serum paraoxonase/lactonase 3	7.00E-01	183000	193000	195000	206000	1.05	1.07	1.13
P04040	Catalase	7.00E-01	3170000	2950000	3060000	2930000	0.93	0.97	0.92
Q8IYB4	PEX5-related protein	7.00E-01	1320000	1320000	1430000	1480000	1.00	1.08	1.12
O75636	Ficolin-3	7.10E-01	382000	326000	340000	349000	0.85	0.89	0.91
Q92954	Proteoglycan 4	7.10E-01	5420000	5080000	5220000	4960000	0.94	0.96	0.92
Q92817	Envoplakin	7.10E-01	7280000	7300000	7250000	6900000	1.00	1.00	0.95
Q00610	Clathrin heavy chain 1	7.10E-01	4530000	4430000	4290000	4180000	0.98	0.95	0.92
P02751	Fibronectin	7.20E-01	515000	474000	495000	474000	0.92	0.96	0.92
P04264	Keratin, type II cytoskeletal 1	7.20E-01	524000	489000	493000	443000	0.93	0.94	0.85
P36980	Complement factor H-related protein 2	7.20E-01	1100000	974000	1010000	1020000	0.89	0.92	0.93
O60524	Nuclear export mediator factor NEMF	7.20E-01	2420000	2090000	2350000	2390000	0.86	0.97	0.99
P57103	Sodium/calcium exchanger 3	7.20E-01	793000	737000	685000	716000	0.93	0.86	0.90
P20366	Protachykinin-1	7.20E-01	61900	52700	56300	55600	0.85	0.91	0.90
P09172	Dopamine beta-hydroxylase	7.30E-01	318000	290000	291000	313000	0.91	0.92	0.98
P04259	Keratin, type II cytoskeletal 6B	7.30E-01	1250000	1310000	1210000	1270000	1.05	0.97	1.02
P08709	Coagulation factor VII	7.30E-01	423000	405000	367000	366000	0.96	0.87	0.87
Q6ZN30	Zinc finger protein basonuclin-2	7.30E-01	1460000	1320000	1390000	1310000	0.90	0.95	0.90
Q6P9F7	Leucine-rich repeat-containing protein 8B	7.30E-01	307000	302000	293000	286000	0.98	0.95	0.93
P27487	Dipeptidyl peptidase 4	7.30E-01	1180000	1080000	1100000	1150000	0.92	0.93	0.97
Q9Y5Z7	Host cell factor 2	7.40E-01	993000	1020000	1100000	1010000	1.03	1.11	1.02
P20929	Nebulin	7.50E-01	31900000	30500000	30700000	29700000	0.96	0.96	0.93
P02656	Apolipoprotein C-III	7.50E-01	1070000	989000	954000	1120000	0.92	0.89	1.05
P0DJI9	Serum amyloid A-2 protein	7.50E-01	43400	40700	39700	45200	0.94	0.91	1.04
Q9Y6K5	2'-5'-oligoadenylate synthase 3	7.50E-01	511000	508000	521000	549000	0.99	1.02	1.07
Q7Z3Y7	Keratin, type I cytoskeletal 28	7.50E-01	2070000	2000000	1990000	1910000	0.97	0.96	0.92
Q9UHC7	E3 ubiquitin-protein ligase makorin-1	7.50E-01	526000	475000	539000	509000	0.90	1.02	0.97
Q92769	Histone deacetylase 2	7.50E-01	2200000	2020000	1930000	1890000	0.92	0.88	0.86
P09871	Complement C1s subcomponent	7.60E-01	2950000	2690000	2880000	2820000	0.91	0.98	0.96
P26927	Hepatocyte growth factor-like protein	7.60E-01	924000	842000	851000	827000	0.91	0.92	0.90
P15169	Carboxypeptidase N catalytic chain	7.60E-01	2140000	1790000	1980000	1980000	0.84	0.93	0.93
Q92820	Gamma-glutamyl hydrolase	7.60E-01	1240000	1260000	1310000	1200000	1.02	1.06	0.97
Q14515	SPARC-like protein 1	7.60E-01	787000	881000	783000	772000	1.12	0.99	0.98
Q9UNP4	Lactosylceramide alpha-2,3-sialyltransferase	7.60E-01	11000	9538.5	9976.91	10000	0.87	0.91	0.91
P68032	Actin, alpha cardiac muscle 1	7.70E-01	534000	493000	485000	564000	0.92	0.91	1.06
Q8NDH2	Coiled-coil domain-containing protein 168	7.70E-01	10600000	10300000	10100000	9960000	0.97	0.95	0.94

A8MT79	Putative zinc-alpha-2-glycoprotein-like 1	7.70E-01	701000	636000	680000	661000	0.91	0.97	0.94
P08107	Heat shock 70 kDa protein 1A/1B	7.70E-01	1720000	1780000	1910000	1750000	1.03	1.11	1.02
O15014	Zinc finger protein 609	7.70E-01	1400000	1370000	1340000	1310000	0.98	0.96	0.94
P19823	Inter-alpha-trypsin inhibitor heavy chain H2	7.80E-01	16800000	15200000	16300000	15600000	0.90	0.97	0.93
Q9NZP8	Complement C1r subcomponent-like protein	7.80E-01	180000	157000	171000	158000	0.87	0.95	0.88
O14791	Apolipoprotein L1	7.80E-01	258000	247000	245000	247000	0.96	0.95	0.96
Q9Y2I6	Ninein-like protein	7.80E-01	1270000	1200000	1280000	1260000	0.94	1.01	0.99
Q9H330	Transmembrane protein 245	7.80E-01	620000	622000	603000	574000	1.00	0.97	0.93
P26599	Polypyrimidine tract-binding protein 1	7.80E-01	491000	468000	471000	451000	0.95	0.96	0.92
P01008	Antithrombin-III	7.90E-01	13200000	12300000	12600000	12300000	0.93	0.95	0.93
Q12805	EGF-containing fibulin-like extracellular matrix protein 1	7.90E-01	218000	218000	235000	221000	1.00	1.08	1.01
Q2TV78	Putative macrophage stimulating 1-like protein	7.90E-01	211000	202000	197000	189000	0.96	0.93	0.90
P31146	Coronin-1A	7.90E-01	1090000	970000	1070000	1110000	0.89	0.98	1.02
P05019	Insulin-like growth factor II	7.90E-01	468000	438000	444000	436000	0.94	0.95	0.93
Q9BYJ9	YTH domain family protein 1	7.90E-01	2020000	1870000	1860000	1830000	0.93	0.92	0.91
P0C0L5	Complement C4-B	8.00E-01	27100000	26600000	25500000	24600000	0.98	0.94	0.91
P02760	Protein AMBP	8.00E-01	3700000	3410000	3550000	3460000	0.92	0.96	0.94
P04004	Vitronectin	8.00E-01	8040000	7730000	7800000	7540000	0.96	0.97	0.94
P01766	Ig heavy chain V-III region BRO;	8.00E-01	367000	393000	392000	368000	1.07	1.07	1.00
Q8IZF3	Probable G-protein coupled receptor 115	8.00E-01	1010000	987000	939000	941000	0.98	0.93	0.93
P22314	Ubiquitin-like modifier-activating enzyme 1	8.00E-01	550000	569000	542000	526000	1.03	0.99	0.96
P0C0L4	Complement C4-A	8.10E-01	26700000	26200000	25200000	24300000	0.98	0.94	0.91
P04003	C4b-binding protein alpha chain	8.10E-01	459000	403000	387000	465000	0.88	0.84	1.01
Q9BXR6	Complement factor H-related protein 5	8.10E-01	956000	958000	932000	877000	1.00	0.97	0.92
P01871	Ig mu chain C region	8.10E-01	425000	353000	385000	399000	0.83	0.91	0.94
Q8NI35	InaD-like protein	8.10E-01	2920000	2880000	2920000	3090000	0.99	1.00	1.06
Q01518	Adenylyl cyclase-associated protein 1	8.10E-01	1520000	1570000	1510000	1450000	1.03	0.99	0.95
P49746	Thrombospondin-3	8.10E-01	2020000	2050000	2110000	2010000	1.01	1.04	1.00
P02671	Fibrinogen alpha chain	8.20E-01	2850000	2830000	2950000	3010000	0.99	1.04	1.06
P27169	Serum paraoxonase/arylesterase 1	8.20E-01	1130000	1230000	1250000	1270000	1.09	1.11	1.12
P61769	Beta-2-microglobulin	8.20E-01	102000	97500	107000	103000	0.96	1.05	1.01
O60287	Nucleolar pre-ribosomal-associated protein 1	8.20E-01	415000	425000	443000	436000	1.02	1.07	1.05
P62937	Peptidyl-prolyl cis-trans isomerase A	8.20E-01	158000	148000	166000	164000	0.94	1.05	1.04
Q70Z53	Protein FRA10AC1	8.20E-01	98300	80000	93300	97100	0.81	0.95	0.99
Q562R1	Beta-actin-like protein 2	8.30E-01	277000	256000	255000	303000	0.92	0.92	1.09
Q03164	Histone-lysine N-methyltransferase 2A	8.30E-01	4130000	3960000	3950000	3940000	0.96	0.96	0.95
P14151	L-selectin	8.30E-01	193000	181000	168000	174000	0.94	0.87	0.90
Q9BYU1	Pre-B-cell leukemia transcription factor 4	8.30E-01	4450000	4280000	4140000	4020000	0.96	0.93	0.90
B5MCN3	Putative SEC14-like protein 6	8.30E-01	1960000	1810000	1840000	1890000	0.92	0.94	0.96
Q99542	Matrix metalloproteinase-19	8.30E-01	683000	626000	665000	657000	0.92	0.97	0.96
Q9HC29	Nucleotide-binding oligomerization domain-containing protein 2	8.30E-01	1360000	1480000	1410000	1470000	1.09	1.04	1.08
O43692	Peptidase inhibitor 15	8.30E-01	48100	41800	45000	48200	0.87	0.94	1.00
Q5SYB0	FERM and PDZ domain-containing protein 1	8.40E-01	1170000	1220000	1150000	1150000	1.04	0.98	0.98
P0C091	FRAS1-related extracellular matrix protein 3	8.40E-01	4320000	4320000	4380000	4060000	1.00	1.01	0.94
P17014	Zinc finger protein 12	8.40E-01	348000	382000	382000	391000	1.10	1.10	1.12
Q6DD88	Atlastin-3	8.40E-01	1020000	954000	945000	964000	0.94	0.93	0.95
A5YKK6	CCR4-NOT transcription complex subunit 1	8.50E-01	7660000	7940000	8050000	8170000	1.04	1.05	1.07
Q8WXW3	Progesterone-induced-blocking factor 1	8.50E-01	2020000	1910000	2010000	1960000	0.95	1.00	0.97
Q92905	COP9 signalosome complex subunit 5	8.50E-01	972000	967000	962000	901000	0.99	0.99	0.93
Q9H4L7	SWI/SNF-related matrix-associated actin-dependent regulator of c	8.50E-01	1360000	1300000	1310000	1350000	0.96	0.96	0.99
O94760	N(G),N(G)-dimethylarginine dimethylaminohydrolase 1	8.50E-01	4860000	4630000	4550000	4450000	0.95	0.94	0.92
Q9Y5K1	Meiotic recombination protein SPO11	8.50E-01	5150000	4890000	5180000	4950000	0.95	1.01	0.96
P29622	Kallistatin	8.60E-01	749000	701000	712000	700000	0.94	0.95	0.93
P18428	Lipopolysaccharide-binding protein	8.60E-01	132000	111000	121000	125000	0.84	0.92	0.95
O43866	CD5 antigen-like	8.60E-01	1980000	2110000	2010000	1850000	1.07	1.02	0.93
P04406	Glyceraldehyde-3-phosphate dehydrogenase	8.60E-01	52600	48500	49200	55400	0.92	0.94	1.05
Q9UL68	Myelin transcription factor 1-like protein	8.60E-01	6400000	6490000	6640000	6630000	1.01	1.04	1.04
O95445	Apolipoprotein M	8.60E-01	147000	137000	143000	155000	0.93	0.97	1.05
P35900	Keratin, type I cytoskeletal 20	8.60E-01	609000	600000	588000	599000	0.99	0.97	0.98
Q6ZNJ1	Neurobeachin-like protein 2	8.60E-01	1730000	1650000	1660000	1640000	0.95	0.96	0.95
A8MW99	Meiosis-specific protein MEI4-like	8.60E-01	2730000	2660000	2630000	2530000	0.97	0.96	0.93
P00748	Coagulation factor XII	8.70E-01	1900000	1670000	1760000	1710000	0.88	0.93	0.90
P04278	Sex hormone-binding globulin	8.70E-01	323000	349000	342000	321000	1.08	1.06	0.99
Q5VST9	Obscurin	8.70E-01	9920000	9270000	9500000	9450000	0.93	0.96	0.95
O75369	Filamin-B	8.70E-01	2370000	2220000	2380000	2190000	0.94	1.00	0.92
Q96BY6	Dedicator of cytokinesis protein 10	8.70E-01	2960000	3050000	2980000	2860000	1.03	1.01	0.97
P35542	Serum amyloid A-4 protein	8.70E-01	223000	231000	235000	245000	1.04	1.05	1.10
O43290	U4/U6.U5 tri-snRNP-associated protein 1	8.70E-01	608000	555000	571000	549000	0.91	0.94	0.90
P01614	Ig kappa chain V-II region Cum	8.70E-01	143000	157000	143000	128000	1.10	1.00	0.90
Q8WZA6	Olfactory receptor 1E3	8.70E-01	102000	110000	110000	101000	1.08	1.08	0.99
P01031	Complement C5	8.80E-01	7320000	7140000	7210000	7100000	0.98	0.98	0.97
P00734	Prothrombin	8.80E-01	11500000	11000000	11200000	10900000	0.96	0.97	0.95
P01042	Kininogen-1	8.80E-01	9600000	9170000	9460000	9390000	0.96	0.99	0.98
P36955	Pigment epithelium-derived factor	8.80E-01	1210000	1160000	1200000	1180000	0.96	0.99	0.98
P63261	Actin, cytoplasmic 2	8.80E-01	1590000	1480000	1470000	1580000	0.93	0.92	0.99
Q8NCM2	Potassium voltage-gated channel subfamily H member 5	8.80E-01	939000	959000	918000	911000	1.02	0.98	0.97
P35443	Thrombospondin-4	8.80E-01	2020000	1990000	2000000	2150000	0.99	0.99	1.06
Q9H892	Tetratricopeptide repeat protein 12	8.80E-01	1940000	1850000	1880000	1860000	0.95	0.97	0.96
P13671	Complement component C6	8.90E-01	3050000	2800000	2980000	2880000	0.92	0.98	0.94
P33151	Cadherin-5	8.90E-01	655000	653000	662000	630000	1.00	1.01	0.96
P04083	Annexin A1	8.90E-01	1610000	1550000	1600000	1570000	0.96	0.99	0.98
Q9BY43	Charged multivesicular body protein 4a	8.90E-01	294000	263000	283000	286000	0.89	0.96	0.97

Q99784	Noelin	8.90E-01	781000	711000	722000	694000	0.91	0.92	0.89
Q08380	Galectin-3-binding protein	8.90E-01	290000	243000	261000	250000	0.84	0.90	0.86
Q9NSB4	Keratin, type II cuticular Hb2	8.90E-01	54500	57100	51400	53300	1.05	0.94	0.98
Q7Z3D4	LysM and putative peptidoglycan-binding domain-containing prote	8.90E-01	622000	619000	638000	645000	1.00	1.03	1.04
P00740	Coagulation factor IX	9.00E-01	414000	440000	450000	434000	1.06	1.09	1.05
P02655	Apolipoprotein C-II	9.00E-01	505000	401000	388000	456000	0.79	0.77	0.90
Q15582	Transforming growth factor-beta-induced protein ig-h3	9.00E-01	847000	809000	798000	762000	0.96	0.94	0.90
P01344	Insulin-like growth factor II	9.00E-01	65000	66000	62800	60800	1.02	0.97	0.94
Q6PKG0	La-related protein 1	9.00E-01	1410000	1470000	1410000	1520000	1.04	1.00	1.08
Q16832	Discoidin domain-containing receptor 2	9.00E-01	1530000	1400000	1450000	1440000	0.92	0.95	0.94
Q9H221	ATP-binding cassette sub-family G member 8	9.00E-01	498000	505000	465000	485000	1.01	0.93	0.97
O75197	Low-density lipoprotein receptor-related protein 5	9.00E-01	389000	358000	375000	360000	0.92	0.96	0.93
A5A3E0	POTE ankyrin domain family member F	9.10E-01	2950000	2920000	3100000	3020000	0.99	1.05	1.02
Q6ZR08	Dynein heavy chain 12, axonemal	9.10E-01	5880000	5790000	5950000	5600000	0.98	1.01	0.95
P11226	Mannose-binding protein C	9.10E-01	531000	460000	500000	521000	0.87	0.94	0.98
P00451	Coagulation factor VIII	9.10E-01	6210000	6090000	6150000	6000000	0.98	0.99	0.97
Q9H6S0	Probable ATP-dependent RNA helicase YTHDC2	9.10E-01	3150000	3090000	3250000	3070000	0.98	1.03	0.97
P07205	Phosphoglycerate kinase 2	9.10E-01	1230000	1280000	1260000	1210000	1.04	1.02	0.98
P19013	Keratin, type II cytoskeletal 4	9.10E-01	1590000	1520000	1540000	1590000	0.96	0.97	1.00
Q9P2D3	HEAT repeat-containing protein 5B	9.10E-01	6490000	6170000	6450000	6280000	0.95	0.99	0.97
Q13586	Stromal interaction molecule 1	9.10E-01	1680000	1580000	1750000	1760000	0.94	1.04	1.05
O75674	TOM1-like protein 1	9.10E-01	527000	500000	526000	509000	0.95	1.00	0.97
A8MPT4	Glutathione S-transferase theta-4	9.10E-01	980000	958000	966000	941000	0.98	0.99	0.96
Q9H4A6	Golgi phosphoprotein 3	9.10E-01	401000	386000	404000	414000	0.96	1.01	1.03
P21333	Filamin-A	9.20E-01	5850000	5740000	5820000	5680000	0.98	0.99	0.97
P08571	Monocyte differentiation antigen CD14	9.20E-01	232000	247000	228000	234000	1.06	0.98	1.01
P78386	Keratin, type II cuticular Hb5	9.20E-01	1010000	901000	1000000	989000	0.89	0.99	0.98
O95497	Pantetheinase	9.20E-01	376000	390000	387000	366000	1.04	1.03	0.97
P04075	Fructose-bisphosphate aldolase A	9.20E-01	341000	318000	316000	318000	0.93	0.93	0.93
P09486	SPARC	9.20E-01	237000	234000	232000	243000	0.99	0.98	1.03
Q96A37	RING finger protein 166	9.20E-01	1040000	1040000	1010000	1010000	1.00	0.97	0.97
P08603	Complement factor H	9.30E-01	16200000	15500000	15600000	15700000	0.96	0.96	0.97
P07225	Vitamin K-dependent protein S	9.30E-01	981000	956000	945000	963000	0.97	0.96	0.98
P80108	Phosphatidylinositol-glycan-specific phospholipase D	9.30E-01	448000	490000	484000	463000	1.09	1.08	1.03
P02743	Serum amyloid P-component	9.30E-01	2920000	2780000	2780000	2780000	0.95	0.95	0.95
Q9Y6R7	IgGFc-binding protein	9.30E-01	1390000	1500000	1520000	1490000	1.08	1.09	1.07
Q02325	Plasminogen-like protein B	9.30E-01	482000	505000	513000	525000	1.05	1.06	1.09
P22891	Vitamin K-dependent protein Z	9.30E-01	39900	41300	40600	37300	1.04	1.02	0.93
P08727	Keratin, type I cytoskeletal 19	9.30E-01	689000	657000	679000	669000	0.95	0.99	0.97
Q9UIF8	Bromodomain adjacent to zinc finger domain protein 2B	9.30E-01	2600000	2740000	2730000	2690000	1.05	1.05	1.03
O00151	PDZ and LIM domain protein 1	9.30E-01	327000	348000	352000	330000	1.06	1.08	1.01
P22692	Insulin-like growth factor-binding protein 4	9.30E-01	13600	14400	13300	13700	1.06	0.98	1.01
P06276	Cholinesterase; EC=3.1.1.8	9.40E-01	2370000	2370000	2420000	2270000	1.00	1.02	0.96
P13796	Plastin-2	9.40E-01	571000	534000	534000	544000	0.94	0.94	0.95
P51587	Breast cancer type 2 susceptibility protein	9.40E-01	9920000	9690000	9850000	9530000	0.98	0.99	0.96
O00187	Mannan-binding lectin serine protease 2	9.40E-01	1380000	1300000	1380000	1330000	0.94	1.00	0.96
Q9P281	BAH and coiled-coil domain-containing protein 1	9.40E-01	5340000	5360000	5210000	5090000	1.00	0.98	0.95
Q6UXB8	Peptidase inhibitor 16	9.40E-01	265000	281000	268000	267000	1.06	1.01	1.01
P20851	C4b-binding protein beta chain	9.40E-01	67800	68100	69900	72700	1.00	1.03	1.07
P00918	Carbonic anhydrase 2	9.40E-01	854000	820000	806000	822000	0.96	0.94	0.96
Q9Y281	Cofilin-2	9.40E-01	652000	601000	584000	605000	0.92	0.90	0.93
P60174	Triosephosphate isomerase	9.40E-01	218000	205000	209000	210000	0.94	0.96	0.96
P22102	Trifunctional purine biosynthetic protein adenosine-3	9.40E-01	1160000	1160000	1100000	1100000	1.00	0.95	0.95
Q13330	Metastasis-associated protein MTA1;	9.40E-01	830000	878000	887000	857000	1.06	1.07	1.03
Q12799	T-complex protein 10A homolog;	9.40E-01	1660000	1720000	1740000	1650000	1.04	1.05	0.99
Q147U7	Single-pass membrane and coiled-coil domain-containing protein	9.40E-01	2480000	2250000	2320000	2180000	0.91	0.94	0.88
Q9NPY3	Complement component C1q receptor	9.40E-01	23600	24700	23000	24800	1.05	0.97	1.05
P19827	Inter-alpha-trypsin inhibitor heavy chain H1	9.50E-01	13500000	13200000	13100000	13000000	0.98	0.97	0.96
P03952	Plasma kallikrein; EC=3.4.21.34	9.50E-01	2220000	2110000	2140000	2130000	0.95	0.96	0.96
P07357	Complement component C8 alpha chain	9.50E-01	1850000	1820000	1910000	1860000	0.98	1.03	1.01
P18206	Vinculin	9.50E-01	9420000	9520000	9710000	9730000	1.01	1.03	1.03
Q7Z794	Keratin, type II cytoskeletal 1b	9.50E-01	1530000	1580000	1530000	1500000	1.03	1.00	0.98
O95678	Keratin, type II cytoskeletal 75	9.50E-01	1030000	1030000	1000000	1010000	1.00	0.97	0.98
O75366	Advillin	9.50E-01	640000	590000	556000	588000	0.92	0.87	0.92
Q6NW34	Uncharacterized protein C3orf17	9.50E-01	627000	672000	610000	598000	1.07	0.97	0.95
P02749	Beta-2-glycoprotein 1	9.60E-01	13400000	12700000	12600000	12300000	0.95	0.94	0.92
P10909	Clusterin	9.60E-01	5140000	5220000	5300000	5270000	1.02	1.03	1.03
P06681	Complement C2	9.60E-01	1840000	1790000	1780000	1730000	0.97	0.97	0.94
P0CG38	POTE ankyrin domain family member I	9.60E-01	2960000	2830000	2890000	2870000	0.96	0.98	0.97
Q86UX7	Fermitin family homolog 3	9.60E-01	79600	72300	77700	81400	0.91	0.98	1.02
A4D1E1	Zinc finger protein 804B	9.60E-01	2290000	2300000	2330000	2180000	1.00	1.02	0.95
P35442	Thrombospondin-2	9.60E-01	921000	908000	918000	875000	0.99	1.00	0.95
Q5T1M5	FK506-binding protein 15	9.60E-01	1750000	1710000	1720000	1780000	0.98	0.98	1.02
P01597	Ig kappa chain V-I region DEE	9.60E-01	35900	35100	35800	33200	0.98	1.00	0.92
Q6EMK4	Vasorin	9.60E-01	9240.63	8718.72	9390.51	9654.85	0.94	1.02	1.04
P12955	Xaa-Pro dipeptidase	9.60E-01	240000	217000	222000	225000	0.90	0.93	0.94
P61160	Actin-related protein 2	9.60E-01	311000	300000	302000	315000	0.96	0.97	1.01
P30043	Flavin reductase (NADPH)	9.60E-01	46600	48000	45500	48100	1.03	0.98	1.03
Q9BTU6	Phosphatidylinositol 4-kinase type 2-alpha	9.60E-01	116000	109000	115000	117000	0.94	0.99	1.01
P03950	Angiogenin	9.60E-01	8368.09	7940.01	7868.98	7822.79	0.95	0.94	0.93
Q8NBT3	Transmembrane protein 145	9.60E-01	38700	38100	37700	37200	0.98	0.97	0.96
P05546	Heparin cofactor 2	9.70E-01	1960000	1890000	1890000	1910000	0.96	0.96	0.97
P25311	Zinc-alpha-2-glycoprotein-	9.70E-01	4150000	4050000	4130000	3960000	``	1.00	0.95

Q96PD5	N-acetylmuramoyl-L-alanine amidase	9.70E-01	1540000	1540000	1520000	1480000	1.00	0.99	0.96
P05155	Plasma protease C1 inhibitor	9.70E-01	2130000	2020000	2020000	2100000	0.95	0.95	0.99
P05452	Tetranectin	9.70E-01	789000	780000	788000	815000	0.99	1.00	1.03
Q16610	Extracellular matrix protein 1	9.70E-01	950000	921000	925000	913000	0.97	0.97	0.96
Q96KN2	Beta-Ala-His dipeptidase	9.70E-01	638000	610000	614000	616000	0.96	0.96	0.97
P02747	Complement C1q subcomponent subunit C	9.70E-01	1260000	1200000	1240000	1230000	0.95	0.98	0.98
P67936	Tropomyosin alpha-4 chain	9.70E-01	398000	383000	385000	383000	0.96	0.97	0.96
Q9UBT6	DNA polymerase kappa	9.70E-01	2330000	2320000	2300000	2370000	1.00	0.99	1.02
P32119	Peroxiredoxin-2	9.70E-01	35600	34300	32900	34200	0.96	0.92	0.96
Q13496	Myotubularin	9.70E-01	1190000	1150000	1200000	1150000	0.97	1.01	0.97
Q8WZ75	Roundabout homolog 4	9.70E-01	1050000	1080000	1110000	1030000	1.03	1.06	0.98
Q5VZB9	Doublesex- and mab-3-related transcription factor A1	9.70E-01	71500	68500	67700	67600	0.96	0.95	0.95
Q9BV40	Vesicle-associated membrane protein 8	9.70E-01	511000	464000	474000	456000	0.91	0.93	0.89
P00747	Plasminogen	9.80E-01	14500000	13900000	14200000	14000000	0.96	0.98	0.97
P02774	Vitamin D-binding protein	9.80E-01	23700000	22900000	23800000	23200000	0.97	1.00	0.98
P02675	Fibrinogen beta chain	9.80E-01	3070000	2980000	2980000	2870000	0.97	0.97	0.93
P01023	Alpha-2-macroglobulin	9.80E-01	935000	917000	917000	875000	0.98	0.98	0.94
Q6S8J3	POTE ankyrin domain family member E	9.80E-01	2880000	2800000	2870000	2890000	0.97	1.00	1.00
Q9UGM5	Fetuin-B	9.80E-01	393000	382000	386000	392000	0.97	0.98	1.00
P04070	Vitamin K-dependent protein C	9.80E-01	630000	647000	652000	625000	1.03	1.03	0.99
P49908	Selenoprotein P	9.80E-01	271000	268000	266000	264000	0.99	0.98	0.97
P49747	Cartilage oligomeric matrix protein	9.80E-01	295000	284000	293000	278000	0.96	0.99	0.94
P22105	Tenascin-X	9.80E-01	1770000	1740000	1780000	1750000	0.98	1.01	0.99
P02533	Keratin, type I cytoskeletal 14	9.80E-01	509000	506000	487000	503000	0.99	0.96	0.99
P13646	Keratin, type I cytoskeletal 13	9.80E-01	458000	441000	450000	457000	0.96	0.98	1.00
Q9NPH3	Interleukin-1 receptor accessory protein	9.80E-01	1200000	1170000	1160000	1170000	0.98	0.97	0.98
Q8TF30	WASP homolog-associated protein with actin, membranes and mic	9.80E-01	2070000	2130000	2110000	2060000	1.03	1.02	1.00
Q15113	Procollagen C-endopeptidase enhancer 1	9.80E-01	96800	92300	94100	96800	0.95	0.97	1.00
P33981	Dual specificity protein kinase TTK	9.80E-01	1860000	1870000	1810000	1870000	1.01	0.97	1.01
Q9NZR1	Tropomodulin-2	9.80E-01	1750000	1680000	1730000	1660000	0.96	0.99	0.95
O75717	WD repeat and HMG-box DNA-binding protein 1	9.80E-01	6490000	6200000	6370000	6230000	0.96	0.98	0.96
P18887	DNA repair protein XRCC1	9.80E-01	787000	752000	776000	759000	0.96	0.99	0.96
P24593	Insulin-like growth factor-binding protein 5	9.80E-01	638000	618000	618000	611000	0.97	0.97	0.96
Q8NCN5	Pyruvate dehydrogenase phosphatase regulatory subunit, mitochc	9.80E-01	216000	218000	229000	190000	1.01	1.06	0.88
P30041	Peroxiredoxin-6 spot 12	9.80E-01	6671.64	6623.73	5851.12	6251.84	0.99	0.88	0.94
Q14624	Inter-alpha-trypsin inhibitor heavy chain H4	9.90E-01	11100000	10800000	10900000	10900000	0.97	0.98	0.98
P00751	Complement factor B	9.90E-01	18200000	17400000	17800000	17600000	0.96	0.98	0.97
P02748	Complement component C9	9.90E-01	2680000	2640000	2740000	2660000	0.99	1.02	0.99
P01024	Complement C3	9.90E-01	7180000	7130000	7240000	7070000	0.99	1.01	0.98
P07358	Complement component C8 beta chain	9.90E-01	1840000	1810000	1830000	1760000	0.98	0.99	0.96
P05156	Complement factor I	9.90E-01	2160000	2140000	2180000	2120000	0.99	1.01	0.98
P08697	Alpha-2-antiplasmin	9.90E-01	3470000	3400000	3440000	3450000	0.98	0.99	0.99
Q06033	Inter-alpha-trypsin inhibitor heavy chain H3	9.90E-01	4660000	4600000	4710000	4600000	0.99	1.01	0.99
P35858	Insulin-like growth factor-binding protein complex acid labile subu	9.90E-01	1110000	1080000	1090000	1070000	0.97	0.98	0.96
P20742	Pregnancy zone protein	9.90E-01	2600000	2540000	2520000	2480000	0.98	0.97	0.95
P22792	Carboxypeptidase N subunit 2	9.90E-01	1690000	1700000	1740000	1720000	1.01	1.03	1.02
P13645	Keratin, type I cytoskeletal 10	9.90E-01	1990000	2000000	1920000	2020000	1.01	0.96	1.02
P00488	Coagulation factor XIII A chain	9.90E-01	1340000	1350000	1290000	1310000	1.01	0.96	0.98
Q96IY4	Carboxypeptidase B2	9.90E-01	374000	373000	367000	377000	1.00	0.98	1.01
P43251	Biotinidase	9.90E-01	402000	401000	393000	389000	1.00	0.98	0.97
P02652	Apolipoprotein A-II	9.90E-01	315000	412000	433000	381000	1.31	1.37	1.21
P48740	Mannan-binding lectin serine protease 1	9.90E-01	1050000	1010000	1030000	1010000	0.96	0.98	0.96
P35527	Keratin, type I cytoskeletal 9	9.90E-01	1390000	1380000	1420000	1360000	0.99	1.02	0.98
P27918	Properdin	9.90E-01	238000	239000	245000	243000	1.00	1.03	1.02
P22352	Glutathione peroxidase 3	9.90E-01	174000	177000	176000	177000	1.02	1.01	1.02
P08519	Apolipoprotein(a)	9.90E-01	145000	144000	136000	143000	0.99	0.94	0.99
Q6KC79	Nipped-B-like protein	9.90E-01	3920000	3920000	3920000	3830000	1.00	1.00	0.98
P04275	von Willebrand factor	9.90E-01	2530000	2460000	2430000	2470000	0.97	0.96	0.98
O75912	Diacylglycerol kinase iota	9.90E-01	1050000	1040000	1060000	1050000	0.99	1.01	1.00
Q01546	Keratin, type II cytoskeletal 2 oral	9.90E-01	923000	911000	911000	933000	0.99	0.99	1.01
O14786	Neuropilin-1	9.90E-01	1360000	1300000	1320000	1310000	0.96	0.97	0.96
P05787	Keratin, type II cytoskeletal 8	9.90E-01	2100000	2190000	2120000	2120000	1.04	1.01	1.01
Q15233	Non-POU domain-containing octamer-binding protein	9.90E-01	1380000	1360000	1390000	1390000	0.99	1.01	1.01
Q5H8C1	FRAS1-related extracellular matrix protein 1	9.90E-01	2290000	2330000	2360000	2320000	1.02	1.03	1.01
P58107	Epiplakin	9.90E-01	3380000	3250000	3340000	3350000	0.96	0.99	0.99
Q9BWP8	Collectin-11	9.90E-01	868000	860000	888000	837000	0.99	1.02	0.96
Q7Z2Q7	Leucine-rich repeat-containing protein 70	9.90E-01	676000	677000	668000	650000	1.00	0.99	0.96
Q96I24	Far upstream element-binding protein 3	9.90E-01	1570000	1590000	1520000	1500000	1.01	0.97	0.96
O14917	Protocadherin-17	9.90E-01	2100000	1960000	2000000	1960000	0.93	0.95	0.93
P00450	Ceruloplasmin	1.00E+00	29400000	29400000	29100000	28000000	1.00	0.99	0.95
P06727	Apolipoprotein A-IV	1.00E+00	14100000	13400000	13600000	14000000	0.95	0.96	0.99
P43652	Afamin	1.00E+00	5210000	4830000	5120000	5100000	0.93	0.98	0.98
P10643	Complement component C7	1.00E+00	1400000	1360000	1390000	1380000	0.97	0.99	0.99
P01019	Angiotensinogen	1.00E+00	2180000	2190000	2170000	2070000	1.00	1.00	0.95
P04196	Histidine-rich glycoprotein	1.00E+00	1220000	1180000	1200000	1180000	0.97	0.98	0.97
P05543	Thyroxine-binding globulin	1.00E+00	745000	712000	729000	713000	0.96	0.98	0.96
P51884	Lumican	1.00E+00	2300000	2250000	2280000	2400000	0.98	0.99	1.04
P02750	Leucine-rich alpha-2-glycoprotein	1.00E+00	1060000	1070000	1120000	1060000	1.01	1.06	1.00
P08185	Corticosteroid-binding globulin	1.00E+00	852000	841000	872000	821000	0.99	1.02	0.96
Q14520	Hyaluronan-binding protein 2	1.00E+00	1010000	1000000	1010000	997000	0.99	1.00	0.99
P02741	C-reactive protein	1.00E+00	205000	202000	209000	205000	0.99	1.02	1.00
Q15848	Adiponectin	1.00E+00	65900	68200	64800	64900	1.03	0.98	0.98
P16070	CD44 antigen	1.00E+00	2540000	2510000	2530000	2490000	0.99	1.00	0.98
P06733	Alpha-enolase	1.00E+00	672000	659000	667000	654000	0.98	0.99	0.97
Q14999	Cullin-7	1.00E+00	881000	872000	864000	870000	0.99	0.98	0.99
Q9Y666	Solute carrier family 12 member 7	1.00E+00	1400000	1380000	1360000	1400000	0.99	0.97	1.00
P62158	Calmodulin	1.00E+00	185000	185000	185000	190000	1.00	1.00	1.03
Q86VB7	Scavenger receptor cysteine-rich type 1 protein M130	1.00E+00	2130000	2170000	2200000	2140000	1.02	1.03	1.00
P57789	Potassium channel subfamily K member 10	1.00E+00	793000	735000	726000	742000	0.93	0.92	0.94
O14717	tRNA (cytosine(38)-C(5))-methyltransferase	1.00E+00	729000	757000	729000	736000	1.04	1.00	1.01
O95721	Synaptosomal-associated protein 29	1.00E+00	371000	383000	395000	394000	1.03	1.06	1.06

Table S5.1 86 proteins significantly regulated between LD and deceased donors with fold change >2

Protein	P value	LD	DBD	DCD	DBD/LD	DCD/LD	LD/DBD	LD/DCD	function
ACT	1.32E-03	4.57E+05	1.43E+06	1.14E+06	3.13	2.49	0.32	0.40	cellular component biogenesis
AGEL	0.02	1.40E+05	7.80E+04	5.30E+04	0.56	0.38	1.79	2.64	
AhR	1.83E-03	4653.05	1419.91	543.9	0.31	0.12	3.28	8.55	Aryl hydrocarbon receptor
AHSG	2.91E-03	6844.51	4011.28	1161.68	0.59	0.17	1.71	5.89	
Alpha-2-AP	0.02	1810.56	1167.27	576.11	0.64	0.32	1.55	3.14	regulation of biological process
ANXA6	0.02	767.82	261.71	238.32	0.34	0.31	2.93	3.22	fatty acid metabolic process
ApoA-IV	0.01	5525.97	2709.09	1208.51	0.49	0.22	2.04	4.57	biosynthetic process
Apo-AIV	1.92E-03	2154.5	1322.15	366.62	0.61	0.17	1.63	5.88	cholesterol metabolic process
Apo-CII	1.25E-04	9175.69	1949.27	3363.62	0.21	0.37	4.71	2.73	fatty acid biosynthetic process
Apo-E	0.01	619.49	391.87	176.2	0.63	0.28	1.58	3.52	homeostatic process
Apo-M	0.02	5634.07	351.51	574.05	0.06	0.10	16.03	9.81	homeostatic process
ARHGAP32	0.03	6007.82	2.63E+04	2.60E+04	4.38	4.33	0.23	0.23	cell cycle
ARHGEF17	2.66E-04	1.47E+04	3522.29	2349.11	0.24	0.16	4.17	6.26	cell cycle
B2M	1.26E-03	1845.38	1.58E+04	3.70E+04	8.56	20.05	0.12	0.05	cellular defence
BCHE	1.09E-04	1485.83	422.39	330.02	0.28	0.22	3.52	4.50	cell signalling
BPA	7.31E-05	3.30E+04	8541.15	4411.47	0.26	0.13	3.86	7.48	cell signalling
C1QB	0.02	998.49	231.56	148.27	0.23	0.15	4.31	6.73	Complement, cellular processes
C3	9.92E-03	2.39E+04	5.14E+04	5.05E+04	2.15	2.11	0.46	0.47	complement activation
C4B	6.12E-04	1577.61	1.97E+04	2.90E+04	12.49	18.38	0.08	0.05	cellular process
C4-B	0.03	1162.14	4052.35	6657.77	3.49	5.73	0.29	0.17	complement activation
C4-B	5.06E-05	8107.67	5.73E+04	8.70E+04	7.07	10.73	0.14	0.09	complement activation
C5	0.02	746.7	483.7	310.85	0.65	0.42	1.54	2.40	cellular process
C5orf25	3.58E-03	875.04	225.43	233.21	0.26	0.27	3.88	3.75	complement
C9	2.11E-03	9.56E+04	2.11E+05	2.35E+05	2.21	2.46	0.45	0.41	Complement component C9
C9	0.02	24.28	272.73	111.24	11.23	4.58	0.09	0.22	Complement factor H
CFB	0.02	2.72E+04	7.59E+04	9.77E+04	2.79	3.59	0.36	0.28	Complement factor B
CFH	0.03	4375.65	9384.24	1.18E+04	2.14	2.70	0.47	0.37	Complement factor B
CLIP-115	0.01	1871.49	823.05	635.16	0.44	0.34	2.27	2.95	
CP	1.17E-03	1.55E+06	2.95E+06	3.51E+06	1.90	2.26	0.53	0.44	blood coagulation
CPU	0.02	2833.2	1635.01	1190.48	0.58	0.42	1.73	2.38	Carboxypeptidase B2
CRP	0.03	2.15E+05	3.38E+05	5.29E+05	1.57	2.46	0.64	0.41	inflammation
DMRT2	2.12E-04	567.66	81.02	21.32	0.14	0.04	7.01	26.63	immune system process
DMXL1	6.90E-03	1096.81	5080.15	7986.66	4.63	7.28	0.22	0.14	exocytosis
DOCK10	5.19E-04	2.93	456.7	1562.76	155.87	533.37	0.01	0.00	Dedicator of cytokinesis protein 10
DPPT-L	0.02	9283.15	5428.32	3807.3	0.58	0.41	1.71	2.44	cell cycle
FARP2	0.01	1.56E+04	6359.61	4752.96	0.41	0.30	2.45	3.28	
FASTKD5	8.47E-03	8022.87	5.41E+04	6.37E+04	6.74	7.94	0.15	0.13	cell cycle
FCN2	0.04	2724.17	3836.8	9550.96	1.41	3.51	0.71	0.29	cell surface receptor signaling pathway
FGA	0.02	9707.85	6.50E+04	6.25E+04	6.70	6.44	0.15	0.16	Fibrinogen alpha chain
FGD2	0.02	616.69	93.02	149.48	0.15	0.24	6.63	4.13	cellular component morphogenesis
FLNA	0.02	1629.98	898.86	2273.74	0.55	1.39	1.81	0.72	
FN	0.04	9.98E+04	1.27E+06	1.29E+06	12.73	12.93	0.08	0.08	blood coagulation
FN	4.52E-03	998.09	1.90E+04	1.46E+04	19.04	14.63	0.05	0.07	blood coagulation
FRYL	2.17E-03	415.78	2596.24	7326.94	6.24	17.62	0.16	0.06	
FXI	0.03	480.3	143.89	187.54	0.30	0.39	3.34	2.56	blood Coagulation factor XI
GSN	4.72E-03	3452.02	990.68	945.39	0.29	0.27	3.48	3.65	cellular component organization
HC-II	2.53E-05	1209.76	361.05	348.49	0.30	0.29	3.35	3.47	
HC-II	2.90E-03	1.13E+05	3.93E+04	3.51E+04	0.35	0.31	2.88	3.22	
HIST3H2A	3.00E-03	6213.34	174.5	1729.91	0.03	0.28	35.61	3.59	biosynthetic process
HSPG	7.48E-03	1.49E+04	7316.89	4407.05	0.49	0.30	2.04	3.38	Syndecan-2
ITI-HC3	7.46E-03	3.16E+04	7.29E+04	7.25E+04	2.31	2.29	0.43	0.44	proteolysis
ITI-HC4	1.30E-03	4.80E+05	8.67E+05	1.21E+06	1.81	2.52	0.55	0.40	proteolysis
KHSRP	0.01	7752.82	1.90E+04	3.92E+04	2.45	5.06	0.41	0.20	
KLKB1	5.40E-05	2.33E+04	7724.1	8369.56	0.33	0.36	3.02	2.78	blood coagulation
LBP	3.11E-04	1738.24	1.19E+04	1.67E+04	6.85	9.61	0.15	0.10	cholesterol metabolic process
LETM1	0.01	933.86	233.4	309.74	0.25	0.33	4.00	3.01	
LRG	4.41E-03	2.13E+04	9.15E+04	1.08E+05	4.30	5.07	0.23	0.20	cellular process
LRG	0.01	1.44E+05	6.29E+05	6.51E+05	4.37	4.52	0.23	0.22	cellular process
MACF1	0.04	1.11E+04	5803.75	1.28E+04	0.52	1.15	1.91	0.87	Microtubule-actin cross-linking factor 1
MSP	0.03	343.98	133.68	77.57	0.39	0.23	2.57	4.43	Transmembrane protease serine 13
ORF1	0.01	7.96E+06	3.11E+06	9.42E+05	0.39	0.12	2.56	8.45	complement activation
PBP	0.05	3610.4	752.53	1257.56	0.21	0.35	4.80	2.87	Platelet basic protein
PI-4	0.01	2.99E+04	1.21E+04	8679.07	0.40	0.29	2.47	3.45	Dedicator of cytokinesis protein 3
PKHD1L1	5.58E-03	6.73	1659.6	1022.72	246.60	151.96	0.00	0.01	Fibrocystin-L
PON 1	0.03	3995.09	8620.67	4.87E+04	2.16	12.19	0.46	0.08	Serum paraoxonase/arylesterase 1
PRDX2	0.02	5526.84	1849.15	839.02	0.33	0.15	2.99	6.59	antioxidant
PROS1	0.01	2539.78	798.4	858.08	0.31	0.34	3.18	2.96	
QSOX1	3.60E-04	6217.89	1412.31	1870.31	0.23	0.30	4.40	3.32	cell death inflammation
RAD23A	6.60E-04	3115.35	12.67	64.09	0.00	0.02	245.88	48.61	UV excision repair protein RAD23 homo
RA-GEF	0.02	3303.73	1625.02	1179.87	0.49	0.36	2.03	2.80	regulation of biological process
S100A9	0.01	496.93	3632.34	2058	7.31	4.14	0.14	0.24	inflammation cell death
SF3B1	7.23E-03	1902.07	664.23	1060.04	0.35	0.56	2.86	1.79	cell signalling
SMADIP1	2.97E-03	6391.86	2468.1	2516	0.39	0.39	2.59	2.54	transmembrane receptor protein tyrosi
SOS-1	8.14E-03	1.17E+04	2469.86	2647.21	0.21	0.23	4.74	4.42	Son of sevenless homolog 1
SPTBN4	0.01	5294.6	587.69	731.05	0.11	0.14	9.01	7.24	Spectrin beta chain, non-erythrocytic 4
TTN	1.54E-03	1.56E+04	4748.91	6869.15	0.30	0.44	3.28	2.27	inflammation
TTN	2.08E-03	2.29E+04	3.59E+04	1.25E+05	1.57	5.46	0.64	0.18	inflammation
TTR	0.02	3273.3	1218.04	817.35	0.37	0.25	2.69	4.00	cell death
TUBA1C	0.04	664.89	3138.57	3529.23	4.72	5.31	0.21	0.19	Tubulin alpha-1C chain
USP31	0.02	9612.09	1693.83	1756.1	0.18	0.18	5.67	5.47	Ubiquitin carboxyl-terminal hydrolase 3
VDB	0.01	5.61E+05	9.49E+05	1.19E+06	1.69	2.12	0.59	0.47	response to stress
WDR90	6.45E-03	1.98E+04	9928.8	7518.88	0.50	0.38	1.99	2.63	induction of apoptosis
YWHAG	0.01	1231.42	3881.54	2.27E+04	3.15	18.43	0.32	0.05	cellular component morphogenesis
Zn-alpha-2-(	6.12E-03	954.69	1579.01	372.01	1.65	0.39	0.60	2.57	cell signalling
tein MGC395	0.02	898.27	340.91	221.04	0.38	0.25	2.63	4.06	cell signalling

Table S5.2 Proteins up regulated in DBD (DGF vs IF) by at least 2 fold change in DGF when compared to IF p<=0.05

Protein	Description	Fold change DGF vs IF	Length (AA)	mw (Da)	Peptide S	% Coverage	Location	Type
P00326	Alcohol dehydrogenase 1C	DGF	375.00	39895.70	13.00	33.60	Cytoplasm	
P04083	Annexin A1;	DGF	346.00	38744.00	9.00	28.60	Plasma Membrane	other
P07355	Annexin A2; AltName:	DGF	339.00	38633.80	8.00	28.30	Plasma Membrane	other
O95445	Apolipoprotein M	DGF	188.00	21257.40	9.00	48.90	Plasma Membrane	transporter
P07738	Bisphosphoglycerate mutase	DGF	259.00	30022.50	12.00	52.90		
Q9NZT1	Calmodulin-like protein 5	DGF	146.00	15900.80	5.00	34.90		
P04040	Catalase	DGF	527.00	59808.80	19.00	38.70		
P11717	Cation-independent mannose-6-phosphate receptor	DGF	2491.00	274631.00	37.00	17.50	Plasma Membrane	transmembrane receptor
Q13740	CD166 antigen	DGF	583.00	65151.20	2.00	4.50		
P36222	Chitinase-3-like protein 1	DGF	383.00	42652.40	21.00	59.80	Extracellular Space	enzyme
P00742	Coagulation factor X	DGF	488.00	54768.60	24.00	48.40	Extracellular Space	peptidase
Q9NZP8	Complement C1r subcomponent-like protein	DGF	487.00	53536.40	18.00	38.00		
Q02985	Complement factor H-related protein 3	DGF	330.00	37352.80	9.00	25.20		
P31146	Coronin-1A	DGF	461.00	51065.80	9.00	25.20		
P99999	Cytochrome c	DGF	105.00	11759.10	2.00	18.10	Cytoplasm	transporter
P30046	D-dopachrome decarboxylase	DGF	118.00	12721.70	7.00	56.80		
Q86UX7	Fermitin family homolog 3	DGF	667.00	76013.10	8.00	14.50		
P23142	Fibulin-1	DGF	703.00	77288.40	22.00	40.30		
P06744	Glucose-6-phosphate isomerase	DGF	558.00	63197.30	12.00	29.60	Extracellular Space	enzyme
P12814	Histone H2B type 1-K; Short=H2B	DGF	892.00	103137.00	10.00	14.00		
Q14520	Hyaluronan-binding protein 2	DGF	560.00	62720.50	22.00	43.60		
O75874	Isocitrate dehydrogenase [NADP] cytoplasmic	DGF	414.00	46701.60	14.00	36.20		
Q9Y468	Lethal(3)malignant brain tumor-like protein 1	DGF	752.00	83956.50	11.00	21.80		
P30740	Leukocyte elastase inhibitor	DGF	379.00	42768.70	16.00	46.70		
P23141	Liver carboxylesterase 1	DGF	567.00	62571.20	18.00	36.00	Cytoplasm	enzyme
P61626	Lysozyme C	DGF	148.00	16544.30	9.00	56.80	Extracellular Space	enzyme
P26038	Moesin	DGF	577.00	67867.80	22.00	35.90	Plasma Membrane	other
Q96PD5	N-acetylmuramoyl-L-alanine amidase	DGF	576.00	62267.90	24.00	64.60		
P30086	Phosphatidylethanolamine-binding protein 1	DGF	187.00	21061.70	10.00	73.80	Cytoplasm	other
P05121	Plasminogen activator inhibitor 1	DGF	402.00	45103.10	6.00	19.20		
O14818	Proteasome subunit alpha type-7	DGF	248.00	27905.60	9.00	43.50	cytoplasm	peptidase
P31151	Protein S100-A7	DGF	101.00	11481.60	6.00	35.60		
P05452	Tetranectin	DGF	202.00	22558.30	15.00	62.40		
P10599	Thioredoxin	DGF	105.00	11747.80	2.00	19.00	Cytoplasm	enzyme
P37837	Transaldolase	DGF	337.00	37570.50	19.00	50.70	Cytoplasm	enzyme
P19320	Vascular cell adhesion protein 1	DGF	739.00	81350.30	16.00	26.40	Plasma Membrane	transmembrane receptor
P08670	Vimentin	DGF	466.00	53691.10	26.00	44.20	Cytoplasm	other
Q9Y5Y7	Lymphatic vessel endothelial hyaluronic acid receptor	96.1	322.00	35245.00	5.00	10.90	Plasma Membrane	transmembrane receptor
P06702	Protein S100-A9	35.1	114.00	13251.50	11.00	86.00	cytoplasm	other
P06732	Creatine kinase M-type	17.7	381.00	43127.90	17.00	48.30	cytoplasm	kinase
Q9ULZ3	Apoptosis-associated speck-like protein containing a (	17.2	195.00	21631.30	5.00	29.70	Cytoplasm	transcription regulator
P80511	Protein S100-A12	16.1	92.00	10568.50	3.00	31.50	Cytoplasm	other
P62491	Ras-related protein Rab-11A	15.9	216.00	24509.50	6.00	28.70	Cytoplasm	enzyme
P21695	Glycerol-3-phosphate dehydrogenase [NAD(+)], cytop	14.8	349.00	37597.30	8.00	24.90		
P13796	Plastin-2	14.6	627.00	70352.00	32.00	54.10	Cytoplasm	other
P68871	Hemoglobin subunit beta	13.0	147.00	16006.30	12.00	84.40	Cytoplasm	transporter
P23141	Protein S100-A8	13.0	93.00	10827.60	11.00	68.80		
P35579	Myosin-9	11.7	1960.00	226734.00	54.00	30.80	Cytoplasm	transporter
P30044	Peroxiredoxin 5 Mitochondria	9.7	690.00	83956.50	30.00	11.00		
P07996	Thrombospondin-1	9.5	1170.00	129498.00	53.00	48.00		
P20742	Pregnancy zone protein	8.2	1482.00	164012.00	57.00	49.90	Extracellular Space	other
O14950	Myosin regulatory light chain 12B	7.5	172.00	19799.50	5.00	28.70	Cytoplasm	other
P00558	Phosphoglycerate kinase 1	6.7	417.00	44658.20	9.00	25.40	Cytoplasm	kinase
P18669	Phosphoglycerate mutase 1	5.8	254.00	28821.90	14.00	70.10		
P55290	Cadherin-13	5.7	713.00	78364.00	7.00	12.20	Plasma Membrane	other
Q9H4G4	Golgi-associated plant pathogenesis-related protein 1	5.5	154.00	17225.50	3.00	27.90	Cytoplasm	other
P00918	Carbonic anhydrase 2	5.3	260.00	29263.90	15.00	62.30		
P62937	Peptidyl-prolyl cis-trans isomerase A	5.1	165.00	18018.90	11.00	58.20	Cytoplasm	enzyme
P16152	Carbonyl reductase [NADPH] 1	5.1	277.00	30391.90	8.00	41.20	Cytoplasm	enzyme
P29508	Serpin B3	4.6	390.00	44590.60	8.00	18.20	Cytoplasm	other
P05062	Fructose-bisphosphate aldolase B	4.5	364.00	39502.10	23.00	48.60		
P21333	Filamin-A	4.5	2647.00	281032.00	46.00	24.40		
P07737	Profilin-1	4.4	140.00	15062.60	11.00	73.60	Cytoplasm	other
Q00796	Sorbitol dehydrogenase	4.4	357.00	38353.80	10.00	37.00		

Protein	Description	Fold change	Length (AA)	mw (Da)	Peptide S	% Coverage	Location	Type
P23528	Cofilin-1	**4.3**	166.00	18508.70	13.00	78.90	Nucleus	other
P63104	14-3-3 protein zeta/delta	**4.2**	245.00	27763.70	18.00	64.10		kinase
P63241	Eukaryotic translation initiation factor 5A-1	**4.1**	154.00	16839.40	4.00	23.40	Cytoplasm	translation regulator
P08833	Insulin-like growth factor-binding protein 1	**4.0**	259.00	27921.30	9.00	28.60	Extracellular Space	other
P40925	Malate dehydrogenase, cytoplasmic	**3.9**	334.00	36457.10	12.00	41.90		
P32119	Peroxiredoxin-2	**3.9**	198.00	21896.20	18.00	77.80	Cytoplasm	enzyme
P62805	Histone H4	**3.9**	103.00	11378.40	5.00	50.50		
P22392	Nucleoside diphosphate kinase B	**3.8**		17305.00	7.00	49.30	Nucleus	kinase
P26447	Protein S100-A4	**3.6**	101.00	11738.70	8.00	48.50		
P10412	Histone H1.4	**3.5**	219.00	21387.80	5.00	19.70	Nucleus	other
P09467	Fructose-1,6-bisphosphatase 1	**3.5**	338.00	36872.80	10.00	37.60		
P07451	Carbonic anhydrase 3	**3.5**	260.00	29574.70	10.00	46.90	Cytoplasm	enzyme
P08319	Alcohol dehydrogenase 4	**3.4**	380.00	40249.70	7.00	20.30		
P36871	Phosphoglucomutase-1	**3.3**	562.00	61500.60	8.00	14.40	Cytoplasm	enzyme
Q14019	Coactosin-like protein	**3.3**	142.00	15953.00	8.00	34.50	Cytoplasm	other
P00491	Purine nucleoside phosphorylase	**3.2**	289.00	32133.20	14.00	63.70	Nucleus	enzyme
P02652	Apolipoprotein A-II	**3.1**	100.00	11167.90	9.00	69.00	Extracellular Space	transporter
P09651	Heterogeneous nuclear ribonucleoprotein A1	**3.1**	372.00	38777.10	6.00	16.40	Nucleus	other
P00734	Prothrombin	**3.1**	622.00	70100.20	43.00	61.60	Extracellular Space	peptidase
Q06830	Peroxiredoxin-1	**3.0**	199.00	22114.30	12.00	55.30		
P37802	Transgelin-2	**3.0**	199.00	22395.20	10.00	47.70	Cytoplasm	other
P09211	Glutathione S-transferase	**3.0**	210.00	23377.00	10.00	66.20	Cytoplasm	enzyme
P03952	Plasma kallikrein	**3.0**	638.00	71430.90	37.00	57.10	Extracellular Space	peptidase
P51884	Lumican	**3.0**	338.00	38458.80	16.00	41.40	Extracellular Space	other
Q9Y490	Talin-1	**2.9**	2541.00	270049.00	49.00	25.30	Cytoplasm	
P09382	Galectin-1 LGALS1	**2.9**	135.00	14724.20	4.00	28.10	Extracellular Space	other
P80188	Neutrophil gelatinase-associated lipocalin	**2.9**	198.00	22591.70	8.00	50.50	Extracellular Space	transporter
P63261	Actin, cytoplasmic 2	**2.9**	375.00	41819.80	26.00	79.20	Cytoplasm	
P02746	Complement C1q subcomponent subunit B	**2.8**	253.00	26740.50	12.00	49.40		
P06753	Tropomyosin alpha-3 chain	**2.8**	285.00	32965.80	10.00	23.50	Cytoplasm	other
P23284	Peptidyl-prolyl cis-trans isomerase B	**2.8**	216.00	23763.60	5.00	23.10	Cytoplasm	enzyme
Q9UGM5	Fetuin-B; AltName	**2.7**	382.00	42082.00	13.00	37.70	Extracellular Space	other
P98160	Basement membrane-specific heparan sulfate proteo	**2.7**	4391.00	469307.00	37.00	11.20	Extracellular Space	enzyme
P14550	Alcohol dehydrogenase [NADP(+)]	**2.7**	325.00	36603.90	8.00	32.30	Cytoplasm	enzyme
P16035	Metalloproteinase inhibitor 2	**2.6**	220.00	24419.10	3.00	14.10	Extracellular Space	other
P18206	Vinculin	**2.6**	1134.00	123920.00	14.00	16.50	Plasma Membrane	enzyme
P68032	Actin, alpha cardiac muscle 1	**2.5**	377.00	42045.90	17.00	48.30	Cytoplasm	enzyme
P26927	Hepatocyte growth factor-like protein (MST1)	**2.5**	711.00	80393.60	26.00	43.20	Extracellular Space	growth factor
Q86YZ3	Hornerin	**2.5**	2850.00	282732.00	21.00	22.00	Cytoplasm	other
P02144	Myoglobin	**2.5**	154.00	17191.00	13.00	73.40	Cytoplasm	transporter
P04196	Histidine-rich glycoprotein	**2.4**	525.00	59630.90	22.00	44.40		
Q15848	Adiponectin	**2.4**	244.00	26433.00	7.00	37.70	Extracellular Space	other
P00325	Alcohol dehydrogenase 1B	**2.4**	375.00	39882.60	17.00	57.10		
P05976	Myosin light chain 1/3, skeletal muscle isoform;	**2.4**	194.00	21149.80	10.00	50.00	Cytoplasm	other
P04075	Fructose-bisphosphate aldolase A	**2.4**	364.00	39449.30	18.00	50.30	Cytoplasm	enzyme
P00740	Coagulation factor IX	**2.4**	461.00	51817.00	20.00	57.00	Extracellular Space	peptidase
Q04828	Aldo-keto reductase family 1 member C1	**2.3**	323.00	36819.10	9.00	26.90	Cytoplasm	enzyme
P30041	Peroxiredoxin-6	**2.3**	224.00	25055.20	16.00	69.60	Cytoplasm	enzyme
P06733	Alpha-enolase	**2.3**	434.00	47211.40	21.00	59.20		
P00338	L-lactate dehydrogenase A chain; Short=LDH-A	**2.3**	332.00	36719.40	16.00	50.00	Cytoplasm	enzyme
P01019	Angiotensinogen	**2.2**	485.00	53192.60	24.00	54.20	Extracellular Space	growth factor
P04114	Apolipoprotein B-100	**2.2**	4563.00	516093.00	480.00	87.20	Extracellular Space	transporter
P52566	Rho GDP-dissociation inhibitor 2	**2.2**	201.00	23009.60	5.00	18.90	Cytoplasm	other
P14174	Macrophage migration inhibitory factor	**2.2**	115.00	12486.20	2.00	17.40	Extracellular Space	cytokine
Q9H299	SH3 domain-binding glutamic acid-rich-like protein 3	**2.1**	93.00	10431.30	4.00	39.80	Nucleus	other
P0C0L5	Complement C4-B	**2.1**	1744.00	192937.00	130.00	80.40		
P24593	Insulin-like growth factor-binding protein 5	**2.1**	272.00	30586.00	7.00	24.60	Extracellular Space	other
P0C0L4	Complement C4-A	**2.1**	1744.00	192971.00	128.00	80.10		
P60174	Triosephosphate isomerase	**2.1**	286.00	30807.70	18.00	75.50	Cytoplasm	enzyme
P69905	Hemoglobin subunit alpha	**2.0**	142.00	15265.90	7.00	62.70		
P12111	Collagen alpha-3(VI)	**2.0**	3177.00	344015.00	35.00	12.90	Extracellular Space	other
P78417	Glutathione S-transferase omega-1	**2.0**	241.00	27584.10	13.00	43.20	Cytoplasm	enzyme

Table S5.3 Proteins up regulated in DCD (DGF vs IF) by at least 2 fold change in DGF when compared to IF p<=0.0

Protein	Description	Fold change	Length (AA)	mw (Da)	Peptide Seqs	% Coverage	Location	Type
P07996	Thrombospondin-1	DGF	1170.00	129498.00	53.00	29.20		
P61604	10 kDa heat shock protein, mitochondrial	DGF	102.00	10942.90	3.00	50.50	Cytoplasm	enzyme
P05387	60S acidic ribosomal protein P2	DGF	115.00	11675.90	2.00	62.40	Cytoplasm	other
P68032	Actin, alpha cardiac muscle 1	DGF	377.00	42045.90	17.00	20.10	Cytoplasm	enzyme
P07327	Alcohol dehydrogenase 1A	DGF	375.00	39886.50	14.00	28.30	Cytoplasm	enzyme
P08319	Alcohol dehydrogenase 4	DGF	380.00	40249.70	7.00	47.10		
Q04828	Aldo-keto reductase family 1 member C1	DGF	323.00	36819.10	9.00	55.30	Cytoplasm	enzyme
P02652	Apolipoprotein A-II	DGF	100.00	11167.90	9.00	44.10	Extracellular Space	transporter
Q562R1	Beta-actin-like protein 2	DGF	376.00	42030.00	10.00	21.80	Nucleus	other
P43251	Biotinidase	DGF	543.00	61183.30	13.00	27.80	Extracellular Space	enzyme
P00918	Carbonic anhydrase 2	DGF	260.00	29263.90	15.00	62.30		
O00299	Chloride intracellular channel protein 1	DGF	241.00	26941.80	8.00	36.50	Nucleus	ion channel
P05160	Coagulation factor XIII B chain	DGF	661.00	75569.20	28.00	18.00	Extracellular Space	enzyme
P00746	Complement factor D	DGF	253.00	27051.90	15.00	59.70	Extracellular Space	peptidase
P31146	Coronin-1A	DGF	461.00	51065.80	9.00	35.60		
P09172	Dopamine beta-hydroxylase	DGF	617.00	69128.70	15.00	39.20	Cytoplasm	enzyme
P68104	Elongation factor 1-alpha 1	DGF	462.00	50225.20	10.00	84.40	Cytoplasm	translation regulator
Q16610	Extracellular matrix protein 1	DGF	540.00	60725.30	24.00	26.90	Extracellular Space	transporter
P47756	F-actin-capping protein subunit beta	DGF	277.00	31366.80	7.00	36.30	Cytoplasm	other
P21333	Filamin-A; Short=FLN-A; AltName:	DGF	2647.00	281032.00	46.00	24.90		
P00738	Haptoglobin	DGF	406.00	45248.60	25.00	51.20	Extracellular Space	peptidase
P08107	Heat shock 70 kDa protein 1A/1B	DGF	641.00	70117.10	18.00	20.30		
P11142	Heat shock cognate 71 kDa protein	DGF	646.00	70962.30	24.00	50.50	Cytoplasm	enzyme
P07900	Heat shock protein HSP 90-alpha	DGF	732.00	84732.80	17.00	48.00	Cytoplasm	enzyme
P68871	Hemoglobin subunit beta	DGF	147.00	16006.30	12.00	37.00	Cytoplasm	transporter
P17936	Insulin-like growth factor-binding protein 3	DGF	291.00	31689.80	9.00	70.10	Extracellular Space	other
O75874	Isocitrate dehydrogenase [NADP] cytoplasmic	DGF	414.00	46701.60	14.00	36.20	Cytoplasm	
Q9Y468	Lethal(3)malignant brain tumor-like protein	DGF	752.00	83956.50	11.00	25.30		
P23141	Liver carboxylesterase 1	DGF	567.00	62571.20	18.00	24.60		
P48740	Mannan-binding lectin serine protease 1	DGF	699.00	79303.30	21.00	75.50	Extracellular Space	peptidase
O00187	Mannan-binding lectin serine protease 2	DGF	686.00	75761.70	14.00	19.80	Extracellular Space	peptidase
P26038	Moesin; AltName: Full=Membrane-organizing extension :	DGF	577.00	67867.80	22.00	48.50		
P05164	Myeloperoxidase; Short=MPO	DGF	745.00	83940.90	14.00	21.70	Cytoplasm	enzyme
P04908	Neural cell adhesion molecule L1-like protein; AltName	DGF						
Q06830	Peroxiredoxin-1	DGF	199.00	22114.30	12.00	18.30		
P05154	Plasma serine protease inhibitor	DGF	406.00	45717.70	15.00	51.00	Extracellular Space	other
Q07954	Prolow-density lipoprotein receptor-related protein 1	DGF	4544.00	505086.00	62.00	23.40	Plasma Membrane	ransmembrane recept
P07237	Protein disulfide-isomerase	DGF	508.00	57170.70	4.00	44.00	Cytoplasm	enzyme
P31949	Protein S100-A11	DGF	105.00	11750.80	5.00	5.80	Cytoplasm	other
P26447	Protein S100-A4; AltName	DGF	101.00	11738.70	8.00	62.30		
P14618	Pyruvate kinase PKM	DGF	531.00	57990.10	21.00	20.90	Cytoplasm	kinase
P0DJI8	Serum amyloid A-1 protein	DGF	122.00	13541.50	11.00	35.10	Extracellular Space	transporter
Q9Y490	Talin-1	DGF	2541.00	270049.00	49.00			
P08670	Vimentin	DGF	466.00	53691.10	26.00	31.60	Cytoplasm	other
P02745	Complement C1q subcomponent subunit A	116.8	245.00	26036.20	9.00	27.80		
P04040	Catalase	24.4	527.00	59808.80	19.00	44.40		
P00325	Alcohol dehydrogenase 1B	14.9	375.00	39882.60	17.00	57.10		
P15924	Desmoplakin	13.3	2871.00	332073.00	74.00	33.30	Plasma Membrane	other
P07355	Annexin A2	12.0	339.00	38633.80	8.00	27.70	Plasma Membrane	other
P00352	Retinal dehydrogenase 1	7.7	501.00	54917.00	12.00	31.30	Cytoplasm	enzyme
P30740	Leukocyte elastase inhibitor; Short=LEI	6.6	379.00	42768.70	16.00	25.20		
P05062	Fructose-bisphosphate aldolase B	5.5	364.00	39502.10	23.00	68.80		
P02763	Alpha-1-acid glycoprotein 1	5.4	201.00	23532.80	5.00	57.80	Extracellular Space	other
P30046	D-dopachrome decarboxylase	5.2	118.00	12721.70	7.00	46.70		
P21695	Glycerol-3-phosphate dehydrogenase [NAD(+)], cytoplas	4.9	349.00	37597.30	8.00	18.60		
P00326	Alcohol dehydrogenase 1C	4.8	375.00	39895.70	13.00	33.60		
P02747	Complement C1q subcomponent subunit C	4.2	245.00	25793.20	7.00	23.90		
P09972	Fructose-bisphosphate aldolase C	4.1	364.00	39485.30	9.00	81.10	Cytoplasm	enzyme
P60660	Myosin light polypeptide 6	4.1	151.00	16937.10	5.00	30.40	Cytoplasm	other
P09467	Fructose-1,6-bisphosphatase 1	3.9	338.00	36872.80	10.00	31.30		
P06733	Alpha-enolase	3.6	434.00	47211.40	21.00	8.70		
P04406	Glyceraldehyde-3-phosphate dehydrogenase	3.6	335.00	36084.40	12.00	12.50	Cytoplasm	enzyme
P40925	Malate dehydrogenase, cytoplasmic	3.5	334.00	36457.10	12.00	26.30		
P09210	Glutathione S-transferase A2	3.4	222.00	25683.60	11.00	37.60	Cytoplasm	enzyme
P63261	Actin, cytoplasmic 2	3.3	375.00	41819.80	26.00	41.90	Cytoplasm	other
P05109	Protein S100-A8	3.3	93.00	10827.60	11.00	37.70	Cytoplasm	other
P08519	Apolipoprotein(a)	3.2	4548.00	501806.00	40.00	44.20		
P24593	Insulin-like growth factor-binding protein 5	3.0	272.00	30586.00	7.00	35.90	Extracellular Space	other
P04196	Histidine-rich glycoprotein;	2.9	525.00	59630.90	22.00	41.20		
P18669	Phosphoglycerate mutase 1	2.9	254.00	28821.90	14.00	24.40		
P14923	Junction plakoglobin;	2.8	745.00	81818.80	13.00	26.60	Plasma Membrane	other
P67936	Tropomyosin alpha-4 chain	2.8	248.00	28540.50	15.00	48.30	Cytoplasm	other
Q03591	Complement factor H-related protein 1	2.7	330.00	37680.00	16.00	26.90		
P31946	14-3-3 protein beta/alpha;	2.7	246.00	28100.90	12.00	52.40		
P27169	Serum paraoxonase/arylesterase 1	2.6	355.00	39760.30	15.00	56.80	Extracellular Space	phosphatase
P01009	Alpha-1-antitrypsin;	2.6	418.00	46779.10	9.00	23.40	Extracellular Space	other
P02144	Myoglobin; taxon_	2.5	154.00	17191.00	13.00	69.00	Cytoplasm	transporter
Q00796	Sorbitol dehydrogenase	2.5	357.00	38353.80	10.00	67.60		
P60174	Triosephosphate isomerase	2.3	286.00	30807.70	18.00	37.10	Cytoplasm	enzyme
P06727	Apolipoprotein A-IV	2.2	396.00	45425.50	47.00	48.30	Extracellular Space	transporter
P05452	Tetranectin	2.2	202.00	22558.30	15.00	72.70		
Q15113	Procollagen C-endopeptidase enhancer 1	2.2	449.00	48014.00	7.00	1.00	Extracellular Space	other
P01011	Alpha-1-antichymotrypsin	2.2	423.00	47692.60	39.00	76.40		
P02765	Alpha-2-HS-glycoprotein;	2.2	367.00	39353.70	16.00	38.70	Extracellular Space	other
P00915	Carbonic anhydrase 1	2.1	261.00	28888.40	14.00	66.30		
P31151	Protein S100-A7;	2.0	101.00	11481.60	6.00	41.90		
P22792	Carboxypeptidase N subunit 2	2.0	545.00	60608.20	18.00	36.00	Extracellular Space	peptidase

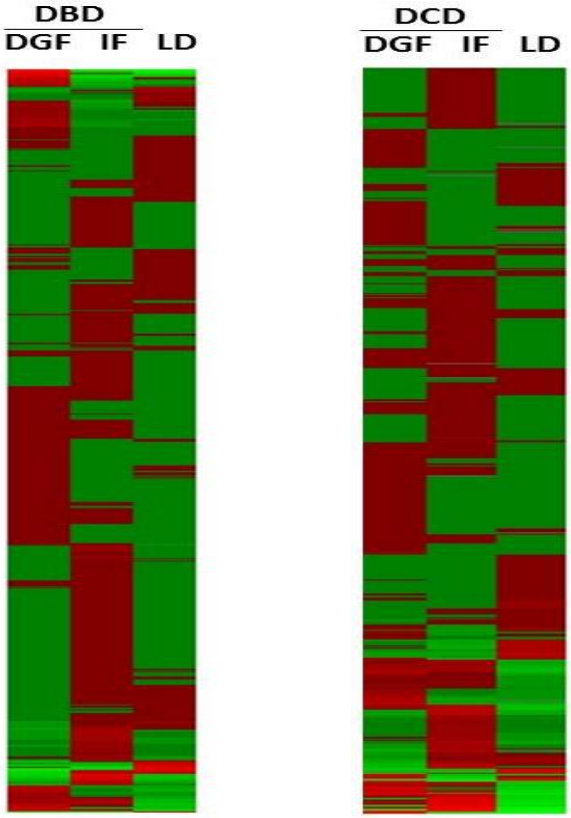

Figure S5.1 Unsupervised HCA for all 640 proteins identified from the comparison DBD (DGF vs IF) and DCD (DGF vs IF) and LD.

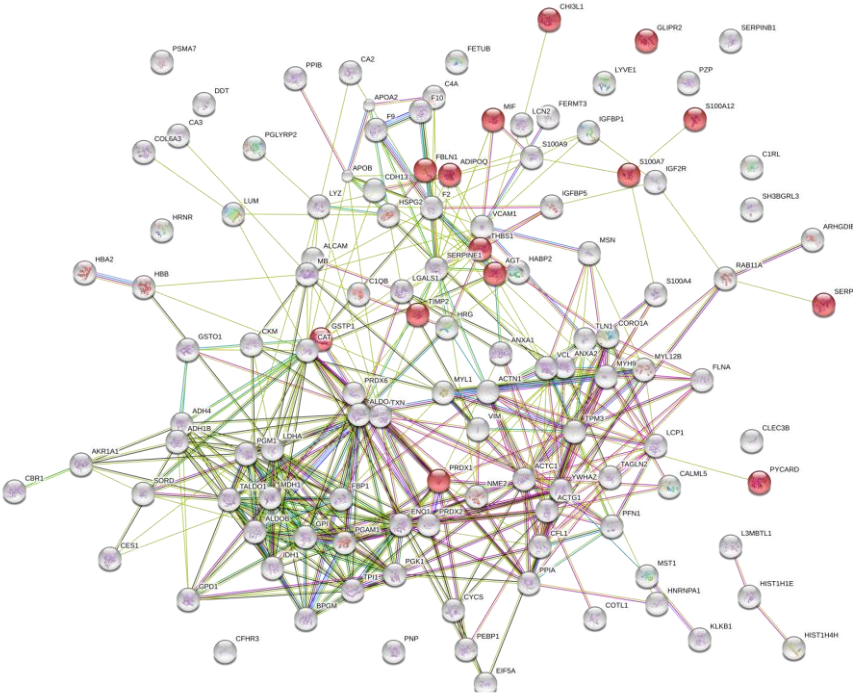

Figure 5S2. Proteins that were assigned as regulators of MAPK and JNK pathways (n=14; FDR 5E10-^{5}) according to String pathway analysis.

Table S5.4 120 proteins identified in urine proteomics DBD (DGF-IF) and LD. Yellow indicates high and green low values of fold change. No changes between DGF and IF were statistically significant. #Div/0*indicates that there was only one value of the abundance from this protein in one of the subgroups and three values in the other subgroup so the t test value could not be accurately defined.*

Protein description	DGF/IF	DGF/LD
Isoform 2B of Desmocollin-2 OS=Homo sapiens GN=DSC2	1.38	
Lipopolysaccharide-binding protein OS=Homo sapiens GN=LBP PE=1 SV=3	0.72	
Lysozyme C OS=Homo sapiens GN=LYZ PE=1 SV=1	8.63	
Napsin-A OS=Homo sapiens GN=NAPSA PE=1 SV=1	0.11	
Carbonic anhydrase 1 OS=Homo sapiens GN=CA1 PE=1 SV=2	1.70	
Collagen alpha-1(I) chain OS=Homo sapiens GN=COL1A1 PE=1 SV=5	313.06	
Cystatin-M OS=Homo sapiens GN=CST6 PE=1 SV=1	0.47	
Dermatopontin OS=Homo sapiens GN=DPT PE=2 SV=2	1.14	
Dystroglycan OS=Homo sapiens GN=DAG1 PE=1 SV=2	1.16	
Isoform 2 of Vascular cell adhesion protein 1 OS=Homo sapiens GN=VCAM1	1.01	
Fructose-bisphosphate aldolase A OS=Homo sapiens GN=ALDOA PE=1 SV=2	#DIV/0!	2.54
Complement C4-B OS=Homo sapiens GN=C4B PE=1 SV=2	0.59	5.42
Lysosomal Pro-X carboxypeptidase OS=Homo sapiens GN=PRCP PE=1 SV=1	0.25	22.19
Complement C3 OS=Homo sapiens GN=C3 PE=1 SV=2	9.89	0.57
Biotinidase OS=Homo sapiens GN=BTD PE=1 SV=2	3.58	8.48
Glutamyl aminopeptidase OS=Homo sapiens GN=ENPEP PE=1 SV=3	0.62	5.80
Retinol-binding protein 4 OS=Homo sapiens GN=RBP4 PE=1 SV=3	0.66	10.62
Lumican OS=Homo sapiens GN=LUM PE=1 SV=2	0.90	7.89
Glutathione S-transferase P OS=Homo sapiens GN=GSTP1 PE=1 SV=2	0.27	0.19
Vesicular integral-membrane protein VIP36 OS=Homo sapiens GN=LMAN2 PE	1.26	47.40
Peptidoglycan recognition protein 1 OS=Homo sapiens GN=PGLYRP1 PE=1 SV	1.34	6.75
Complement C1r subcomponent-like protein OS=Homo sapiens GN=C1RL PE	0.41	1.91
Galectin-3-binding protein OS=Homo sapiens GN=LGALS3BP PE=1 SV=1	2.14	22.81
Aminopeptidase N OS=Homo sapiens GN=ANPEP PE=1 SV=4	19.29	13.16
Profilin-1 OS=Homo sapiens GN=PFN1 PE=1 SV=2	2.06	16.49
14-3-3 protein gamma	#DIV/0!	0.18
Fructose-bisphosphate aldolase B OS=Homo sapiens GN=ALDOB PE=1 SV=2	2.98	2.42
Prostatic acid phosphatase OS=Homo sapiens GN=ACPP PE=1 SV=3	278.30	412.21
Complement factor I OS=Homo sapiens GN=CFI PE=1 SV=2	4.70	0.90
Inter-alpha-trypsin inhibitor heavy chain H2 OS=Homo sapiens GN=ITIH2 PE=	11.81	0.22
Coactosin-like protein OS=Homo sapiens GN=COTL1 PE=1 SV=3	1.59	54.73
N(G),N(G)-dimethylarginine dimethylaminohydrolase 2 OS=Homo sapiens G	0.99	26.03
Apolipoprotein A-IV OS=Homo sapiens GN=APOA4 PE=1 SV=3	2.97	0.98
Low-density lipoprotein receptor-related protein 2 OS=Homo sapiens GN=LR	0.80	0.42
Peroxiredoxin-1 OS=Homo sapiens GN=PRDX1 PE=1 SV=1	#DIV/0!	6.42
Keratin, type II cytoskeletal 2 epidermal OS=Homo sapiens GN=KRT2 PE=1 SV	0.35	2.98
Collagen alpha-1(VI) chain OS=Homo sapiens GN=COL6A1 PE=1 SV=3	1.84	10.45
Glyceraldehyde-3-phosphate dehydrogenase OS=Homo sapiens GN=GAPDH	2.25	1.81
Lysosomal protective protein OS=Homo sapiens GN=CTSA PE=1 SV=2	6.61	39.45
N-acetylglucosamine-6-sulfatase OS=Homo sapiens GN=GNS PE=1 SV=3	21.73	244.12
Complement C4-A OS=Homo sapiens GN=C4A PE=1 SV=2	0.79	4.29
Pigment epithelium-derived factor OS=Homo sapiens GN=SERPINF1 PE=1 SV	2.42	4.07
Basement membrane-specific heparan sulfate proteoglycan core protein OS	0.15	1.13
Cubilin OS=Homo sapiens GN=CUBN PE=1 SV=5	1.72	0.66
Fibrinogen alpha chain OS=Homo sapiens GN=FGA PE=1 SV=2	1.44	1.00
Complement factor B OS=Homo sapiens GN=CFB PE=2 SV=1	14.58	1.75
Isoform Sap-mu-6 of Prosaposin OS=Homo sapiens GN=PSAP	0.06	0.03
6-phosphogluconolactonase OS=Homo sapiens GN=PGLS PE=1 SV=2	1.74	11.30
Keratin, type I cytoskeletal 9 OS=Homo sapiens GN=KRT9 PE=1 SV=3	3.00	5.84
Isoform 3 of Vitamin D-binding protein OS=Homo sapiens GN=GC	16.27	0.44
Dipeptidyl peptidase 1 OS=Homo sapiens GN=CTSC PE=1 SV=2	7.35	56.73
Eukaryotic translation initiation factor 6 OS=Homo sapiens GN=EIF6 PE=1 SV=	1.91	5.00
Keratin, type II cytoskeletal 1 OS=Homo sapiens GN=KRT1 PE=1 SV=6	0.84	3.04
L-lactate dehydrogenase B chain OS=Homo sapiens GN=LDHB PE=1 SV=2	1.48	1.31
Alpha-1-acid glycoprotein 2 OS=Homo sapiens GN=ORM2 PE=1 SV=2	0.22	27.34
Keratin, type I cytoskeletal 10 OS=Homo sapiens GN=KRT10 PE=1 SV=6	1.04	1.80
Alpha-2-antiplasmin OS=Homo sapiens GN=SERPINF2 PE=1 SV=3	1.18	0.81
Thyroxine-binding globulin OS=Homo sapiens GN=SERPINA7 PE=1 SV=2	4.05	5.81
Inter-alpha-trypsin inhibitor heavy chain H4 OS=Homo sapiens GN=ITIH4	1.68	1.26
Cathepsin D OS=Homo sapiens GN=CTSD PE=1 SV=1	5.28	4.45
Polymeric immunoglobulin receptor OS=Homo sapiens GN=PIGR PE=1 SV=4	2.03	3.24
Vasorin OS=Homo sapiens GN=VASN PE=1 SV=1	1.96	13.23
Isoform 5 of Osteopontin OS=Homo sapiens GN=SPP1	2.07	7.13
SH3 domain-binding glutamic acid-rich-like protein 3 OS=Homo sapiens G	0.41	4.52
Apolipoprotein D OS=Homo sapiens GN=APOD PE=1 SV=1	1.18	0.72
Isoform 3 of Pro-epidermal growth factor OS=Homo sapiens GN=EGF	0.61	0.90
Transthyretin OS=Homo sapiens GN=TTR PE=1 SV=1	0.63	1.49
Leucine-rich alpha-2-glycoprotein OS=Homo sapiens GN=LRG1 PE=1 SV=2	0.67	60.77
Corticosteroid-binding globulin OS=Homo sapiens GN=SERPINA6 PE=1 SV=1	2.05	1.48
Alpha-2-macroglobulin OS=Homo sapiens GN=A2M PE=1 SV=3	1.85	0.62
Keratin, type II cuticular Hb6 OS=Homo sapiens GN=KRT86 PE=1 SV=1	0.20	0.40
Alpha-1B-glycoprotein OS=Homo sapiens GN=A1BG PE=1 SV=4	1.11	0.69
Ceruloplasmin OS=Homo sapiens GN=CP PE=1 SV=1	15.11	2.91
Isoform D of Osteopontin OS=Homo sapiens GN=SPP1	2.57	12.65
Alpha-1-acid glycoprotein 1 OS=Homo sapiens GN=ORM1 PE=1 SV=1	0.30	14.26
Beta-2-microglobulin OS=Homo sapiens GN=B2M PE=1 SV=1	0.23	23.15
Hemoglobin subunit alpha OS=Homo sapiens GN=HBA1 PE=1 SV=2	14.80	76.31
Hemoglobin subunit beta OS=Homo sapiens GN=HBB PE=1 SV=2	12.94	45.84
Antithrombin-III OS=Homo sapiens GN=SERPINC1 PE=1 SV=1	1.20	1.52
Actin, cytoplasmic 1 OS=Homo sapiens GN=ACTB PE=1 SV=1	2.08	0.93
Prothrombin OS=Homo sapiens GN=F2 PE=1 SV=2	0.82	2.70
Monocyte differentiation antigen CD14 OS=Homo sapiens GN=CD14 PE=1	1.31	61.29
Hemopexin OS=Homo sapiens GN=HPX PE=1 SV=2	1.35	1.13
Beta-2-glycoprotein 1 OS=Homo sapiens GN=APOH PE=1 SV=3	0.27	0.29
Angiotensinogen OS=Homo sapiens GN=AGT PE=1 SV=1	0.57	2.33
Alpha-1-antichymotrypsin OS=Homo sapiens GN=SERPINA3 PE=1 SV=2	0.73	2.81
Alpha-2-HS-glycoprotein OS=Homo sapiens GN=AHSG PE=1 SV=1	0.86	2.30
CD59 glycoprotein OS=Homo sapiens GN=CD59 PE=1 SV=1	0.55	1.27
Protein AMBP OS=Homo sapiens GN=AMBP PE=1 SV=1	0.38	11.61
Haptoglobin OS=Homo sapiens GN=HP PE=1 SV=1	0.07	0.05
Isoform LMW of Kininogen-1 OS=Homo sapiens GN=KNG1	0.51	0.53
Apolipoprotein A-I OS=Homo sapiens GN=APOA1 PE=1 SV=1	2.34	0.16
Apolipoprotein A-II OS=Homo sapiens GN=APOA2 PE=1 SV=1	1.24	0.08
Alpha-1-antitrypsin OS=Homo sapiens GN=SERPINA1 PE=1 SV=3	1.59	1.91
3-mercaptopyruvate sulfurtransferase OS=Homo sapiens GN=MPST PE=1	0.36	6.48
Alpha/beta hydrolase domain-containing protein 14B OS=Homo sapiens (	1.92	28.13
Apolipoprotein E OS=Homo sapiens GN=APOE PE=1 SV=1	1.12	0.63
Betaine--homocysteine S-methyltransferase 1 OS=Homo sapiens GN=BHI	2.31	1.60
Carboxypeptidase N subunit 2 OS=Homo sapiens GN=CPN2 PE=1 SV=3	0.06	0.19
Cathepsin Z OS=Homo sapiens GN=CTSZ PE=1 SV=1	0.29	0.28
Coagulation factor XII OS=Homo sapiens GN=F12 PE=1 SV=3	#DIV/0!	0.52
Dipeptidyl peptidase 2 OS=Homo sapiens GN=DPP7 PE=1 SV=3	19.71	40.91
Endonuclease domain-containing 1 protein OS=Homo sapiens GN=ENDOD	0.03	0.35
Fatty acid-binding protein, adipocyte OS=Homo sapiens GN=FABP4 PE=1 S	0.05	1.28
Fibrinogen beta chain OS=Homo sapiens GN=FGB PE=1 SV=2	128.22	1.27
Fructose-1,6-bisphosphatase 1 OS=Homo sapiens GN=FBP1 PE=1 SV=5	1.59	0.14
Gelsolin OS=Homo sapiens GN=GSN PE=1 SV=1	0.91	1.94
Hemoglobin subunit delta OS=Homo sapiens GN=HBD PE=1 SV=2	#DIV/0!	39.79
Isoform 2 of N-acetylmuramoyl-L-alanine amidase OS=Homo sapiens GN=	9.05	127.95
Isoform 2 of Roundabout homolog 4 OS=Homo sapiens GN=ROBO4	0.63	1.74
Isoform B of Fibulin-1 OS=Homo sapiens GN=FBLN1	0.82	3.08
Isoform Gamma-A of Fibrinogen gamma chain OS=Homo sapiens GN=FGG	49.22	1.26
Keratin, type I cytoskeletal 14 OS=Homo sapiens GN=KRT14 PE=1 SV=4	0.50	1.78
Myoglobin OS=Homo sapiens GN=MB PE=1 SV=2	6.58	5701.28
Ribonuclease T2 OS=Homo sapiens GN=RNASET2 PE=1 SV=2	5.59	87.59

Table S5.5136 proteins identified in urine proteomics DCD (DGF-IF) and LD

Yellow indicates high and green low values of fold change. No changes between DGF and IF were statistically significant Div/0 *indicates that there was only one value of the abundance from this protein in one of the subgroups and three values in the other subgroup so the t test value could not be accurately defined.*

Protein description	DGF /IF	DGF /LD
Myoglobin OS=Homo sapiens GN=MB PE=1 SV=2	3.18	11749.63
Ig kappa chain V-III region VH (Fragment) OS=Homo sap	216.1	265.2742
Beta-2-microglobulin OS=Homo sapiens GN=B2M PE=1 S	0.92	216.2411
Fatty acid-binding protein, adipocyte OS=Homo sapiens	157.74	80.58928
MPST	151.58	63.29737
Vesicular integral-membrane protein VIP36 OS=Homo s	1.47	62.17933
Coactosin-like protein OS=Homo sapiens GN=COTL1 PE=	1.14	60.28189
Retinol-binding protein 4 OS=Homo sapiens GN=RBP4 P	1.06	53.11067
Monocyte differentiation antigen CD14 OS=Homo sapie	1.09	50.6329
Leucine-rich alpha-2-glycoprotein OS=Homo sapiens GN	0.91	50.3511
Lysosomal Pro-X carboxypeptidase OS=Homo sapiens G	0.09	29.10959
ABHD14B	0.88	27.0335
Dipeptidyl peptidase 1 OS=Homo sapiens GN=CTSC PE=	1.96	27.00267
SH3 domain-binding glutamic acid-rich-like protein 3 OS	9.3	24.20499
Endonuclease domain-containing 1 protein OS=Homo sa	1.73	21.04893
Isoform D of Osteopontin OS=Homo sapiens GN=SPP1	0.51	19.66168
Endothelial protein C receptor OS=Homo sapiens GN=PI	11.36	19.50747
Profilin-1 OS=Homo sapiens GN=PFN1 PE=1 SV=2	2.21	18.78088
Hemoglobin subunit alpha OS=Homo sapiens GN=HBA1	0.18	17.20349
Hemoglobin subunit delta OS=Homo sapiens GN=HBD P	0.34	16.21665
Protein AMBP OS=Homo sapiens GN=AMBP PE=1 SV=1	0.35	15.11792
Isoform B of Fibulin-1 OS=Homo sapiens GN=FBLN1	3.1	14.02049
Ig kappa chain V-III region HAH OS=Homo sapiens PE=2 S	2.45	13.80509
Hemoglobin subunit beta OS=Homo sapiens GN=HBB PE	0.29	12.51765
Lysosomal protective protein OS=Homo sapiens GN=CTS	3.11	12.33216
Collagen alpha-1(VI) chain OS=Homo sapiens GN=COL6A	3.79	11.96683
Glutamyl aminopeptidase OS=Homo sapiens GN=ENPEP	10.3	11.38199
Basement membrane-specific heparan sulfate proteogl	1.58	11.37178
Isoform 5 of Osteopontin OS=Homo sapiens GN=SPP1	0.67	10.53015
Isoform 2 of N-acetylmuramoyl-L-alanine amidase OS=H	#DIV/0!	9.292051
N(G),N(G)-dimethylarginine dimethylaminohydrolase 2	0.46	9.172099
Peroxiredoxin-1 OS=Homo sapiens GN=PRDX1 PE=1 SV=	#DIV/0!	9.040205
Cathepsin Z OS=Homo sapiens GN=CTSZ PE=1 SV=1	3.1	7.672662
PGLS	5.95	7.081024
Biotinidase OS=Homo sapiens GN=BTD PE=1 SV=2	1.2	7.013818
Galectin-3-binding protein OS=Homo sapiens GN=LGALS	0.69	6.607103
Betaine--homocysteine S-methyltransferase 1 OS=Hom	#DIV/0!	6.196917
N-acetylglucosamine-6-sulfatase OS=Homo sapiens GN=	0.63	6.126657
ORM1	0.08	6.082052
Lumican OS=Homo sapiens GN=LUM PE=1 SV=2	1.63	5.984422
Alpha-1-acid glycoprotein 2 OS=Homo sapiens GN=ORM	0.05	5.903398
Vasorin OS=Homo sapiens GN=VASN PE=1 SV=1	0.51	5.084778
Peptidoglycan recognition protein 1 OS=Homo sapiens (	1.69	5.068841
Group XV phospholipase A2 OS=Homo sapiens GN=PLA2	2.57	4.84375
Alpha-2-HS-glycoprotein OS=Homo sapiens GN=AHSG P	2.08	4.842398
Thyroxine-binding globulin OS=Homo sapiens GN=SERP	11.04	4.779333
Secreted and transmembrane protein 1 OS=Homo sapie	#DIV/0!	4.568609
Ig heavy chain V-III region BRO OS=Homo sapiens PE=1 S	1.16	4.555384
Eukaryotic translation initiation factor 6 OS=Homo sapie	103.07	4.322378
Fibrinogen alpha chain OS=Homo sapiens GN=FGA PE=1	2.32	4.141809
Ribonuclease T2 OS=Homo sapiens GN=RNASET2 PE=1 S	#DIV/0!	3.744146
Alpha-1-antichymotrypsin OS=Homo sapiens GN=SERPI	0.98	3.734112
Aminopeptidase N OS=Homo sapiens GN=ANPEP PE=1 S	4.8	3.622643
Cathepsin D OS=Homo sapiens GN=CTSD PE=1 SV=1	0.26	3.586578
Transthyretin OS=Homo sapiens GN=TTR PE=1 SV=1	1.13	3.408932
Isoform 2 of Roundabout homolog 4 OS=Homo sapiens (	2.55	3.330996
Complement C4-B OS=Homo sapiens GN=C4B PE=1 SV=2	0.51	2.990196
Complement C1r subcomponent-like protein OS=Homo	1.04	2.806874
Prothrombin OS=Homo sapiens GN=F2 PE=1 SV=2	1.73	2.776494
Complement C4-A OS=Homo sapiens GN=C4A PE=1 SV=1	0.67	2.573173
Angiotensinogen OS=Homo sapiens GN=AGT PE=1 SV=1	1.88	2.556607
Dipeptidyl peptidase 2 OS=Homo sapiens GN=DPP7 PE=	4.34	2.372925
Ig lambda-2 chain C regions OS=Homo sapiens GN=IGLC2	2.49	2.181263
Isoform 3 of Pro-epidermal growth factor OS=Homo sap	1.99	2.123079
Fructose-bisphosphate aldolase B OS=Homo sapiens GN	#DIV/0!	2.081624
Keratin, type II cuticular Hb6 OS=Homo sapiens GN=KRT	#DIV/0!	2.077637
CD59 glycoprotein OS=Homo sapiens GN=CD59 PE=1 SV=	0.32	2.05176
Ig lambda chain V-III region LOI OS=Homo sapiens PE=1	3.3	2.025933
Ig kappa chain V-II region TEW OS=Homo sapiens PE=1 S	1.15	1.987217
Polymeric immunoglobulin receptor OS=Homo sapiens	0.26	1.91375

Protein description	DGF/IF	DGF/LD
Pigment epithelium-derived factor OS=Homo sapiens	1.26	1.699437
Alpha-1-antitrypsin OS=Homo sapiens GN=SERPINA1	0.61	1.69424
Alpha-2-macroglobulin OS=Homo sapiens GN=A2M PI	1	1.584135
L-lactate dehydrogenase B chain OS=Homo sapiens G	0.31	1.550108
Gelsolin OS=Homo sapiens GN=GSN PE=1 SV=1	0.47	1.522645
Isoform LMW of Kininogen-1 OS=Homo sapiens GN=K	1.93	1.355261
Isoform Sap-mu-6 of Prosaposin OS=Homo sapiens GI	4.45	1.33655
Inter-alpha-trypsin inhibitor heavy chain H4 OS=Hom	2.39	1.327273
Prostatic acid phosphatase OS=Homo sapiens GN=AC	9.67	1.279951
Ig lambda chain V-I region WAH OS=Homo sapiens PE	1.2	1.26688
Alpha-1B-glycoprotein OS=Homo sapiens GN=A1BG P	1.35	1.224455
Keratin, type II cytoskeletal 2 epidermal OS=Homo sa	0.26	1.191292
Glyceraldehyde-3-phosphate dehydrogenase OS=Hor	0.23	1.171993
Corticosteroid-binding globulin OS=Homo sapiens GN	2.02	1.164432
Fructose-bisphosphate aldolase A OS=Homo sapiens	0.2	1.093868
ACTB	0.14	1.063751
Immunoglobulin lambda-like polypeptide 5 OS=Hom	1.12	1.032768
Ig kappa chain V-III region VG (Fragment) OS=Homo s	0.87	1.016146
Keratin, type I cytoskeletal 9 OS=Homo sapiens GN=K	0.3	0.869172
Keratin, type II cytoskeletal 1 OS=Homo sapiens GN=I	0.36	0.857806
Hemopexin OS=Homo sapiens GN=HPX PE=1 SV=2	0.98	0.855419
Haptoglobin OS=Homo sapiens GN=HP PE=1 SV=1	0.95	0.752001
Keratin, type I cytoskeletal 10 OS=Homo sapiens GN=	0.43	0.668941
Carboxypeptidase N subunit 2 OS=Homo sapiens GN=	0.92	0.657649
Apolipoprotein D OS=Homo sapiens GN=APOD PE=1 S	0.18	0.655042
Ig lambda chain V-I region NEW OS=Homo sapiens PE	1.14	0.643611
Low-density lipoprotein receptor-related protein 2 O	0.7	0.612766
Antithrombin-III OS=Homo sapiens GN=SERPINC1 PE=	0.91	0.571812
Cubilin OS=Homo sapiens GN=CUBN PE=1 SV=5	0.43	0.571712
Glutathione S-transferase P OS=Homo sapiens GN=GS	0.34	0.56441
Pepsin A-3 OS=Homo sapiens GN=PGA3 PE=1 SV=1	0.03	0.508653
Ceruloplasmin OS=Homo sapiens GN=CP PE=1 SV=1	0.5	0.478948
Immunoglobulin J chain OS=Homo sapiens GN=IGJ PE	0.2	0.453416
Nuclear transport factor 2 OS=Homo sapiens GN=NUT	#DIV/0!	0.452359
Beta-2-glycoprotein 1 OS=Homo sapiens GN=APOH PI	2.44	0.412717
Epididymal secretory protein E1 OS=Homo sapiens GI	0	0.331106
Complement factor I OS=Homo sapiens GN=CFI PE=1	1.39	0.235006
Apolipoprotein A-IV OS=Homo sapiens GN=APOA4 PE	1	0.230268
Apolipoprotein E OS=Homo sapiens GN=APOE PE=1 S	0.04	0.173531
Alpha-2-antiplasmin OS=Homo sapiens GN=SERPINF2	0.08	0.146203
Isoform Gamma-A of Fibrinogen gamma chain OS=Ho	0.42	0.142278
Complement factor B OS=Homo sapiens GN=CFB PE=2	0.17	0.13755
Fibrinogen beta chain OS=Homo sapiens GN=FGB PE=	0.53	0.11362
Apolipoprotein A-II OS=Homo sapiens GN=APOA2 PE=	0.07	0.096345
Apolipoprotein A-I OS=Homo sapiens GN=APOA1 PE=	0.18	0.092406
Inter-alpha-trypsin inhibitor heavy chain H2 OS=Hom	0.12	0.066871
Complement C3 OS=Homo sapiens GN=C3 PE=1 SV=2	0.21	0.055001
Isoform 3 of Vitamin D-binding protein OS=Homo sap	0.09	0.052754
Lithostathine-1-alpha OS=Homo sapiens GN=REG1A P	0.07	
Lysozyme C OS=Homo sapiens GN=LYZ PE=1 SV=1	0.09	
Isoform 3 of Immunoglobulin superfamily member 8	0.19	
Glia maturation factor gamma OS=Homo sapiens GN=	0.23	
Collagen alpha-1(I) chain OS=Homo sapiens GN=COL1	0.39	
Cystatin-M OS=Homo sapiens GN=CST6 PE=1 SV=1	0.43	
Carbonic anhydrase 1 OS=Homo sapiens GN=CA1 PE=	0.49	
Insulin-like growth factor-binding protein 1 OS=Hom	0.73	
Glia maturation factor beta OS=Homo sapiens GN=GN	0.75	
Fatty acid-binding protein, heart OS=Homo sapiens G	1.38	
Myocilin OS=Homo sapiens GN=MYOC PE=1 SV=2	1.85	
Isoform Alpha of Poliovirus receptor-related protein	1.9	
Isoform 2 of V-set and immunoglobulin domain-cont	2.68	
Dystroglycan OS=Homo sapiens GN=DAG1 PE=1 SV=2	3.2	
Isoform 2B of Desmocollin-2 OS=Homo sapiens GN=D	3.45	
Dermatopontin OS=Homo sapiens GN=DPT PE=2 SV=2	3.86	
Heat shock protein beta-6 OS=Homo sapiens GN=HSP	4.13	
Isoform 2 of Vascular cell adhesion protein 1 OS=Hom	4.44	

Chapter 6S

Table S6.1 significantly increased proteins in donor kidneys with suboptimal outcomes, fold change>2

Protein	Description	Fold change Sub/Good	Good/Sub	p values
O60826|CCD22_	Coiled-coil domain-containing protein 22 OS=Homo sapiens GN=CCDC22 PE=1 SV=1	Sub only	0.00	ND
Q53T59|H1BP3_	HCLS1-binding protein 3 OS=Homo sapiens GN=HS1BP3 PE=1 SV=1	Sub only	0.00	ND
P10644-2|KAP0_	Isoform 2 of cAMP-dependent protein kinase type I-alpha regulatory subunit OS=Homo sapiens GN=PRKAR1A	Sub only	0.00	ND
Q53SF7-2|COBL1_	Isoform 2 of Cordon-bleu protein-like 1 OS=Homo sapiens GN=COBLL1	Sub only	0.00	ND
Q16625-2|OCLN_	Isoform 2 of Occludin OS=Homo sapiens GN=OCLN	Sub only	0.00	ND
Q86VB7-2|C163A_	Isoform 2 of Scavenger receptor cysteine-rich type 1 protein M130 OS=Homo sapiens GN=CD163	Sub only	0.00	ND
O14828-2|SCAM3_	Isoform 2 of Secretory carrier-associated membrane protein 3 OS=Homo sapiens GN=SCAMP3	Sub only	0.00	ND
P67812-2|SC11A_	Isoform 2 of Signal peptidase complex catalytic subunit SEC11A OS=Homo sapiens GN=SEC11A	Sub only	0.00	ND
Q9NY33-4|DPP3_	Isoform 4 of Dipeptidyl peptidase 3 OS=Homo sapiens GN=DPP3	Sub only	0.00	ND
Q9NX40|OCAD1_	OCIA domain-containing protein 1 OS=Homo sapiens GN=OCIAD1 PE=1 SV=1	Sub only	0.00	ND
P26196|DDX6_	Probable ATP-dependent RNA helicase DDX6 OS=Homo sapiens GN=DDX6 PE=1 SV=2	Sub only	0.00	ND
Q9UHJ6|SHPK_	Sedoheptulokinase OS=Homo sapiens GN=SHPK PE=1 SV=3	Sub only	0.00	ND
P53041|PPP5_	Serine/threonine-protein phosphatase 5 OS=Homo sapiens GN=PPP5C PE=1 SV=1	Sub only	0.00	ND
P62316|SMD2_	Small nuclear ribonucleoprotein Sm D2 OS=Homo sapiens GN=SNRPD2 PE=1 SV=1	Sub only	0.00	ND
Q15393|SF3B3_	Splicing factor 3B subunit 3 OS=Homo sapiens GN=SF3B3 PE=1 SV=4	Sub only	0.00	ND
O75954|TSN9_	Tetraspanin-9 OS=Homo sapiens GN=TSPAN9 PE=1 SV=1	Sub only	0.00	ND
Q9Y2W1|TR150_	Thyroid hormone receptor-associated protein 3 OS=Homo sapiens GN=THRAP3 PE=1 SV=2	Sub only	0.00	ND
P27216-2|ANX13_	Isoform B of Annexin A13 OS=Homo sapiens GN=ANXA13	No ID	20.00	ND
O43681|ASNA_	ATPase ASNA1 OS=Homo sapiens GN=ASNA1 PE=1 SV=2	No ID	20.00	ND
P36222|CH3L1_	Chitinase-3-like protein 1 OS=Homo sapiens GN=CHI3L1 PE=1 SV=2	No ID	20.00	ND
P42677|RS27_	40S ribosomal protein S27 OS=Homo sapiens GN=RPS27 PE=1 SV=3	17.76	0.06	ND
O43294|TGFI1_	Transforming growth factor beta-1-induced transcript 1 protein OS=Homo sapiens GN=TGFB1I1 PE=1 SV=2	7.42	0.13	4.53E-02
P42224|STAT1_	Signal transducer and activator of transcription 1-alpha/beta OS=Homo sapiens GN=STAT1 PE=1 SV=2	6.94	0.14	3.00E-04
Q00688|FKBP3_	Peptidyl-prolyl cis-trans isomerase FKBP3 OS=Homo sapiens GN=FKBP3 PE=1 SV=1	6.19	0.16	ND
P21964-2|COMT_	Isoform Soluble of Catechol O-methyltransferase OS=Homo sapiens GN=COMT	5.09	0.20	ND
P18827|SDC1_	Syndecan-1 OS=Homo sapiens GN=SDC1 PE=1 SV=3	4.86	0.21	ND
P05109|S10A8_	Protein S100-A8 OS=Homo sapiens GN=S100A8 PE=1 SV=1	4.65	0.22	4.84E-03
Q07157-2|ZO1_	Isoform Short of Tight junction protein ZO-1 OS=Homo sapiens GN=TJP1	3.98	0.25	4.29E-02
Q14624-2|ITIH4_	Isoform 2 of Inter-alpha-trypsin inhibitor heavy chain H4 OS=Homo sapiens GN=ITIH4	3.96	0.25	ND
Q9UBV8|PEF1_	Peflin OS=Homo sapiens GN=PEF1 PE=1 SV=1	3.92	0.26	ND
Q15181|IPYR_	Inorganic pyrophosphatase OS=Homo sapiens GN=PPA1 PE=1 SV=2	3.68	0.27	1.05E-02
P49914-2|MTHFS_	Isoform 2 of 5-formyltetrahydrofolate cyclo-ligase OS=Homo sapiens GN=MTHFS	3.63	0.28	ND
Q8TCC7-2|S22A8_	Isoform 2 of Solute carrier family 22 member 8 OS=Homo sapiens GN=SLC22A8	3.33	0.30	ND
Q9NTJ5-2|SAC1_	Isoform 2 of Phosphatidylinositide phosphatase SAC1 OS=Homo sapiens GN=SACM1L	3.23	0.31	ND
Q92896-2|GSLG1_	Isoform 2 of Golgi apparatus protein 1 OS=Homo sapiens GN=GLG1	3.10	0.32	4.25E-02
P05387|RLA2_	60S acidic ribosomal protein P2 OS=Homo sapiens GN=RPLP2 PE=1 SV=1	3.03	0.33	3.57E-03
P08237-3|PFKAM_	Isoform 3 of ATP-dependent 6-phosphofructokinase, muscle type OS=Homo sapiens GN=PFKM	2.89	0.35	5.03E-03
Q01813|PFKAP_	ATP-dependent 6-phosphofructokinase, platelet type OS=Homo sapiens GN=PFKP PE=1 SV=2	2.87	0.35	3.45E-02
Q13885|TBB2A_	Tubulin beta-2A chain OS=Homo sapiens GN=TUBB2A PE=1 SV=1	2.86	0.35	7.41E-04
Q96G03|PGM2_	Phosphoglucomutase-2 OS=Homo sapiens GN=PGM2 PE=1 SV=4	2.83	0.35	5.03E-02
P49327|FAS_	Fatty acid synthase OS=Homo sapiens GN=FASN PE=1 SV=3	2.83	0.35	ND
P31946-2|1433B_	Isoform Short of 14-3-3 protein beta/alpha OS=Homo sapiens GN=YWHAB	2.81	0.36	1.97E-02
Q14764|MVP_	Major vault protein OS=Homo sapiens GN=MVP PE=1 SV=4	2.73	0.37	1.75E-02
P05413|FABPH_	Fatty acid-binding protein, heart OS=Homo sapiens GN=FABP3 PE=1 SV=4	2.68	0.37	8.68E-03
P16615|AT2A2_	Sarcoplasmic/endoplasmic reticulum calcium ATPase 2 OS=Homo sapiens GN=ATP2A2 PE=1 SV=1	2.61	0.38	9.04E-03
Q07075|AMPE_	Glutamyl aminopeptidase OS=Homo sapiens GN=ENPEP PE=1 SV=3	2.60	0.38	1.85E-02
P50990-2|TCPQ_	Isoform 2 of T-complex protein 1 subunit theta OS=Homo sapiens GN=CCT8	2.60	0.38	4.41E-05
Q04637-3|IF4G1_	Isoform B of Eukaryotic translation initiation factor 4 gamma 1 OS=Homo sapiens GN=EIF4G1	2.54	0.39	ND
O14976-2|GAK_	Isoform 2 of Cyclin-G-associated kinase OS=Homo sapiens GN=GAK	2.53	0.39	ND
Q9Y2R0|COA3_	Cytochrome c oxidase assembly factor 3 homolog, mitochondrial OS=Homo sapiens GN=COA3 PE=1 SV=1	2.50	0.40	5.09E-03
P50552|VASP_	Vasodilator-stimulated phosphoprotein OS=Homo sapiens GN=VASP PE=1 SV=3	2.45	0.41	ND
Q99436|PSB7_	Proteasome subunit beta type-7 OS=Homo sapiens GN=PSMB7 PE=1 SV=1	2.44	0.41	3.68E-02
Q9UNF0-2|PACN2_	Isoform 2 of Protein kinase C and casein kinase substrate in neurons protein 2 OS=Homo sapiens GN=PACSIN2	2.44	0.41	2.00E-02
P07814|SYEP_	Bifunctional glutamate/proline--tRNA ligase OS=Homo sapiens GN=EPRS PE=1 SV=5	2.39	0.42	1.21E-02
Q07955|SRSF1_	Serine/arginine-rich splicing factor 1 OS=Homo sapiens GN=SRSF1 PE=1 SV=2	2.36	0.42	3.20E-02
Q01844-2|EWS_	Isoform EWS-B of RNA-binding protein EWS OS=Homo sapiens GN=EWSR1	2.35	0.43	3.87E-02
O14818-2|PSA7_	Isoform 2 of Proteasome subunit alpha type-7 OS=Homo sapiens GN=PSMA7	2.33	0.43	7.48E-03
Q96HC4|PDLI5_	PDZ and LIM domain protein 5 OS=Homo sapiens GN=PDLIM5 PE=1 SV=5	2.31	0.43	1.10E-02
P14868-2|SYDC_	Isoform 2 of Aspartate--tRNA ligase, cytoplasmic OS=Homo sapiens GN=DARS	2.29	0.44	3.04E-02
Q16851|UGPA_	UTP--glucose-1-phosphate uridylyltransferase OS=Homo sapiens GN=UGP2 PE=1 SV=5	2.28	0.44	4.00E-02
P63010-2|AP2B1_	Isoform 2 of AP-2 complex subunit beta OS=Homo sapiens GN=AP2B1	2.28	0.44	3.34E-03
P18859-2|ATP5J_	Isoform 2 of ATP synthase-coupling factor 6, mitochondrial OS=Homo sapiens GN=ATP5J	2.26	0.44	2.11E-02
Q16851-2|UGPA_	Isoform 2 of UTP--glucose-1-phosphate uridylyltransferase OS=Homo sapiens GN=UGP2	2.25	0.45	4.55E-02
P53420|CO4A4_	Collagen alpha-4(IV) chain OS=Homo sapiens GN=COL4A4 PE=1 SV=3	2.24	0.45	ND
Q14204|DYHC1_	Cytoplasmic dynein 1 heavy chain 1 OS=Homo sapiens GN=DYNC1H1 PE=1 SV=5	2.20	0.46	1.58E-03
Q9UI09|NDUAC_	NADH dehydrogenase [ubiquinone] 1 alpha subcomplex subunit 12 OS=Homo sapiens GN=NDUFA12 PE=1 SV=	2.19	0.46	2.54E-02
P51659|DHB4_	Peroxisomal multifunctional enzyme type 2 OS=Homo sapiens GN=HSD17B4 PE=1 SV=3	2.17	0.46	5.22E-03
P52209-2|6PGD_	Isoform 2 of 6-phosphogluconate dehydrogenase, decarboxylating OS=Homo sapiens GN=PGD	2.14	0.47	4.15E-03
Q14247-3|SRC8_	Isoform 3 of Src substrate cortactin OS=Homo sapiens GN=CTTN	2.13	0.47	3.24E-02
P36507|MP2K2_	Dual specificity mitogen-activated protein kinase kinase 2 OS=Homo sapiens GN=MAP2K2 PE=1 SV=1	2.13	0.47	ND
P28482|MK01_	Mitogen-activated protein kinase 1 OS=Homo sapiens GN=MAPK1 PE=1 SV=3	2.11	0.47	3.55E-02
P0DJI8|SAA1_	Serum amyloid A-1 protein OS=Homo sapiens GN=SAA1 PE=1 SV=1	2.11	0.47	ND
Q16527|CSRP2_	Cysteine and glycine-rich protein 2 OS=Homo sapiens GN=CSRP2 PE=1 SV=3	2.09	0.48	2.48E-02
P12277|KCRB_	Creatine kinase B-type OS=Homo sapiens GN=CKB PE=1 SV=1	2.08	0.48	3.47E-02
P21397|AOFA_	Amine oxidase [flavin-containing] A OS=Homo sapiens GN=MAOA PE=1 SV=1	2.08	0.48	4.94E-02
P09497-2|CLCB_	Isoform Non-brain of Clathrin light chain B OS=Homo sapiens GN=CLTB	2.07	0.48	2.52E-02
Q8NFV4-4|ABHDB_	Isoform 4 of Alpha/beta hydrolase domain-containing protein 11 OS=Homo sapiens GN=ABHD11	2.06	0.49	2.01E-02
P39023|RL3_	60S ribosomal protein L3 OS=Homo sapiens GN=RPL3 PE=1 SV=2	2.05	0.49	1.89E-02
Q7KZF4|SND1_	Staphylococcal nuclease domain-containing protein 1 OS=Homo sapiens GN=SND1 PE=1 SV=1	2.03	0.49	1.70E-02
Q99832-3|TCPH_	Isoform 3 of T-complex protein 1 subunit eta OS=Homo sapiens GN=CCT7	2.01	0.50	7.20E-03
P14854|CX6B1_	Cytochrome c oxidase subunit 6B1 OS=Homo sapiens GN=COX6B1 PE=1 SV=2	2.01	0.50	3.78E-03
P33176|KINH_	Kinesin-1 heavy chain OS=Homo sapiens GN=KIF5B PE=1 SV=1	1.98	0.50	4.37E-03
P51580|TPMT_	Thiopurine S-methyltransferase OS=Homo sapiens GN=TPMT PE=1 SV=1	1.98	0.51	4.53E-02
P35613-2|BASI_	Isoform 2 of Basigin OS=Homo sapiens GN=BSG	1.96	0.51	2.09E-05

Sub only indicates uniquely identified in SO group.

ND: (not determined) indicates that there was only one value of the abundance from this protein in one of the subgroups and three values in the other subgroup so the t test value could not be accurately defined.

Table S6.2 Proteins significantly increased in expression in donor kidneys with good outcome compared to suboptimal outcome

Protein	Description	Fold change Sub/Good	Fold change Good/Sub	p values
O15143|ARC1B_	Actin-related protein 2/3 complex subunit 1B OS=Homo sapiens GN=ARPC1B PE=1 SV=3	0.47	2.12	3.85E-02
P05093|CP17A_	Steroid 17-alpha-hydroxylase/17,20 lyase OS=Homo sapiens GN=CYP17A1 PE=1 SV=1	0.05	20.59	ND
P27216-2|ANX13_	Isoform B of Annexin A13 OS=Homo sapiens GN=ANXA13	0.00	Good only	ND
O43681|ASNA_	ATPase ASNA1 OS=Homo sapiens GN=ASNA1 PE=1 SV=2	0.00	Good only	ND
P36222|CH3L1_	Chitinase-3-like protein 1 OS=Homo sapiens GN=CHI3L1 PE=1 SV=2	0.00	Good only	ND
Q9NRX4-2|PHP14_	Isoform 2 of 14 kDa phosphohistidine phosphatase OS=Homo sapiens GN=PHPT1	0.07	13.46	2.63E-02
P47897-2|SYQ_	Isoform 2 of Glutamine--tRNA ligase OS=Homo sapiens GN=QARS	0.15	6.87	ND
P02766|TTHY_	Transthyretin OS=Homo sapiens GN=TTR PE=1 SV=1	0.19	5.25	2.58E-02
P11234-2|RALB_	Isoform 2 of Ras-related protein Ral-B OS=Homo sapiens GN=RALB	0.20	4.89	2.20E-03
Q9HAV7|GRPE1_	GrpE protein homolog 1, mitochondrial OS=Homo sapiens GN=GRPEL1 PE=1 SV=2	0.22	4.50	3.96E-03
Q9UGB7|MIOX_	Inositol oxygenase OS=Homo sapiens GN=MIOX PE=1 SV=1	0.24	4.25	ND
Q9NZ45|CISD1_	CDGSH iron-sulfur domain-containing protein 1 OS=Homo sapiens GN=CISD1 PE=1 SV=1	0.25	4.07	3.79E-02
P26885|FKBP2_	Peptidyl-prolyl cis-trans isomerase FKBP2 OS=Homo sapiens GN=FKBP2 PE=1 SV=2	0.26	3.89	ND
Q15124-2|PGM5_	Isoform 2 of Phosphoglucomutase-like protein 5 OS=Homo sapiens GN=PGM5	0.29	3.40	4.78E-03
Q9NNW7-2|TRXR2	Thioredoxin reductase 2, mitochondrial OS=Homo sapiens GN=TXNRD2	0.5	3.3	4.00E-02
Q9BSW2-2|EFC4B_	Isoform 2 of EF-hand calcium-binding domain-containing protein 4B OS=Homo sapiens GN=CRACR2A	0.37	2.72	ND
O00151|PDLI1_	PDZ and LIM domain protein 1 OS=Homo sapiens GN=PDLIM1 PE=1 SV=4	0.37	2.72	1.20E-02
Q9NPJ3|ACO13_	Acyl-coenzyme A thioesterase 13 OS=Homo sapiens GN=ACOT13 PE=1 SV=1	0.38	2.65	3.36E-02
Q15424-2|SAFB1_	Isoform 2 of Scaffold attachment factor B1 OS=Homo sapiens GN=SAFB	0.38	2.64	ND
Q8IUX7|AEBP1_	Adipocyte enhancer-binding protein 1 OS=Homo sapiens GN=AEBP1 PE=1 SV=1	0.38	2.60	ND
P19823|ITIH2_	Inter-alpha-trypsin inhibitor heavy chain H2 OS=Homo sapiens GN=ITIH2 PE=1 SV=2	0.40	2.47	ND
Q93077|H2A1C_	Histone H2A type 1-C OS=Homo sapiens GN=HIST1H2AC PE=1 SV=3	0.42	2.41	5.78E-03
Q9Y2A7-2|NCKP1_	Isoform 2 of Nck-associated protein 1 OS=Homo sapiens GN=NCKAP1	0.42	2.37	ND
Q9NRZ7-2|PLCC_	Isoform 2 of 1-acyl-sn-glycerol-3-phosphate acyltransferase gamma OS=Homo sapiens GN=AGPAT3	0.43	2.33	ND
P80294|MT1H_	Metallothionein-1H OS=Homo sapiens GN=MT1H PE=1 SV=1	0.43	2.33	1.32E-02
Q695T7|S6A19_	Sodium-dependent neutral amino acid transporter B(0)AT1 OS=Homo sapiens GN=SLC6A19 PE=1 SV=1	0.45	2.23	1.18E-03
Q15637-2|SF01_	Isoform 2 of Splicing factor 1 OS=Homo sapiens GN=SF1	0.45	2.22	ND
O95428-4|PPN_	Isoform 4 of Papilin OS=Homo sapiens GN=PAPLN	0.45	2.21	4.96E-02
Q6P1X6-2|CH082_	Isoform 2 of UPF0598 protein C8orf82 OS=Homo sapiens GN=C8orf82	0.45	2.21	2.53E-02
P43034|LIS1_	Platelet-activating factor acetylhydrolase IB subunit alpha OS=Homo sapiens GN=PAFAH1B1 PE=1 SV=2	0.46	2.19	ND
Q9NZB2-4|F120A_	Isoform D of Constitutive coactivator of PPAR-gamma-like protein 1 OS=Homo sapiens GN=FAM120A	0.46	2.17	ND
Q16531|DDB1_	DNA damage-binding protein 1 OS=Homo sapiens GN=DDB1 PE=1 SV=1	0.46	2.16	ND

ND: (not determined) indicates that there was only one value of the abundance from this protein in one of the subgroups and three values in the other subgroup so the t test value could not be accurately defined.

Table S6.4 Cytoskeletal proteins identified by LFQ-MS/MS, were statistically significantly regulated among the two cohorts

Protein	Description	Fold change Sub/Good	Fold change Good/Sub	p values
Q16625-2|OCLN_	Isoform 2 of Occludin OS=Homo sapiens GN=OCLN	20.00	#DIV/0!	ND
O43294|TGFI1_	Transforming growth factor beta-1-induced transcript 1 protein	7.42	0.13	4.53E-02
P18827|SDC1_	Syndecan-1 OS=Homo sapiens GN=SDC1 PE=1 SV=3	4.86	0.21	ND
Q07157-2|ZO1_	Isoform Short of Tight junction protein ZO-1 OS=Homo sapiens GN=TJP1	3.98	0.25	4.29E-02
Q13885|TBB2A_	Tubulin beta-2A chain OS=Homo sapiens GN=TUBB2A PE=1 SV=1	2.86	0.35	7.41E-04
Q96HC4|PDLI5_	PDZ and LIM domain protein 5 OS=Homo sapiens GN=PDLIM5 PE=1 SV=5	2.31	0.43	1.10E-02
P53420|CO4A4_	Collagen alpha-4(IV) chain OS=Homo sapiens GN=COL4A4 PE=1 SV=3	2.24	0.45	ND
Q14204|DYHC1_	Cytoplasmic dynein 1 heavy chain 1 OS=Homo sapiens GN=DYNC1H1 PE=1 SV=5	2.20	0.46	1.58E-03
Q14247-3|SRC8_	Isoform 3 of Src substrate cortactin OS=Homo sapiens GN=CTTN	2.13	0.47	3.24E-02
Q16527|CSRP2_	Cysteine and glycine-rich protein 2 OS=Homo sapiens GN=CSRP2 PE=1 SV=3	2.09	0.48	2.48E-02
P33176|KINH_	Kinesin-1 heavy chain OS=Homo sapiens GN=KIF5B PE=1 SV=1	1.98	0.50	4.37E-03
P35580-3|MYH10_	Isoform 3 of Myosin-10 OS=Homo sapiens GN=MYH10	1.86	0.54	ND
Q9HBL0|TENS1_	Tensin-1 OS=Homo sapiens GN=TNS1 PE=1 SV=2	1.76	0.57	2.56E-02
P35221|CTNA1_	Catenin alpha-1 OS=Homo sapiens GN=CTNNA1 PE=1 SV=1	1.73	0.58	4.33E-02
Q07092-2|COGA1_	Isoform 2 of Collagen alpha-1(XVI) chain OS=Homo sapiens GN=COL16A1	1.68	0.59	ND
P26641|EF1G_	Elongation factor 1-gamma OS=Homo sapiens GN=EEF1G PE=1 SV=3	1.64	0.61	8.40E-03
Q01082|SPTB2_	Spectrin beta chain, non-erythrocytic 1 OS=Homo sapiens GN=SPTBN1 PE=1 SV=2	1.21	0.83	4.62E-03
Q12792-4|TWF1_	Isoform 4 of Twinfilin-1 OS=Homo sapiens GN=TWF1	1.08	0.93	ND
Q99569-2|PKP4_	Isoform 2 of Plakophilin-4 OS=Homo sapiens GN=PKP4	0.94	1.06	ND
Q7Z406-2|MYH14_	Isoform 2 of Myosin-14 OS=Homo sapiens GN=MYH14	0.87	1.15	ND
P68366-2|TBA4A_	Isoform 2 of Tubulin alpha-4A chain OS=Homo sapiens GN=TUBA4A	0.76	1.32	4.96E-02
P52907|CAZA1_	F-actin-capping protein subunit alpha-1 OS=Homo sapiens GN=CAPZA1 PE=1 SV=3	0.72	1.38	3.79E-02
P15924-3|DESP_	Isoform DSPIa of Desmoplakin OS=Homo sapiens GN=DSP	0.69	1.44	ND
O15143|ARC1B_	Actin-related protein 2/3 complex subunit 1B OS=Homo sapiens	0.47	2.12	3.85E-02
O00151|PDLI1_	PDZ and LIM domain protein 1 OS=Homo sapiens GN=PDLIM1 PE=1 SV=4	0.37	2.72	1.20E-02

ND: (not determined) indicates that there was only one value of the abundance from this protein in one of the subgroups and three values in the other subgroup so the t test value could not be accurately defined.

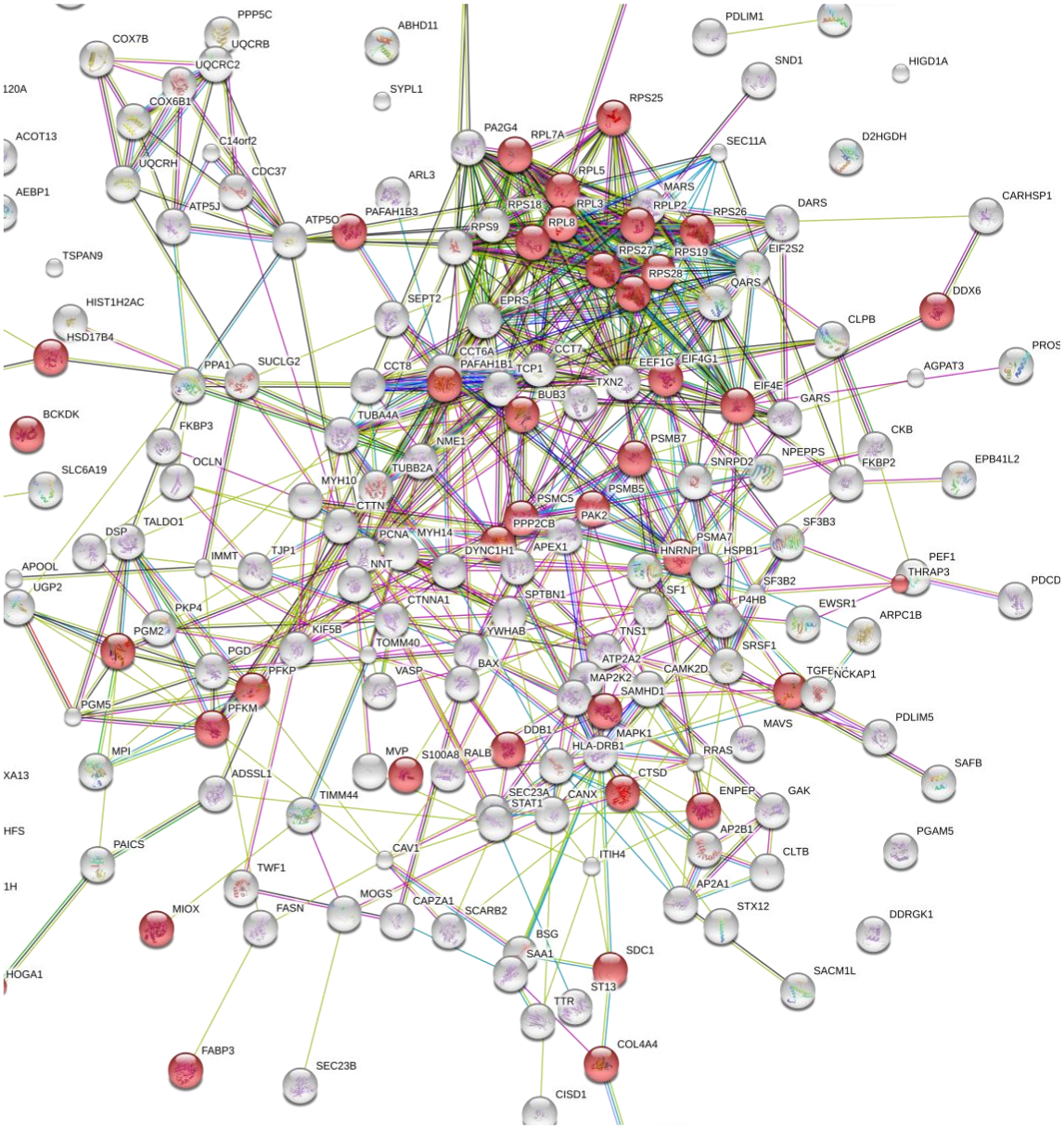

Figure S6.1. Proteins associated with catabolic processes

40 proteins identified were found to be associated with this pathway (FDR 2.27 10^{-5}). The string analysis include only the proteins that were found to be regulated in a statistically significant manner between the two subgroups (214 proteins). The red spheres represent the proteins associated with catabolic processes. The rest of the spheres represent the proteins identified by LC-MS/MS.

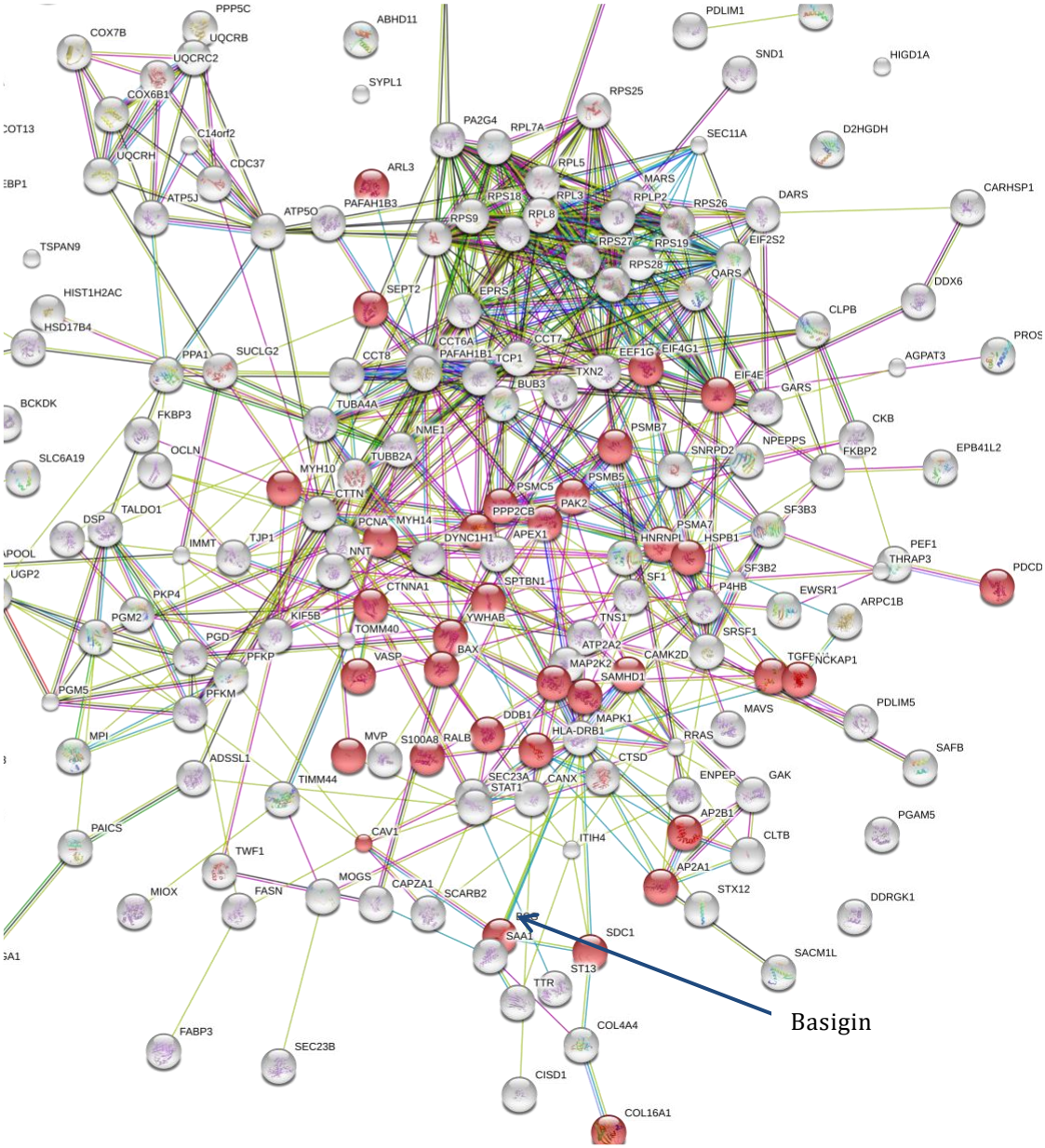

Figure S6.2 Cell surface receptor signalling pathways

30 proteins with a calculated FDR of 0.03 were found to be associated with cell surface signalling pathways including basigin (BSG). The string analysis included only the proteins that were found to be regulated in a statistically significant manner between the two subgroups (214 proteins). The red spheres represent the proteins associated with catabolic processes. The rest of the spheres represent the proteins identified by LC-MS/MS

Gel 1

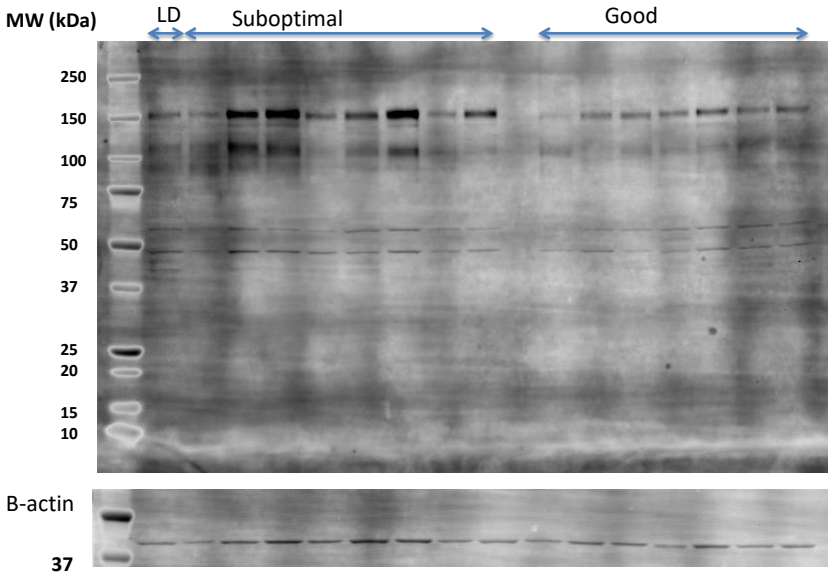

Gel 2

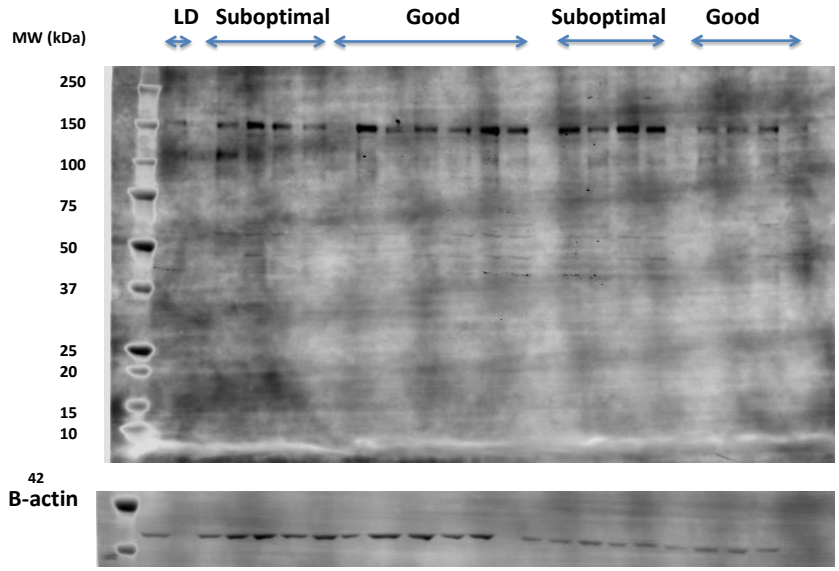

Figure S6.3 Western blot of PDGFRα.
Western blot analysis of a cohort of n=28 kidney biopsy samples. n=14 per outcome. The second gel contains some of the donor kidney samples analysed by LC-MS/MS (in blue boxes) and were not included in the blot analysis because they were tissue biopsies included in the proteomic analysis. A single LD kidney biopsy sample was included in the western blot but not included in the overall validation analysis.

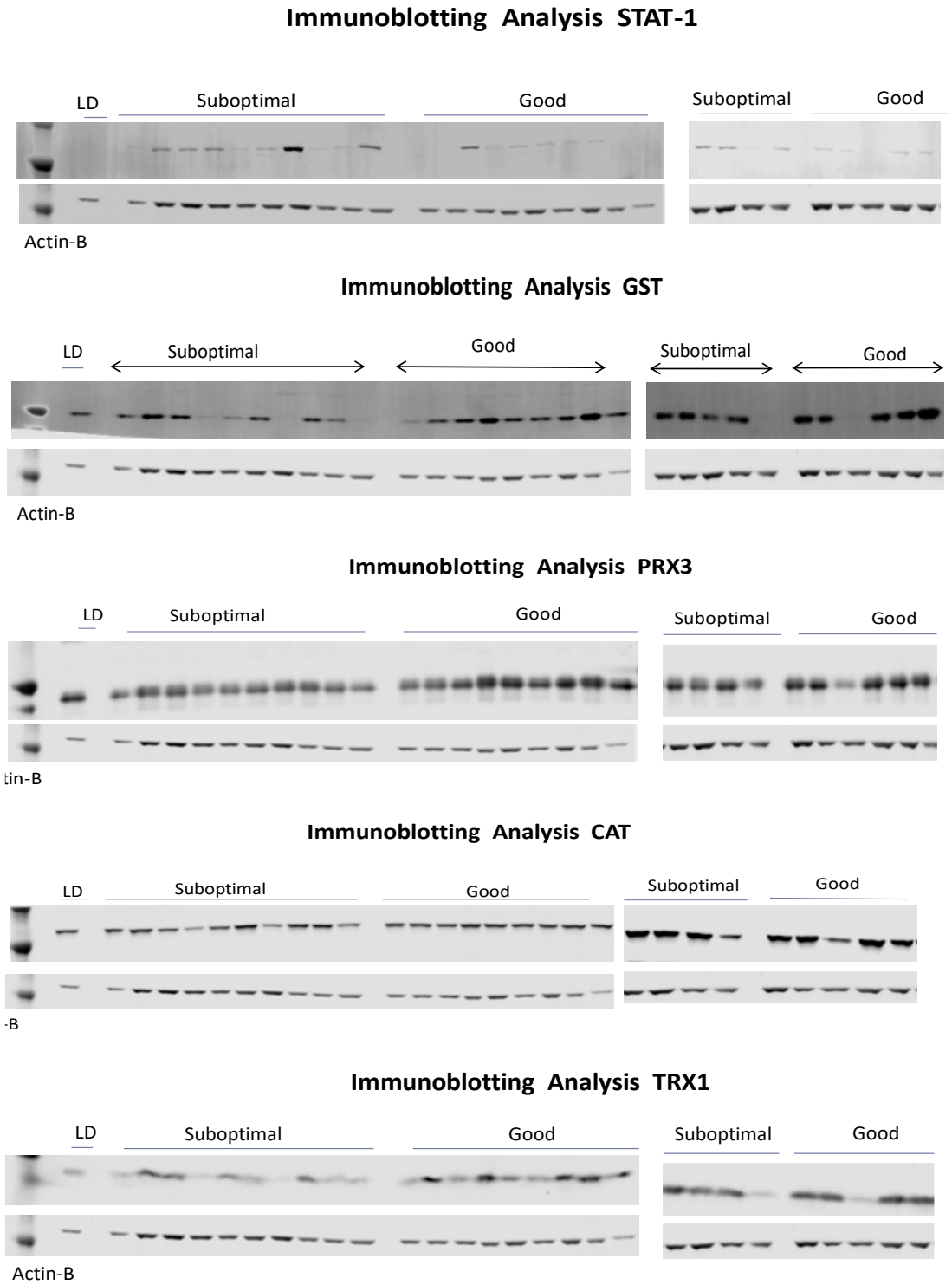

Figure S6.4 Western blot analysis of kidney biopsy samples

Western blot analysis of a cohort of n=28 kidney biopsy samples. n=14 per outcome. A single LD kidney biopsy sample was included in the western blot but not included in the overall analysis.